Studies on Intramolecular Excimer Formation in Polymer Systems(Dissertation_全文)

AUTHOR(S):

Ito, Shinzaburo

CITATION:

Ito, Shinzaburo. Studies on Intramolecular Excimer Formation in Polymer Systems. 京都大学, 1981, 工学博士

ISSUE DATE:

1981-03-23

URL:

https://doi.org/10.14989/doctor.k2550

STUDIES ON INTRAMOLECULAR EXCIMER FORMATION IN POLYMER SYSTEMS

SHINZABURO ITO

DEPARTMENT OF POLYMER CHEMISTRY
KYOTO UNIVERSITY
KYOTO

1981

STUDIES ON INTRAMOLECULAR EXCIMER FORMATION IN POLYMER SYSTEMS

SHINZABURO ITO

DEPARTMENT OF POLYMER CHEMISTRY
KYOTO UNIVERSITY
KYOTO

1981

CONTENTS

CHAPTER 1

Introduction

1-1. Introduction to 'Excimer'

Electronically excited states of chromophores and their relaxation phenomena in polymer systems have become of interest in recent years. There have been a great deal of interests in the relaxation processes as a photophysical subject in polymer science. In addition, much attention has been paid to the excited state of polymers in connection with the photochemical reaction and the photobiological phenomena. The most striking characteristic of polymer systems is the fact that a great number of chromophores gather together in a given polymer domain, even in the extremely dilute conditions. This provides various specific functions in polymer systems.

A number of investigations for the excited state of simple molecules, e.g., aromatic molecules and their derivatives, have clarified the fundamental photophysical and photochemical relaxation processes. Besides the unimolecular relaxation processes, bimolecular photophysical processes take place in such locally concentrated systems as polymer molecules. These processes are closely related to the specific functions of polymer systems. One of the bimolecular processes is the formation of 'Excimer'. Here, a few fundamental matters about the excimer are described below.

Excimer is an electronically excited dimer formed by the attractive interaction between an excited molecule and another molecule of the same kind in the ground state. It exists only in the excited state, and dissociates in the ground state due to the repulsive force between the monomeric molecules. In this point, excimer is distinguished from the excited dimer produced by light absorption of a dimer stable in the ground state. Excimer fluorescence appears as a broad structureless band in a longer wavelength range than the ordinary fluorescence from the excited monomeric molecule. The emission spectra vary markedly with concentration of chromophores, although there is no appreciable change in the absorption spectra.

Since the first observation of excimer fluorescence of pyrene in concentrated solutions was reported by Förster and Kasper in 1954,[1] many systematic investigations have been carried out, and several excellent reviews have been published.[2-7] Since the work of Förster and Kasper, the excimer formation processes have been studied in detail mainly for pyrene molecule as a chromophore, because of its advantageous photophysical characteristics. Since then, excimer emission was found for a lot of aromatic molecules.[8,9] It was shown that excimer formation is a common phenomenon for most aromatic molecules.

The first important characteristic of excimers is on the dynamic properties due to the diffusion controlled process of excimer formation. In fluid solution, intermolecular excimer is formed by a collision between an excited molecule and a ground state one during its excited lifetime. Then, the formation

of excimers is expected to be controlled by the mutual diffusion of chromophores. The diffusion controlled process of excimer formation has been verified mainly for pyrene molecule.[10,11] The experimental value of the association rate constant agree with the theoretical rate of a diffusion controlled collision, and the activation energy obtained from the Arrhenius plot shows the same value as that of solvent viscosity. The excimer formation process is thus directly governed by the ratio of temperature to viscosity for the system.

The second important characteristic of excimers is the geometrical requirement for the excimer formation; rather strict sandwich parallel geometry is needed. The potential diagram for the formation of excimers is given by the sum of energy due to the π orbital repulsion of aromatic molecules and the attractive force in the excited state. Theoretical treatments for the interaction energy are based on the configuration interaction model between charge resonance interaction and excitation resonance interaction. The arrangement of interacting chromophores was calculated by the semi-empirical MO theory, and the potential minima were found at the distance of 3 - 4 Å between two aromatic planes.[12-15] The sandwich parallel arrangement is the most stable one for various chromophores. As for the experimental studies of the geometrical requirement of chromophores, crystals of aromatic molecules[16] and various aromatic compounds where two chromophores are fixed in the molecule such as (m,n)-paracyclophanes.[17,18] have been studied. The results also indicate that

the stable excimer arrangement is the sandwich parallel geometry at the distance of 3 - 4 Å. A well-known study is Hirayama's work,[19] where fluorescence spectra of various diphenyl- and triphenylalkanes were measured. He observed excimer emission only for the compounds in which two aromatic groups along the alkane chain are separated by three carbon atoms. It has been confirmed since that the n = 3 rule holds for other kinds of chromophores such as dinaphthylalkanes[20] and dicarbazolylalkanes.[21,22] Chandross and Dempster[20] studied the fluorescence spectra of various dinaphthylalkanes over the wide range of temperature. They observed efficient intramolecular excimer formation only for two symmetrical di-α-naphthylpropane and di-β-naphthylpropane. Unsymmetrical αβ-dinaphthylpropane showed little excimer formation. Therefore, they concluded that the stable excimer geometry is the symmetrical sandwich arrangement and the compounds other than n = 3 cannot achieve the parallel conformation because of the instability of alkane chain.[23]

Vinyl aromatic polymers such as polystyrene satisfy the configurational condition for efficient excimer formation, where the pendant fluorescent aromatic groups are separated by three carbon atoms of polymer chain. Since the first observation of excimer emission in polystyrene,[24] excimer fluorescence has been measured for a number of aromatic polymers[25]: poly(vinyltoluene), poly(vinylnaphthalene), poly(vinylcarbazole), poly(vinylpyrene), and various kinds of vinyl polymers: poly(allylnaphthalene), poly(naphthyl methacrylate), poly(naphthyl-

ethyl vinyl ether) and so on.

In dilute solution, the monomer and excimer fluo rescence bands of there polymers agree with those of monomeric and dimeric model compounds, although the excimer formation in polymers is usually more efficient than the formation in model compounds. Each intensity of the monomer fluorescence and excimer one does not vary with the concentration of polymers, and this shows that the observed excimers are formed by intramolecular interaction between adjacent aromatic groups on the polymer chain. As mentioned above, the arrangement of chromophores in the excimer state is the sandwich parallel geometry. The adjacent side groups must take place rotational motion to achieve the favorable conformation of excimers during the excited lifetime. The ratio of excimer to monomer quantum yields markedly depends on tempera tures,[26,27] and the excimer formation is inhibited at a low temperature, 77 K in the dilute solution. Thus, the intramolecular excimer formation in polymer solution is governed by the micro-Brownian motion of the polymer chain. The effects of stereo-regularity of polymer chain on the excimer formation have been discussed in polystyrene,[28,29] and poly-α-methylstyrene.[6] The samples having high values of isotactic content exhibit relatively high efficiency of excimer formation. These effects, i.e., temperature and stereo-regularity, suggest that the intramolecular excimers in solution are closely related to the two fundamental physical properties of polymers: molecular motion of polymer segments and their micro-structures.

In solid state of polymers, both intra- and intermolecular excimer formation is possible, but the distinction is not easy. As the excimer conformation is unstable in the ground state, only a little fraction of the chromophores seem to take the parallel arrangement. The emission spectra of films of polystyrene, poly(vinylnaphthalene), and poly(vinylcarbazole) consist of predominant excimer fluorescence, and even if the films are cooled at 4.2 K, the excimer emission can be still observed.[30] Since conformational changes of polymer segments are suppressed in solid films, the efficient excimer formation is attributable to the energy migration from a chromophore absorbing the excitation light to another chromophore taking the suitable arrangement for excimer formation in the ground state. By the fluorescence quenching experiments in polymer films, the diffusion length of excitation energy and fraction of excimer forming site in poly(vinylcarbazole)[31] were estimated to be 200 Å and 10^{-3} mole per mole of the base unit of the polymer, respectively. In solid, thus, energy migration plays an important role in the excimer formation.

In dilute solution, the effect of energy migration process on the intramolecular excimer formation, have not been clarified. Quenching experiments for the monomer emission suggest that the singlet energy migrates among chromophores with a fairly fast rate constant, since the fluorescence quenching is more effective than that for the monomeric model compounds.[32,33] A number of investigations have been continued,[34-37] but the problems such as the

mechanism of energy migration in polymers and the determination of migration rate, are still subjects for further investigation.

Recent developments in the time-resolved technique for photoluminescence measurements enable determination of individual rate constants of photophysical processes including the excimer formation process.[38-41] It can be said that quantitative study on various polymers and their model compounds is necessary to clarify the excimer formation mechanism in polymer systems. In addition to photostationary measurements, the time-resolved fluorescence method provides further advances in the elucidation of polymer excimers.

In this thesis, the author intends to clarify the mechanism of intramolecular excimer formation in polymer systems. There are two purposes for the study of the excimer.

The first is fundamental interest for the relaxation processes of excitation energies, as a subject of polymer science. The detailed knowledge of the intramolecular excimers seems to be essential for understanding of the photophysical and photochemical behavior of polymer systems. The importance has already been mentioned at the beginning of this section.

The second is applications of the excimers for the study of physical properties of polymers. Particularly, the segment motion of polymers in solution has the relaxation times in the range of 10^{-10}- 10^{-7}s, which are the same range of the excited lifetimes for

usual aromatic molecules. As mentioned above, the intramolecular excimers formed by the short range interactions are closely related to the molecular motion of polymer segments. Hence, the quantitative study on the intramolecular excimers provides information about the rotational relaxation times of polymer chains.

1-2. Outline of This Thesis

This thesis aims to elucidate the excimer formation mechanism in polymer systems. For this purpose, two approaches are taken; one is the study of the fluorescence behavior of various model compounds, whose molecular structures are designed to clarify the interactions of a pair of chromophores, and another is the study of transient behavior in the time range of 10^{-9} - 10^{-6} s, where the relaxation processes of the excitation energy are directly observed. The former approach is described mainly in Part II and the latter one is presented in Part III. The outline will be hereinafter mentioned briefly.

In Chapter 1, a few fundamental properties of the excimers are described. This chapter is the general introduction of this thesis, and its outline is also mentioned.

Part I deals with fundamental characteristics of inter- and intramolecular excimers of naphthalene derivatives. Chapter 2 states the experimental methods for studying the excimer formation processes of naphthalene chromophore. Detailed procedures for photostationary and time-resolved measurements

are described. Next, the kinetic treatments under steady state and transient conditions are mentioned. The kinetic treatments enable us to determine all the photophysical rate constants in the kinetic scheme. In Chapter 3, the inter- and intramolecular excimer formation of the monomeric and dimeric model compounds are analyzed in practice by the kinetic treatments mentioned in Chapter 2. Characteristics of inter- and intramolecular excimers of the model compounds, 2-ethylnaphthalene and 1,3-dinaphthylpropane, are discussed. Chapter 4 provides the geometrical requirements for excimer formation of naphthalene chromophores. The $n = 3$ rule is examined for α,ω-dinaphthylalkanes. Emission properties of a few unstable excimers are also measured. The extraordinary emission behaviors of the naphthyl groups are discussed with respect to the configuration.

Part II deals with studies on the intramolecular excimers of model compounds and their conformational relaxation processes. In Chapter 5, various dimeric model compounds are synthesized, and the photophysical rate constants are determined by the time-resolved measurements. On the basis of association rate contants, the relationship between the molecular structure and the conformational relaxation processes are discussed. In Chapter 6, the conformation analysis of dinaphthylalkanes is carried out. The pathway of the internal rotation from the stable conformation to the excimer conformation is described. The configurational effects on the excimer formation rate obtained in Chapter 5, are explained by the calculation of conformation energies. In Chapter 7, excimer

formation processes in trimer model compounds are described. By the kinetic study and conformation analysis, the individual interaction of each pair of chromophores are discussed. The trimers can be regarded as the smallest model compounds having polymer effects on the relaxation processes of excitation energy. The photophysical behavior provides some basic information for the excimer formation mechanism in polymer systems.

Part III deals with the intramolecular excimers in polymer systems. The emission behavior of poly-(2-vinylnaphthalene) and its copolymers in solution or in rigid matrix are presented, and two important photophysical processes in the polymers: energy migration and excimer formation, are discussed. Chapter 8 provides the fluorescence behavior of poly(2-vinylnaphthalene) and its block copolymers: temperature effect, molecular weight effect, and solvent effect. The mechanism of intramolecular excimer formation are discussed on the basis of the kinetic rate constants, which are compared with those obtained for various model compounds. In Chapter 9, the time-resolved technique is applied to the vinylnaphthalene-styrene copolymer systems. Here, effects of the sequence distribution of chromophores, the migration rate of excitation energy, and the rotational relaxation rate of polymer segments are discussed. With a kinetic treatment taken account of these effects, the observed transient and steady state behavior is explained. In Chapter 10, the excimer formation mechanism of poly(2-vinylnaphthalene) in rigid matrix are described. The marked molecular

weight dependence of the excimer formation efficienc is explained as the results of energy migration on the polymer chain. The concentration of excimer forming site and migration rate of the excitation energy are discussed.

References

1) Th. Förster and K. Kasper, Z. Phys. Chem. N.F., 1, 275 (1954).
2) Th. Förster, Angew. Chem., 81, 364 (1969).
3) J.B. Birks, "Photophysics of Aromatic Molecules, Chap. 7, Wiley-Interscience, London, 1970.
4) W. Klöpffer, "Organic Molecular Photophysics," J.B. Birks Ed., Vol. 1, Chap. 7, Wiley-Interscience, London, 1973.
5) Y. Nishijima, J. Macromol. Sci.-Phys., B8, 389 (1973).
6) H. Odani, Bull. Inst. Chem. Res., Kyoto Univ., 51, 351 (1973).
7) S.W. Beavan, J.S. Hargreaves, and D. Phillips, "Adv. in Photochem.," J.N. Pitts, Jr.G.S. Hammon and K. Gollnick Eds., Vol. 11, Wiley, New York, 1979.
8) J.B. Birks and L.G. Christophorou, Nature, 197, 1064 (1963).
9) J.B. Birks and L.G. Christophorou, Spectrochim. Acta, 19, 401 (1963).
10) J.B. Birks, D.J. Dyson, and I.H. Munro, Proc. R. Soc., A275, 575 (1963).
11) R. Speed and B. Selinger, Aust. J. Chem., 22, 9 (1969).

12) T. Azumi and H. Azumi, Bull. Chem. Soc. Jpn., 39, 1829 (1966).
13) F.J. Smith, A.T. Armstrong, and S.P. McGlynn, J. Chem. Phys., 44, 442 (1966).
14) A.K. Chandra and B.S. Sudhindra, Mol. Phys., 28, 695 (1974).
15) A.K. Chandra and E.C. Lim, Chem. Phys. Lett., 45, 79 (1977).
16) H. Braun and Th. Förster, Ber. Bunsenges. Phys. Chem., 70, 1091 (1966).
17) D.J. Cram, N.L. Allinger, and H. Steinberg, J. Am. Chem. Soc., 76, 6132 (1954).
18) M.T. Vala, Jr.,J. Haebig, and S.A. Rice, J. Chem. Phys., 43, 886 (1965).
19) F. Hirayama, J. Chem. Phys., 42, 3163 (1965).
20) E.A. Chandross and C.J. Dempster, J. Am. Chem. Soc., 92, 3586 (1970).
21) W. Klöpffer, Ber. Bunsenges. Phys. Chem., 74, 693 (1970).
22) Y. Nishijima, Y. Sasaki, K. Hirota, and M. Yamamoto, Repts. Progr. Polym. Phys. Japan, 15, 449 (1972).
23) K. Zachariasse and W. Kühnle, Z. Phys. Chem. N.F., 101, 267 (1976). The excimer emission for the compounds, Py-$(CH_2)_n$-Py, (n=2-22) was reported. This seems to be the results of the large binding energy and long lifetime of pyrene chromophores.
24) L.J. Basile, J. Chem. Phys., 36, 2204 (1962).
25) A number of spectroscopic investigations of vinyl aromatic polymers have been reported in the 1970's. The literatures are listed in the references of Chaper 8.

26) C. David, M. Piens, and G. Geuskens, Eur. Polym. J., 8, 1019 (1972).
27) Y. Nishijima, Y. Sasaki, M. Tsujisaki, and M. Yamamoto, Repts. Progr. Polym. Phys. Japan, 15, 453 (1972).
28) J.W. Longworth, Biopolymers, 4, 1131 (1966).
29) C. David, N.P. Lavareille, and G. Gueskens, Eur. Polym. J., 10, 617 (1974).
30) C.W. Frank and L.A. Harrah, J. Chem. Phys., 61, 1526 (1974).
31) W. Klöpffer, J. Chem. Phys., 50, 2337 (1969).
32) A.M. North and M.F. Treadaway, Eur. Polym. J., 9, 609 (1973).
33) E. Leory, C.F. Lapp, and G. Laustriat, Biopolymers 13, 507 (1974).
34) A.M. North and D.A. Ross, J. Polym. Sci., Symposium, 55, 259 (1976).
35) J. Fouassier, D. Lougnot, and J. Faure, Makromol. Chem., 179, 437 (1978).
36) J.S. Aspler, C.E. Hoyle, and J.E. Guillet, Macromolecules, 11, 925 (1978).
37) I. McInally, R.F. Reid, H. Rutherford, and I. Soutar, Eur. Polym. J., 15, 723 (1979).
38) G.E. Johnson, J. Chem. Phys., 61, 3002 (1974).
39) P.A. Avouris, J. Kordas, and M.A. El-Bayoumi, Chem. Phys. Lett., 26, 373 (1974).
40) C. David, M. Piens, and G. Geuskens, Eur. Polym. J., 12, 621 (1976).
41) K.A. Zachariasse, W. Kühnle, and A. Weller, Chem. Phys. Lett., 59, 375 (1978).

PART I

Fundamental Properties of Naphthalene Excimers

CHAPTER 2

Experimental and Kinetic Treatment for the Inter- and Intramolecular Excimer Formation Processes

2-1. Introduction

Since the evidence of excimer formation in the mechanism of dynamic quenching was reported by Förster and Kasper[1] for concentrated solutions of pyrene, many detailed studies on the kinetic treatment of the excimer formation processes have been carried out for pyrene solutions.[2] Pyrene molecule possesses many advantageous photophysical characteristics for study of excimer formation, i.e., the long wavelength of the absorption and emission bands, the large quantum yields of the fluorescence, and the high efficiency of the excimer formation at room temperature. The mechanism of the excimer formation processes have been elucidated quantitatively in this compound. Before long, it was found that a lot of aromatic compounds form excimers, which then emit luminescence in a longer wavelength range of the spectra than the ordinary fluorescence.[3] Naphthalene chromophore is one of the typical compounds which can form excimers. Its dynamic quenching mechanism was elucidated by the analysis of the photophysical behavior, using the procedure developed for the intermolecular excimers in pyrene solutions.[4]

In this chapter, the experimental methods for studying the excimer formation processes of naph-

thalene chromophore, are described. Next, the kinetic treatments under steady state and transient conditions are discussed on the basis of the kinetic scheme.

2-2. Experimental Method

2-2, 1. Steady State Measurements

In the measurements of dilute solutions, the concentration of samples were adjusted to ca. 10^{-4} mol/l. In such dilute solutions, the naphthalene derivatives show no interaction between excited chromophores during their lifetime. Tetrahydrofuran (THF) and 2-methyltetrahydrofuran (2MTHF) were chosen for the solvent in the present experiments, since they are good solvents for the investigated polymers, having very low freezing temperatures, and showing no quenching effect on the chromophores. In particular, 2MTHF was used for the measurement at the temperature, 77 K, since the solvent gives a transparent rigid glass under the freezing temperature (-136 ^{o}C). The solvents were purified by vacuum distillation after preliminary distillation over sodium metal. The solutions were degassed by several freeze-to-thaw cycles at 10^{-5} mmHg. Measurements were carried out on the solutions in rectangular quartz cells (1 cm square cross section and 4 cm long). Absorption spectra were obtained with a Shimadzu UV-200S spectrophotometer. Fluorescence spectra were measured with a Shimadzu spectrofluorophotometer model RF502, whose spectral response is corrected by a standard tungsten lamp. The emission spectra of dilute solutions were observed at a right angle to the incident light. In the concentrated

solutions, emission spectra were measured by front surface irradiation. The quantum yields of emissions were determined relative to that of quinine sulfate in 1 N sulfuric acid, which has several advantages as a standard; it is not quenched by oxygen, exhibits little concentration quenching, has no significant overlap between its absorption and emission spectra, and is stable in solution.[5] The reported quantum yield is 0.508 at 5×10^{-3} mol/l and 0.546 for concentrations below 10^{-4} mol/l at 25 °C, which is constant to ±5% for excitation in the region 250-370 nm.[6] The samples were excited by the light of wavelength, 276 nm which corresponds to the L_a band (ε = 5000) of naphthalene chromophore. For dilute solutions, the concentrations of the samples and the standard were adjusted to the same optical density at 276 nm (O.D. = 0.7 - 0.8) in order to observe the emissions under an equivalent optical condition. In such concentration of quinine sulfate, the value, 0.51 was adopted for the quantum yield of the standard. For concentrated solutions, the measurements of quantum yields were carried out with the excitation wavelength of 310 nm, at this wavelength, both the sample solution and the standard solution (5×10^{-3} mol/l) absorbed completely the incident excitation light in the region near the front surface. Under such conditions, the quantum yield of standard solution was taken as 0.51. The fluorescence spectra were separated into the monomer and excimer fluorescence parts by the reference of the spectrum for 2-ethylnaphthalene at each temperature. On the recorded emission spectra, the areas below the spec-

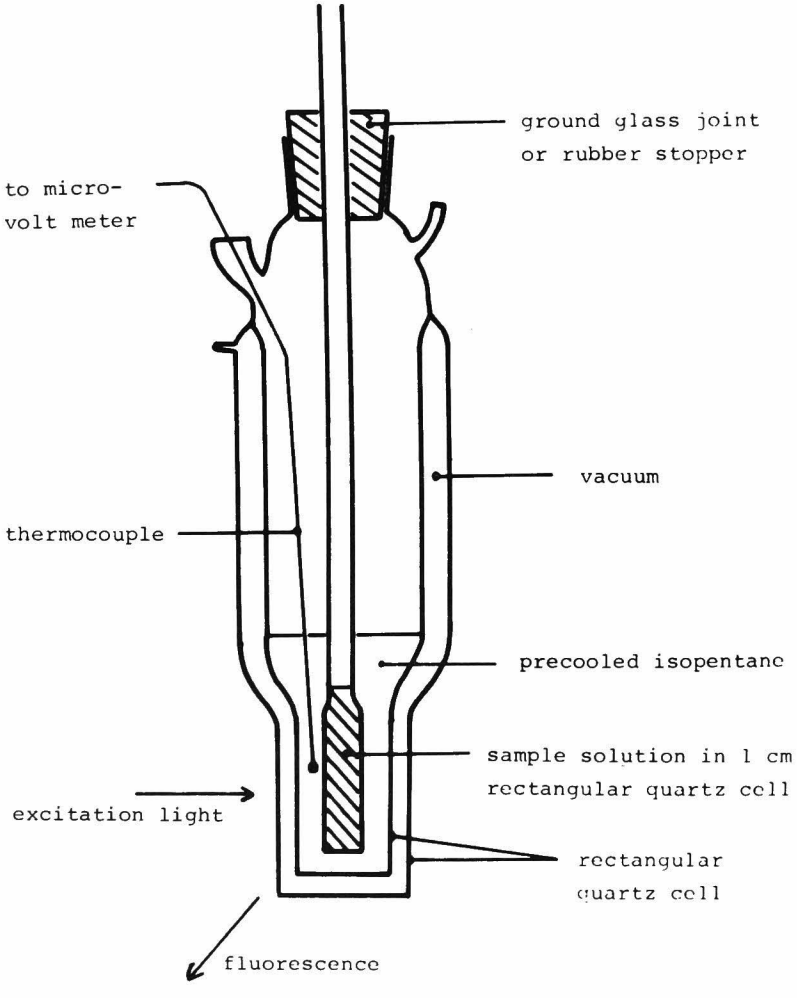

Fig. 1. Dewar cell for measurements at low temperatures.

tral curves for quinine sulfate (S_q) and sample (S) were measured. The quantum yield of the sample (Φ) are given as follows,

$$\Phi = n^2 S \Phi_q / (n_q^2 S_q),$$

where Φ_q is the quantum yield of the standard, n and n_q are the refractive indices of the sample solution and the standard solution, respectively.

In the measurements at temperatures above 0 °C, the cell containing sample solution was set in a thermo-regulated holder. The measurements at low temperatures were carried out by dipping the cell into isopentane precooled by liquid nitrogen in a quartz dewar equipped with a thermocouple, illustrated in Fig. 1. Since isopentane has a very low freezing point (-160 °C) and good transmittance for short wavelength light down to 220 nm, it is favorable for the medium of the cells. The quantum yields at low temperatures were obtained relative to that at room temperature under the same optical conditions The values were corrected for the changes of the refractive index and the density of solvent.

2-2, 2. Time-Resolving Measurements

A single photon counting method was used for the measurement of fluorescence decay curves at temperatures above 0 °C.[7] The apparatus consists of an Ortec nanosecond fluorescence spectrometer and a Hitachi multi-channel analyzer. At low temperatures, the decay curves were measured by a pulse fluorometer, TRW model 31 B.[8] The cells containing sample solutions were set in a thermo-regulated holder or

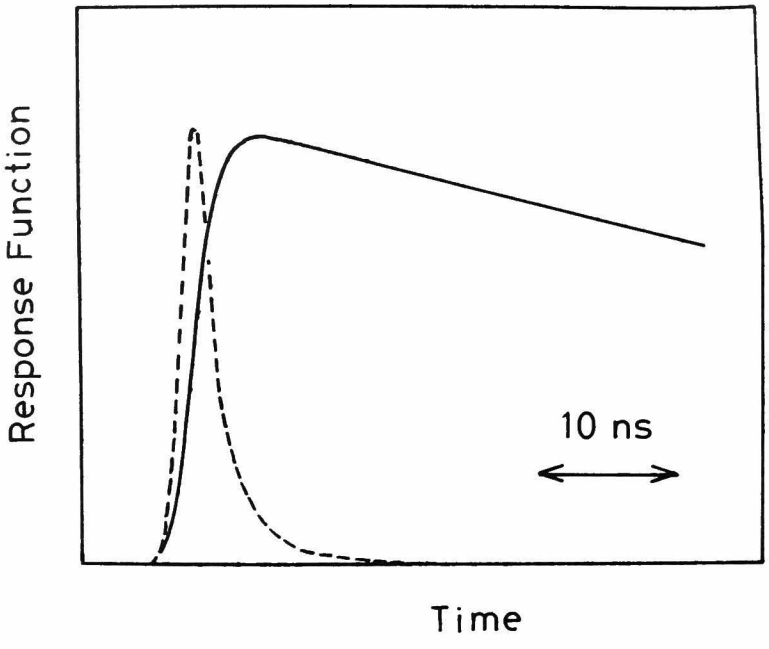

Fig. 2. A typical rise and decay curve of the excimer emission measured with the single photon counting method. The broken line shows the excitation light generated by an air gap pulser with a halfwidth of 2.5 ns.

a quartz dewar, and the fluorescence decay was observed at a right angle to the excitation light. In the single photon counting method, the excitation light pulse was generated by an air gap pulser with a halfwidth of about 2.5 ns. The typical time function of the excitation pulse and a fluorescence decay curve are shown in Fig. 2. In the measurement with TRW fluorometer, a deuterium lamp was used for the pulsed light source whose halfwidth was ca.

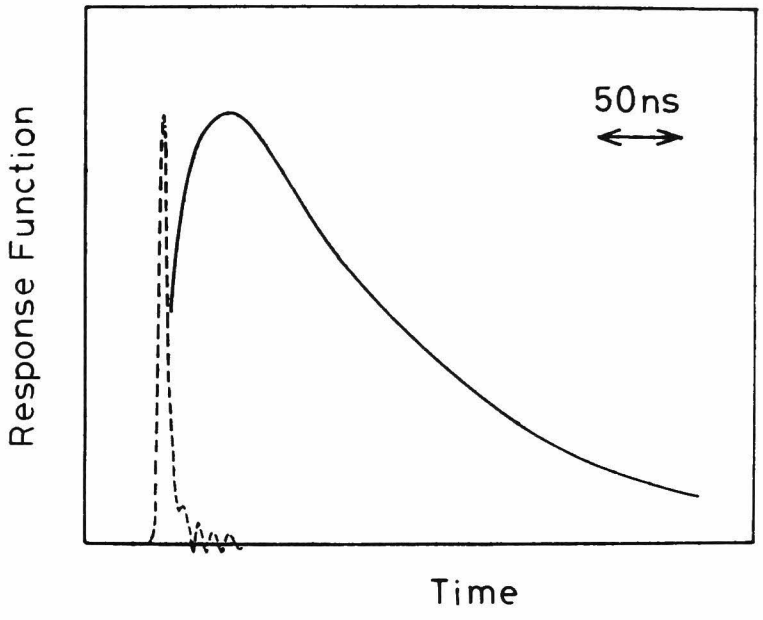

Fig. 3. A typical rise and decay curve of the excimer emission measured with the TRW fluorometer. The broken line shows the excitation light pulse generated by a deuterium lamp with a halfwidth of 7.5 ns.

7.5 ns. The typical response functions for the excitation light pulse and decay curve are shown in Fig. 3. Suitable combinations of optical filters were used for the excitation light and for the observation of the monomer fluorescence and excimer fluorescence. The absorption and fluorescence spectra of 2-ethylnaphthalene and fluorescence spectra of poly(2-vinylnaphthalene) at room temperature are shown in Fig. 4, and the optical characteristics of

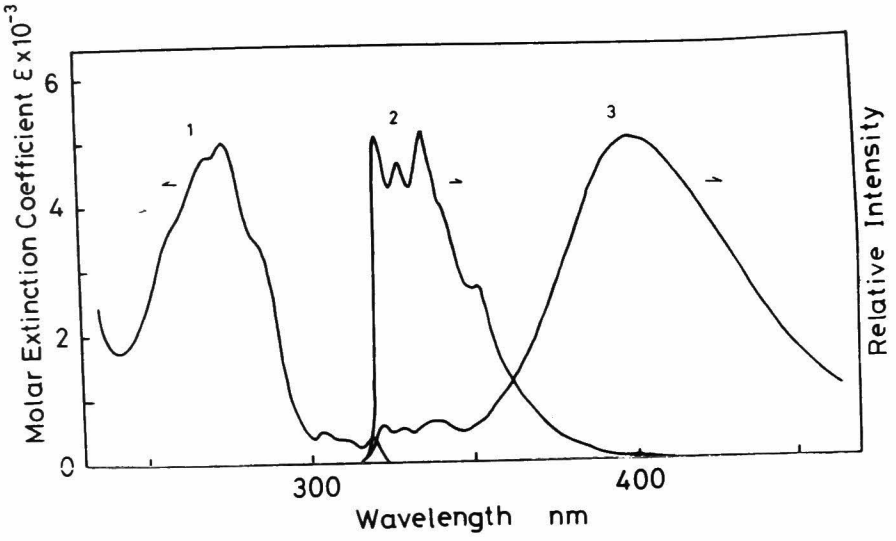

Fig. 4. Absorption and emission spectra of naphthalene chromophore. (1) Absorption spectrum of 2-ethylnaphthalene. (2) Fluorescence spectrum of 2-ethylnaphthalene. (3) Fluorescence spectrum of poly(2-vinylnaphthalene) at room temperature.

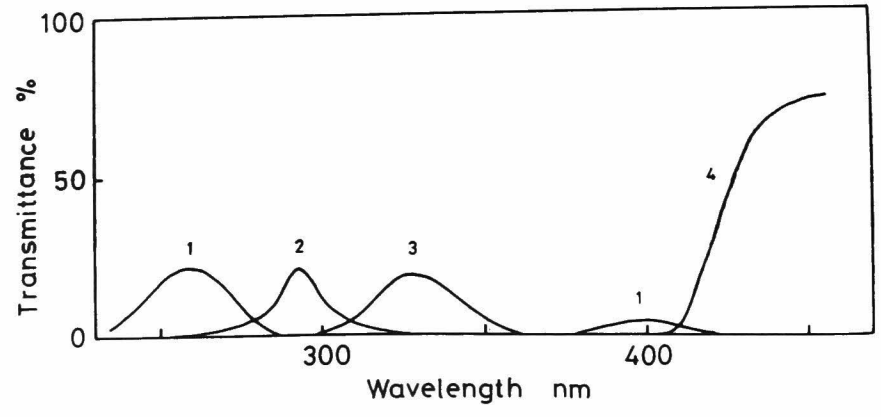

Fig. 5. Transmittance of filters. (1) Chlorine filter + UV-D25 filter. (2) 293 nm interference filter. (3) Chrome alum filter + UV-D25 filter. (4) SC-42 filter.

the filters are shown in Fig. 5. The combination, chlorine + UV-D25 (Toshiba) filters or 293 nm interference filter + UV-D25 filter were used for the excitation. The chlorine filter was made by enclosing chlorine gas with a rectangular quartz cell (1 cm) at a pressure of 4 atm. In the former combination of filters, the lines at 259 nm and 270 nm of the air gap pulser were used as the excitation light, and in the latter combination, the lines at 296 nm and 315 nm were used. The monomer fluorescence was selected by chrome alum filter + UV-D25 filter. The chrome alum ($KCr(SO_4)_2 \cdot 12H_2O$) was prepared by reducing recrystallized potassium dichromate with ethanol. A 15% chrome alum solution in 1 N sulfuric acid was sealed in a glass cell (1.5 cm). The excimer fluorescence was separated from the monomer fluorescence by SC-42 filter (Fuji), which cuts off the light below the wavelength of 400 nm.

The methods for preparation of materials will be described in each chapter. From the measurements of quantum yields and decay curves, the rate constants of the excimer formation processes are determined on the basis of the transient reaction kinetics. The relationship between the rate constants and the experimental data will be mentioned in the following section.

2-3. Kinetic Treatment of the Excimer Formation Processes

2-3, 1. Steady State Kinetics

The formation of the excimer in solution occurs via a collision between an excited chromophore and

the same kind of chromophore in the ground state. The kinetic scheme of such excimer formation is given in Fig. 6. The rate parameters for the photophysical processes are denoted as follows,

$^1M + h\nu$	$\rightarrow$	$^1M^*$	k_{10}
$^1M^*$	$\rightarrow$	$^1M + h\nu'$	k_{01}^f
$^1M^*$	$\rightarrow$	^1M	k_{01}^n
$^1M^* + {}^1M$	$\rightarrow$	$^1D^*$	k_{21}
$^1D^*$	$\rightarrow$	$^1M^* + {}^1M$	k_{12}
$^1D^*$	$\rightarrow$	$^1M + {}^1M + h\nu''$	k_{02}^f
$^1D^*$	$\rightarrow$	$^1M + {}^1M$	k_{02}^n

where ^1M and $^1M^*$ represent the chromophores in the ground state and the excited singlet state, respectively, and $^1D^*$ represents the singlet excimers. In the present system, all the photophysical processes associated with the triplet excited states are radiationless, hence those processes can be included in the scheme into the radiationless processes together with the internal conversion processes.

The rate constants for steady excitation can be written as follows,

$$d[^1M^*]/dt = I_o + k_{12}[^1D^*] - (k_{01}^f + k_{01}^n + k_{21}[^1M])[^1M^*] \quad (1)$$

$$d[^1D^*]/dt = k_{21}[^1M][^1M^*] - (k_{02}^f + k_{02}^n + k_{12})[^1D^*] \quad (2)$$

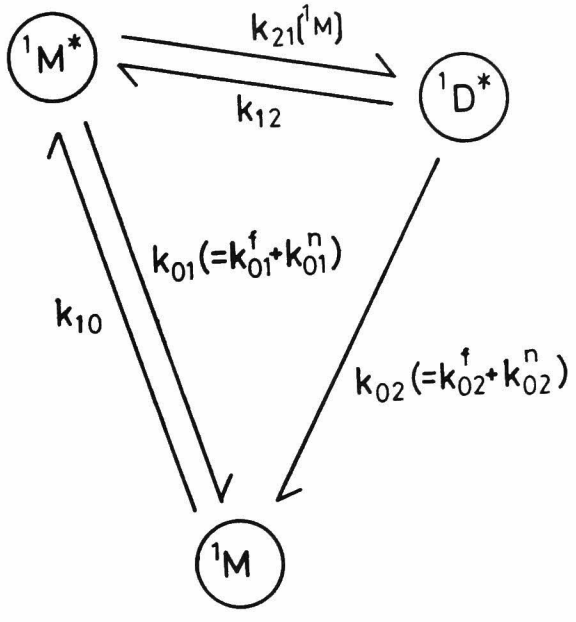

Fig. 6. Kinetic scheme of the intermolecular excimer formation processes.

where I_o is the intensity of excitation light. Under photostationary conditions, $d[^1M^*]/dt = d[^1D^*]/dt = 0$, the concentrations of the excited molecules are given in the following forms,

$$[^1M^*] = I_o\, k_2 / (k_1\, k_2 - k_{21}\, k_{12}[^1M]) \qquad (3)$$

$$[^1D^*] = I_o\, k_{21}[^1M] / (k_1\, k_2 - k_{21}\, k_{12}[^1M]), \qquad (4)$$

where the parameters, k_1 and k_2 are defined as follows,

$$k_1 = k_{21}[^1M] + k_{01}, \quad k_2 = k_{12} + k_{02}, \tag{5}$$

$$k_{01} = k_{01}^f + k_{01}^n, \quad k_{02} = k_{02}^f + k_{02}^n . \tag{6}$$

Using these parameters, the quantum yields of the monomer fluorescence (Φ_M) and the excimer fluorescence (Φ_D) are written,

$$\Phi_M = k_{01}^f \, k_2 \, / \, (k_1 \, k_2 - k_{21} \, k_{12}[^1M]) \tag{7}$$

$$\Phi_D = k_{02}^f \, k_{21}[^1M] \, / \, (k_1 \, k_2 - k_{21} \, k_{12}[^1M]) . \tag{8}$$

The ratio of the quantum yields, Φ_D/Φ_M can be expressed in a simple form,

$$\Phi_D/\Phi_M = k_{02}^f \, k_{21}[^1M] \, / \, k_{01}^f \, k_2 . \tag{9}$$

The equation shows that the ratio should be proportional to the concentration of chromophore at a given temperature. Moreover, k_{01}^f and k_{02}^f is generally independent of temperature, and then in such low temperature region that the rate constants, k_{12} and k_{02}^n are negligibly small compared to k_{02}^f, Eq. 9 can be written as

$$\Phi_D/\Phi_M = k_{21}[^1M] \, / \, k_{01}^f$$

$$= (N_a \, [^1M] \, / \, k_{01}^f) \exp(-E_a/RT), \tag{10}$$

where N_a and E_a are the frequency factor and the activation energy for the excimer formation process.

By the measurements of the temperature dependence of the ratio Φ_D/Φ_M, we can obtain the activation energy, E_a as a slope of Arrhenius plot. The ratio Φ_D/Φ_M, takes a peak value at a temperature which is

called a critical temperature (T_c). In the high temperature range above T_c, the condition, $k_{21}[^1M]$, $k_{12} \gg k_{01}$, k_{02} is satisfied in solution, and Eq. 9 is expressed as

$$\ln (\Phi_D/\Phi_M) = - \Delta H / (RT) + \text{const.} \qquad (11)$$

and $\Delta H = E_d - E_a$,

where ΔH is the enthalpy change of the excimer formation, and E_d is the activation energy of dissociation process of the excimer. Hence, the Arrhenius plot in the high temperature region gives the values of ΔH and E_d. Under this condition, Eq. 2 is modified,

$$[^1D^*] / ([^1M^*][^1M]) = k_{21} / (k_{12} + k_{02})$$

$$\rightarrow \quad k_{21} / k_{12} = K_e \qquad (12)$$

where K_e is the molar equilibrium constant of the excimer formation and dissociation processes. Using Eqs. 9 and 12, the following relation is obtained,

$$\Phi_D/\Phi_M = k_{02}^f \, K_e \, [^1M] / k_{01}^f \, . \qquad (13)$$

From the thermodynamic relation for the change of free energy, ΔG,

$$\Delta G = - R \, T \ln K_e = \Delta H - T \, \Delta S \, . \qquad (14)$$

The entropy change (ΔS) for the excimer formation process can be derived from Eqs. 13 and 14,

$$\Phi_D/\Phi_M = (k_{02}^f[^1M]/ k_{01}^f) \exp(\Delta S/R) \exp(-\Delta H/RT). \qquad (15)$$

Then, if the ratio. k_{02}^f/k_{01}^f is known, ΔS can be evalu——

ated. Thus, by the steady state measurements in the wide range of temperatures, thermodynamic parameters such as E_a, E_d, ΔH, and ΔS for the excimer formation processes can be estimated.

These treatments are applicable to the intramolecular excimer formation processes only by regarding its association process as a pseudo-first order reaction, where the concentration of chromophore in the ground state is omitted in the above equations. In order to determine the individual rate constants, time-resolved fluorescence measurements are required. But, the rate constants for the intramolecular excimer formation processes were estimated with steady state measurements by Klöpffer and Liptay,[9] using an appropriate quencher such as oxygen for the monomer and excimer fluorescence. The treatments are briefly outlined below. In the measurements for the monomeric model compounds in dilute solution, the quantum yield of the monomer fluorescence and its decay time are observed. The quantum yield (Φ_M^o) and the decay time (τ_M^o) are expresses as follows,

$$\Phi_M^o = k_{01}^f/(k_{01}^f + k_{01}^n), \quad \tau_M^o = (k_{01}^f + k_{01}^n)^{-1}, \qquad (16)$$

and the fluorescence yield with quencher, $\Phi_{M,q}^o$ is,

$$\Phi_{M,q}^o = k_{01}^f / (k_{01}^f + k_{01,q}^n). \qquad (17)$$

From Eqs. 16 and 17, the rate constants of the radiative process of the excited monomer and its nonradiative process in the absence and presence of quencher are written,

$$k_{01}^{f} = \Phi_{M}^{o} / \tau_{M}^{o}, \qquad k_{01}^{n} = (\Phi_{M}^{o-1} - 1) k_{01}^{f} \tag{18}$$

$$k_{01,q}^{n} = (\Phi_{M,q}^{o-1} - 1) k_{01}^{f} \tag{19}$$

The ratios of the fluorescence yields, Φ_{M}^{o}/Φ_{D} and Φ_{M}/Φ_{D} are given,

$$\Phi_{M}^{o}/\Phi_{D} = \{(k_{02}^{f} + k_{02}^{n} + k_{12})(k_{01}^{f} + k_{01}^{n}) + (k_{02}^{f} + k_{02}^{n})k_{21}\} \times k_{01}^{f} / \{(k_{01}^{f} + k_{01}^{n})\, k_{02}^{f}\, k_{21}\} \tag{20}$$

$$\Phi_{M}/\Phi_{D} = (k_{02}^{f} + k_{02}^{n} + k_{12})\, k_{01}^{f} / (k_{02}^{f}\, k_{21}), \tag{21}$$

and the ratios of the fluorescence yields with quencher, Φ_{M}^{o}/Φ_{D} and Φ_{M}/Φ_{D} are given by replacing the non-radiative rate constants k_{01}^{n} and k_{02}^{n} by $k_{01,q}^{n}$ and $k_{02,q}^{n}$, respectively. Then the ratios of the non-radiative rate constant to the radiative one are derived as follows,

$$k_{02}^{n}/k_{02}^{f} = \{(\Phi_{M}^{o}/\Phi_{D}) - (\Phi_{M}/\Phi_{D})\}/ \Phi_{M}^{o} - 1 \tag{22}$$

$$k_{02,q}^{n}/k_{02}^{f} = \{(\Phi_{M,q}^{o}/\Phi_{D,q}) - (\Phi_{M,q}/\Phi_{D,q})\}/\Phi_{M,q}^{o}-1. \tag{23}$$

Furthermore, Eq. 21 can be rewritten,

$$\Phi_{M}/\Phi_{D} = (k_{01}^{f}/k_{21})\{(k_{02}^{f} + k_{12})/k_{02}^{f} + k_{02}^{n}/k_{02}^{f}\} \tag{24}$$

$$\Phi_{M,q}/\Phi_{D,q} = (k_{01}^{f}/k_{21})\{(k_{02}^{f} + k_{12})/k_{02}^{f} + k_{02,q}^{n}/k_{02}^{f}\}. \tag{25}$$

Using Eqs. 22, 23, 24, and 25, the association rate constant k_{21} is obtained,

$$k_{21} = (k_{02,q}^{n}/k_{02}^{f} - k_{02}^{n}/k_{02}^{f})\, k_{01}^{f} / (\Phi_{M,q}/\Phi_{D,q} - \Phi_{M}/\Phi_{D}). \tag{26}$$

From these equations, the rate constants, k_{01}^{f}, k_{01}^{n}, and k_{21} can be evaluated. However, further assumption is necessary for determination of all rate constants. They assumed that the monomer and excimer fluorescence are equally quenched by the additional quencher. Under such conditions, k_{02}^{f}, k_{02}^{n}, and k_{12} can be determined by steady state measurements.

However, for the intramolecular excimers, especially, for the excimers in polymers, their kinetic treatment is unsuitable, since the effeciency of quenching of the excited monomer fluorescence in polymers must be different from that in the monomeric compounds. The collisional quenching of chromophores is influenced directly by the mutual diffusion of molecules, then the quenching efficiency in polymers seems to be smaller than that in the monomer model compounds. On the other hand, the presence of the delocalization of excited state in polymers should make the quenching more effective than the monomeric compounds. Hence, these kinetic treatments can not be used in the study of polymer systems. In order to determine all rate constants in Fig. 6, time-resolved measurements of the monomer and excimer fluorescence are required.

2-3, 2. Transient Kinetics

In the time-resolved measurements, the chromophores regarded to be excited by a δ-function light pulse. The rate equations are written by the similar forms to Eqs. 1 and 2.

$$d[{}^{1}M^{*}]/dt = k_{12}[{}^{1}D^{*}] - k_{1}[{}^{1}M^{*}] \qquad (27)$$

$$d[^1D^*]/dt = k_{21}[^1M^*][^1M] - k_2[^1D^*] \quad . \qquad (28)$$

Under the initial conditions at t = 0, $[^1M^*] = [^1M^*]_o$, $[^1D^*] = 0$, the equations can be solved as follows,

$$[^1M^*] = [^1M]_o\{(\lambda_2 - k_1)\exp(-\lambda_1 t) + (k_1 - \lambda_1)\exp(-\lambda_2 t)\}/(\lambda_2 - \lambda_1) \qquad (29)$$

$$[^1D^*] = k_{21}[^1M][^1M^*]_o\{\exp(-\lambda_1 t) - \exp(-\lambda_2 t)\}/(\lambda_2 - \lambda_1), \qquad (30)$$

where the parameters, λ_1 and λ_2 are defined,

$$\lambda_{1,2} = \tfrac{1}{2}[k_1 + k_2 \mp \{(k_2 - k_1)^2 + 4k_{21}k_{12}[^1M]\}^{\frac{1}{2}}]. \qquad (31)$$

Then, the response functions for the monomer fluorescence $f_M(t)$ and the excimer one $f_D(t)$ after δ-pulse excitation are derived,

$$f_M(t) = k_{01}^f(\lambda_2 - k_1)\{\exp(-\lambda_1 t) + A\exp(-\lambda_2 t)\}/(\lambda_2 - \lambda_1) \qquad (32)$$

$$f_D(t) = k_{02}^f k_{21}[^1M]\{\exp(-\lambda_1 t) - \exp(-\lambda_2 t)\}/(\lambda_2 - \lambda_1), \qquad (33)$$

where A is defined as, $A = (k_1 - \lambda_1)/(\lambda_2 - k_1)$. Thus, the response functions can be represented by two exponential functions.

In order to indicate the properties of these response functions, we shall consider the typical two conditions. First one is that the rate constants for the association and dissociation processes are sufficiently small compared with the values for k_1 and

k_2, then the following relation is fulfilled,

$$4\, k_{21}\, k_{12}\, [^1M] \,/\, (\, k_1 - k_2\,)^2 \ll 1 \,. \qquad (34)$$

This condition is often satisfied in solution below a critical temperature T_c. λ_1 and λ_2 can be written as,

$$\lambda_1 = k_2 - k_{21}\, k_{12}\, [^1M] \,/\, (k_1 - k_2) \qquad (35)$$

$$\lambda_2 = k_1 - k_{21}\, k_{12}\, [^1M] \,/\, (k_1 - k_2) \,. \qquad (36)$$

If the dissociation rate constant, k_{12} is negligibly small, λ_1 and λ_2 are given approximately,

$$\lambda_1 = k_{02} \,, \qquad \lambda_2 = k_{01} + k_{21}\, [^1M] \,. \qquad (37)$$

Secondly, the condition, $k_{21}[^1M]$, $k_{12} \gg k_{01}$, k_{02}, is satisfied in the intermolecular excimer formation at the high temperature region, then Eq. 31 can be approximated as follows,

$$\lambda_1 = (k_{01} + k_{02})/2 \,, \quad \lambda_2 = k_{12} + k_{21}[^1M] \,. \qquad (38)$$

Since λ_2 takes extremely large value than λ_1 under this condition, the response functions both for the monomer and excimer fluorescence decay exponentially with the same lifetime λ_1^{-1} except for the time range immediately after excitation, as follows,

$$f_M(t),\ f_D(t) \propto \exp\{-(k_{01} + k_{02})t/2\} \,. \qquad (39)$$

The relations are obtained from Eq. 31,

$$\lambda_1 + \lambda_2 = k_1 + k_2 \,, \qquad (40)$$

$$\lambda_1\, \lambda_2 = k_1\, k_2 - k_{21}\, k_{12}\, [^1M] \,. \qquad (41)$$

Equation 40 shows that the association rate constant, k_{21} is evaluated from the measurement of the concentration dependence of $\lambda_{1,2}$, because at all $[^1M]$, the following relation is derived,

$$\partial(\lambda_1 + \lambda_2)/\partial[^1M] = k_{21} \quad . \tag{42}$$

On the other hand, Eq. 41 can be used for Eqs. 7 and 8, and the quantum yields are written as,

$$\Phi_M = k_{01}^f k_2/\lambda_1\lambda_2 \quad , \qquad \Phi_D = k_{02}^f k_{21}[^1M]/\lambda_1\lambda_2 \quad . \tag{43}$$

In the actual time-resolved measurement, the time function of excitation light pulse can not be regarded as δ-function as shown in Figs. 2 and 3. Hence, the observed decay curves of the monomer fluorescence, $I_M(t)$ and excimer one, $I_D(t)$ are given by

$$I_M(t) = \int_o^t p(t')\, f_M(t-t')\, dt' \tag{44}$$

$$I_D(t) = \int_o^t p(t')\, f_D(t-t')\, dt' \quad . \tag{45}$$

where $p(t)$ represents the overall time function of the excitation pulse and the detector. λ_1 and λ_2 are determined so as to fit the calculated $I_M(t)$ or $I_D(t)$ with the observed decay curves. From the data, λ_1, λ_2, Φ_M, and Φ_D, all rate constants shown in Fig. 6 can be determined. The treatment for evaluation of the intramolecular excimer formation processes is somewhat different from the intermolecular one. It will be described in the next chapter on the basis of the data with photostationary and time-resolved measurements for inter- and intramolecular systems.

References

1) Th. Förster and K. Kasper, Z. Phys. Chem. N.F., 1, 275 (1954).
Th. Förster and K. Kasper, Z. Electrochem., 59, 976 (1955).

2) E. Döller and Th. Förster, Z. Phys. Chem. N.F., 34, 132 (1962).
J.B. Birks and L.G. Christophorou, Spectrochim. Acta, 19, 401 (1963).
J.B. Birks, D.J. Dyson, and I.H. Munro, Proc. R. Soc., A275, 575 (1963).
J.B. Birks, M.D. Lumb, and I.H. Munro, Proc. R. Soc., A280, 289 (1964).
Th. Förster and H.P. Seidel, Z. Phys. Chem. N.F., 45, 58 (1965).
R. Speed and B. Selinger, Aust. J. Chem., 22, 9 (1969).
M. Hauser and G. Heidt, Z. Phys. Chem. N.F., 69, 201 (1970).
J.B. Birks, "Photophysics of Aromatic Molecules," Chap. 7, Wiley-Interscience, London, 1970.

3) J.B. Birks and L.G. Christophorou, Proc. R. Soc. A274, 552 (1963).
J.B. Birks and L.G. Christophorou, Nature, 197, 1064 (1963).
J.B. Birks and L.G. Christophorou, Proc. R. Soc., A277, 571 (1964).
B. Stevens and M.I. Ban, Trans. Faraday Soc., 60, 1515 (1964).
J.B. Birks, C.L. Braga, and M.D. Lumb, Proc. R. Soc., A283, 83 (1965).
J.B. Aladekomo and J.B. Birks, Proc. R. Soc.,

A284, 551 (1965).
L. Barnes and J.B. Birks, Proc. R. Soc., A291, 570 (1966).
M.D. Lumb and D.A. Weyl, J. Mol. Spectr., 23, 365 (1967).
4) B.K. Selinger, Aust. J. Chem., 19, 825 (1966).
N. Mataga, M. Tomura, and H. Nishimura, Mol. Phys. 9, 367 (1965).
J.B. Birks and T.A. King, Proc. R. Soc., A291, 244 (1966).
5) J.N. Demas and G.A. Crosby, J. Phys. Chem., 75, 991 (1971).
6) W.H. Melhuish, J. Phys. Chem., 65, 229 (1961).
7) S. Nishimoto and Y. Nishijima, Ann. Rept. Res. Inst. Chem. Fibers, 32, 41 (1975).
8) M. Yamamoto, K. Hirota, and Y. Nishijima, Repts. Progr. Polym. Phys. Japan, 13, 429 (1970).
E.T. Meserve, "Excited States of Proteins and Nucleic Acids," R.F. Steiner and I. Weinryb Eds., Plenum Press, New York, 1971.
9) W. Klöpffer and W. Liptay, Z. Naturforsch, 25a, 1091 (1970).
W. Klöpffer, "Organic Molecular Photophysics," J.B. Birks Ed., Vol. 1, Chap. 7, Wiley-Interscience, London 1973.

CHAPTER 3

Characteristics of the Inter- and Intramolecular Excimers

3-1. Introduction

Naphthalene derivatives are well-known compounds having the ability to form excimers in solution, and show a new broad fluorescence band in a longer wavelength range of the spectra than the ordinary monomer fluorescence. These excimers can be formed not only intermolecularly but also intramolecularly in the molecules having two or more chromophores. For example, polyvinylnaphthalene and its dimeric model compound, 1,3-dinaphthylpropane exhibit high efficiencies of the intramolecular excimer formation.

Excimers are formed by the interaction between an excited state chromophore and a ground state one. It is known that the intermolecular excimer formation process in solution is controlled by the mutual diffusion of chromophores.[1] On the other hand, intramolecular excimers are formed by the interaction between two chromophores attached to one molecule. Therefore, the intramolecular excimer emission relates to the molecular structures and the molecular motion of the compounds. A kinetic study using the time-resolved technique makes possible to determine the individual rate constants of the photophysical processes of the intramolecular excimers as well as the intermolecular excimers.[2] It seems that such quantitative investigation provides significant information for the micro-Brownian motion of molecules and the intramolecular reactions.

In this chapter, the inter- and intramolecular excimer formation processes are analyzed on the basis of photophysical reaction kinetics as mentioned in the previous chapter. 2-Ethylnaphthalene and 1,3-di(2-naphthyl)propane are chosen as the samples which are corresponding to the monomeric and dimeric units of poly(2-vinylnaphthalene), respectively. Individual rate constants of the photophysical processes can be determined by the measurements in photostationary and transient conditions. From these kinetic analysis, the characteristics of inter- and intramolecular excimers are clarified.

3-2. Experimental

1,3-Di(2-naphthyl)propane (1,3-DNPr) was prepared by the same method of Chandross.[3] 1,3-di(2-naphthyl)-2-propen-1-one was obtained by condensation of 2-naphthaldehyde and 2-acetonaphthone in an alkaline ethanol solution. After recrystallization from chloroform, the product was reduced in acetic acid solution by addition of zinc dust and refluxing for a few minutes. The mixture was filtered and the filtrate was extracted with dichloromethane. After removing the solvent, the residue was recrystallized from carbon tetrachloride to give colorless crystals of 1,3-di(2-naphthyl)-1-propanone. The ketone was reduced by Wolff-Kishner reduction. The reaction mixture was extracted with benzene. After removing the solvent, the product was chromatographed on silica gel with hexane-dichlomethane (5:1): mp 104-105 $^{\circ}$C; IR(KBr) 3050, 2950, 2850, 1630, 1600, 1510, 1460, 815, 740, and 480 cm^{-1}; NMR(CS_2) δ= 1.90-2.25 (2H, m), 2.77 (4H, t, J=7.2Hz), and 7.10-

7.74 (14H, m). Found: C, 93.01; H, 6.99%. Calcd for $C_{23}H_{20}$: C, 93.20; H, 6.80%.

2-Ethylnaphthalene(MNEt) (Aldrich Chemical Co. Inc.) was used as a monomeric compound without further purification.

Solutions of these samples were prepared in 2MTHF and deaerated. Procedures for measuring fluorescence spectra, quantum yields, and decay curves were described in Chapter 2.

3-3. Results and Discussion

3-3, 1. Photophysical Behavior of the Intermolecular Excimer

Fluoresence spectra for MNEt at various concentrations were measured. Figure 1 shows the spectra at -80 °C. The absorption spectra do not show any appreciable change with concentration, whereas the fluorescence spectra show marked change at high concentrations. In the solutions of high concentrations, the normal fluorescence at 320-340 nm decreases and a broad new emission band appears in the longer wavelength range. The structured shorter wavelength band and the broad longer wavelength band are assigned, respectively, to the monomer fluorescence from non-associated excited state chromophores and to the excimer fluorescence from excited state chromophores interacting with another chromophores in the ground state. In the spectra, the contributions from the monomor and excimer fluorescence at a wavelength were estimated by the spectra for dilute solution of MNEt at the same temperature. The areas below the spectral curves give the fluorescence intensities proportional to the

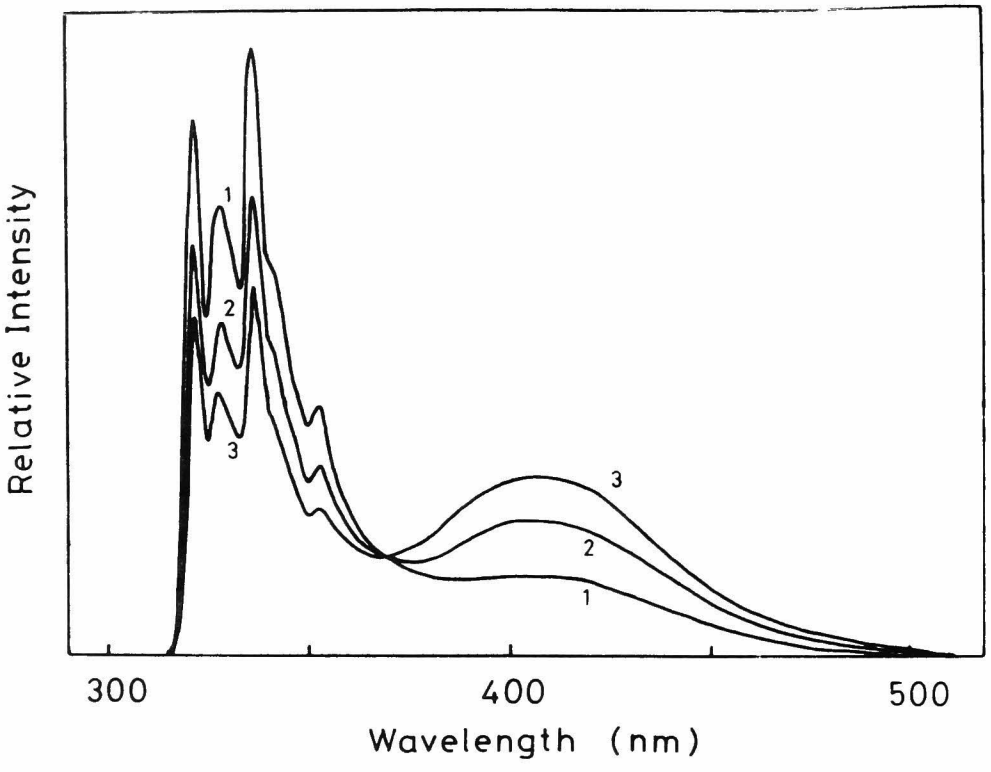

Fig. 1. Fluorescence spectra of MNEt in 2MTHF at -80 °C. Concentrations of MNEt: (1) 5.8×10^{-2} mol/l, (2) 1.2×10^{-1} mol/l, (3) 2.0×10^{-1} mol/l.

quantum yields.

The quantum yields of the monomer fluorescence (Φ_M) and excimer fluorescence (Φ_D) for MNEt solution at various temperatures are shown in Fig. 2. At the low temperature region below -100 °C, the quantum yields, Φ_M for the concentrated solutions give the similar values as that for dilute solution of MNEt which show no excimer fluorescence. At the liquid nitrogen temperature, all of the samples show no excimer emission. This indicates that the excited naphthalene chromophore during its lifetime can not encounter with another molecule of the same kind in the ground state, since the molecular motions are suppressed. As the temperature increases, translational diffusion of molecules takes place so sufficiently that excimers become to be formed. There, Φ_M decreases while Φ_D increases with rise in temperature, and Φ_D takes a maximum value at -80 °C. At temperatures above -80 °C, Φ_D decreases monotonously accompanied by the increasing of Φ_M. This shows that the dissociation process of the excimer before its emission becomes predominant. The logarithms of the quantum yield ratio, Φ_D/Φ_M are plotted against the reciprocal of the temperature in Fig. 3. From the slope in the low temperature region, the activation energy, E_a for the excimer formation rate constant, k_{21} can be estimated according to Eq. 2-10. From the slope in the high temperature region, the enthalpy change of the excimer formation, ΔH and the activation energy for the dissociation process of the excimer, E_d can be estimated according to Eq. 2-11. The values of E_a and ΔH are independent of the concentration, and found

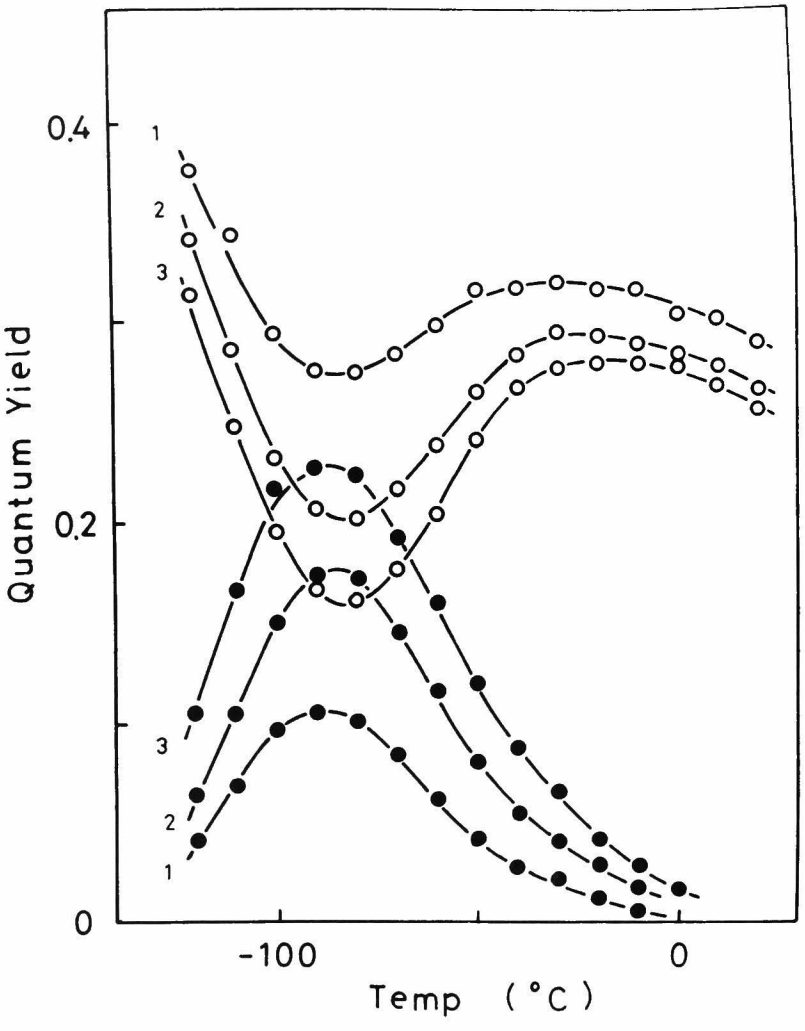

Fig. 2. Temperature dependence of the fluorescence quantum yields. ○ : monomer fluorescence yield, Φ_M. ● : excimer fluorescence yield, Φ_D. Concentrations of MNEt: (1) 5.8 x 10^{-2} mol/l, (2) 1.2 x 10^{-1} mol/l, (3) 2.0 x 10^{-1} mol/l.

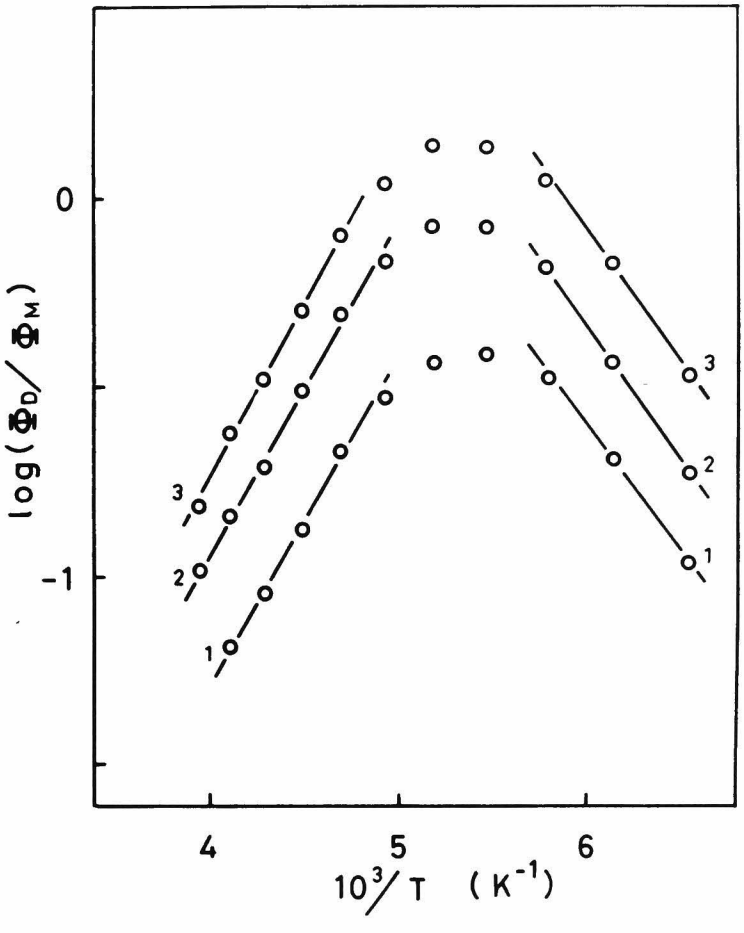

Fig. 3. The logarithm plot of the quantum yield ratio, Φ_D/Φ_M against the reciprocal of temperature. Concentrations of MNEt: (1) 5.8 x 10^{-2} mol/l, (2) 1.2 x 10^{-1} mol /l, (3) 2.0 x 10^{-1} mol/l.

to be: E_a=3.4 kcal/mol, ΔH=4.3 kcal/mol, and E_d=7.7 kcal/mol.

In order to determine the rate costants, time-resolved measurement was carried out. Rise and Decay curves of the excimer emission at various temperatures were measured. The observed curves can be analyzed by two exponential functions according to Eq. 2-30, and the parameters, λ_1 and λ_2 are determined. At the temperatures above -50 ^{o}C, the rise component, λ_2 can not be determined, since the excimers are formed within much shorter time than the resolving time scale of this experiments. The sums of λ_1 and λ_2 are plotted against the concentration of MNEt at various temperatures in Fig. 4. According to Eq. 2-42, the slope (α) of each line in Fig. 4 gives the association rate constant, k_{21}, and the extrapolated values (β) to the concentration [M]=0, give the sums of other rate constants except k_{21}.

$$\alpha = k_{21}, \quad \beta = k_{01} + k_2, \tag{1}$$

where $k_2=k_{02}+k_{12}$. The rate constant, k_{01} is obtained by the measurement of lifetime (τ_M) for dilute solution of MNEt. Then, the rate, k_2 can be evaluated. On the other hand, Eq. 2-9 indicates that the ratio, Φ_D/Φ_M should be proportional to the concentration [M]. This plots were shown in Fig. 5. The slope (γ) in Fig 5 is given as follows

$$\gamma = k_{02}^{f} \cdot k_{21} / (k_{01}^{f} \cdot k_2) \tag{2}$$

The rate constants, k_{21} and k_2 are already known, then the ratios of radiative rate constants, k_{02}^{f}/k_{01}^{f} is

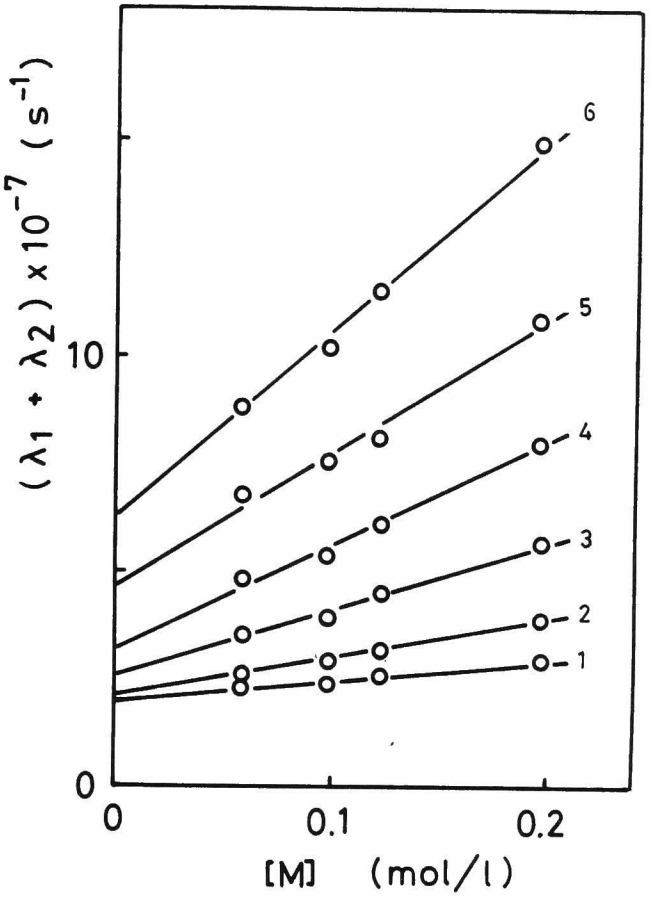

Fig. 4. Concentration dependence of the sums of λ_1 and λ_2 at various temperatures: (1) -110 °C, (2) -100 °C, (3) -90 °C, (4) -80 °C, (5) -70 °C, (6) -60 °C.

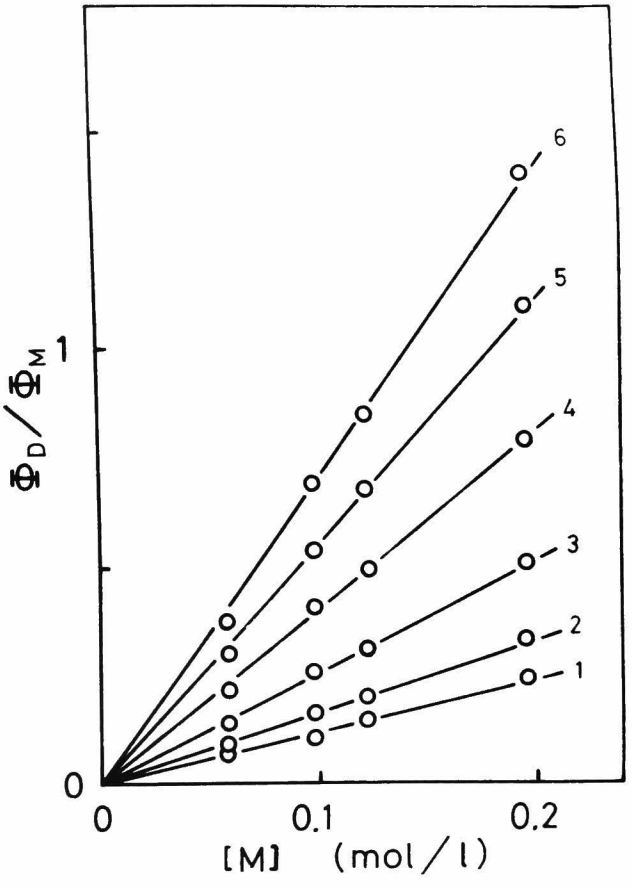

Fig. 5. Concentration dependence of the quantum yield ratio, Φ_D/Φ_M at various temperatures: (1) -30 °C, (2) -40 °C, (3) -50 °C, (4) -60 °C, (5) -70 °C, (6) -80 °C.

obtained from this slope. The value of this ratio is found to be ca. 0.5, and it is independent of temperature in the range of measurements. Assuming that the ratio of the radiative rate constants k^f_{02}/k^f_{01}, maintains the constant value even in high temperature region, k_2 can be estimated from the slope γ, in the steady state measurement. It has been known that the radiative rate constant is almost independent of temperature, and the constancy is confirmed in the measurements of lifetime and quantum yield in dilute solution on MNEt.

$$\tau_M = (k^f_{01} + k^n_{01})^{-1} = 1/k_{01}, \quad \Phi_M = k^f_{01}/k_{01}, \qquad (3)$$

then, $k^f_{01} = \Phi_M/\tau_M$. The radiative rate constant, k^f_{01} is found to be 0.40×10^7 s^{-1} in the temperature range of measurement. The rate constant k^f_{02}, are obtained: 0.20×10^7 s^{-1}. All of these values estimated at various temperatures are listed in Table 1. It is shown that the temperature dependence of Φ_M and τ_M of the dilute solution of MNEt are due to the change of radiationless transition rate, and the radiative transition rate, k^f_{01} is independent of temperature. The rate constants, k_{12} and k_2 are plotted against the reciprocal of the temperature in Fig. 6. The thermally activated process in k_2 is mainly the dissociation rate, k_{12}. The lines in Fig. 6 give the temperature dependence of the association and dissociation rate constants, and their activation energies, E_a and E_d are given: E_a = 3.2 kcal/mol, E_d = 7.7 kcal/mol. They are consistent with the value obtained by the plots in Fig. 3. The rates, k_{21} and k_{12} are formulated as follows,

Table 1. Fluorescence properties of the concentrated solutions of 2-ethylnaphthalene at various temperatures.

Temp. (°C)	$\alpha \cdot 10^{-7}$(l/mol·s)	$\beta \cdot 10^{-7}(s^{-1})$	Φ_M*	τ_M(ns)*	$k_{01}^f \cdot 10^{-7}(s^{-1})$	γ (l/mol)	k_{02}^f/k_{01}^f	$k_2 \cdot 10^{-7}(s^{-1})$**
-20	-	-	0.25	63	0.40	0.82	-	98.
-30	-	-	0.25	64	0.40	1.2	-	52.
-40	-	-	0.26	66	0.39	1.7	-	29.
-50	-	-	0.27	67	0.40	2.6	-	14.
-60	43.	6.3	0.27	68	0.40	4.1	0.46	5.2
-70	32.	4.6	0.28	70	0.40	5.5	0.54	2.9
-80	24.	3.2	0.29	71	0.41	6.9	0.51	1.7
-90	16.	2.6	0.30	73	0.42	6.8	0.53	1.1
-100	8.8	2.2	0.31	74	0.42	5.5	0.50	0.80
-110	4.9	2.0	0.33	76	0.43	3.4	0.47	0.72

* This value is obtained for the dilute solution of 2-ethylnaphthalene.

** This value is estimated from γ using the relation, $k_{02}^f/k_{01}^f = 0.5$.

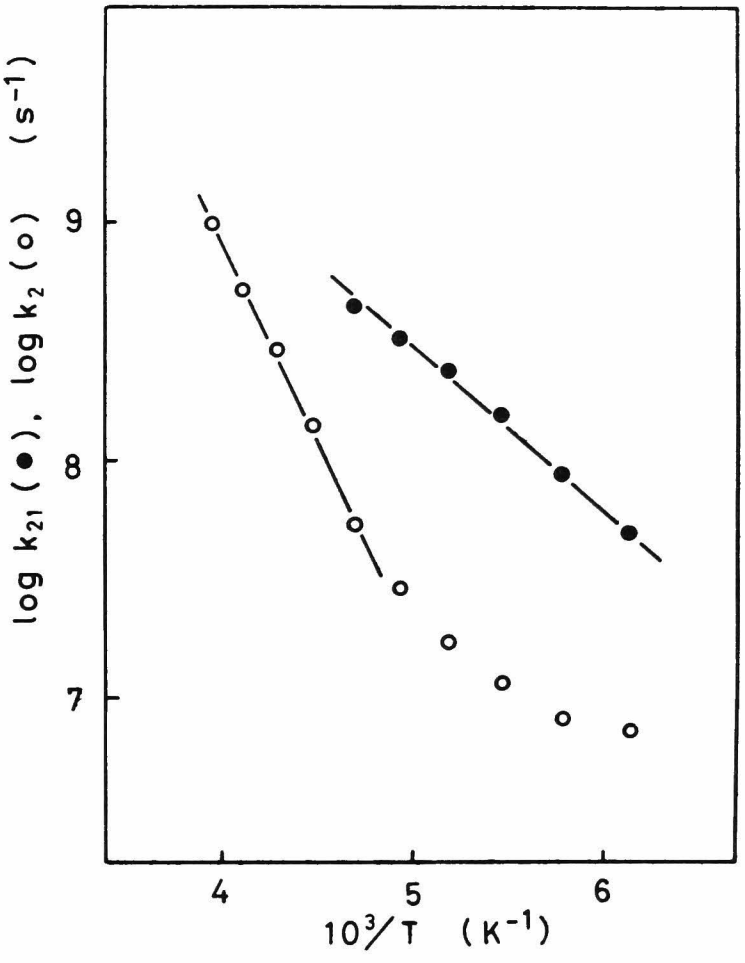

Fig. 6. Arrhenius plots of k_{21} and k_2 for the intermolecular excimer of MNEt.
● : k_{21}, ○ : k_2.

Table 2. Thermodynamic and kinetic data for 2-ethylnaphthalene

k^f_{01} /s^{-1}	0.40×10^7
k^f_{02} /s^{-1}	0.20×10^7
E_a /kcal mol^{-1}	3.2
E_d /kcal mol^{-1}	7.7
N_a /l $mol^{-1}s^{-1}$	9.4×10^{11}
N_d / s^{-1}	4.4×10^{15}
ΔH /kcal mol^{-1}	- 4.5
ΔS /cal $mol^{-1}deg^{-1}$	- 17

$$k_{21} = 9.4 \times 10^{11} \exp(-3200/RT) ,$$

$$k_{12} = 4.4 \times 10^{15} \exp(-7700/RT) .$$

From the ratio, k_{21}/k_{12}, the entropy change ΔS for the excimer formation can be evaluated : ΔS = -17 cal/(mol deg). The results are summarized in Table 2.

3-3, 2. Photophysical Behavior of the Intramolecular Excimer

Absorption spectra for 1,3-DNPr are identical to that for MNEt. Fluorescence spectra consist of two emission bands, which are the same as the concentrated solutions of MNEt. This shows that the excited electronic states of the naphthalene units of these samples are very much alike. The quantum yields of the monomer fluorescence and excimer fluorescence for the dilute solution of 1,3-DNPr are shown in Fig. 7. The behavior for changing the temperature from extremely low region are similar to that for the intermolecular excimers. In this case, the excimer is not formed by the interaction between different molecules, since the concentration of 1,3-DNPr was about 1×10^{-4} mol/l. The naphthalene groups in the same molecule. As the temperature increases, the intramolecular excimer is formed efficiently and the monomer fluorescesce is quenched. The remarkable change of Φ_D and Φ_M with the temperature is caused by the change of the internal rotation of the part attached to chromophores. Since the total quantum yields, $\Phi_D+\Phi_M$ diminish with the excimer formation, the excitation energy dissipates radiationlessly on the process pathing through the excimer state.

The kinetic scheme for intramolecular excimers are considered as shown in Fig. 8, which is the same as that for the intermolecular one except for the rate constant, k_{21}. This is a pseudo-first order rate constant for the intramolecular excimers. If the dissociation of the excimer and its quenching rates are small compared to the rate of excimer emission,

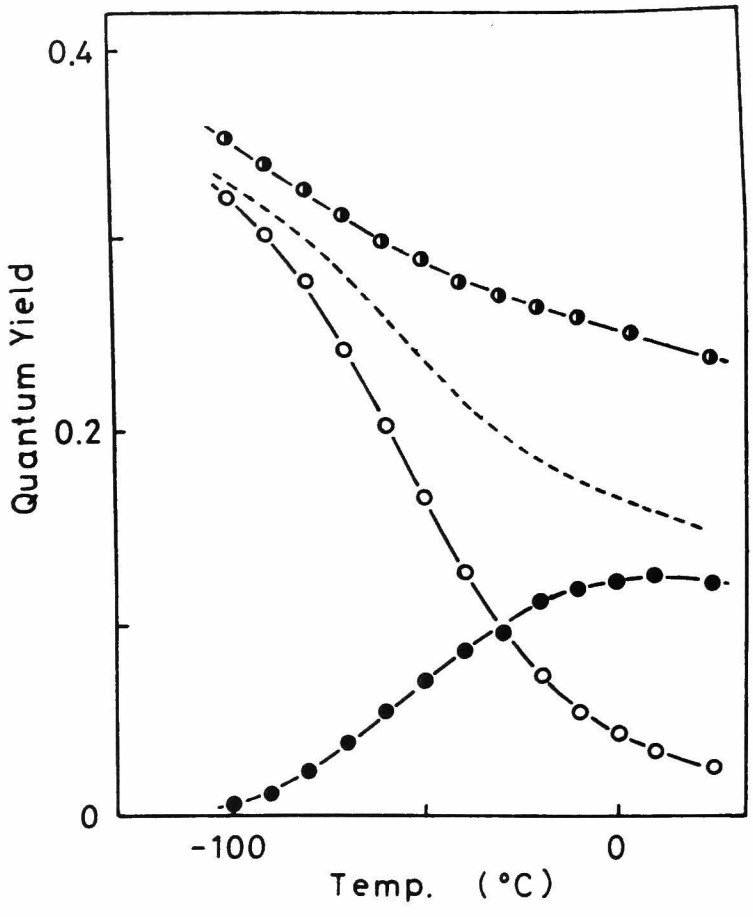

Fig. 7. Temperature dependence of the fluorescence quantum yields. ◑ : monomer fluorescence yield of the dilute solution of MNEt. ○ : monomer fluorescence yield of 1,3-DNPr. ● : excimer fluorescence yield of 1,3-DNPr. The broken line represents the total quantum yield, $\Phi_M + \Phi_D$ of 1,3-DNPr.

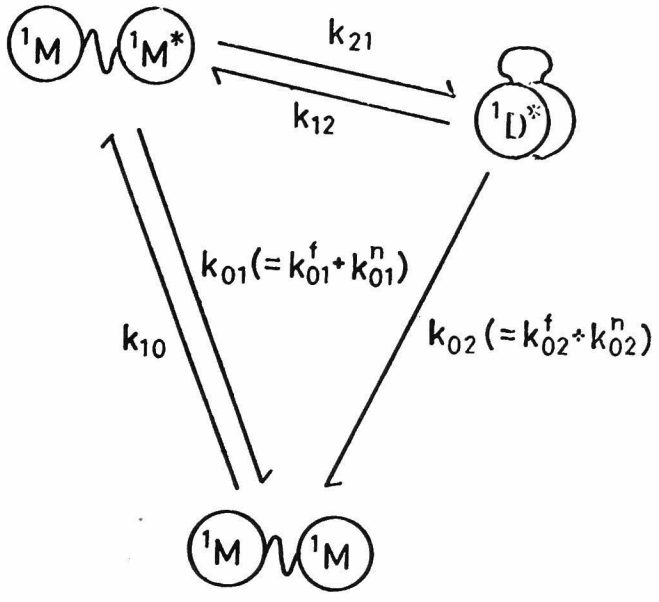

Fig. 8. Kinetic scheme of the energy dissipation processes in the intramolecular excimer system.

or independent of the temperature, the activation energy for excimer formation can be obtained by the photostationary measurements using Eq. 2-10. The activation energy, E_a=4.8 kcal/mol was obtained for 1,3-DNPr. This value is larger than that for the intermolecular excimer formation of MNEt, 3.4 kcal/mol, and the value, 2.8 kcal/mol for 2-methylnaphthalene in ethanol solution reported by Selinger.[4)]

The behavior in the high temperature region in

Fig. 7 are quite different between inter- and intramolecular excimers. In the case of 1,3-DNPr, the Φ_D curve has a maximum at a higher temperature than the case of MNEt, ca. 10 ^{o}C, and Φ_M decreases monotonously. In the case of MNEt, the intermolecular excimer is formed efficiently in low temperature region, and the Φ_D becomes the maximum at -80 ^{o}C, which is much lower than that for 1,3-DNPr. Above this temperature, the Φ_M increases temporarily. These phenomena will be discussed on the basis of the rate constants.

The measurements of the quantum yields and decay curves as a function of the concentration, were carried out for the determination of the rate constants of the intermolecular excimer formation processes. But, in the case of the intramolecular excimers, the rate constants of excimer formation can not be determined by the concentration dependence. However, in the dilute solution, quantum yields are determined more accurately than those for the concentrated solution, since the effects of the depth of penetration of excitation light and the reabsorption can be negligible. From the rise and decay curves of the excimer emission at various temperatures, λ_1 and λ_2 are obtained. As mentioned previously, the rate constants, k_{01}^{f} and k_{01} ($= k_{01}^{f} + k_{01}^{n}$) are determined by the measurements of the dilute solution of MNEt. According to Eq. 2-43, the rate constant k_2 is given by,

$$k_2 = \lambda_1 \cdot \lambda_2 \cdot \Phi_M / k_{01}^{f} \quad . \qquad (4)$$

From λ_1, λ_2, and k_2, the rate constant, k_1 is obtained as follows,

$$k_1 = \lambda_1 + \lambda_2 - k_2 \quad , \tag{5}$$

and k_{21} is determined by Eq. 2-5. Equation 2-43 is rewritten as follows for intramolecular excimers,

$$\Phi_D = k_{02}^f \cdot k_{21} / (\lambda_1 \cdot \lambda_2) \quad . \tag{6}$$

Then, k_{02}^f is obtained. The relation of Eq. 2-41 is used for the determination of the dissociation rate constant, k_{12},

$$\lambda_1 \cdot \lambda_2 = k_1 \cdot k_2 - k_{21} \cdot k_{12} \quad . \tag{7}$$

In this equation, λ_1, λ_2, k_1, k_2, and k_{21} are known

Table 3. Rate constants for 1,3-DNPr at various temperatures

Temp. (°C)	k_{01}^f	k_{01}^n	k_{21}	k_{12}	k_{02}^f	k_{02}^n
25	0.40	1.3	26.	0.86	0.16	1.0
0	0.40	1.3	12.	0.54	0.16	0.94
-20	0.40	1.2	5.5	0.37	0.17	0.92
-40	0.39	1.1	2.0	0.17	0.17	0.91
-60	0.40	1.1	0.7	0.05	0.18	0.91

already. The last rate constant, k_{02}^{n} is derived easely from Eqs. 2-5 and 2-6. The results at various temperatures are listed in Table 3. A marked temperature dependence in these rate constants in found only for the association rate, k_{21}, and others show a little change with temperature. The dissociation rate constant k_{12} is found to be very small values in the observed range of temperature. Then, the thermodynamic properties, ΔH, ΔS, and E_d concerned with this dissociation process in the high temperature region, can

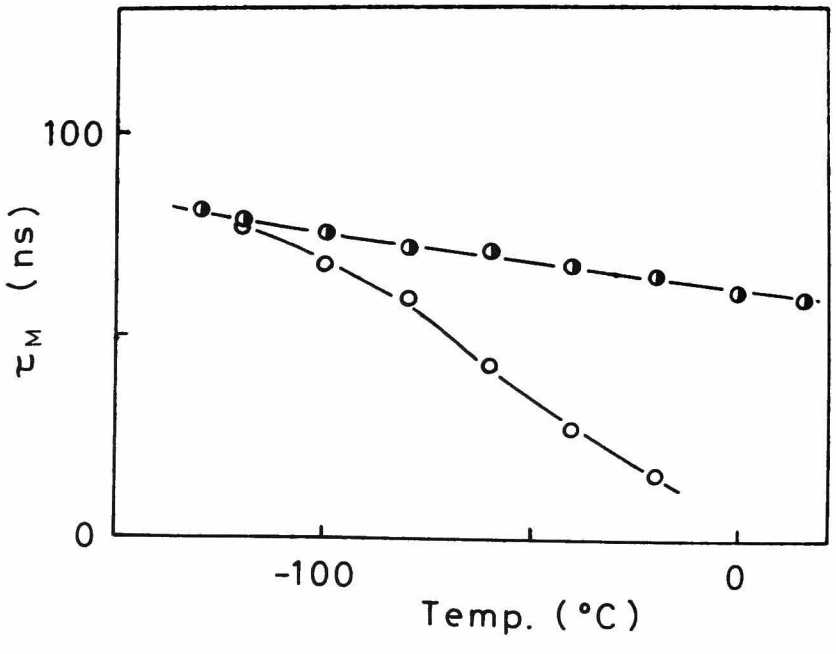

Fig. 9. Temperature dependence of the monomer fluorescence lifetime. ◑: MNEt, ○: 1,3-DNPr.

not be obtained in the case of the intramolecular excimers. Since the dissociation rate is sufficiently small, the decay curves of the monomer fluorescence, $I_M(t)$ for 1,3-DNPr can be approximated by single exponential function, $\exp(-t/\tau_M)$. The temperature dependence of the τ_M is shown in Fig. 9, and the value at a temperature is consistent with the rise component, λ_2 of the excimer emission. Arrhenius plot of the rate constant, k_{21} gives the activation energy for the intramolecular excimer formation process, E_a: 5.4 kcal /mol. Then, the rate is rewritten as follows,

$$k_{21} = 2.3 \times 10^{12} \exp(-5400 / RT) .$$

3-3. 3. Comparison of the Rate Constants for Inter- and Intramolecular Excimers

On the process determining the rate constants for the intramolecular excimers, the values of k_{01}^f and k_{01}^n for the dilute solution of MNEt, were used. This assumption can be justified by the following experimental facts. First, 1,5-dinaphthylpentane which shows no excimer fluorescence, gives the same rate constants as that for MNEt. Secondly, in the measurements at low temperatures, the intramolecular excimer is hardly observed, since the molecular motion are suppressed. In such condition, the Φ_M and τ_M for 1,3-DNPr become close to those for MNEt. This behavior can be expected in the Eq. 2-7, where Φ_M is approximated by k_{01}^f/k_{01}, if k_{21} becomes sufficiently small. From these facts, the rate constants, k_{01}^f and k_{01}^n for the dilute solution of MNEt were used in the analysis of the intramolecular excimer formation. The radiative rate constant of the excimer state, k_{02}^f are obtained the same value

both in the inter- and intramolecular excimers. This indicates that the electronic states of the excimers are much alike each other. The total quantum yield diminishes with increasing the excimer formation as shown in Fig. 7, since the quantum efficiency of the intramolecular excimer emission, k_{02}^f/k_{02} is smaller than that of the excited monomer state, k_{01}^f/k_{01}.

The photophysical behavior of the intramolecular excimer is characterized with the association and dissociation rate constants. The intermolecular excimer formation is governed by the mutual diffusion of the naphthalene chromophores. The rate constant for the association process k_{21} should be given using the Einstein-Smoluchowski and Stokes-Einstein equations for diffusion-controlled processes,

$$k_{21} = (8RT/3000\eta)(p\ a/b) \qquad (8)$$

where η is the solvent viscosity, a is the interaction radii, b is the Stokes' radii of chromophore, and p is the reaction probability per collision. For 2MTHF solution at 0 °C, Eq. 8 yields a value of 1.0×10^{10} l/(mol·s), if $p \cdot a/b = 1$. The observed value of k_{21} at 0 °C is 0.25×10^{10} l/(mol·s). This shows that $p = 0.25$ in Eq. 8, at 0 °C. The activation energy of the association rate constant is predicted by the Eq. 8 as follows,

$$k_{21} \propto \exp (-W\eta / RT) \qquad (9)$$

where $W\eta$ is the activation energy of the solvent viscosity. For 2MTHF, $W\eta$ is reported to be 1.8 kcal/mol.[5] The observed value of E_a is 3.2 kcal/mol. In the

study of pyrene solution,[1] the observed values were consistent with the theoretical values in various solvents. The difference between pyrene and naphthalene derivatives may be attributed to the difference in binding energy of the excimers: 10 kcal/mol for pyrene, 5 kcal/mol for naphthalene. These facts indicate that the steric condition necessary for excimer formation is more strict in the case of naphthalene chromophore than in the case of pyrene chromophre.

It is interesting to compare the association rate constants of 1,3-DNPr with those for intermolecular excimer formation in MNEt. Since the k_{21} for 1,3-DNPr is a pseudo-first order rate constant, effective concentrations of naphthalene units of 1,3-DNPr can be calculated by the relation, $C_{eff} = k_{21}^{intra} / k_{21}^{inter}$. This effective concentrations at various temperatures, are found between one hundredth and tenth of the apparent concentration that is calculated by using equilibrium distance between two naphthalene unit of 1,3-DNPr in the ground state. This reflects that the motion of naphthalene units is depressed by the methlene chain. The activation energies of k_{21} are interpreted in the same way. The activation energy for MNEt was found to be 3.2 kcal/mol, which is smaller than that of 1,3-DNPr. The larger activation energy of intramolecular excimer formation indicates that the methylene chain forces the molecule to take a higher energy conformation in the excimer formation process in which the conformational change is needed to take parallel sandwich geometry from the stable ground state conformation. The dissociation rate constant, k_{12} for 1,3-DNPr is much smaller than that for MNEt. The

temperature dependence above -80 °C for MNEt in Fig. 2 are attributed to the large dissociation rate of MNEt. In the case of the intramolecular excimer, the dissociaton process is depressed by the methylene chain restriction. Hence, the Φ_D's increase with increasing temperature until much higher temperature range. The differences of the k_{21} and k_{12} between 1,3-DNPr and MNEt lead to the emission properties of Φ_M and Φ_D as shown in Figs. 2 and 7.

From these results, it is clear that the characteristics of intramolecular excimers exist in the association and dissociation processes, which are controlled by the internal ratotion of the methylene chain. Then, it can be expected that the information of the micro-Brownian motion of molecules is given by the quantitative study of these rate constants of intramolecular excimers.

References

1) J.B. Birks, D.J. Dyson, and I.H. Munro, Proc. R. Soc., A275, 575 (1963).
J.B. Birks, M.D. Lumb, and I.H. Munro, Proc. R. Soc., A280, 289 (1964).
2) G.E. Johnson, J. Chem. Phys., 61, 3002 (1974).
P.A. Avouris, J. Kordas, and M.A. El-Bayoumi, Chem. Phys. Lett., 26, 373 (1974).
Y. Nishijima, Y. Sasaki, and M. Yamamoto, Repts. Progr. Polym. Phys. Japan, 16, 505 (1973).
K. Hirota, M. Yamamoto, and Y. Nishijima, Repts. Progr. Polym. Phys. Japan, 16, 509 (1973).
S. Ito, M.Yamamoto. and Y. Nishijima, Repts. Progr.

Polym. Phys. Japan, 19, 421 (1976).
3) E.A. Chandross and C.J. Dempster, J. Am. Chem. Soc., 92, 3586 (1970).
4) B.K. Selinger, Aust. J. Chem., 19, 825 (1966).
5) M. Szwarc,"Carbanions Living Polymers and Election Transfer Processes," Interscience, New York, 1968.

CHAPTER 4

Geometrical Requirements for Intramolecular Excimer Formation

4-1. Introduction

In the previous chapter, the characteristics of the intramolecular excimers were discussed in comparison with the intermolecular excimers. The compound, 1,3-DNPr was used as a typical compound which corresponds the dimeric model of vinyl polymers. The photophysical properties were interpreted by the binding effect of the methylene chain whose internal rotations control the excimer formation and dissociation processes. The characteristics observed for 1,3-DNPr are common to the compounds satisfying the n=3 rule such as 1,3-diarylpropanes.[1-6] It is due to the existence of the favorable conformations for the formation of the stable excimers without any appreciable instabilities of the methylene chains. But, in general, almost all compounds having the molecular structure except for n=3 do not show such high efficient formation of stable excimers,[1,3] and in this view point, it can be said that the diarylpropane is one of the specific compounds forming the intramolecular excimers.

The geometrical arrangement of interacting chromophores in a given compound seems to be related to the following two factors: (a) the binding energies in the excited state at various arrangements of

two chromophores, and (b) the chain instabilities at those conformations. The former problem (a), has been studied theoretically and experimentally by many workers. The binding energies calculated by the semi-empirical molecular orbital theory predict various minima on the potential maps as a function of the distance and angles of aromatic planes.[7-10] It has been said that the sandwich parallel conformation is the most stable one and the distance between aromatic rings is estimated to be 3.2 - 3.8 Å. Experimentally, the investigations of this problem have been carried out by measuring absorption and fluorescence properties of crystals of aromatic compounds[11] and various compounds in which two chromophores are fixed by a rigid link.[12-18] The typical experiments for paracyclophane indicated that the normal excimer emission are observed for (4,4)-paracyclophane whose distance between the aromatic planes is calculated to be 3.7 Å.

The latter problem (b), has been discussed using a number of experimental results for various dimeric compounds. One of the well known results is the Hirayama's n=3 rule which was confirmed with diphenyl- and triphenylalkanes.[1] Thereafter, it has been said that the n=3 rule holds for the other kind of chromophores such as dinaphthylalkanes[3] and dicarbazolylalkanes.[2,4] This shows that the parallel sandwich arrangement is the stable excimer conformation and compounds other than n=3 can not achieve the parallel conformation because of the instability of the methylene chain. However, the intramolecular excimer emission was observed for various α,ω-di-

pyrenylalkanes, Py-$(CH_2)_n$-Py (n=2-22).[19] The results indicate that pyrene excimer has the large binding energy enough to overcome the geometrical disadvantages, together with the long enough lifetime to achieve the encounters of the terminal chromophores.

The ability of the intramolecular excimer formation is thus based on the equlibrium between the binding energy of chromophores and the instability of backbone chain at the excimer conformation. Then, the configurational requirements for the excimer formation are different in each chromophore, although the compound, n=3 gives the most stable intramolecular excimers.

In this chapter, requirements of molecular configuration for excimer formation of naphthalene chromophores are discussed on the basis of the photophysical properties of the various naphthalene derivatives. First, the n=3 rule is examined for α,ω-dinaphthylalkanes up to n=12. Corresponding dipyrenylalkanes having the same number of carbons show the efficient excimer formation. Next, the emission behavior of unstable excimers are reported. The molecular structures are close to the sandwich arrangement, but their axes of naphthalene units are not parallel because of the structural restraint. It is interesting to measure the photophysical properties of such compounds, because they seem to give the information about the geometrical limits of fluorescent excimer formation and the arrangement of chromophores at the stable excimer state.

4-2. Experimental

Preparation of 1,3-di(2-naphthyl)propane (1,3-DNPr) was described in Chapter 3. 1-Ethylnaphthalene (α-MNEt) and 2-ethylnaphthalene (β-MNEt) were used as a monomeric compound without further purification. The other samples were prepared by the following methods.

1,5-Di(2-naphthyl)pentane (1,5-DNPe): the mixture of 2-naphthaldehyde (0.1 mol) and acetone (0.05 mol) in ethanol (200 ml) was added to the ethanol solution of sodium hydroxide (30 g). After stirring at room temperature for an hour, the insoluble yellow product was filtered and washed with water. Then, the product was recrystallized from benzene-chloroform, and gave yellow crystalline 1,5-dinaphthyl-1,4-pentadien-3-one: mp 241-243 °C. This was reduced with zinc dust in acetic acid using the same procedure as that for 1,3-DNPr. The extracted product was crystallized from ethanol and gave the colorless crystalline 1,5-dinaphthyl-3-pentanone: mp 126-127 °C; IR(KBr) 3050, 2950, 1685, 1600, 825, 735, and 470 cm^{-1}. Found: C, 88.98; H, 6.50; O, 4.93%. Calcd for $C_{25}H_{22}O$: C, 88.72; H, 6.55; O, 4.73%.

The ketone was reduced with hydrazine and sodium hydroxide in triethylene glycol. The reaction mixture was extracted with benzene and washed several times. The residue was purified by chromatography on silica gel with benzene-hexane (1:9) as eluent. The colorless crystal of 1,5-DNPe was obtained by recrystallization from ethanol: mp 92-93 °C; IR(KBr) 3050, 2950, 2850, 1600, 820, 740, and

480 cm^{-1}; NMR(CS_2) δ= 1.3-1.9 (3H, m), 2.71 (2H, t, J= 7Hz), and 7.1-7.7 (7H, m). Found: C, 92.53; H, 7.59%. Calcd for $C_{25}H_{24}$: C, 92.54; H, 7.46%.

1,7-Di(2-naphthyl)heptane (1,7-DNHp): The dry ether solution of 1,5-dibromopentane (8g) was added dropwise to the stirred magnesium (2.5 g) in dry ether (25 ml). After refluxing for an hour, the tetrahydrofuran solution (50 ml) of 2-naphthonitrile (10 g) was added dropwise. The solution was refluxed for 4 hours with removing the ether from the reaction mixture. After cooling the mixture in an ice bath, 6 N hydrochloric acid (80 ml) was added, and the solution was refluxed for 7 hours with removing the tetrahydrofuran. The reaction mixture was extracted with dichloromethane and washed with water. The product was purified by column chromatography on silica gel with dichloromethane and recrystallized from ethanol. The colorless crystalline 1,5-di-(2-naphthoyl)pentane was obtained: mp 119-120 °C; IR(KBr) 3050, 2950, 1680, 1625, 810, 740, and 490 cm^{-1}.

The ketone was reduced by the same method as for 1,5-DNPe. The product was purified by column chromatography on silica gel and recrystallized from methanol. The colorless crystalline 1,7-DNHp was obtained: mp 78-79 °C; IR(KBr) 3050, 2930, 2850, 1600, 820, 740, and 480 cm^{-1}; NMR(CS_2) δ= 1.2-1.5 (3H, m), 1.5-1.8 (2H, m), 2.70 (2H, t, J= 7Hz), and 7.1-7.7 (7H, m). Found: C, 91.86; H, 8.00%. Calcd for $C_{27}H_{28}$; C, 91.99; H, 8.01%.

1,12-Di(2-naphthyl)dodecane (1,12-DNDd): This

compound was prepared by the same method as that for 1,7-DNHp. 1,10-Dibromodecane was used instead of 1,5-dibromopentane. The product was crystallized from ethanol, and gave the colorless crystalline 1,12-DNDd: mp 93-94 °C; IR(KBr) 3050, 2910, 2850, 1600, 820, 740, and 480 cm^{-1}; NMR(CS_2) δ= 1.15-1.48 (8H, m), 1.48-1.84 (2H, m), 2.70 (2H, t, J= 7Hz), and 7.1-7.7 (7H, m). Found: C, 90.48; H, 9.15%. Calcd for $C_{32}H_{38}$: c, 90.94; H, 9.06%.

1-(1-naphthyl)-3-(2-naphthyl)propane (αβ-DNPr): An alkaline ethanol solution was added to the equimolar mixture of 1-naphthaldehyde and 2-acetonaphthone in ethanol, and the solution was stirred for an hour. The product was reduced to αβ-DNPr by the same procedure as that for 1,3-DNPr. The final product was recrystallized from hexane and gave the colorless crystalline αβ-DNPr: mp 61-62 °C; IR(KBr) 3050, 2940, 1595, 1505, 820, 780, and 475 cm^{-1}; NMR (CS_2) δ= 2.08 (1H, q, J= 8Hz), 2.70-3.14 (2H, m), and 7.1-7.9 (7H, m). Found: C, 93.44; H, 6.78%. Calcd for $C_{23}H_{20}$: C, 93.20, H, 6.80%.

Trans-1,2-di(2-naphthyl)cyclobutane (trans-DNCb) and cis-1,2-di(2-naphthyl)cyclobutane (cis-DNCb) were prepared by the photo-dimerization of 2-vinylnaphthalene. The benzene solution of 2-vinylnaphthalene (0.6 mol/l) was degassed in a pyrex tube, and irradiated by a high pressure mercury lamp for 20 hours. The products were fractionated by column chromatography on silica gel with hexane-dichloromethane (7:1) as eluent. The detailed procedures were referred to the literature.[20)]

trans-DNCb: mp 106-107 °C; NMR(CCl_4) δ= 2.2-2.5

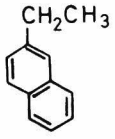

β-MNEt

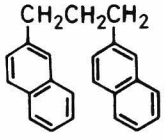

1,3-DNPr

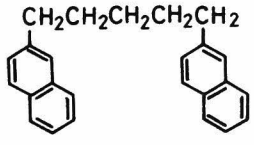

1,5-DNPe

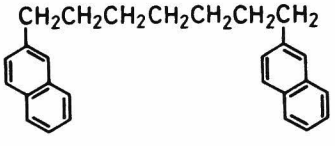

1,7-DNHp

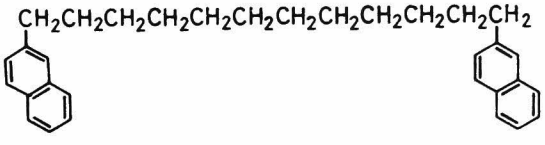

1,12-DNDd

Fig. 1. The structures of α,ω-dinaphthylalkanes

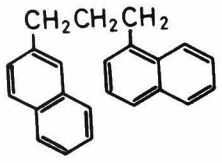

αβ-DNPr

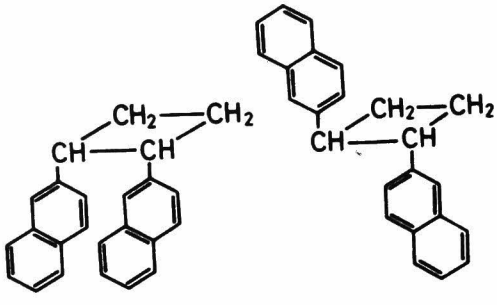

cis-DNCb trans-DNCb

Fig. 2. The structures of αβ-DNPr, trans-DNCb, and cis-DNCb.

(2H, m), 3.7-3.9 (1H, m), and 7.2-7.8 (7H, m).

cis-DNCb: mp 95-97 °C; NMR(CCl_4) δ= 2.5-2.7 (2H, m), 4.1-4.3(1H, m), and 6.8-7.6 (7H, m).

Tetrahydrofuran (THF) and hexane were used as solvents. THF was purified with the procedure described in Chapter 2. Spectro-grade hexane was used without further purification. All measurements were carried out for the degassed solutions of samples, and detailed method were mentioned in the previous chapter. The molecular structures of the com-

pounds used in this chapter are shown in Figs. 1 and 2.

4-3. Results and Discussion

4-3, 1. Photophysical Properties of α,ω-Dinaphthylalkanes

The efficient intramolecular excimer formation was observed for 1,3-DNPr which has the molecular structure satisfying the n=3 rule. However, it has not yet been clear that the rule holds in naphthalene chromophore. It is necessary to investigate the photophysical properties of the alkanes substituted with naphthyl groups which are the chromophore mainly dealt with this thesis. The fluorescence spectra of 1,5-DNPe, 1,7-DNHp, and 1,12-DNDd are the same as that for β-MNEt and show the monomer fluorescence alone. The fluorescence intensities are the same each other. The decay curves of these compounds in THF at dilute concentration at 25 °C are shown in Fig. 3. The lifetime of all samples are found to be 54 - 57 ns, which agree each other within the experimental error. Then, it seems to have no interaction between the naphthalene chromophores on a same molecule at the room temperature.

The fluorescence spectra are measured at temperatures from -100 to 25 °C, and the quantum yields are determined as shown in Fig. 4. All samples show no excimer emission at the whole temperature range. There is no indication of the monomer fluorescence quenching by the interaction between chromophores. Chandross and Dempster reported the fluorescence spectra of 1,2-di(1-naphthyl)ethane and 1,4-di(1-

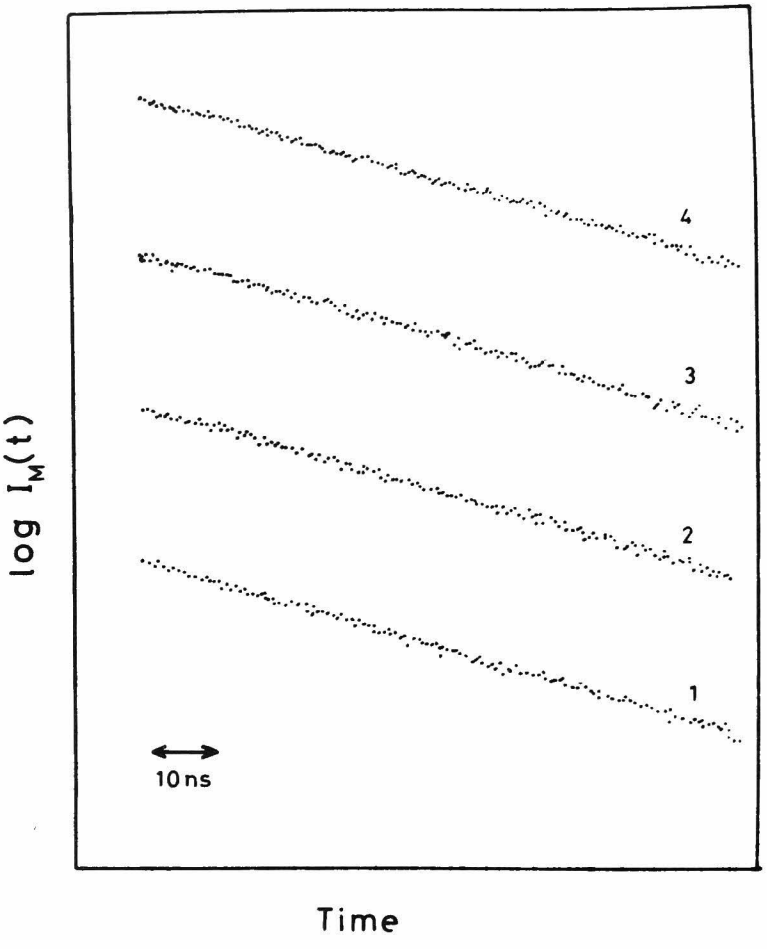

Fig. 3. Decay curves of α,ω-dinaphthylalkanes in THF at 25 °C: (1) β-MNEt, (2) 1,5-DNPe, (3) 1,7-DNHp, (4) 1,12-DNDd.

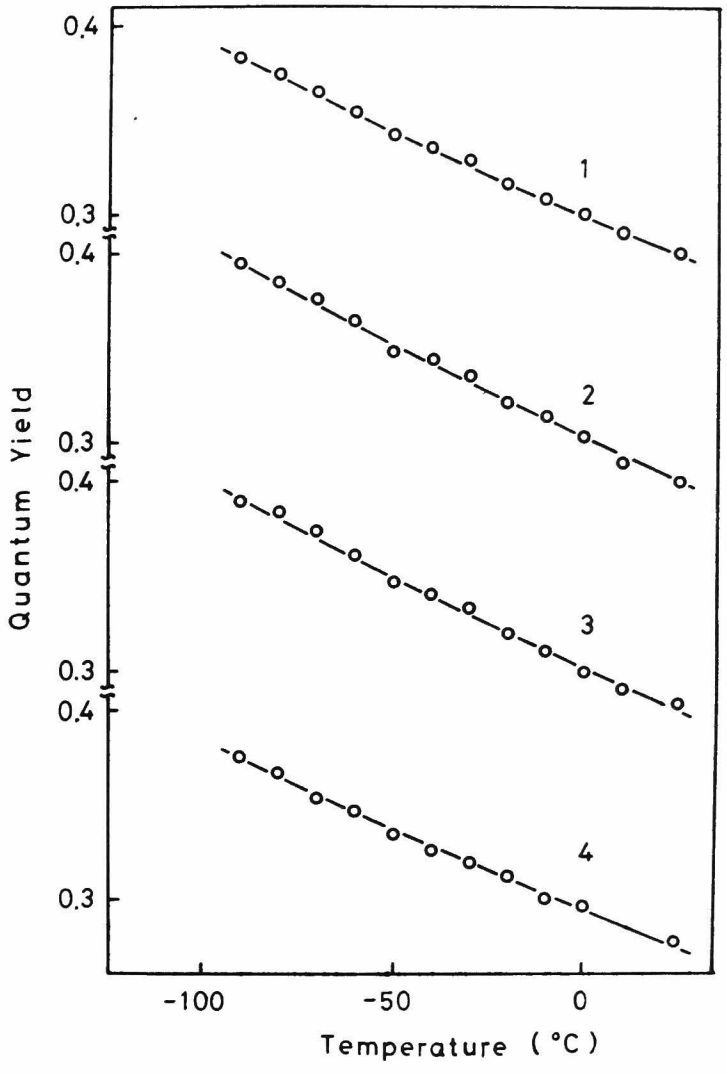

Fig. 4. Temperature dependence of the quantum yields of α,ω-dinaphthylalkanes in THF: (1) β-MNEt, (2) 1,5-DNPe, (3) 1,7-DNHp, (4) 1,12-DNDd.

naphthyl)butane.[3] The spectra of dinaphthylethane shows no variation from that of 1-methylnaphthalene. The fluorescence spectra of dinaphthylbutane indicate a weak excimer formation only at low temperatures. The fluorescence spectra of α,ω-dipyrenylalkanes were measured by Zachariasse and Kühnle,[19] and showed the intramolecular excimer emission except for n=7 and 8. The excimer formation efficiencies recover again as increasing n, and show almost constant value for the compounds having the longer methylene chains than n=10. In the case of dinaphthlyalkanes, no appreciable excimer emission can be observed for the compounds having smaller or larger value of n than n=7. The enthalpy change of the intermolecular excimer formation in THF were reported to be ca. 4.5 kcal /mol in the previous chapter. On the other hand, the enthalpy for pyrene derivatives have been reported to be ca. 10 kcal/mol,[21] which is very larger than that of naphthalene derivatives. Furthermore, the lifetime of pyrene have been found to be 250 ns, then the pyrene chromophores have many encounter chances during their lifetime as compared to the naphthalene chromophores.

Thus, the intramolecular excimer formation of dinaphthylalkanes are in accordance with the n=3 rule. It is due to the small stabilization energy of excimers and short lifetime of naphthalene chromophore. These results indicate that there are strict conditions for the excimer formation and the efficiency seems to reflect sensitively the configuration of the molecules and their rotational motions.

4-3, 2. Photophysical Properties of αβ-DNPr

The parallel sandwich arrangement of chromophores is not attainable in this compound. The chromophores can take sandwich arrangements overlapping with various angles between corresponding axes of two naphthalene chromophores. The fluorescence spectra in hexane at various temperatures are shown in Fig. 5. The spectra show weak excimer fluorescence only at low temperatures. The monomer and excimer emission are separated with reference to that of α-MNEt and β-MNEt at the same temperature. The muximum wavelength of the excimer emission appears at 370 - 380 nm which shifts to the blue side of the normal excimer emission (400 nm) of 1,3-DNPr. This result shows that in such unsymmetrical compound, the naphthalene chromophores can not approach the most stable arrangement and the binding energy is much less than that of the symmetrical dimer. The quantum yields of αβ-DNPr, α-MNEt, and β-MNEt at various temperatures are shown in Fig. 6. As increasing temperature, the intramolecular excimer emission is observed and its intensity takes a maximum value at -60 °C, which is very lower than that for 1,3-DNPr. At the temperature above -50 °C, the excimer emission decreases monotonously. Corresponding to this behavior, the monomer fluorescence intensity of αβ-DNPr is quenched as increasing temperature, and at the temperature, ca. -40 °C, the decrease of fluorescence intensity stops temporarily with the dissociation of the excimers. At high temperatures, the monomer fluorescence is quenched again as compared with α-MNEt and β-MNEt. If there

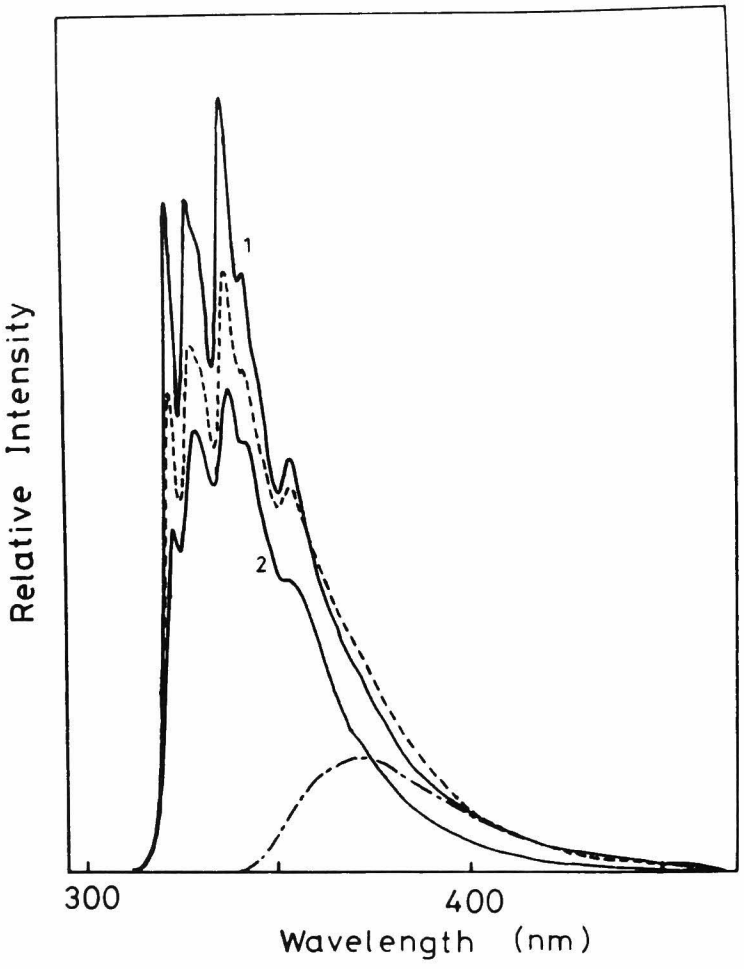

Fig. 5. Fluorescence spectra of αβ-DNPr in hexane at various temperatures. Full lines; (1) -80 °C, (2) 0 °C. Broken lines;(----) fluorescence spectra at -50 °C, (—-——-——) excimer emission spectra estimated at -50 °C.

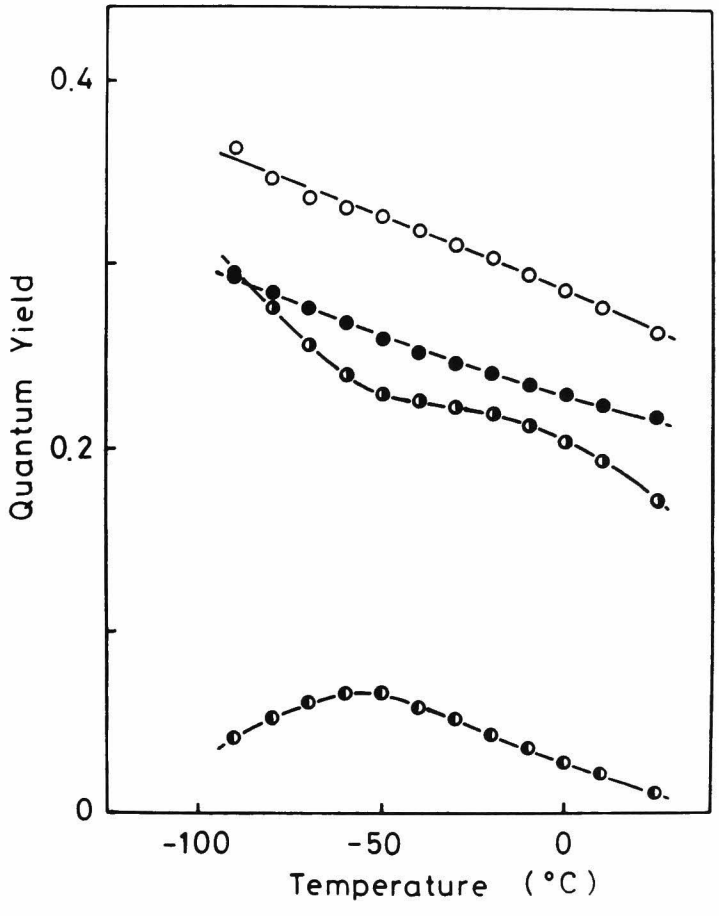

Fig. 6. Temperature dependence of the quantum yields in hexane; ●: α-MNEt, ○: β-MNEt, ◑: monomer fluorescence of αβ-DNPr, ◐: excimer fluorescence of αβ-DNPr.

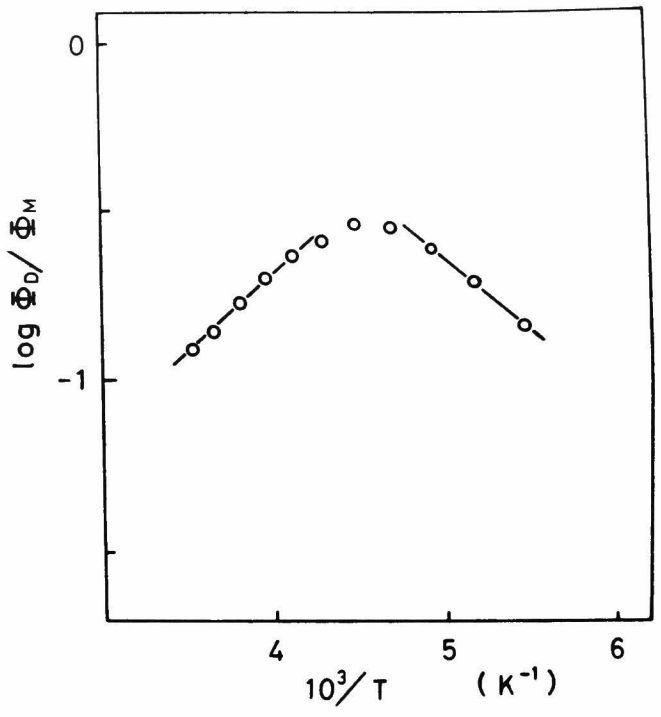

Fig. 7. Logarithm plot of the quantum yield ratio, Φ_D/Φ_M against 1/T for αβ-DNPr in hexane.

is no quenching process of excited chromophores, the quantum yield of αβ-DNPr should be the values between the quantum yields of α-MNEt and β-MNEt at a given temperature, which is proportianal to a fraction of the excited α- and β-MNEt. Then, the decrease of Φ_M at high temperatures indicates that the excitation energy is thermally dissipated by the interaction of chromophores.

According to Eqs. 2-10 and 2-11, the logarithms

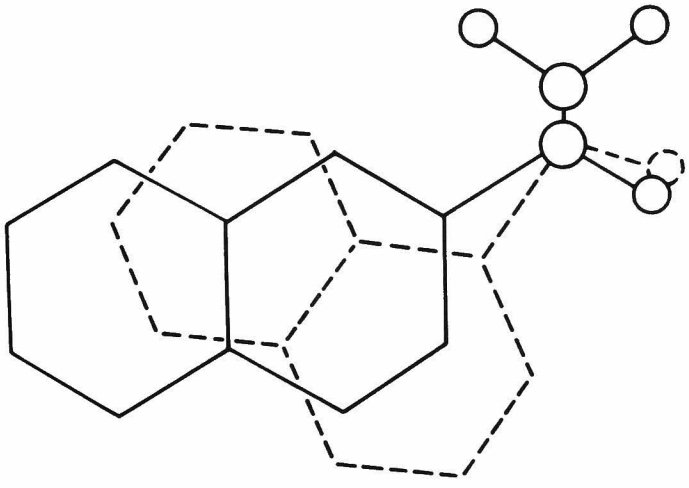

Fig. 8. Arrangement of two naphthalene chromophores of αβ-DNPr at the most overlapped conformation.

of the quantum yield ratio, Φ_D/Φ_M are plotted against the reciprocal of the temperature in Fig. 7. From this slopes, apparent activation energy of intramolecular excimer formation process, E_a and enthalpy change of the excimer formation, ΔH are estimated as follows,

$$E_a = 2.0 \text{ kcal/mol}, \qquad \Delta H = -2.1 \text{ kcal/mol}.$$

These values are very small as compared with those

for the symmetrical dimer, 1,3-DNPr. Although a little twist of each bond angle of the methylene chain gets the chromophores to take various sandwich arrangements, the most overlapped conformation is achieved at the rotated angle of ca. 40° of aromatic axes with keeping the sandwich arrangement, as shown in Fig. 8. A theoretical calculation of the interaction energy as a function of the rotation angle predicts that the binding energy becomes small at the angle about 40°, and the excimer state turns to be an unstable one.[7] It has been reported that the compound, chiral [2,2](1,5)-naphthalenophane which takes a similar rotated arrangement, shows the fluorescence spectra much alike to the excimer's.[17] However, the result cannot be applied to the spectra of αβ-DNPr, since the interplanar distance of the naphthlene chromophores is held to be so short as compared with that of αβ-DNPr. Therefore, the small enthalpy gain of the excimer formation indicates that the stable excimer conformation is the parallel sandwich arrangement, and that the unsymmetrical dimer, αβ-DNPr cannot form the stable intramolecular excimer such as 1,3-DNPr, owing to the configurational restriction of the molecule. This restraint causes the enhancement of the dissociation of excimers.

Figure 9 shows the molar extinction coefficients (ε) of α-MNEt and β-MNEt in hexane at various wavelengths. Since the solution of αβ-DNPr consists on the equal number of α and β isomers of naphthalene, the fraction of the excited α and β chromophores varies in proportion to the ε's of α and β

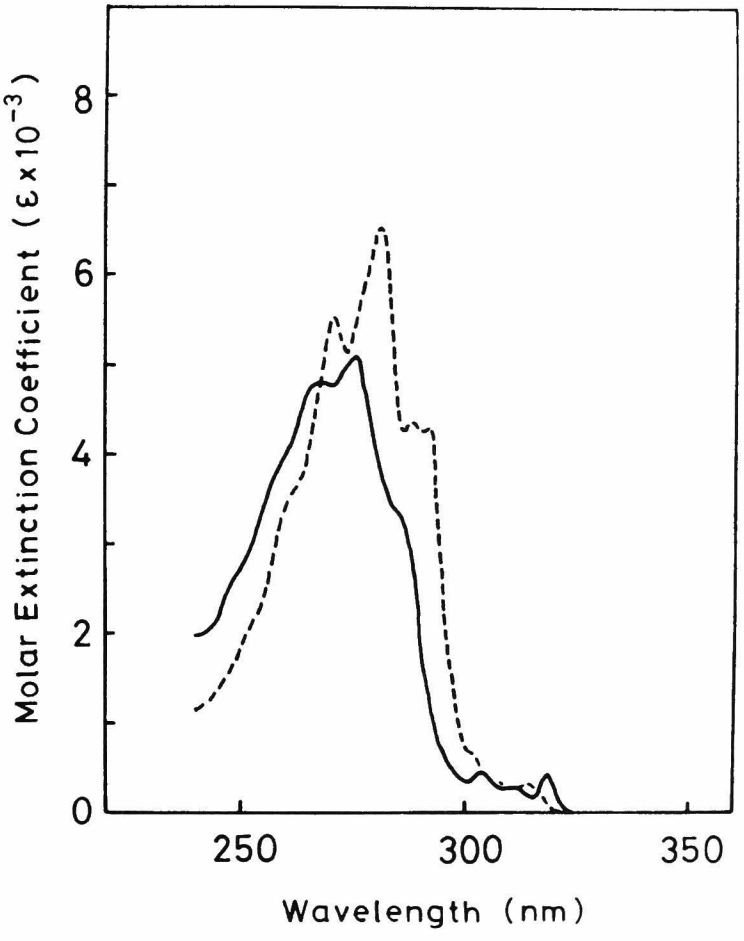

Fig. 9. Molar extinction coefficient (ε) of α-MNEt (----) and β-MNEt (——) in hexane at room temperature.

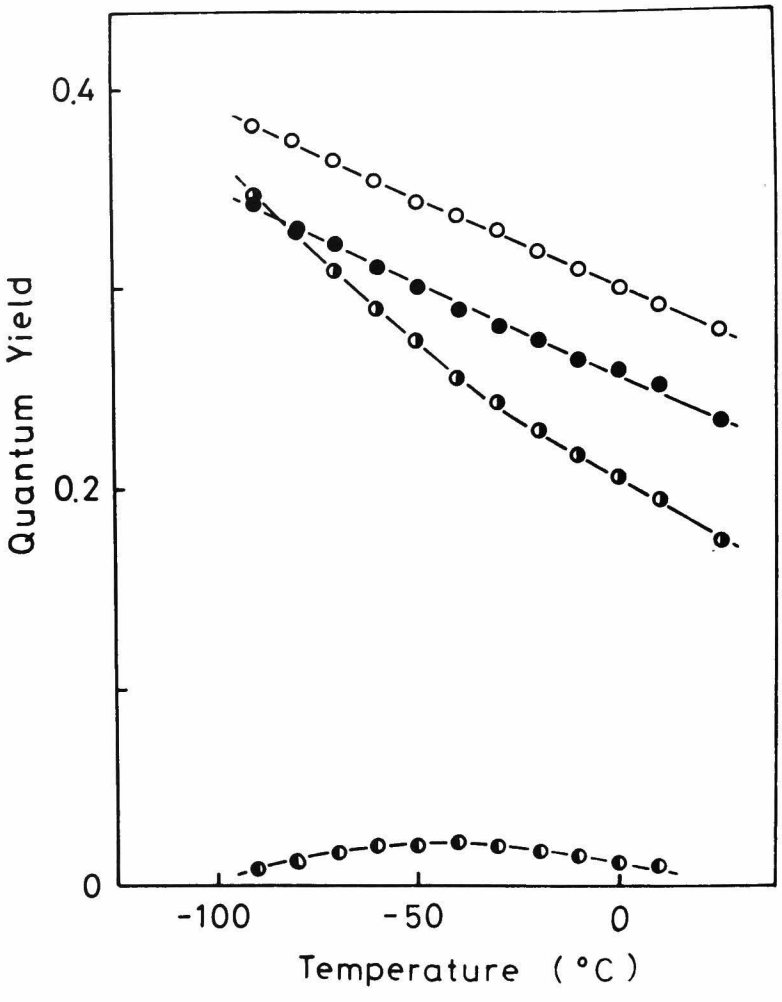

Fig. 10. Temperature dependence of the quantum yields of αβ-DNPr in THF; ●: α-MNEt, ○: β-MNEt, ◑: monomer fluorescence of αβ-DNPr, ◐: excimer fluorescence of αβ-DNPr.

isomers with the change of the excitation wavelength. However, the fluorescence spectra of the monomer emission band is independent of the excitation wavelength in the range of 260 - 310 nm. This shows that the excitation energy is exchanged rapidly between α and β chromophores and the fraction of the excited states reaches the equilibrium distribution before dissipating to the ground state as the monomer fluorescence. The fraction is estimated by the fluorescence spectra with reference to those of α- and β-MNEt, and found to be 0.34 at -20 °C and 0.24 at -80 °C for α-chromophore.

The similar measurements are carried out in THF solutions of αβ-DNPr. Figure 10 shows the quantum yields of the monomer and excimer fluorescence of αβ-DNPr and the monomer fluorescence of α-MNEt and β-MNEt at various temperatures. The excimer emission intensity is very weak in this solvent, and it appears in the tail of the monomer fluorescence band on the spectra. This solvent effect seems to be due to the solvation of chromophores, as mentioned in Chap. 8. The monomer fluorescence is quenched as the increase of temperature, and this shows that the excited chromophores interact with another ground state one on the processes of excimer formation, but almost all of them return to the monomer state or lose the excitation energy due to the instability of excimer state. The decay curves of monomer fluorescence are observed as a simple exponential function, $\exp(-t/\tau_M)$, and the lifetime, τ_M is shown in Fig. 11, together with those of α- and β-MNEt. At low temperatures about -100 °C, τ_M for αβ-DNPr is

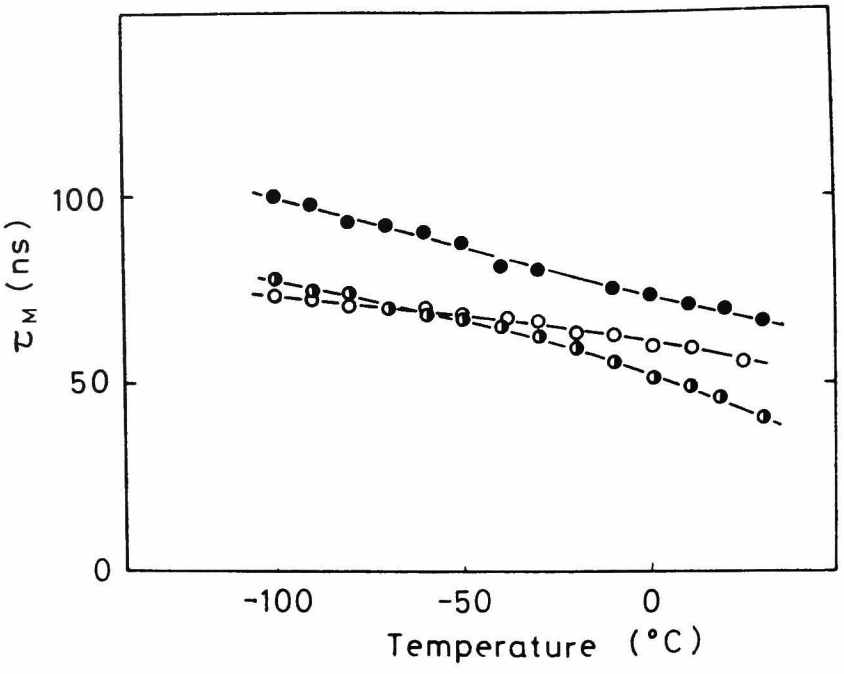

Fig. 11. Temperature dependence of the lifetimes for the monomer emission of αβ-DNPr; ● : α-MNEt, ○ : β-MNEt, ◑ : αβ-DNPr.

ca. 80 ns, which can be reasonably estimated from the partition of excited state between α- and β-naphthalenes as described above. Hence, at this low temperature region, the interaction between chromophores leading to radiationless transitions are negligible, even though efficient energy migration between chromophores takes place. With increasing temperature, the lifetime for αβ-DNPr

decreases more sharply than the corresponding monomeric α- and β-naphthalenes. This implies that the energy migration between chromophores take place with fairly long distance interaction, but the quenching process is caused by the short distance interaction, which is assisted by the rotational motion of methylene chain, and occurs in the course of intramolecular excimer formation.

The results for the unsymmetrical compound, αβ-DNPr indicate the following facts: The binding energy of the excimer is much less than that of 1,3-DNPr. This shows that the symmetrical sandwich arrangement of naphthyl groups is the stable excimer conformation, which cannot be attained in this compound because of its structural restriction. This effect appears in the photophysical behavior as quenching of the excited states and increasing of the dissociation process at low temperatures. On the other hand, the excitation energies are exchanged between α and β chromophores with sufficiently rapid rate as compared with the lifetime of chromophores, and the distribution equilibrium is attained before emission. The migration of excitation energies will become an important phenomenon in order to interpret the excimer formation in polymer systems.

4-3, 3. Photophysical Properties of trans- and cis-DNCb

In the cis compound, the naphthalene rings face to each other without deformation of the aromatic rings, and it can be expected to form intramolecular

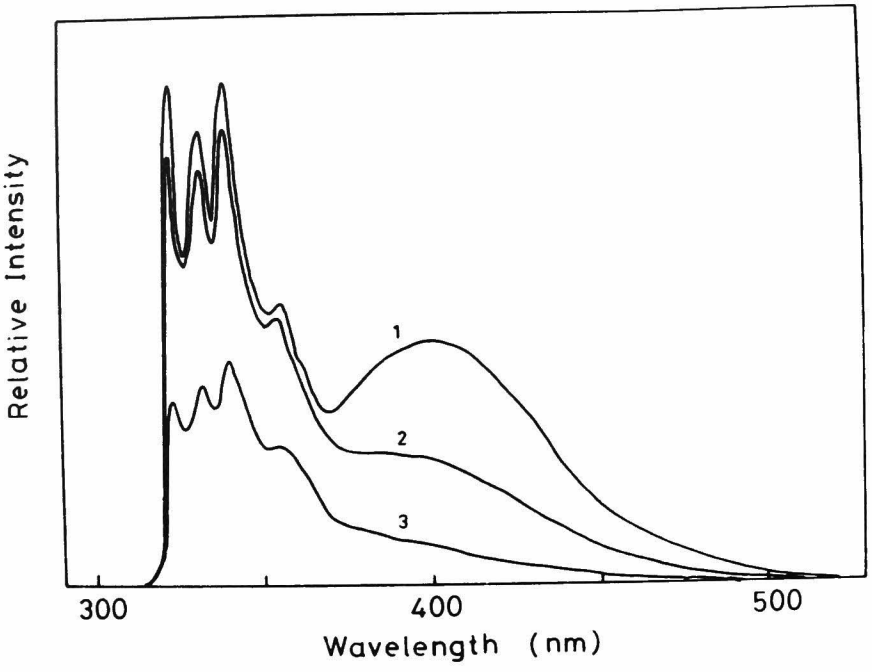

Fig. 12. Fluorescence spectra of cis-DNCb in hexane at various temperatures; (1) -80 °C, (2) -50 °C, (3) -20 °C.

excimers because of the similar arrangement of aromatic rings to the sandwich conformation.

Absorption spectra of cis-DNCb, trans-DNCb, and β-MNEt are much alike each other, although a little red shift of 2 nm is observed for both DNCb's. Such red shift has been reported for the similar compound, cis-1,2-diphenylcyclopentane.[12] The fluorescence spectra of cis- and trans-DNCb in hexane

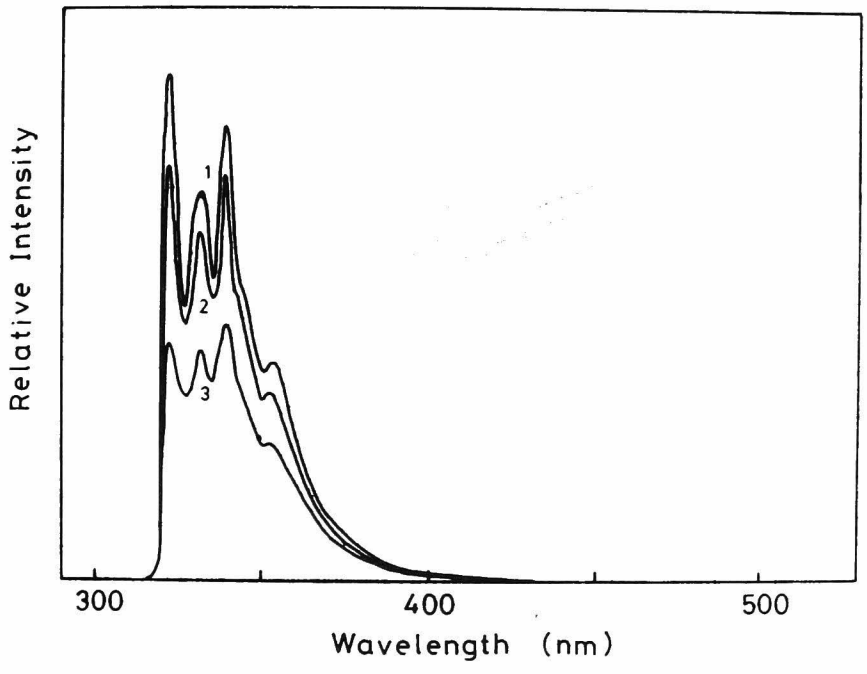

Fig. 13. Fluorescence spectra of trans-DNCb in hexane at various temperatures; (1) -80 °C, (2) -50 °C, (3) -20 °C.

at various temperatures are shown in Figs. 12 and 13. There is no indication of the excimer formation for trans-DNCb, but for cis-DNCb, the spectra show clearly the broad excimer emission at 400 nm in the low temperature range. The quantum yields of these samples are shown in Fig. 14. The fluorescence spectra and its quantum yields of trans-DNCb are similar to those of β-MNEt, but the thermal quenching is observed at high temperatures. The decay time of the monomer

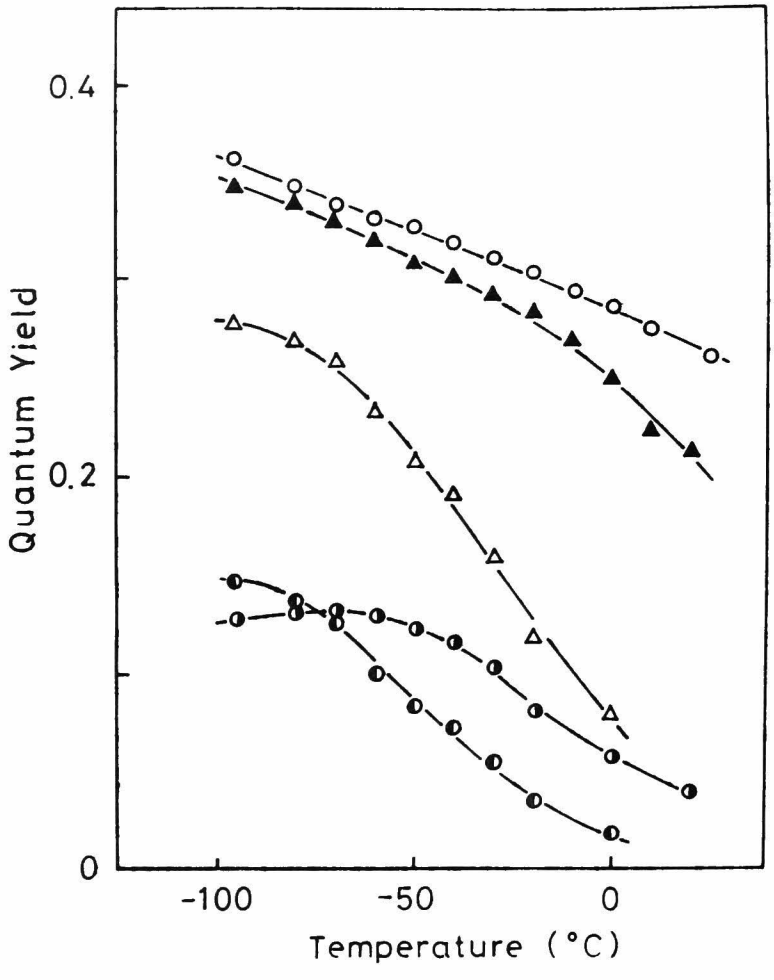

Fig. 14. Temperature dependence of the quantum yields in hexane; ○ : β-MNEt, ▲ : trans-DNCb, △ : total quantum yield of cis-DNCb, ◑ : monomer fluorescence quantum yield of cis-DNCb, ◐ : excimer fluorescence quantum yield of cis-DNCb.

fluorescence of trans-DNCb shows the same tendency with increasing temperature as that of the quantum yields as shown in Fig. 15. The lifetimes coincide with those of β-MNEt at the whole temperatures except for high temperatures. The fluorescence spectra of cis-DNCb show the intramolecular excimer emission at 400 nm, and their quantum yields become the largest value at the extremely low temperature, -95 °C, which is the freezing point of the solvent. As increasing temperature, Φ_D decreases monotonously, and Φ_M increases slightly. Then, both of the monomer and excimer fluorescence intensities decrease rapidly. This shows that large conformational changes are not necessary in this compound to form intramolecular excimers, and the formation processes are very fast even at low temperatures. But, the excimer state is not stable as well as αβ-DNPr, so the excimers go back to the monomer state or dissipate radiationlessly to the ground state with increasing the temperature. Since the rate of the non-radiative process changes too markedly with temperatures, the value of enthalpy change for the excimer formation given by Eq. 2-11, may include large error. But, the decay curves for excimer emission are the same as those of monomer emission at temperatures above -60 °C. This fact shows that the association and dissociation rate constants are fairly large as compared with the other rate constants. Therefore, the enthalpy change for excimer formation process is roughly estimated using the ordinary method, and found to be 1.7 kcal/mol.

At the low temperatures below -70 °C, the rise

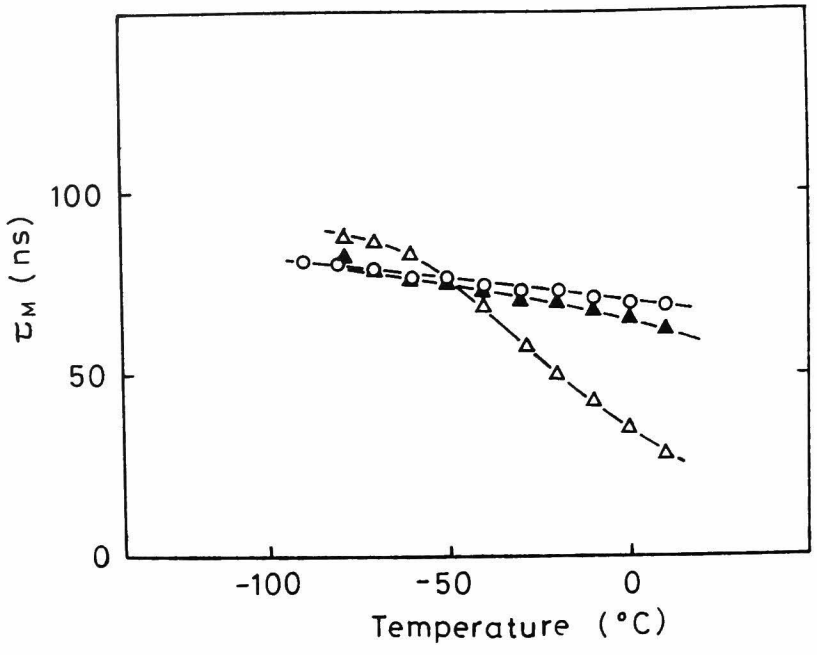

Fig. 15. Temperature dependence of the lifetimes in hexane; ○ : β-MNEt, ▲ : trans-DNCb, △ : cis-DNCb.

components are observed for transient curves of the excimer emission. Moreover, there is no excimer fluorescence in the spectra at 77 K. These facts indicate that there are some conformational relaxation process of the molecule from the ground state conformation to the excimer state one after excitation of the chromophores. The relaxation process may correspond with the bending motion of the cyclobutane

ring between puckered forms as shown in Fig. 16.[22] Two naphthalene chromophores of cis-DNCb can take an overlapped arrangement at the planar form of cyclobutane ring, which is attained in the course of the bending motion. The planar conformation has said to be a little higher energy state, ca. 1.4 kcal/mol than the puckered form, therefore the conformational transition rate seems to be considerably fast. The overlapped arrangement at the planar form of the cyclobutane ring is not parallel sandwich arrangement. Assuming the angle, R-C-H, to be 110°, the planes of naphthalene rings face to each other with the angle, ca. 50°, and the distance of aromatic rings are estimated to be 2.8 Å and 6.7 Å for the nearest and farthest aromatic carbon atoms, respectively. The instability of the excimer state is due to this structural restriction which prevents the nephthalene rings from the stable parallel conformation.

On the other hand, the compound, trans-DNCb takes diaxial and diequatorial conformations as shown in Fig. 16. But, this compound can not achieve the overlapped arrangement of chromophores. Then, the naphthalene groups have no appreciable interaction each other and behave like an isolated chromophore such as β-MNEt.

These results in the various dimeric compounds indicate that there are strict conditions for the intramolecular excimer formation of naphthalene derivatives. The aromatic rings must take the parallel sandwich arrangement spaced with appropriate interplanar distance in order to form a stable ex-

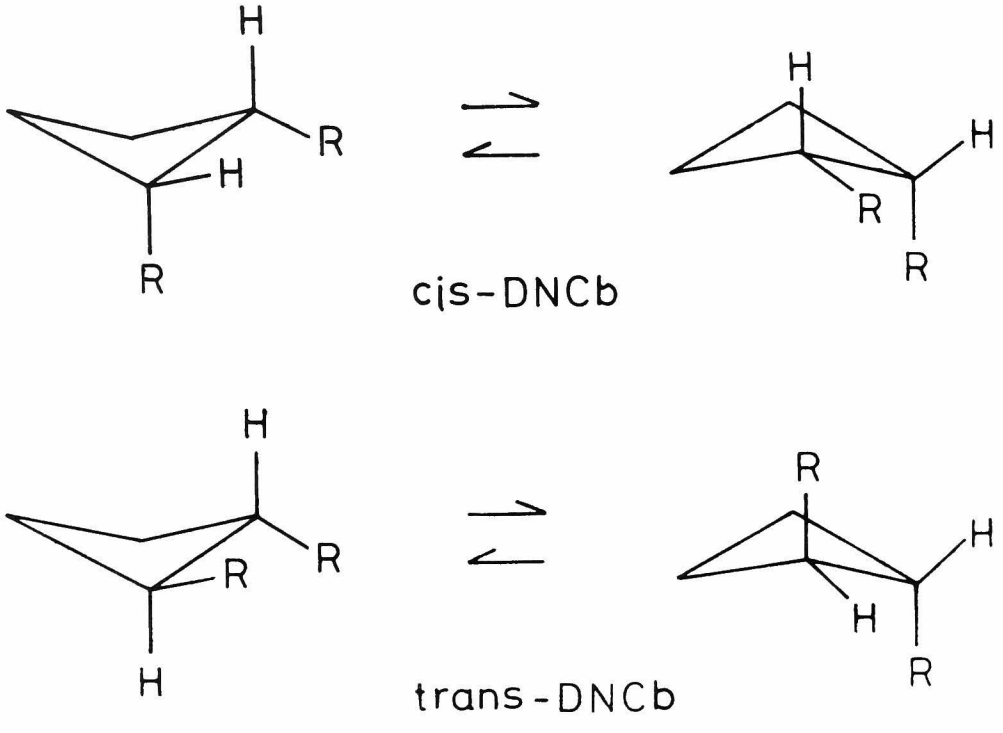

Fig. 16. Bending motion between two puckered conformations of 1,2-di(2-naphthyl)-cyclobutanes: R= 2-naphthyl-.

cimer. The specifically efficient formation of the stable excimer in 1,3-DNPr which satisfies the n=3 rule, is due to the easy attainment of this sandwich conformation without any structural restrictions. The other compounds having the molecular structure except for n=3 can not form intramolecular excimers, and behave like as isolated chromophores.

The compounds taking the conformation close to an overlapped arrangement, but slightly different from the parallel sandwich one, show the intramolecular excimer formation with low efficiencies, and the formed excimers have much different properties from the stable excimers: small enthalpy gain for the excimer formation process, large dissociation rate of the excimers, and increase of non-radiative dissipation rate from the excimer state. This strict configurational requirement seems to be useful for study of the conformation of molecules and their rotational motions through the observation of the intramolecular excimers.

References

1) F. Hirayama, J. Chem. Phys., 42, 3163 (1965).
2) W. Klöpffer, Ber. Bunsenges. Phys. Chem., 74, 693 (1970).
3) E.A. Chandross and C.J. Dempster, J. Am. Chem. Soc., 92, 3586 (1970).
4) Y. Nishijima, Y. Sasaki, K. Hirota, and M. Yamamoto, Repts. Progr. Polym. Phys. Japan, 15, 449 (1972).
5) G.E. Johnson, J. Chem. Phys., 61, 3002 (1974).

6) K. Zachariasse, W. Kühnle, and A. Weller, Chem. Phys. Lett., 59, 375 (1978).
7) T. Azumi and H. Azumi, Bull. Chem. Soc. Jpn., 39, 1829 (1966).
8) F.J. Smith, A.T. Armstrong, and S.P. McGlynn, J. Chem. Phys., 44, 442 (1966).
9) A.K. Chandra and B.S. Sudhindra, Mol. Phys., 28, 695 (1974).
10) A.K. Chandra and E.C. Lim, Chem. Phys. Lett., 45, 79 (1977).
11) H. Braun and Th. Förster, Ber. Bunsenges. Phys. Chem., 70, 1091 (1966).
12) D.J. Cram, N.L. Allinger, and H. Steinberg, J. Am. Chem. Soc., 76, 6132 (1954).
13) J.W. Longworth and F.A. Bovey, Biopolymers, 4, 1115 (1966).
14) J.R. Froines and P.J. Hagerman, Chem. Phys. lett., 4, 135 (1969).
15) M.W. Haenel, Tetrahedron Lett., 35, 3053 (1974).
16) D. Schweitzer, J.P. Colpa, J. Behnke, K.H. Hausser, M. Haenel, and H.A. Staab, Chem. Phys., 11, 373 (1975).
17) D. Schweitzer, J.P. Colpa, K.H. Hausser, M. Haenel, and H.A. Staab, J. Lumin., 12/13, 363 (1976).
18) N.E. Blank and M.W. Haenel, Tetrahedron Lett., 16, 1425 (1978).
19) K. Zachariasse and W. Kühnle, Z. Phys. Chem., N. F., 101, 267 (1976).
20) T. Asanuma, Doctoral thesis, Kyoto University, Kyoto, Japan, 1977.
21) E. Doller and Th. Förster, Z. Phys. Chem. N.F.,

34, 132 (1962).
22) R.M. Moriarty, "Topics in Stereochemistry," E.L. Eliel and N.L. Allinger, Ed., Vol. 8, Interscience, New York, 1974.

PART II

Intramolecular Excimer Formation in Model Compounds and Conformational Relaxation Processes

CHAPTER 5

Kinetic Studies on Intramolecular Excimer Formation in Dinaphthylalkanes

5-1. Introduction

Excimer is an excited dimer existing only in the excited state by the attractive interaction between an excited chromophore and one in the ground state. It turns unstable in the ground state due to the steric hindrance between chromophores. The formation of intermolecular excimers is thus expected to be controlled by the mutual diffusion of chromophores. Verification of the diffusion controlled process has been carried out mainly using pyrene molecule as a chromophore.[1,2] For naphthalene chromophore, the diffusion controlled process was studied in chapter 3, and it was shown that the steric condition necessary for excimer formation is more strict in the case of naphthalene chromophore than in the case of pyrene chromophore.

The formation of intramolecular excimers is considered to be governed by the micro-structures of molecules to which chromophores are attached. It seems that there are two controlling factors for the intramolecular excimer formation: (a) conformational changes of the molecule which corresponds to the mutual diffusion process in the case of intermolecular excimer formation, and (b) the geometrical arrangement of two chromophores in an excimer state which is determined by the micro-structure of the molecule. Concerning (b), Hirayama proposed the n=3 rule for the

intramolecular excimer formation.[3] The results indicate that the most favorate arrangement of chromophores is a symmetrical parrallel sandwich arrangement which can be formed specifically in a compound having a molecular structure in which two aromatic groups along the alkane chain separated by three carbon atoms.[4] It was also shown in Chapter 4, that the configurational requirements for intramolecular excimer formation are strict in the naphthalene excimers and they have fairly tight arrangements in the excited state.

This chapter deals with (a), the relationship between the micro-structures of molecules and their rotational relaxation processes within the lifetime of a chromophore. As mentioned above, the naphthalene chromophore seems to have fairly strict arrangements in the excimer state, its emission properties being favorable for detection in spectroscopic analyses. The photophysical characteristics are useful for investigating the rotational relaxation processes. In order to clarify the problem (a), quantitative study on various model compounds by the time-resolved fluorescence method, is necessary. Advance in the time-resolved technique for photoluminescence measurements enables us to determine the rate constants of the kinetic scheme including the intramolecular excimer formation process.[5-9] Various dinaphthylalkanes satisfying the n=3 rule, are investigated under photostationary and transient conditions. The individual rate constant of photophysical processes is determined. From the results, the relationship between the molecular structure and its conformational relaxation is

discussed. The compounds examined are regarded as the dimeric model compounds of vinyl polymers. Their photophysical behavior provides useful information on the intramolecular excimers in polymer systems.

5-2. Experimental

Materials. 1,3-Di(2-naphthyl)propane (1,3-DNPr) was synthesized by the procedure of Chandross and Dempster.[4] The other samples were prepared by as follows.

1,3-Di(2-naphthyl)butane (1,3-DNBu): 1,3-Di(2-naphthyl)-1-propanone, obtained as an intermediate product in the synthesis of 1,3-DNPr, was reacted with methylmagnesium iodide in ether solution. The oily product was purified by a column chromatography on silica gel. 2,4-Di(2-naphthyl)-2-butanol thus obtained was reduced in acetic acid solution by addition of zinc dust and hydrochloric acid. The product was chromotographed on silica gel with hexane-dichloromethane (4:1) : mp 65-66 °C; IR(KBr) 3050, 2950, 2930, 2850, 1630, 1600, 1510, 815, 740, and 475 cm^{-1}; NMR(CS_2) δ= 1.35 (3H, d, J=6.5 Hz), 1.90-2.16(2H, m), 2.52-2.96(3H, m) and 7.06-7.74(14H, m). Found: C, 92.69; H, 7.18%. Calcd for $C_{24}H_{22}$: C, 92.86; H, 7.14%.

1,3-Di(2-naphthyl)pentadecane (1,3-DNPd) and 1,3-di(2-naphthyl)-5-phenylpentane (1,3-DN-5-PhPe) were synthesized by the same method as that for 1,3-DNBu, 1-bromododecane and 1-bromo-2-phenylethane being used for 1,3-DNPd and 1,3-DN-5-PhPe, respectively, instead of methyl iodide. 1,3-DNPd: IR(KBr) 3050, 2930, 2850, 1630, 1600, 1510, 815, 740, and 475 cm^{-1}; NMR(CS_2) δ = 0.75-0.95(3H, m), 1.17(20H, s), 1.54-1.83(2H, m),

1.92-2.18(2H, m), 2.50-2.80(3H, m), and 7.05-7.76(14H, m). Found: C, 90.67; H, 9.82%. Calcd for $C_{35}H_{44}$: C, 90.46; H, 9.54%. 1,3-DN-5-PhPe: IR(KBr) 3050, 2930, 2850, 1630, 1600, 1510, 815, 740, 695, and 475 cm^{-1}; NMR(CS_2) δ= 1.85-2.22(4H, m), 2.30-2.82(5H, m), and 6.85-7.80(19H, m). Found: C, 92.87; H, 6.99%; M^+, 400. Calcd for $C_{31}H_{28}$: C, 92.95; H, 7.05%; M, 400.

2,4-Di(2-naphthyl)pentane (2,4-DNPe): 1,3-Di(2-naphthyl)-2-propen-1-one, obtained in the course of the synthesis of 1,3-DNPr, was reacted with methylmagnesium iodide in the presence of a trace amount of cuprous chloride, and the product was extracted with benzene. After benzene had been removed, the residue was recrystallized from carbon tetrachloride to give colorless crystalline 1,3-di(2-naphthyl)-1-butanone : mp 148-150 °C. The ketone was reacted again with methylmagnesium iodide in either solution. The product, 2,4-dinaphthyl-2-pentanol, was reduced by the same method as that for 1,3-DNBu. The residual oil was purified by a column chromatography on silica gel. The oily product consists of meso and racemo isomers (ca. 1:2). The isomers were separated by a recycle gel permeation chromatography. After seventy cycles, fractionated samples were used for measurements. The purity of the isomers was found to be 85% for both isomers by the methyl proton resonance in NMR spectra. Emission intensity was corrected by this proportion of isomers. 2,4-DNPe: IR(KBr) 3050. 2950, 2920, 2860, 1630, 1600, 1505, 815, 740, and 475 cm^{-1}; NMR(CS_2) for meso isomer, δ= 1.35(3H, d, J=7 Hz), 1.7-2.3(1H, m), 2.5-2.95(1H, m), and 7.16-7.80(7H, m), NMR(CS_2) for racemo isomer, δ= 1.24(3H, d, J=6.8 Hz), 1.96-2.18(1H,

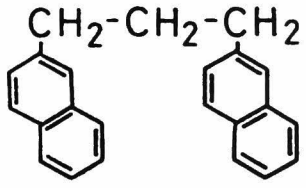

1,3-DNPr

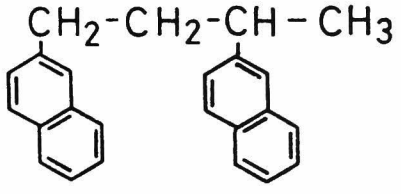

1,3-DNBu

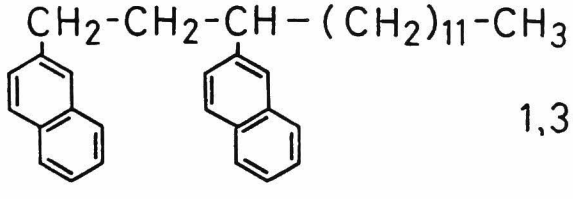

1,3-DNPd

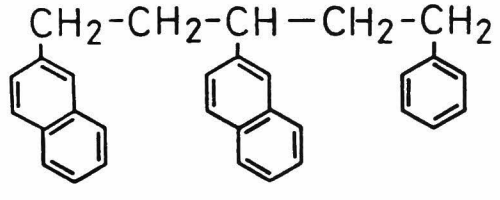

1,3-DN-5-PhPe

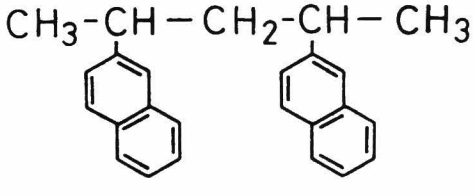

2,4-DNPe

Fig. 1. Molecular structures of dinaphthyl-alkanes studied in this chapter.

m), 2.42-2.85(1H, m), and 7.18-7.80(7H, m). Found: C, 92.53; H, 7.48%; M^+, 324. Calcd for $C_{25}H_{24}$: C. 92.54; H, 7.46%; M, 324.

Measurements. Photoluminescence measurements were carried out for the degassed THF solutions, and the detailed methods were mentioned in the previous chapter.

5-3. Results and Discussion

5-3, 1. Photostationary Measurements

Structual formulas of dinaphthylakanes are summarized in Fig. 1. The alignment of aromatic groups favorable for intramolecular excimer formation can be achieved when two adjacent aromatic groups are separated by three carbon atoms of alkane chain. Hence, effective intramolecular excimer formation can be expected in these compounds. Absorption spectra for these samples are nearly the same and similar to those of 2-ethylnaphthalene (MNEt) corresponding to the monomeric unit. This indicates that there is no specific interaction between naphthyl groups in th ground state, each chromophore behaving like an isolated naphthalene unit. Figure 2 shows the fluorescence spectra of three typical compounds at -20 ^{o}C. They consist of two emission bands. The structured shorter wavelength band and the broad longer wavelength band are assigned to the monomer fluorescence and intramolecular excimer fluorescence, respectively. Relative fluorescence intensities of these bands differ considerably with sample. Although the molecular structures of these samples are very much alike as a common dimer unit, they show different efficiency in excimer formation.

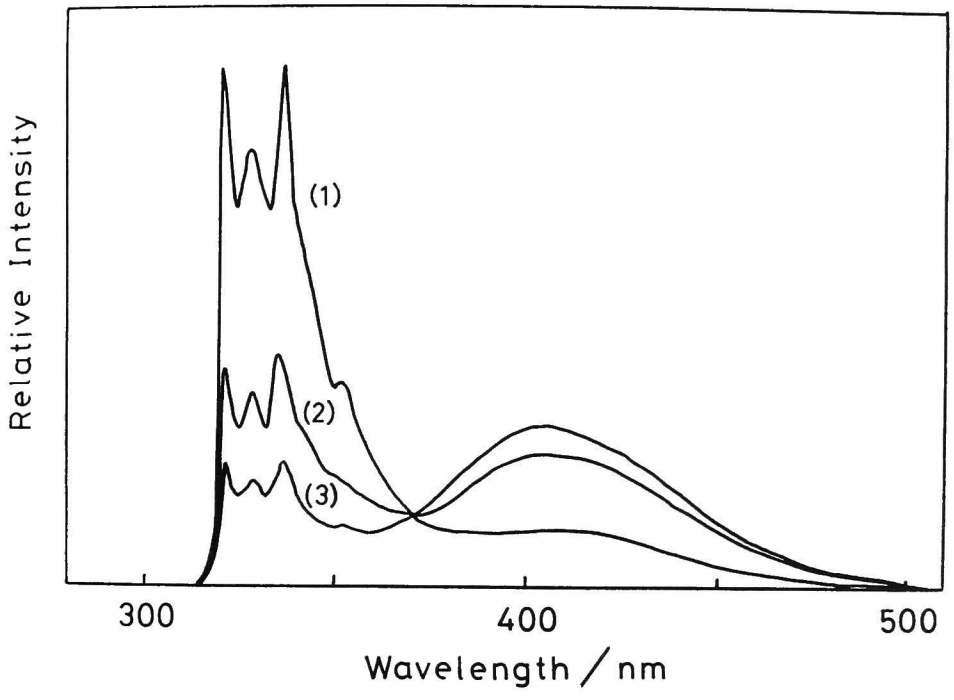

Fig. 2. Fluorescence spectra of the solutions of three typical compounds in THF at -20 °C: (1) 2,4-DNPe(rac), (2) 1,3-DNPr, (3) 2,4-DNPe(meso).

This can be attributed to the conformational relaxation processes after excitation of chromophores, from identity of the absorption and emission bands on the spectra of these samples.

The ratios of quantum yield (Φ_D) of excimer fluorescence to that of monomer fluorescence (Φ_M) for all samples at various temperatures are given in Table 1. Figure 3 shows the temperature dependence of Φ_M and Φ_D for three typical samples. Below -100 °C, fluorescence spectra of all samples are almost the same as those

Table 1. Ratios of the quantum yield of excimer fluorescence to that of monomer fluorescence at various temperatures.

Temp/°C	1,3-DNPr	1,3-DNBu	1,3-DNPd	1,3-DN-5-PhPe	2,4-DNPe (meso)	2,4-DNPe (rac)
0	2.6	3.2	3.6	3.6	5.2	0.59
-20	1.4	1.7	2.0	2.0	3.3	0.27
-40	0.61	0.83	0.89	0.98	1.9	0.10
-60	0.22	0.33	0.35	0.38	0.87	0.05

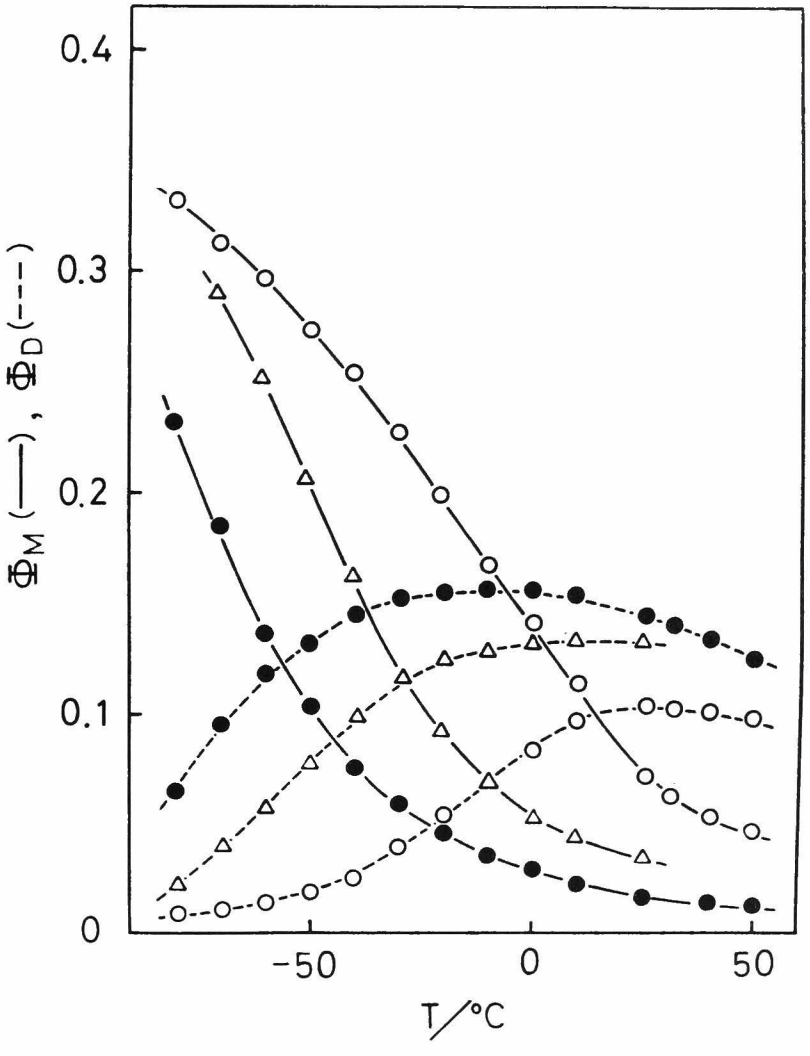

Fig. 3. Temperature dependence of quantum yields, Φ_M and Φ_D. ○ : 2,4-DNPe(rac), △ : 1,3-DNPr, and ● : 2,4-DNPe(meso).

of MNEt. There is no indecation of interaction between the naphthalene groups in the excited state when the molecular motion is suppressed. With rise in temperature, the monomer fluorescence is quenched steadily with increase in the excimer fluorescence. This shows that intramolecular excimer formation is governed by the conformational changes of the molecules. Some remarks are given concerning Table 1. (1) The compounds having alkyl substituents at one side of the dimer unit such as 1,3-DNBu, 1,3-DNPd, 1,3-DN-5-PhPe, show the same efficiency of excimer formation, the efficiency being independent of the kind of substituent. (2) 1,3-DNPr shows lower efficiency than that of 1,3-DNBu. (3) The highest efficiency of excimer formation is observed for 2,4-DNPe(meso), but its isomer 2,4-DNPe(rac) gives the lowest efficiency among the measured compounds. The effect of molecular configuration for intramolecular excimer formation appears typically in these isomers. This large difference in excimer formation for 2,4-DNPe between (meso) and (rac) is similar to the result of the steady state observation for diphenylpentanes.[10)]

The activation energy, E_a, for the excimer formation process can be obtained in the low temperature region by the equation

$$\Phi_D/\Phi_M = K \exp(-E_a/RT) ,$$

where K is a constant. The plots are shown in Fig. 4. In all samples except for 2,4-DNPe(rac), E_a was found to be 4.8-5.3 kcal/mol. 2,4-DNPe(rac) gives a somewhat larger value of E_a, 5.5 kcal/mol. The activation ener-

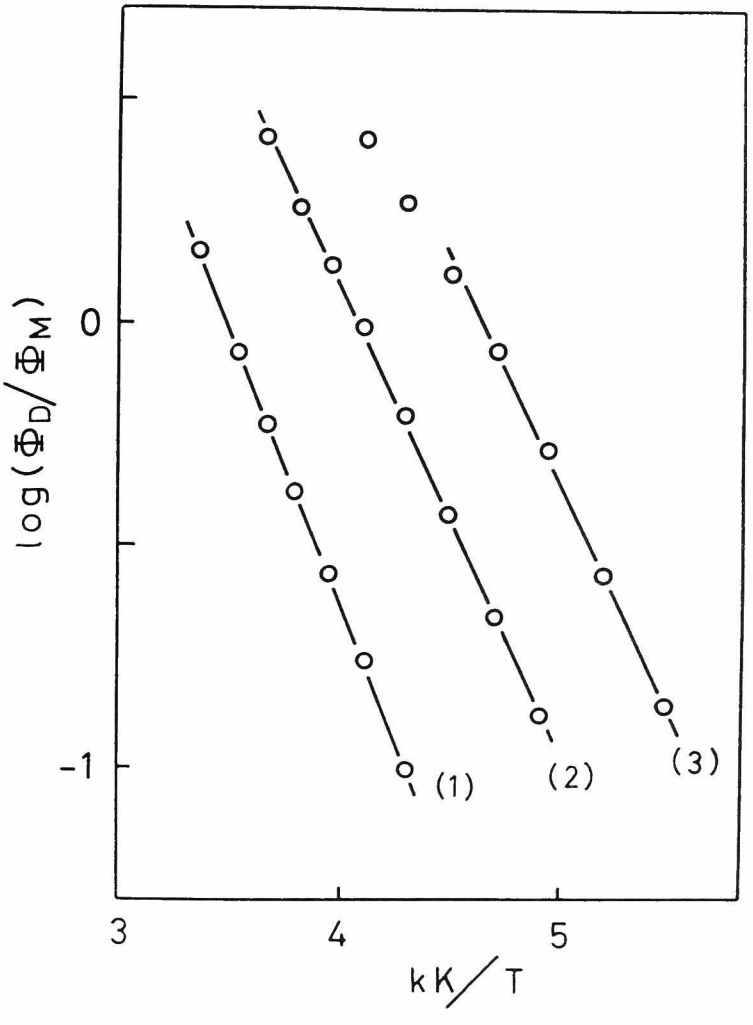

Fig. 4. Arrhenius plots of the ratio, Φ_D/Φ_M. (1) 2,4-DNPe(rac), (2) 1,3-DNPr, and (3) 2,4-DNPe(meso).

gy required for intermolecular excimer formation of MNEt in THF was found to be 3.2-3.4 kcal/mol.[11] The larger activation energies of intramolecular excimers indicate methylene chain restriction in the conformational changes. Somewhat larger activation energy for 2,4-DNPe(rac) suggests that some other conformational restraints in the excimer formation process are imposed on this compound. Although the activation energies for meso- and rac-diphenylpentanes were reported by Bokobza et al.[10] to be 2.0 and 4.6 kcal/mol, respec-

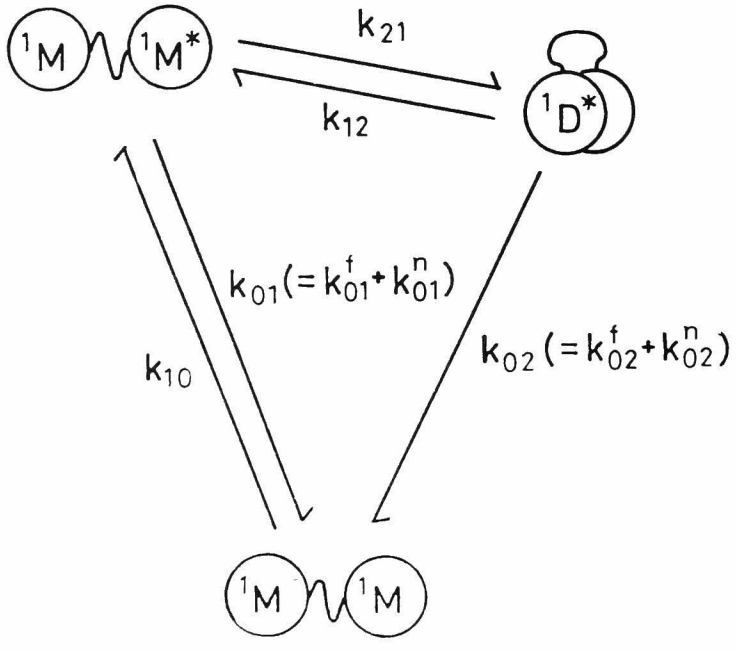

Fig. 5. Photophysical kinetic scheme of the energy dissipation processes. ^1M, $^1M^*$, and $^1D^*$ represent the ground state of monomer, the excited state of monomer, and the intramolecular excimer, respectively.

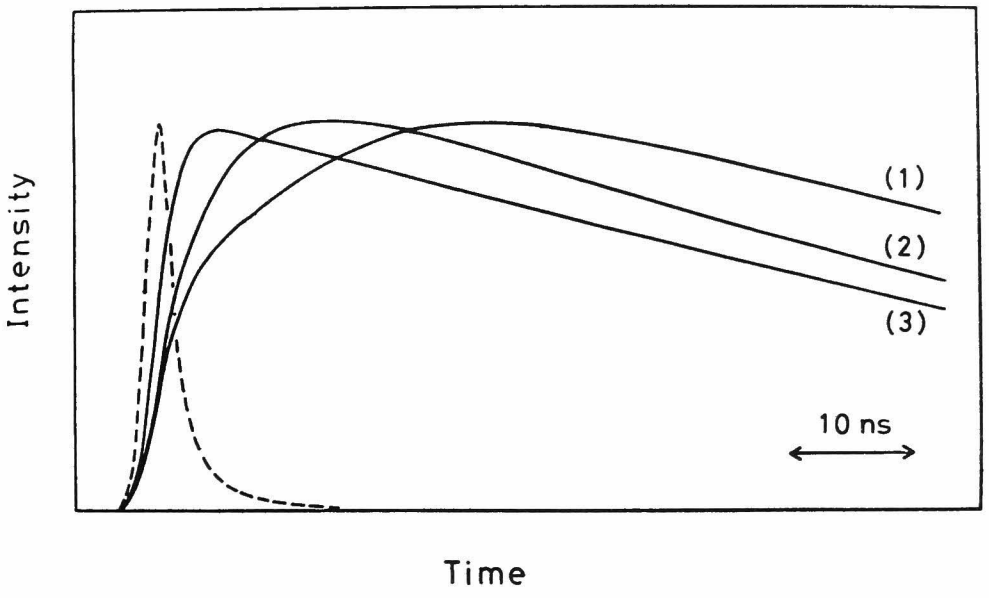

Fig. 6. Rise and decay curves of the intramolecular excimer fluorescence in THF at 25 °C. (1) 2,4-DNPe(rac), (2) 1,3-DNPr, (3) 2,4-DNPe(meso). The broken line is the excitation light pulse.

tively, no such large difference was found for the two isomers of 2,4-DNPe in the present investigation.

5-3, 2. Kinetic Rate Constants

The scheme of photophysical kinetics including the intramolecular excimer formation process is given in Fig. 5. However, it is not clear which process causes the difference in the efficiency of excimer formation for these compounds. For the sake of clarification, all the rate constants in the kinetic scheme should be

determined by the time-resolved measurements. Rise and decay curves of excimer emission after excitation by a pulse with a half-width of about 2.5 ns, are shown in Fig. 6 for three typical samples at 25 °C. On the assumption that the actual lifetime of the monomer emission in the absence of the excimer formation process is equal to the lifetime of MNEt under the same conditions, all the rate constants given in Fig. 5 can be determined by analysis of the transient curves and the quantum yields, Φ_M and Φ_D. The detailed procedures were mentioned in Chapter 2.

The rate constant k_{21} values measured at various temperatures are given in Table 2, other rate constants at 25 °C for all the samples being summarized in Table 3. There is an appreciable difference in the pseudo-1st order rate constant k_{21} values of the association process among these compounds, although little change is seen in the other rate constants. It is apparent that the marked increase of the excimer formation efficiency observed in the steady state measurements is due to the large values of the association rate constant k_{21}.

The observed compounds seem to have the same geometrical alignment of the naphthyl groups in the excimer state. We might conclude that the rate constant k_{02} dose not vary so much with sample. There is no consederable change in the dissociation rate constant k_{12}, although somewhat a larger value is obtained for 2,4-DNPe(meso). The value of k_{12} for the intermolecular excimers in concentrated solution of MNEt in THF is given by

Table 2. Intramolecular excimer formation rate constants and their activation energies

Temp/°C	$k_{21}/10^7 s^{-1}$ 1,3-DNPr	1,3-DNBu	1,3-DNPd	1,3-DN-5-PhPe	2,4-DNPe (meso)	2,4-DNPe (rac)
50						17
25	21	28	29	29	79	8.7
0	12	17	17	17	41	3.6
-20	4.8	7.0	7.0	7.1	17	
-40	1.9	2.6	2.8	2.9	7.8	
-60	0.7	1.0	1.0	1.0	3.3	
E_a/kcal mol^{-1}	5.1	5.2	5.3	5.3	4.8	5.5

Table 3. Kinetic rate constants at 25 °C

$k_{01}^{f}/10^{7}s^{-1}$	0.49
$k_{01}^{n}/10^{7}s^{-1}$	1.3
$k_{02}^{f}/10^{7}s^{-1}$	0.16 - 0.22
$k_{02}^{n}/10^{7}s^{-1}$	0.8 - 1.2
$k_{12}/10^{7}s^{-1}$	2.6 - 0.8

$$k_{12} = A \exp(-E_d/RT) ,$$

where A, E_d, and R are the Arrheius factor, the activation energy of the dissociation process, and the gas constant, respectively. The values for A and E_d were found to be 4.4×10^{15} s^{-1} and 7.7 kcal/mol, respectively. A much smaller value is obtained for k_{12} in the case of the intramolecular excimer than in the case of the intermolecular excimer. This is due to the binding dffect of the methylene chain. The binding energy of the excimer state seems to be the same in the compounds we studied because of a similar molecular structure in the dimer unit. Therefore, it is understandable that there is no appreciable difference in the value of k_{12}. The methyl group of

2,4-DNPe(rac) should be situated in an unstable gauche position in the excimer conformation. However, the unstable energy is too small to affect the dissociation rate constant.

For the association rate constant k_{21}, the compounds 1,3-DNBu, 1,3-DNPd, and 1,3-DN-5-PhPe show the same value. This indicates that the association rates are determined only by the configuration of the common dimer units, and the conformations in the dimer units are not much influenced by the substituent groups of the 3-position for these model compounds. This indicates that the rate of conformational relaxation in the terminal dimer units is not strongly affected by the increase of mass or chain length of these substituent groups. The effect of molecular weight on the rotational relaxation times was reported, e.g., by the measurement of fluorescence depolarization,[12,13] ^{13}C NMR,[14] and ESR.[15] The results indicate that the relaxation time of molecular motions increases with increasing molecular wight. However, no such changes were observed in the case of intramolecular excimers. The observed rate constants of excimer formation reflect the local segment motions of the end group of the molecule with respect to the molecular coordinate system. It seems that tha molecular size of the alkane chain such as pentadecane, is too small to cause changes in the local segment motion and the local environment around the end groups.

5-3, 3. Excimer Formation Rate Constants and Rotational Relaxation Processes

Large differences in the association rate

constants for 1,3-DNPr, 1,3-DNBu, 2,4-DNPe(meso) and (rac) are observed (Table 2). First, let us discuss the results for 2,4-DNPe(rac) which gives the smallest value of k_{21}. The rate of intramolecular excimer formation is controlled by the internal rotational motion of the molecule from the equilibrium conformation in the ground state to the excimer one. From the analysis of NMR spectra,[16-18] we know that the preferred conformation for racemo dimers is situated at tt, indicating a planar conformation for the alkane chain. In order to reach the excimer conformation from the tt conformation, it is necessary to carry out an unfavorable conformational change, $g^+ \not\rightleftarrows g^-$ with respect to the naphthyl groups. This seems to be the cause of small values of k_{21} and the somewhat larger value of E_a for 2,4-DNPe(rac). Secondly, there are considerable difference in 1,3-DNPr, 1,3-DNBu, and 2,4-DNPe(meso). These differences are due to the equilibrium distribution of conformation at the ground state, whose distribution determines the initial positions of the naphthalene chromophores immediately after their excitation. Particularly, the population of the nighboring conformation to the excimer conformation seems to play an important role in the excimer fomation rate (Fig. 7). The results are interpreted as follows: In 1,3-DNPr where $R_1 = R_2 = H$, the planar conformation with respect to the naphthyl groups (a) is most stable, the fraction of the neighboring conformation such as (b) not being large. In 1,3-DNBu where $R_1 = H$ and $R_2 = CH_3$, the neighboring conformation (b) becomes favorable owing to the steric hindrance of the methyl group. In 2,4-DNPe(meso) where $R_1 = R_2 = CH_3$, the

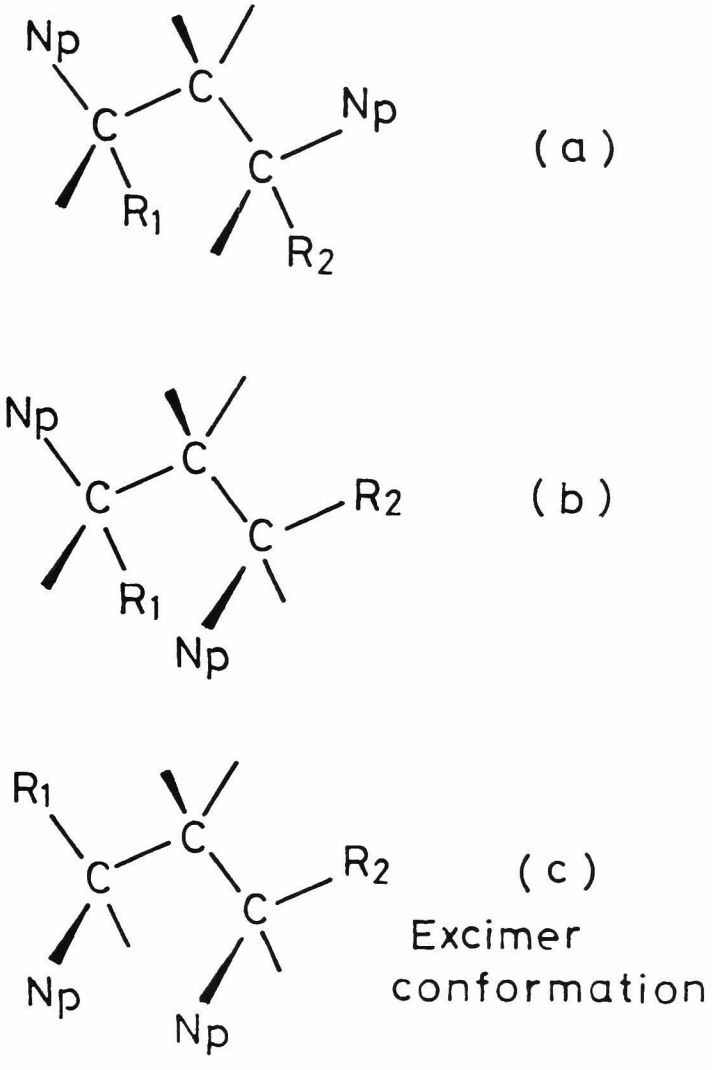

Fig. 7. Stable conformations of (a) 1,3-DNPr, (b) 1,3-DNBu and 2,4-DNPe(meso), and (c) the excimer conformation. Np: 2-naphthyl.

conformational distribution seems to be predominantly in the neighboring conformation (b). According to the analysis of NMR spectra for meso-diphenylpentane,[16-18] all other conformations have no appreciable fractions. The observed k_{21} values of the three compounds increase in this order. Thus, the association rate constants reflect the population of the neighboring conformation to the excimer state (c), and the rotational motion from this neighboring one to the excimer state.

The compounds studied here can be regarded as model compounds of poly(2-vinylnaphthalene) (PVN), which shows efficient intramolecular excimer formation.[7] 2,4-DNPe(meso) is considered to be model compound of the isotactic sequence in PVN, the large value of k_{21} indicating the important role of isotactic sequence in the intramolecular excimer formation in vinyl aromatic polymers.

In this chapter, photophysical rate constants are determined for various dinaphthylalkanes satisfying the n=3 rule, and it was found that the association rate constants change markedly for each sample in spite of the similar molecular structures in the common dimer units. This indicates that the intramolecular excimer formation is directly controlled by the rotational relaxation processes of the molecules, particularly, the relaxation processes from the neighboring conformations to the excimer conformation. More detailed discussion about the relationship between the relaxation process and the micro-structures are described in the next chapter.

References

1) J.B. Birks, D.J. Dyson, and I.H. Munro, Proc. R. Soc., A275, 575 (1963).
2) R. Speed and B. Selinger, Aust. J. Chem., 22, 9 (1969).
3) F. Hirayama, J. Chem. Phys., 42, 3163 (1965).
4) E.A. Chandross and C.J. Dempster, J. Am. Chem. Soc., 92, 3586 (1970).
5) G.E. Johnson, J. Chem. Phys., 61, 3002 (1974).
6) P.A. Avouris, J. Kordas, and M.A. El-Bayoumi, Chem. Phys. Lett., 26, 373 (1974).
7) S. Ito, M. Yamamoto, and Y. Nishijima, Repts. Progr. Polym. Phys. Japan, 19, 421 (1976).
8) C. David, M. Piens, and G. Geuskens, Eur. Polym. J., 12, 621 (1976).
9) K.A. Zachariasse, W. Kühnle, and A. Weller, Chem. Phys. Lett., 59, 375 (1978).
10) L. Bokobza, B. Jasse, and L. Monnerie, Eur. Polym. J., 13, 921 (1977).
11) B.K. Selinger reported the activation energy for 2-methylnaphthalene in ethanol: 2.8 kcal/mol (Aust. J. Chem., 19, 825 (1966)). But, the activation energy for MNEt in THF was found to be 3.2-3.4 kcal/mol in this work.
12) M. Uchida, Doctoral Thesis, Kyoto University, Kyoto, Japan, 1977.
13) S. Murase, Y. Suzuki, M. Yamamoto, and Y. Nishijima, Repts. Progr. Polym. Phys. Japan, 21, 405 (1978).
14) A. Allerhand and R.K. Hailstone, J. Chem. Phys., 56, 3718 (1972).
15) A.T. Bullock, G.G. Cameron, and P.M. Smith, J. Phys. Chem., 77, 1635 (1973).

16) F.A. Bovey, F.P. Hood, E.W. Anderson, and L.C. Snyder, J. Chem. Phys., 42, 3900 (1965).
17) H. Pivcova, M. Kolinsky, D. Lim, and B. Schneider, J. Polym. Sci., Polym. Symp., 22, 1093 (1969).
18) T. Moritani and Y. Fujiwara, J. Chem. Phys., 59, 1175 (1973).

CHAPTER 6
Conformation Analysis for Intramolecular Excimer Formation in Dinaphthylalkanes

6-1. Introduction

Since intramolecular excimers have been observed in various vinyl aromatic polymers and their model compounds, it has been known that the efficiency of excimer formation is greatly governed by their molecular structures. Particularly, Hirayama,[1] Longworth,[2] Chandross,[3] and Klöpffer[4] studied configurational requirements for the intramolecular excimer formation, and elucidated that the molecular structure in which two aromatic groups are separated with three carbon atoms of methylene chain is the most favorable configuration for the intramolecular excimer formation. Their results show that the parallel sandwich arrangement of the aromatic groups can be formed with propane chain, and that in the other type of compounds with shorter or longer chains than the propane chain, such as ethane, butane, pentane, two aromatic groups cannot approach each other, owing to conformational instability. This selectivity for the excimer formation in diarylalkanes is generally accepted as n=3 rule.

Considering the fact that the intramolecular excimers are formed in conformational relaxation processes after excitation of chromophores, this phenomenon has to be explained by the equilibrium conformations of the molecule and their internal

rotation processes. In fact, the different efficiencies of the excimer formation even for the compounds holding n=3 rule, were reported by Hirayama,[1] and similar results were observed by Davidson[5] and Bokobza,[6] recently. But in order to discuss the process of the intramolecular excimer formation in greater detail, quantitative data for the rate constant of the formation processes are required.

In Chapter 5, a large difference in the efficiency of the excimer formaion for the compounds satisfying the n=3 rule was observed, and it was shown by the time-resolved measurement that the association rate constants vary with the microstructure of the molecules.[7] In this chapter, the configurational effect on the rate of intramolecular excimer formation process will be studied. The pathway of the internal rotation from the most stable conformation to the excimer conformation, is discussed on the basis of the calculations of conformation energies. The calculated results account for the configurational effect on the excimer formation rates.

6-2. Procedures for the Calculation

In this study, calculation of conformation energy was carried out for the following compounds: 1,3-di(2-naphthyl)propane (1,3-DNPr), 1,3-di(2-naphthyl)butane (1,3-DNBu), meso-2,4-di(2-naphthyl)-pentane (2,4-DNPe(meso)), and racemo-2,4-di(2-naphthyl)pentane (2,4-DNPe(rac)).

The conformation energies of dinaphthylalkanes were calculated with the following procedure:[8]

Potentioal energies due to the van der Waals interaction between nonbonded atoms and due to the intrinsic torsional potential energies associated with the rotation about the bonds are considered. For calculation of the van der Waals interaction, a potential function of Lennard-Jones type is used as follows,

$$P_{ij} = B_{ij} / (r_{ij})^{12} - A_{ij} / (r_{ij})^{6},$$

where P_{ij} is the potential energy between the i-th and j-th nonbonded atoms, r_{ij} is the distance between the i-th and j-th nondonded atoms, A_{ij} and B_{ij} are suitable parameters. The potential function is modified by considering the molecule-solvent interaction according to Flory et al.[9] The total potential energy due to the van der Waals interaction is calculated as the sum over all pairs of nonbonded atoms. The intrinsic torsional potential energy for skeletal alkane chain, $E(\phi)$, is calculated for the rotation angle, ϕ, which is regarded to have a three fold periodicity as follows,

$$E(\phi) = (E_o/2) (1 - \cos 3\phi),$$

where E_o is the torsional barrier energy, and taken to be 2.8 kcal/mol.[10] The torsional energy for the rotation of naphthalene units, θ_i, is neglected, since the rotational potential has a sixfold periodicity and the potential barrier is too small. The total potential energy is given by the sum of the potential energy due to the van der Waals interaction and the intrinsic torsional potentials.

Structural parameters used in this calculation

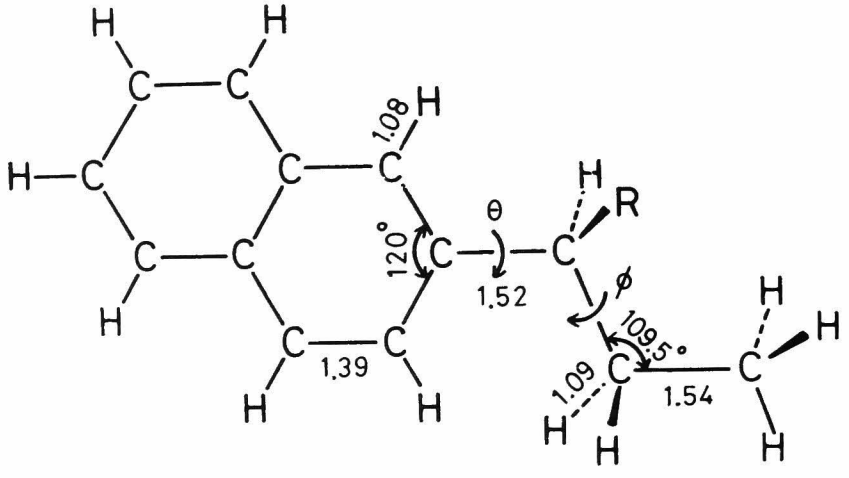

Fig. 1. Structural parameters of 1-(2-naphthyl)propane (R=H) and 2-(2-naphthyl)-butane ($R=CH_3$). These parameters are used for the calculation of the dimer model compounds.

are shown in Fig. 1. We must consider four independent angles to generate a given conformation of the dimers: two rotation angles, ϕ_1 and ϕ_2 for chain skeleton and two rotation angles, θ_1 and θ_2 for the naphthyl groups, which are denoted as shown in Fig. 2. Angles are taken as 0° in the trans conformation. The naphthalene substituents are adopted as a reference conformation for the nota-

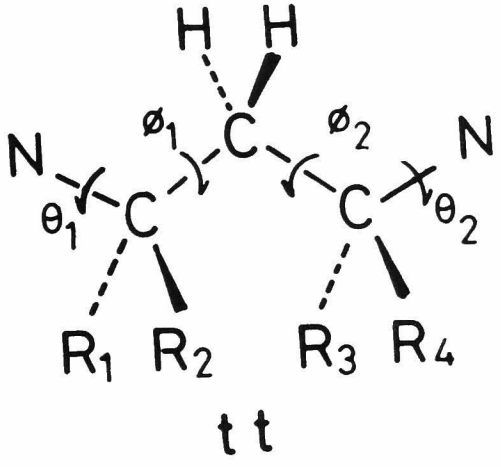

Fig. 2. Molecular formula at a tt conformation of dinaphthylalkanes: 1,3-DNPr (R_1=H, R_2=H, R_3=H, R_4=H), 1,3-DNBu (R_1=H, R_2=H, R_3=CH_3, R_4=H), 2,4-DNPe (meso) (R_1=CH_3, R_2=H, R_3=CH_3, R_4=H), 2,4-DNPe(rac) (R_1=H, R_2=CH_3, R_3=CH_3, R_4=H).

tion of trans and gauche conformations, in order to represent consistently the conformations of all compounds used in this study. For example, the tt conformation of meso-dinaphthylpentane (2,4-DNPe (meso)), which is situated at (ϕ_1, ϕ_2) = (0^o, 0^o), represents the conformation in which two naphthalene units are extended at the ends of trimethylene chain as shown in Fig. 2, and it does not mean the planar zigzag conformation of the skeletal bonds.

Conformation maps can be drawn as a function of four angles, θ_1, ϕ_1, ϕ_2, θ_2. But, in order to make the survey easier of the energy maps, they are given as a function of skeletal bond rotations, ϕ_1 and ϕ_2. The other rotational angles, θ_1 and θ_2 are fixed on the angles giving a minimum energy at the most stable position of ϕ_1 and ϕ_2. For some specific region on the energy maps, conformation energy is calculated as a function of all four angles, and the minimum energy was adopted. With the rotation of the skeletal angles, several stable conformations appear on the confomational map. The fraction of i-th conformation, f_i is calculated assuming that the distribution of conformations obeys the Boltzmann distribution including a weighting factor, W_i,

$$f_i = \{W_i \exp(-E_i/RT)\} \; / \; \sum_i W_i \exp(-E_i/RT) \; ,$$

where E_i is the minimized potential energy for i-th conformation. The weighting factor is estimated by the 2-dimensional local energy maps for the rotation angles, (θ_1, ϕ_1) and (θ_2, ϕ_2), where an angle set is fixed at the values chosen to minimize the energy, and the values of another set are varied. The area surrounded by the contour of 500 cal/mol higher than the energy of each minimum position is measured in their local energy maps, and the weighting factor is calculated by $W_i = w_{1,i} \times w_{2,i}$, where $w_{1,i}$ and $w_{2,i}$ are proportional to calculated areas on the local energy maps for (θ_1, ϕ_1) and (θ_2, ϕ_2), respectively, corresponding to i-th conformation.

6-3. Conformation Energies of Dinaphthylalkanes

All rate constants in the photophysical kinetic scheme were determined by the time-resolved measurements.[7] The obtained rate constants for the compounds used in this chapter are shown again in Table 1, and the association rate constant k_{21}, at various temperatures and their activation energies E_a, are given in Table 2. As shown in these tables, all rate constants except k_{21} are the same for all the compounds, but the excimer formation rate constant k_{21}, is much different for different compounds. In order to discuss the relationship between the excimer formation rate constants and the configuration of the compounds, it is necessary to follow the pathway of conformational changes on the potential energy map for each compound.

The calculation is made at first for 1-(2-naph-

Table 1. Kinetic rate constants of photophysical processes except for the association process, in THF at 25 °C.

$k_{01}^{f} \times 10^{-7}$	$k_{01}^{n} \times 10^{-7}$	$k_{02}^{f} \times 10^{-7}$	$k_{02}^{n} \times 10^{-7}$	$k_{12} \times 10^{-7}$
0.49	1.3	0.19±0.03	1.0±0.2	0.8–2.6

unit: s^{-1}

Table 2. Intramolecular excimer formation rate constants and their activation energies

Temp/°C	1,3-DNPr	1,3-DNBu	2,4-DNPe (meso)	2,4-DNPe (rac)
50				17
25	21	28	79	8.7
0	12	17	41	3.6
-20	4.8	7.0	17	
-40	1.9	2.6	7.8	
-60	0.7	1.0	3.3	
E_a/kcal mol^{-1}	5.1	5.2	4.8	5.5

Unit: $10^7 s^{-1}$

thyl)propane (R=H in Fig. 1) and 2-(2-naphthyl)-butane (R=CH_3 in Fig. 1) which are the model compounds corresponding to the monomer units of dinaphthylalkanes. Conformation energy maps for these compounds are shown in Figs. 3 and 4, where the potential energies are calculated at intervals of 5° for each rotation angle. For 1-(2-naphthyl)-

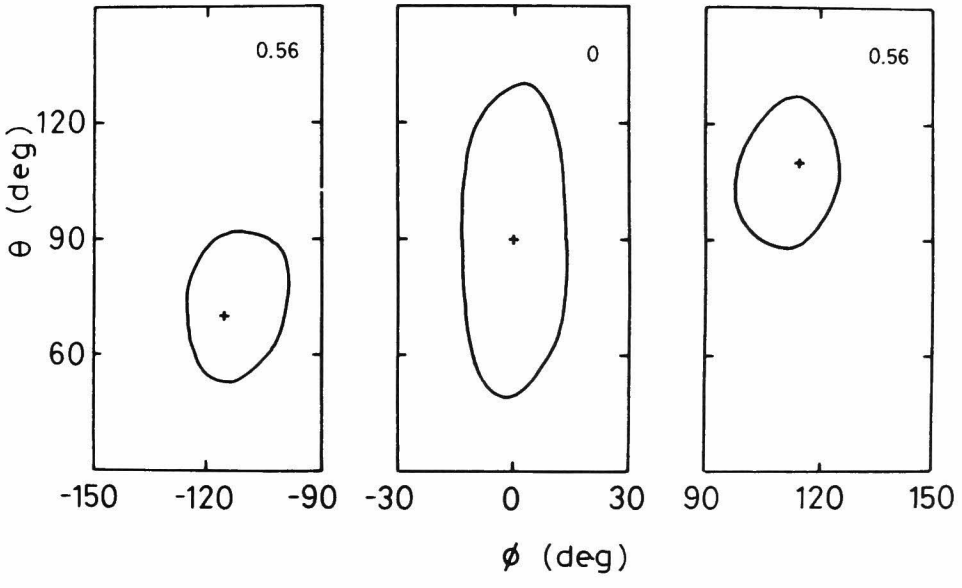

Fig. 3. Conformation energy maps for 1-(2-naphthyl)propane. The energy minima are marked by + signs. The contour lines indicate the 500 cal/mol higher energies than each minimum. Numerals in the figure show the potential energy at the minimum position (kcal/mol).

propane, the potential minima are situated at (θ, ϕ) = (90°, 0°), (70°, -115°), and (110°, 115°). The potential minima for 2-(2-naphthyl)butane, are found to be at (θ, ϕ) = (60°, -15°), (60°, -115°), and (110°, 125°). The stable conformations considerably deviate from the trans or gauche positions owing to the repulsion between the methyl and naphthyl units.

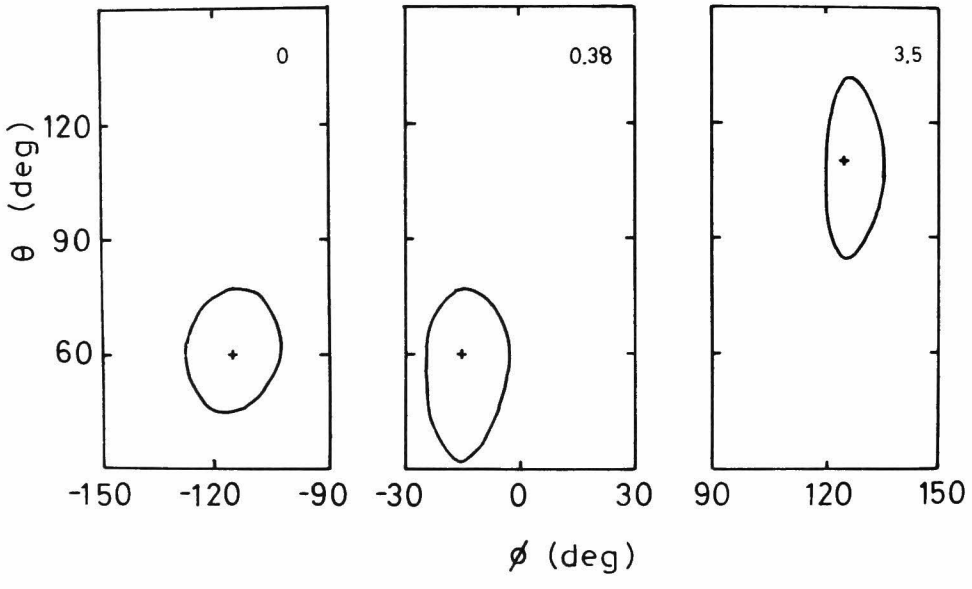

Fig. 4. Conformation energy maps for 2-(2-naphthyl)butane. The energy minima are marked by + signs. The contour lines indicate the 500 cal/mol higher energies than each minimum. Numerals show the potential energy at the minimum position (kcal/mol).

The area surrounded by the contour for each energy minimum significantly differs one from the other. The areas for the trans conformations are larger than that for gauche conformation; they are about 2.4 times and 1.2 times larger than the other potential minima in 1-(2-naphthyl)propane and 2-(2-naphthyl)butane, respectively. Therefore, it must be reflected in calculation for the fraction of each conformation. In the next place, the local energy

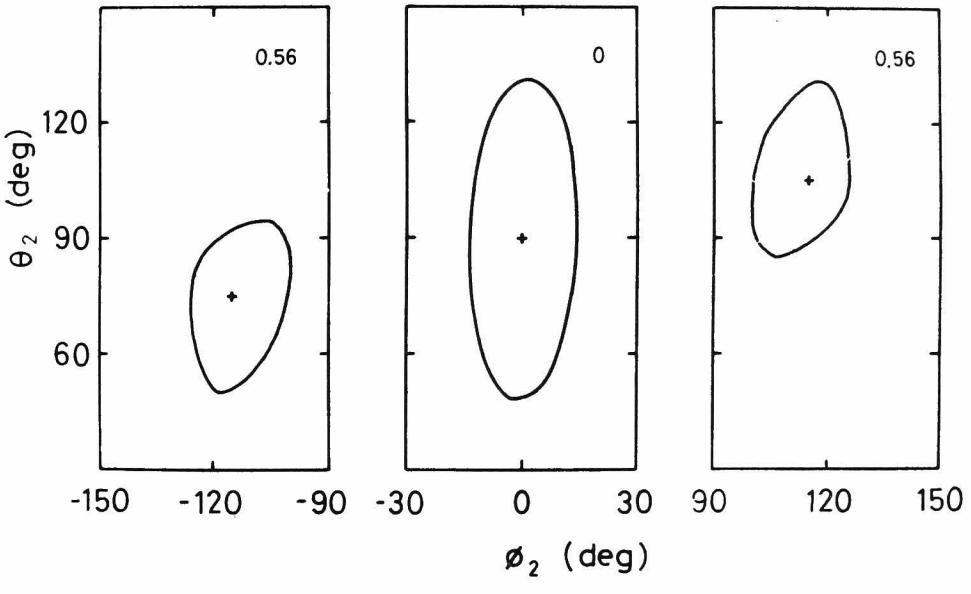

Fig. 5. Energy maps for 1,3-DNPr as a function of θ_2 and ϕ_2, where θ_1 and ϕ_1 are fixed at trans position ($\theta_1=90^\circ$, $\phi_1=0^\circ$). Notations of the contour lines and numerals are the same as Fig. 3.

maps as a function of θ_2 and ϕ_2 for the dimer compounds were calculated, where the angles, θ_1 and ϕ_1 are held to the values obtained by the calculation for the monomeric model compounds. The local maps for 1,3-DNPr are shown in Figs. 5 and 6. The energy maps were calculated once more, changing the rotation angle set to θ_1 and ϕ_1, holding θ_2 and ϕ_2 to the minimum positions obtained on the previous maps. These procedures are repeated until the mini-

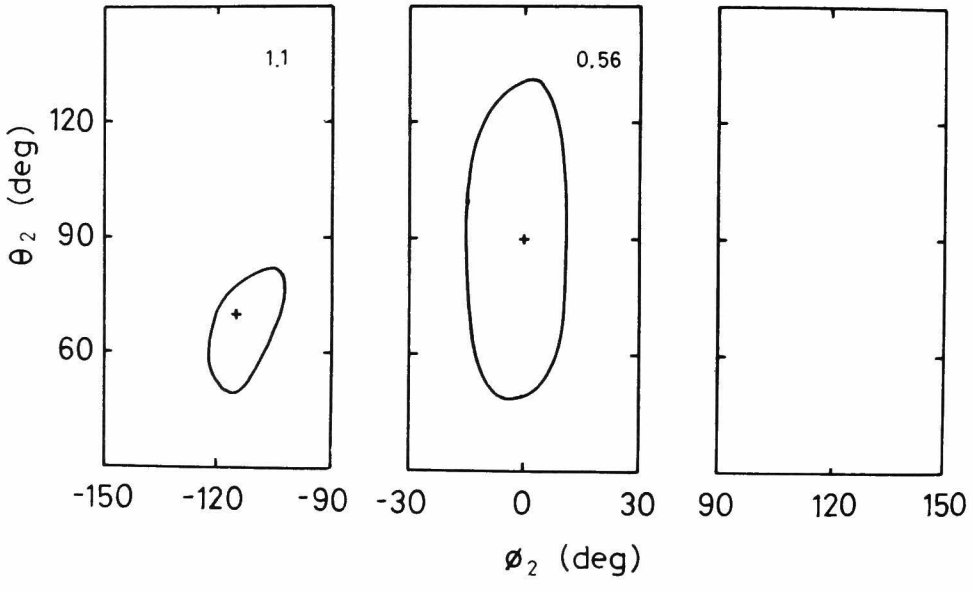

Fig. 6. Energy maps for 1,3-DNPr as a function of θ_2 and ϕ_2, where θ_1 and ϕ_1 are fixed at gauche position ($\theta_1=70^{\circ}$, $\phi_1=-115^{\circ}$). Notations of the contour lines and numerals are the same as Fig. 3.

Table 3. Conformations and their energies and fractions of 1,3-DNPr. Weighting factors are given by the ratios of areas to the smallest one.

	θ_1 (deg)	ϕ_1 (deg)	ϕ_2 (deg)	θ_2 (deg)	W_i	E_i (kcal/mol)	f_i
t t	90	0	0	90	22	0	0.57
t g^+	90	0	115	105	10	0.56	0.10
t g^-	90	0	-115	75	10	0.56	0.10
g^+ t	105	115	0	90	10	0.56	0.10
g^- t	75	-115	0	90	10	0.56	0.10
$g^+ g^+$	110	115	115	110	1	1.1	0.01
$g^- g^-$	70	-115	-115	70	1	1.1	0.01

Table 4. Conformations and their energies and fractions of 1,3-DNBu.

	θ_1 (deg)	ϕ_1 (deg)	ϕ_2 (deg)	θ_2 (deg)	W_i	E_i (kcal/mol)	f_i
t t	90	0	15	120	5.0	0.31	0.35
t g^+	90	0	115	120	4.7	0	0.56
t g^-	90	5	-125	70	3.0	3.6	0.0
g^- t	70	-110	15	120	2.0	1.1	0.04
g^+g^+	110	115	115	120	1.0	0.5	0.05

Table 5. Conformations and their energies and fractions of 2,4-DNPe.

	θ_1 (deg)	ϕ_1 (deg)	ϕ_2 (deg)	θ_2 (deg)	W_i	E_i (kcal/mol)	f_i
meso							
t g^+	-120	-15	115	-120	4.4	0	0.49
g^-t	-120	-115	15	-120	4.4	0	0.49
g^-g^+	-120	-105	100	-120	1.0	1.1	0.02
racemo							
t t	-60	15	15	120	1.4	1.1	0.18
g^+g^+	-60	115	115	120	1.0	0	0.82

mum position in consistent with that obtained on the previous map. For each stable conformation, angles, minimized potential energy, weighting factor, and fraction of the conformation at 25 °C are listed in Tables 3, 4, and 5.

For 1,3-DNPr, conformation energy map as a function of skeletal bond rotations, ϕ_1 and ϕ_2, is shown in Fig. 7, where the angles, θ_1 and θ_2 are fixed at $\theta_1=90^\circ$ and $\theta_2=90^\circ$. In this figure, a minimum position (tt) is marked by +, and the excimer conformations (g^+g^- or g^-g^+) are represented by ●. The most stable conformation is situated at tt, and is surrounded by four equivalent tg conformations. The potential energy of tg conformation is ca. 500 cal/mol larger than that of tt. The minimized energy by the rotation of all angles at the important region of Fig. 7 are calculated. The result indicates that the barrier energies corresponding to the transitions of tt - tg and tt - g^+g^- (tt - g^-g^+), are about 3.6 kcal/mol and 7 kcal/mol, respectively. These potential energies mainly result from the intrinsic torsional energies.

For 1,3-DNBu, conformation energy map is shown in Fig. 8. The fixed angles, θ_1 and θ_2 are chosen to be $\theta_1=90^\circ$, $\theta_2=120^\circ$ for 1- and 3-naphthyl substituents, respectively, according to the result obtained by the local potential maps. The most stable conformation is found at tg^+, and metastable confomations appear at tt, g^-t, and g^+g^+. The barrier energy corresponding to the transition of tt - tg^+ and tt - g^-g^+ show the same values as that for 1,3-DNPr.

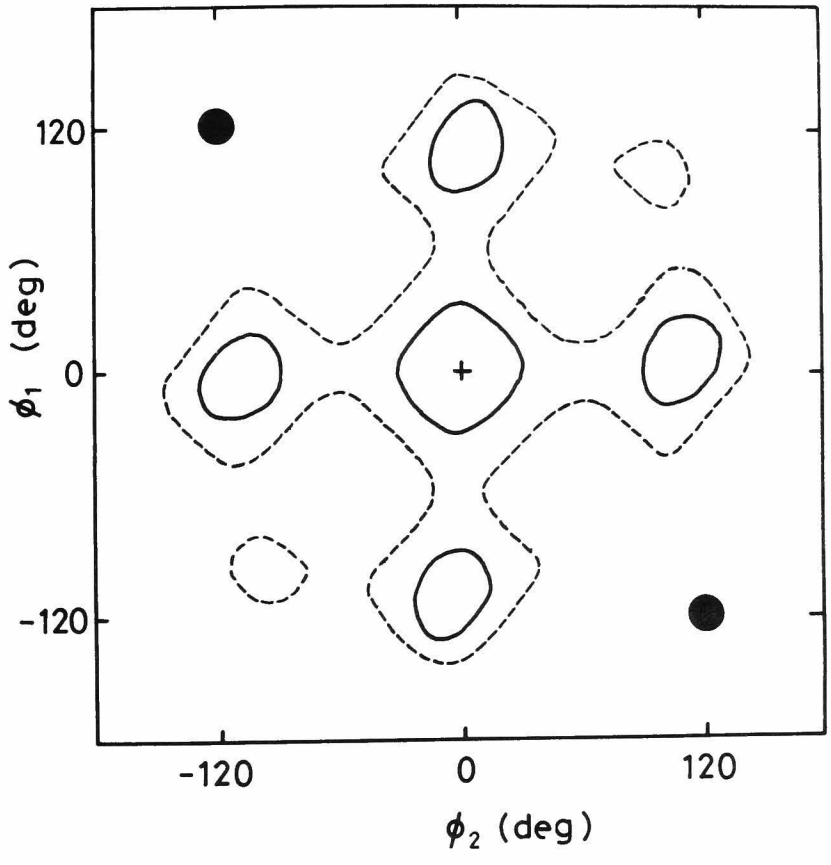

Fig. 7. Conformation energy map for 1,3-DNPr as a function of ϕ_1 and ϕ_2. The rotation angles of naphthalene units, θ_1 and θ_2 are fixed at $\theta_1=\theta_2=90^{\circ}$. The most stable position and the excimer conformations are marked by + and ●, respectively. Full lines indicate the 2 kcal/mol higher energy than the minimum. Dotted lines indicate the 4 kcal/mol higher energy than the minimum.

For 2,4-DNPe, conformation energy maps are shown in Fig. 9 for meso isomer and Fig. 10 for racemo isomer. In these compounds, most of the conformations are unstable due to the steric hindrance of methyl substituents. Only two conformations are allowed: tg^+ and g^-t conformations for meso isomer, tt and g^+g^+ conformations for racemo isomer. In Fig. 9, the third potential minimum is observed beside the excimer conformation, g^-g^+, but its fraction is so small that it can be neglected as shown in Table 5.

6-4. Pathway of Conformational Changes and Excimer Formation Processes

In the ground state, the excimer conformation marked by ● , is one of the unstable conformations by the steric hindrance of naphthalene units. However, in the excited state, this conformation can be stabilized by the electronic interactions between two naphthalene groups. The enthalpy change due to excimer formation is found to be ca. 4.5 kcal/mol for the intermolecular excimer formation in THF. This electronic interaction acts mainly in the parallel alignment of two naphthalene units, and the investigations on various dinaphthylalkanes have demonstrated the strict geometrical requirements for the interaction of chromophores. The initial distribution of the molecular conformations at the instance of photo-excitation is the same as that in the ground state, and conformational relaxation to the excimer state occurs from the initial distribution. When the molecular motion is frozen in

the low temperature region, there is no indication of specific interaction between naphthalene units both in the ground state and excited state for the compounds studied in this chapter. Hence, the relaxation processes are considered hereinafter assuming that there is no excimer interaction between two naphthalene units except in the excimer conformation.

For 1,3-DNPr, conformation energy map shows that the tt position is the minimum conformation where the naphthalene units are furthest apart from each other. Two excimer conformations, g^+g^- (g^-g^+) are equivalent in this compounds. As for the pathway to the excimer conformations, the direct conformational changes from tt to g^+g^- (g^-g^+), which require a co-operative motion of two rotation angles, ϕ_1 and ϕ_2, are unfavorable, since such transitions need to overcome the barrier, ca. 7 kcal /mol. This barrier comes from the intrinsic torsional potential. This calculated energy for the rotational barrier of the co-operative motion is higher than the activation energy, ca. 5 kcal/mol observed experimentally for the association rate constant, k_{21}. In order to reach the excimer conformations, it is necessary to pass through the tg conformations which are neighboring both the stable tt and the excimer conformations. For the fraction of tg, a fairly large value is obtained: 0.4. The barrier energy for the conformational change from tt to tg is found to be 3.6 kcal/mol, and this value is sufficiently smaller than the activation energy of excimer formation. Hence, the occurrence of tg

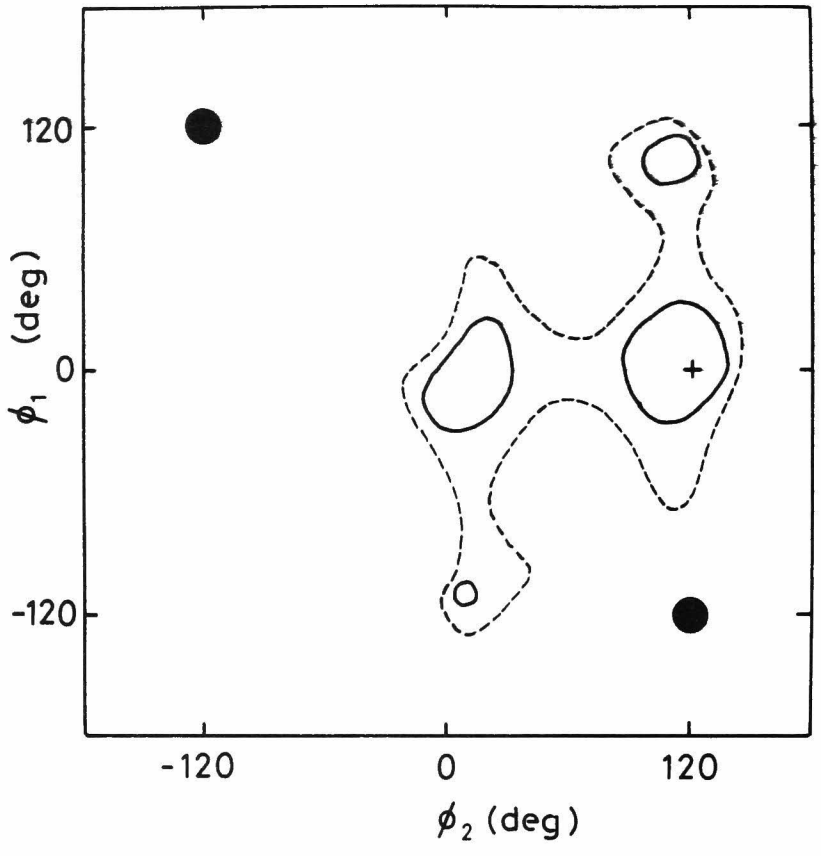

Fig. 8. Conformation energy map for 1,3-DNBu as a function of ϕ_1 and ϕ_2. The rotation angles of naphthalene units, θ_1 and θ_2 are fixed at $\theta_1=90^o$, $\theta_2=120^o$. The most stable position and the excimer conformations are marked by + and ●, respectively. Full lines indicate the 2 kcal/mol higher energy than the minimum. Dotted lines are the 4 kcal/mol higher energy than the minimum.

conformations under the equilibrium, tt $\rightleftarrows$ tg, contributes to the intramolecular excimer formation in 1,3-DNPr, since the tg conformation can be considered as a precursory conformation of the intramolecular excimer.

For 1,3-DNBu, the energy map indicates that the most stable conformation is tg^+ which corresponds to the planar conformation of skeletal chain. The minimized energy for the tt conformation is 300 cal /mol higher than that of lowest conformation, and the barrier energy for the transition from the tt conformation to the excimer state is the same as that of 1,3-DNPr. The fractions of the conformations except for tg^+, tt, are negligibly small owing to the steric hindrance of methyl substituent. In this compound, two excimer conformations, g^+g^- and g^-g^+ are not equivalent. The g^+g^- conformation which lies to the upper left-hand corner in Fig. 8, is unsuitable for the excimer site, since there is no available conformation adjacent to the excimer conformation. The intramolecular excimers in 1,3-DNBu, therefore, are formed at the g^-g^+ conformation. The sum of fractions for tg^+ and g^-t which are neighboring the excimer site, are found to be 0.6. This predicts a larger association rate constant for 1,3-DNBu than that for 1,3-DNPr.

For 2,4-DNPe(meso), the calculation shows three potential minima, tg^+ of lowest energy, its mirror image g^-t, and g^-g^+ which corresponds to the trans conformation of the methyl groups. All other conformations cannot have appreciable fractions. The distribution is found predominantly in the tg^+ and

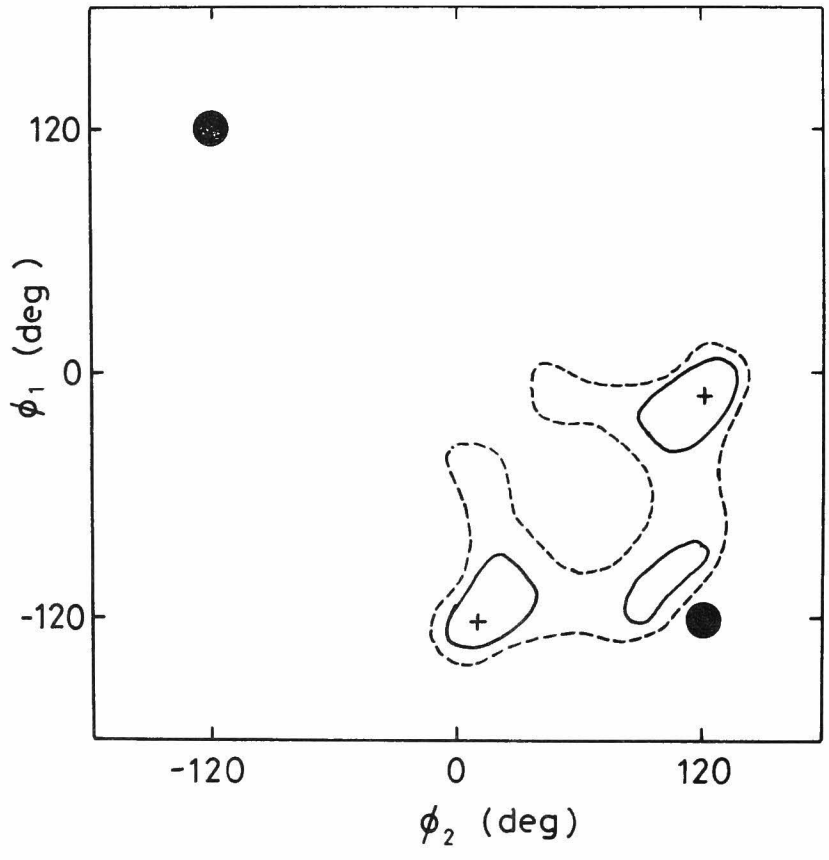

Fig. 9. Conformation energy map for 2,4-DNPe (meso). The rotation angles of naphthalene units, θ_1 and θ_2 are fixed at θ_1=-120°, θ_2=-120°. The most stable position and the excimer conformations are marked by + and ●, respectively. Notations of lines are the same as Fig. 7.

g^-t forms, which are available conformations adjacent to the excimer one, g^-g^+. There is a little fraction for the excimer conformation, g^-g^+ in the ground state. This rotational isomer was found in the calculations for meso-diphenylpentane and its derivatives.[11,12] The fraction of this g^-g^+ conformation has been reported to be a few percent by NMR spectroscopy.[13] In this calculation, it was estimated to be 1 - 2% at 25 °C. If appreciable fraction of 2,4-DNPe(meso) takes this conformation, a fast rising component of almost no time-lag from excitation pulse should be observed in the time-resolved excimer fluorescence measurement. However, such indication cannot be observed at the present measurement. Efficient intramolecular excimer formation can be expected for 2,4-DNPe(meso), since the large part of molecules take the adjacent conformations to the excimer state, g^-g^+. Another excimer conformation, g^+g^- can be ignored, because it has no available conformation in the neighboring positions, moreover, there is a steric hindrance between two methyl substituents at this excimer state.

The calculation for the three compounds, 1,3-DNPr, 1,3-DNBu, and 2,4-DNPe(meso) indicates that the intramolecular excimers are formed by the internal rotation, $t \rightarrow g$, from the tg^+ and g^-t forms. Since the activation energies for excimer formation processes are observed to be almost the same as each other, the difference between the rate constants of the excimer formation is due to the frequency factors of their rates. These factors should be proportional to the fraction of the adjacent conformations, tg^+

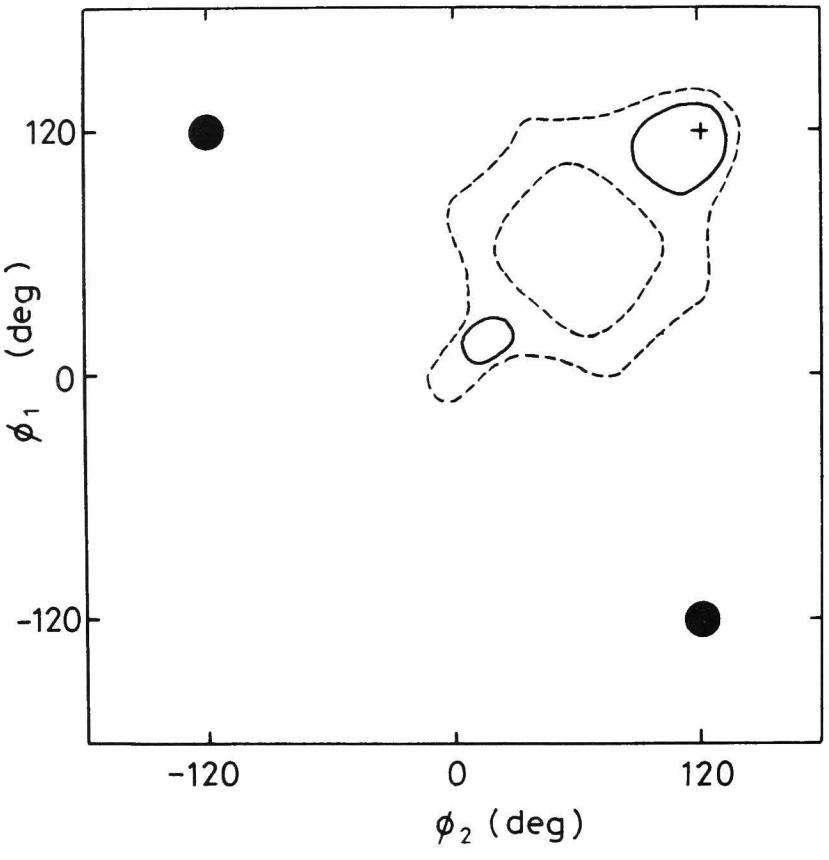

Fig. 10. Conformation energy map for 2,4-DNPe (rac). The rotation angles of naphthalene units, θ_1 and θ_2 are fixed at θ_1=-60°, θ_2=120°. The most stable position and the excimer conformations are marked by + and ●, respectively. Notations of lines are the same as Fig. 7.

and g^-t, if the intramolecular excimers are formed by the same rotational mode. Calculated fractions increase in the order, 1,3-DNPr, 1,3-DNBu, and 2,4-DNPe(meso). This is consistent with the result of the association rate constants determined experimentally. For 2,4-DNPe(meso), somewhat larger values than that expected by the calculation are obtained in the experiments. This fact may come from the existence of the metastable g^-g^+ conformation in the ground state, which lowers slightly the activation energy for the association process.

For 2,4-DNPe(rac), the situation is different from that described above. Calculations reveal the g^+g^+ form of the lowest energy which corresponds to the planar trans conformation of the skeletal chain, and which is neighboring the excimer conformation. However, the internal rotations, $g^+g^+ \rightarrow g^+g^-$ ($g^+g^+ \rightarrow g^-g^+$), are required for the excimer formation, which are a different type of rotations from that of other three compounds. It is known that the barrier to the interconversion of gauche forms, $g^+ - g^-$ ($g^- - g^+$) is higher than that between t and g forms, and the barrier energy has been reported to be about 6.5 kcal/mol.[14] Furthermore, the direction of an approach to the sandwich alignment of two naphthalene units is restricted to a slide of the aromatic plane holding the parallel arrangement. On the route to the excimer state, it is also possible to take the tg^+ (g^+t) conformations which are unstable conformations with the steric hindrance, and imposed the energy, 3 - 4 kcal/mol.[15] This conformational energy is smaller than the activation energy of

excimer formation process. In this respect, the excimers are formed by a t → g transition. But, when viewed from the side of methyl substituents, the t → g transition for the naphthalene units turns to a $g^+ \rightarrow g^-$ ($g^- \rightarrow g^+$) transition for the methyl groups. In either case of rotation for 2,4-DNPe(rac) it is necessary to carry out the interconversion $g^+ \rightarrow g^-$ ($g^- \rightarrow g^+$) to reach the excimer conformation. The small value of the association rate constant and somewhat larger activation energy obtained for this compound is not due to the fraction of the adjacent conformation but due to the different transition mode of the internal rotation.

Since the calculation includes no interaction between naphthalene units in the excited monomer state, the relationship between the activation energy of the excimer formation process and the conformation energy near to the excimer conformation, is not clear. However, the rate of intramolecular excimer formation can be interpreted reasonably by this conformation analysis. Observed rate constants and the results of calculations indicate that the intramolecular excimers are mainly formed by the internal rotation, t → g, and the fraction of the tg state which is the adjacent conformation to the excimer one, serves as an effective concentration in the intramolecular reaction. Figures 11, 12, and 13 are schematic figures of favorable conformational changes and excimer formation processes for 1,3-DNPr, 1,3-DNBu, and 2,4-DNPe(meso), respectively.

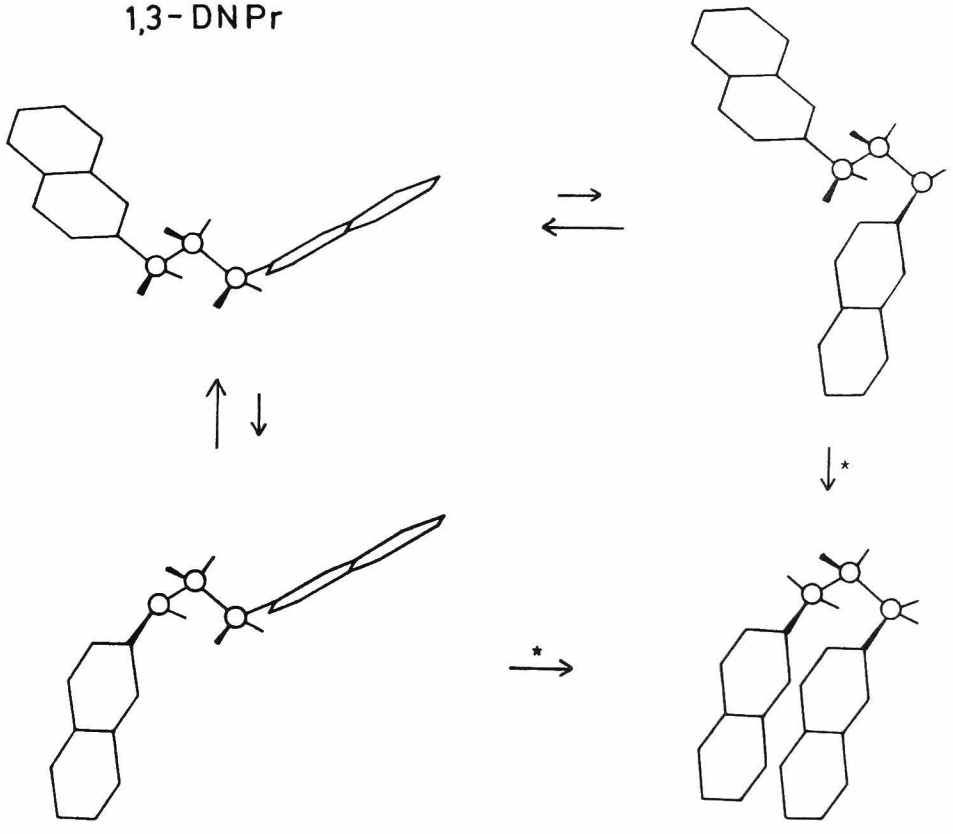

Fig. 11. Schematic diagram of favorable conformational changes in 1,3-DNPr. The sign, * shows the excimer formation process which is efficient only in the excited state.

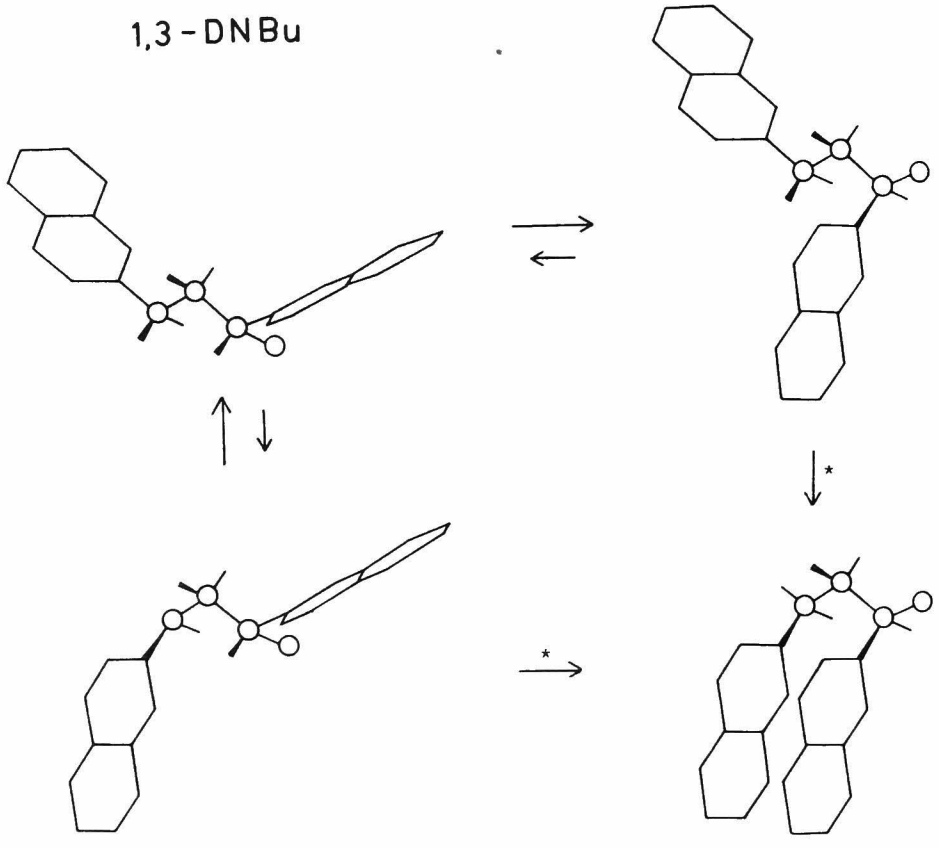

Fig. 12. Schematic diagram of favorable conformational changes in 1,3-DNBu. The sign, * shows the excimer formation process which is efficient only in the excited state.

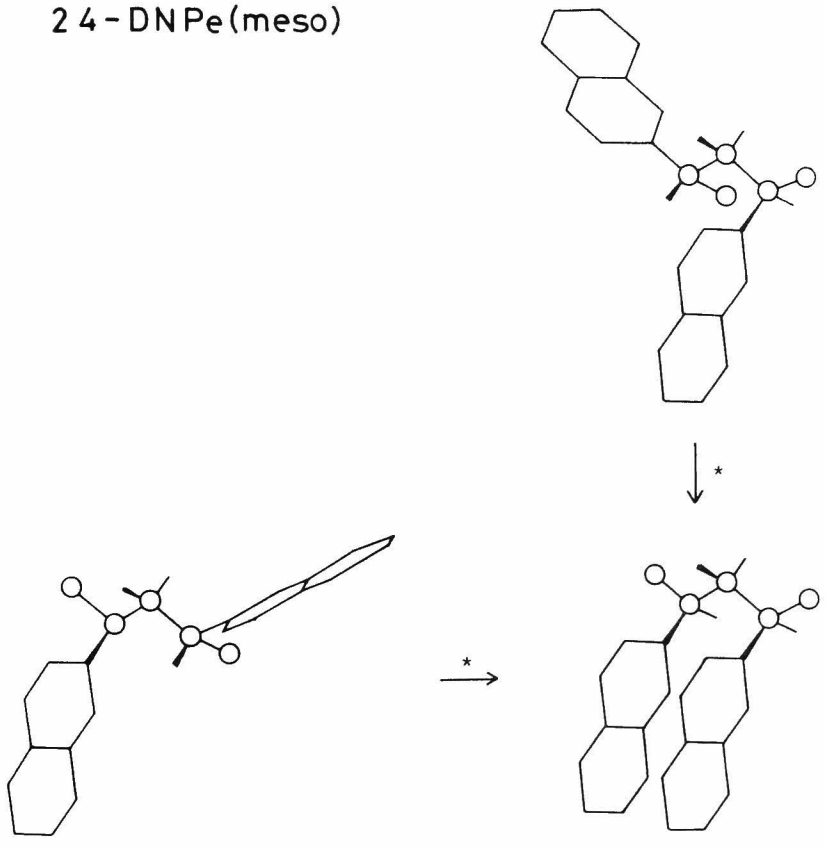

Fig. 13. Schematic diagram of favorable conformational changes in 2,4-DNPe(meso). The sign, * shows the excimer formation process which is efficient in the excited state.

References

1) F. Hirayama, J. Chem. Phys., 42, 3163 (1965).
2) J.W. Longworth and F.A. Bovey, Biopolymers, 4, 1115 (1966).
3) E.A. Chandross and C.J. Dempster, J. Am. Chem. Soc., 92, 3586 (1970).
4) W. Klöpffer, Ber. Bunsenges. Phys. Chem., 74, 693 (1970).
5) R.S. Davidson and T.D. Whelan, J. C. S., Chem. Commun., 1977, 361.
6) L. Bokobza, B. Jasse, and L. Monnerie, Eur. Polym. J., 13, 921 (1977).
7) S. Ito, M. Yamamoto, and Y. Nishijima, Bull. Chem. Soc. Jpn., in press.
8) T. Kanaya, Y. Hatano, M. Yamamoto, and Y. Nishijima, Bull. Chem. Soc. Jpn., 52, 2079 (1979).
9) D.A. Brant and P.J. Flory, J. Am. Chem. Soc., 87, 2791 (1965).
10) A. Abe, R.L. Jernigan, and P.J. Flory, J. Am. Chem. Soc., 88, 631 (1966).
11) S. Gorin and L. Monnerie, J. Chim. Phys. Phys.-Chim. Biol., 67, 869 (1970).
12) B. Froelich, B. Jasse, C. Noel, and L. Monnerie, J. C. S., Faraday Trans. II, 74, 445 (1978).
13) T. Moritani and Y. Fujiwara, J. Chem. Phys., 59, 1175 (1973).
14) J.E. Piercy and M.G.S. Rao, J. Chem. Phys., 46, 3951 (1967).

CHAPTER 7

Intramolecular Excimer Formation in Trimer Model Compounds

7-1. Introduction

The mechanism of intramolecular excimer formation has been clarified by the study of various dimer model compounds using the time-resolved technique. Generally, the formation process is controlled by a conformational relaxation of the skeletal chain, that is, internal rotation from the equilibrium conformation to the excimer conformation after excitation of the chromophore. This implies that these phenomena provide significant information regarding the microstructure of molecules and their relaxation processes.

On the other hand, various vinyl aromatic polymers such as polystyrene, poly(vinylnaphthalene), show efficient intramolecular excimer formation under various conditions. A number of investigations have been reported on the phenomena of excimer formation in polymers. However, the detailed mechanism is not yet to be clarified, owing to the complexity of polymer systems. Quantitative studies of various compounds designed to have simple but similar molecular structures to the dimeric unit of polymer chains, are useful to elucidate the micro-structural factors on the excimer formation processes in polymers.

In comparing the polymer systems with the model dimeric compounds, it should be noted that the micro

environments of an excited chromophore are markedly different in these two systems. In polymers, an excited chromophore is surrounded with the same kind of chromophores in the ground state. Therefore, additional photophysical processes, e.g., energy migration among chromophores, excimer formation between non-adjacent chromophores, seem to be introduced to the kinetic scheme. From this view point, it is interesting to observe the photophysical behavior of the trimer model compound, because its simple molecular structure enables discussion of the relaxation processes quantitatively, and it can be regarded as one of the smallest molecules having the characteristic photophysical process of polymers.

In this chapter, photoluminescence properties of three trimer model compounds are reported. Through the analysis of these model compounds, it becomes possible to clarify the individual interactions of each pair of chromophores in the trimer medel compounds. On the basis of quantitative rate constants from the time-resolved measurements, the relaxation processes of the excitation energy are discussed. It seems that their photophysical behavior provides some useful information for the intramolecular excimers in polymer systems.

7-2. Experimental

Preparation of 1,3-DNPr and 1,5-DNPe was described in Chapter 3 and Chapter 4, respectively. The compound, 1,3-di(2-naphthyl)-5-phenylpentane, which was used in Chapter 5, is abbreviated as NNS in this chapter. The other samples were pre-

pared by the following methods.

1,5-Di(2-naphthyl)-3-phenylpentane (NSN): 1,5-Di(2-naphthyl)-3-pentanone which was obtained in the process of the synthesis of 1,5-DNPe, was reacted with phenylmagnesium bromide in ether solution. The oily product was recrystallized from cyclohexane to give the colorless crystalline 1,5-di(2-naphthyl)-3-phenylpentane-3-ol: mp 120 - 121 °C. The pentanol thus obtained was reduced in acetic acid solution

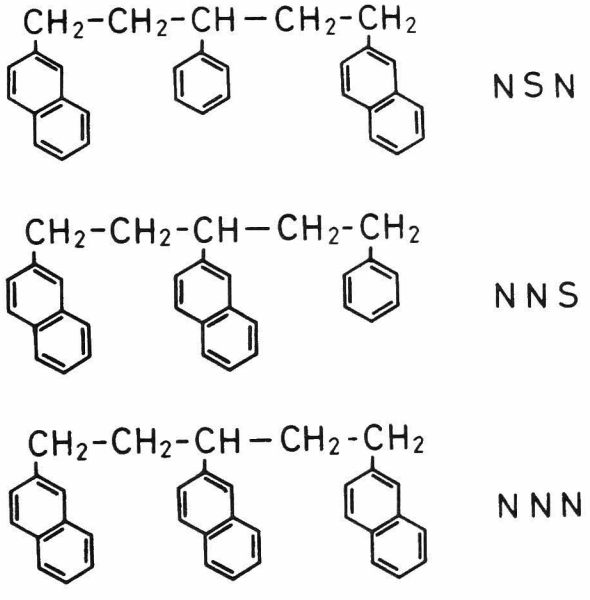

Fig. 1. Molecular structures of trimer model compounds used in this chapter.

by addition of zinc dust and hydrochloric acid. The reaction mixture was extracted with benzene. The product was purified by a column chromatography on silica gel with hexane-dichloromethane (4:1) as eluent: IR(KBr) 3050, 2940, 1630, 1600, 1510, 820, 740, 700, and 475 cm^{-1}. Found: C, 92.85; H, 6.91%; M^+, 400. Calcd for $C_{31}H_{28}$: C, 92.95; H, 7.05%; M, 400.

1,3,5-Tri(2-naphthyl)pentane (NNN) was synthesized by the same method as that used for NSN. 2-Bromonaphthalene was used instead of bromobenzene. After the purification by column chromatography on silica gel, the colorless oily product was obtained: IR(KBr) 3050, 2940, 1630, 1600, 1500, 815, 740, and 475 cm^{-1}; NMR(CS_2) δ = 1.95-2.30 (4H, m), 2.46-2.90 (5H, m), and 7.0 - 7.8 (21H, m). Found: C, 93.49; H, 6.99%; M^+, 450. Calcd for $C_{35}H_{30}$: C, 93.29; H, 6.71%; M, 450.

The molecular fomula of the trimer model compounds were shown in Fig. 1. Photoluminescence measurements were carried out for the degassed THF solutions. Detailed methods were described in the previous chapters.

7-3. Results

7-3, 1. Photophysical Behavior

Photophysical properties of three trimer model compounds, NSN, NNS, and NNN are observed. The singlet excited state of the phenyl chromophore lies at considerably higher energy level than that of the naphthalene chromophore. Because of the excitation wavelength (ca. 276 nm) used in these measurements,

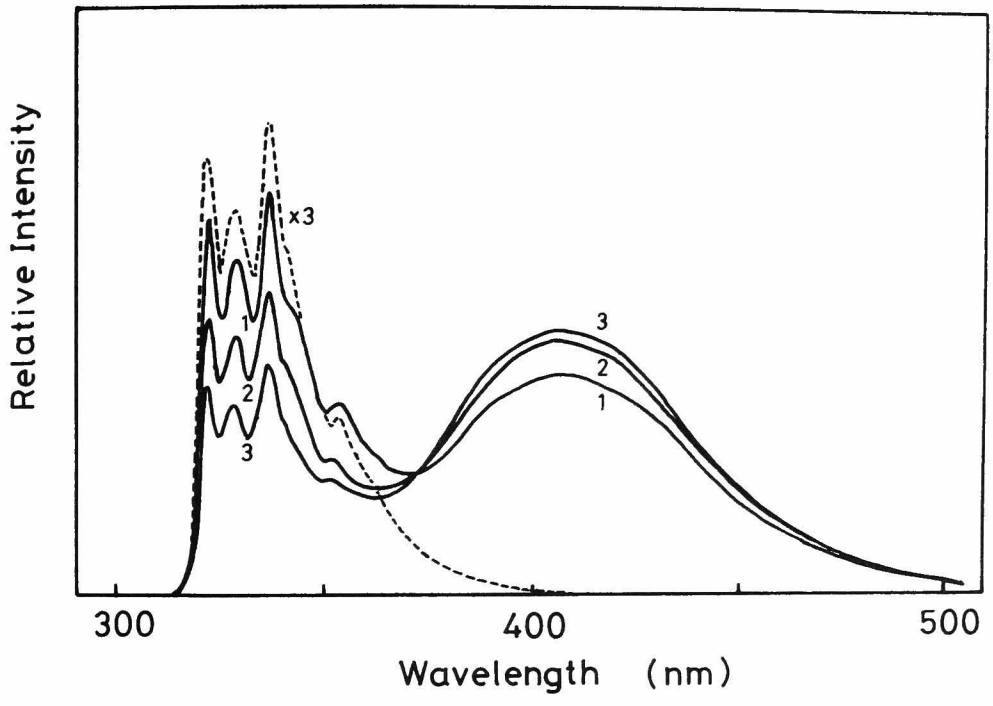

Fig. 2. Fluorescence spectra in THF at -20 °C. Full line: (1) 1,3-DNPr, (2) NNS, and (3) NNN. Broken line: NSN.

the phenyl chromophore is photophysically inert, although the phenyl group affects the molecular conformation as the naphthalene units. Absorption spectra of these trimers are essentially identical. Fluorescence spectra at - 20 °C are shown in Fig. 2, together with the dimeric model compound, 1,3-DNPr. There is no emission of intramolecular excimers in the compound, NSN which does not satisfy the n = 3

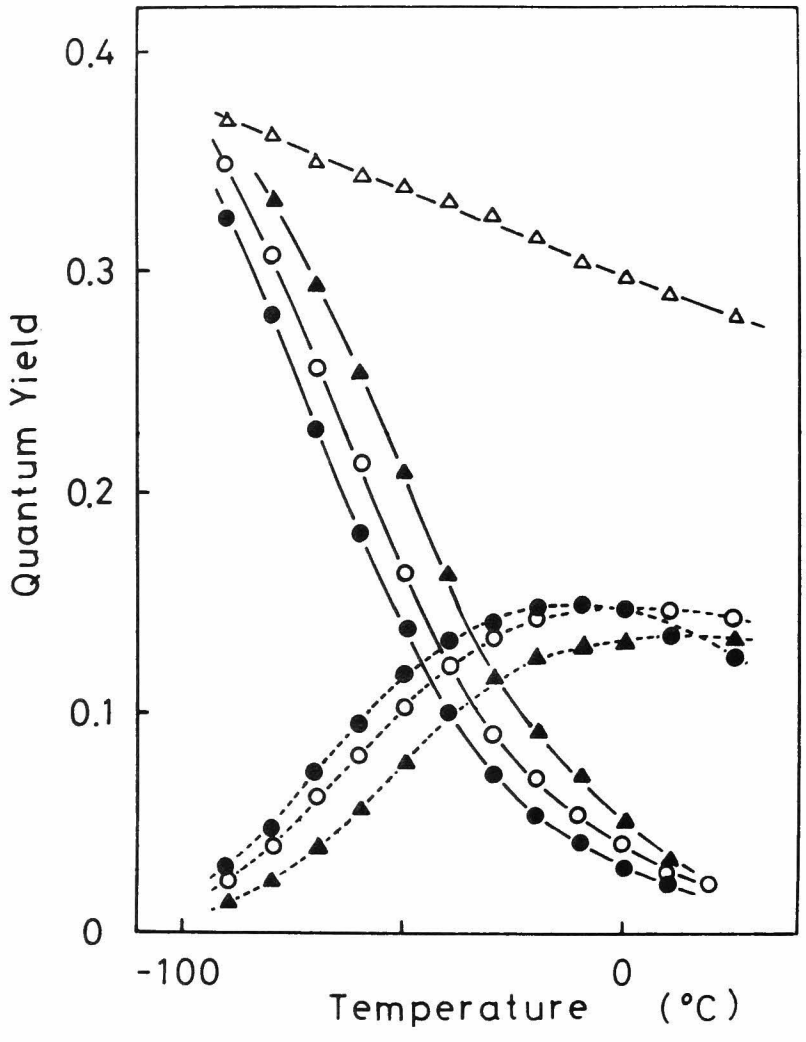

Fig. 3. Temperature dependence of the quantum yields in THF. ● : NNN, ○ : NNS, △ : NSN, and ▲ : 1,3-DNPr. Full lines are the quantum yields of the monomer fluorescence and broken lines are the quantum yields of the excimer fluorescence.

rule. But, for NNS and NNN, efficient intramolecular excimer formation are observed. The monomer and excimer fluorescence bands of the trimers are the same as those of the dimer model compound. The temperature dependence of the quantum yields for the monomer and excimer fluorescence are shown in Fig. 3. NSN shows no indication of the excimer formation in the whole temperature range as for the case of 1,5-

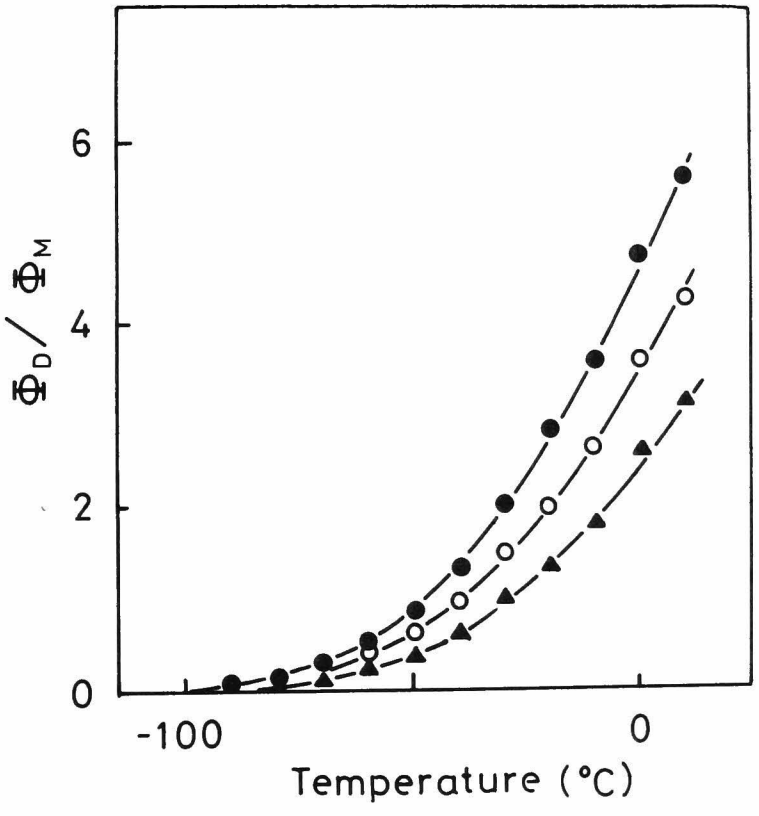

Fig. 4. Temperature dependence of the quantum yield ratio, Φ_D/Φ_M. ● : NNN, ○ : NNS, and ▲ : 1,3-DNPr.

Table 1. Intramolecular excimer formation rate constants and their activation energies

Temp. (°C)	$k_{21} \times 10^{-7}$ (s^{-1})		
	1,3-DNPr	N N S	N N N
25	21.	29.	49.
0	12.	17.	26.
-20	4.8	7.0	10.
-40	1.9	2.8	4.4
-60	0.7	1.0	1.4
E_a (kcal/mol)	5.1	5.3	5.4

DNPe, and the quantum yield of the monomer fluorescence and lifetime agree with those of MNEt. Hence, it can be concluded that there is no interaction between two naphthalene chromophores at the end of trimer model compound. The ratios of the excimer fluorescence quantum yield (Φ_D) to the monomer fluorescence quantum yield (Φ_M) of NNS, NNN, and 1,3-DNPr at various temperatures are shown in Fig. 4. NNS and NNN show similar temperature dependence to 1,3-DNPr. As mentioned in Chapter 5, the intramolecular excimer in NNS is formed more effi-

ciently than 1,3-DNPr, and its efficiency is almost identical with 1,3-DNBu, because of the configurational effect of the equilibrium conformations. Furthermore, NNN shows higher efficiency of excimer formation than NNS, although the equilibrium conformations seems to be little affected by the change of the molecular structure from S to N at one end of the trimer model compound.

In order to clarify the fluorescence behavior, the individual rate constants in the photophysical kinetic scheme are determined by the measurements of the rise and decay curves for the excimer fluorescence. The differences in the rate constants for NNS and NNN are mainly in the association rate constant, k_{21}, and the values are listed in Table 1, together with those of 1,3-DNPr. The rates k_{21} for NNN are 1.4 - 1.6 times larger than those for NNS. Other rate constants for both NNS and NNN are quite similar, although a little difference is found in the dissociation rate, k_{12} in high temperatures. The logarithms of k_{21} against the reciprocal of temperature are plotted in Fig. 5. The activation energies for the excimer formation process are given as the slopes and are found to be almost the same value, 5.1 - 5.4 kcal/mol.

7-3, 2. Conformation Analysis

Conformation energies of the trimer model compounds are calculated. The pathway from the stable conformation to the excimer conformation after excitation of a chromophore is estimated from the results. The procedures are the same as those for

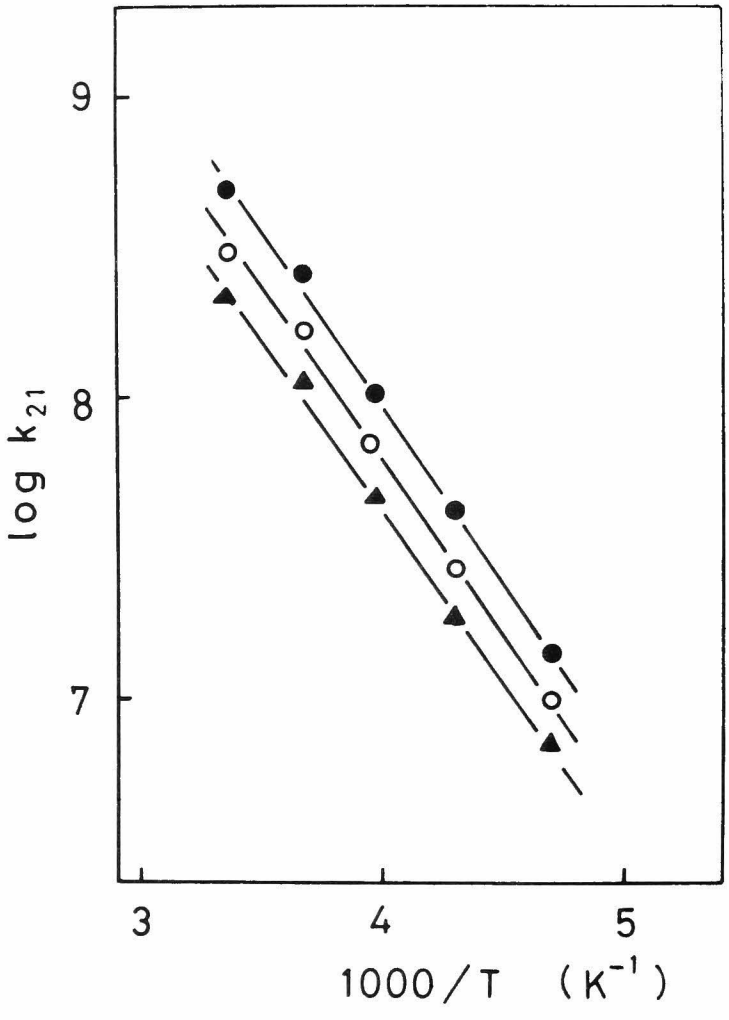

Fig. 5. Arrhenius plot of the association rate constant, k_{21}. ● : NNN, ○ : NNS, and ▲ : 1,3-DNPr.

dimers described in Chapter 6. But, for the trimers, there are some difficulties in calculating their energies in addition to the procedure for dimers. We must consider seven independent rotational angles to generate a given conformation of a trimer: four rotational angles, ϕ_1, ϕ_2, ϕ_3, and ϕ_4 for the skeletal chain and three rotational angles, θ_1, θ_2, and θ_3 for the aromatic groups, which are denoted in

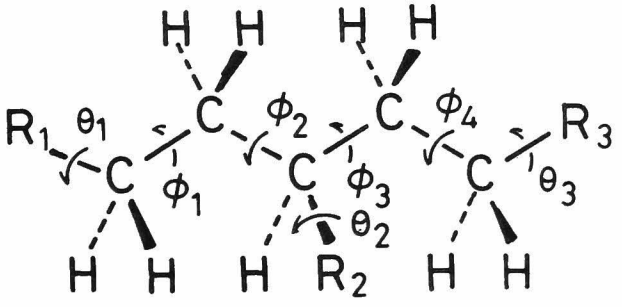

	R_1	R_2	R_3
3-PhPe	H	Ph	H
N S N	Naph	Ph	Naph
N N S	Naph	Naph	Ph
N N N	Naph	Naph	Naph

Fig. 6. Structural parameters of trimer model compounds.

Fig. 6. The angles, ϕ_i are taken as 0^o in the trans conformation. The angles for terminal aromatic groups, θ_1 and θ_3 are taken as 0^o when the carbon atoms, C_2 or C_4 lie in the aromatic planes of R_1 or R_3, respectively. The angle, θ_2 is taken as 0^o, when the hydrogen atom attached to C_3 lies in the aromatic plane of R_2. Even if the rotational angles, θ_i for the aromatic groups are eliminated from consideration, a large number of conformations seem to take minimum energies as a function of ϕ_i: 3^4 = 81. Furthermore, the stable rotation angle, θ_2 for the middle aromatic group, R_2 and the breadth of the potential map around the minimum position, must be estimated, although they relate closely to the conformation of either side of the skeletal chain.

To begin with, calculation was carried out for 3-phenylpentane (3-PhPe), in which three rotation angles, ϕ_2, ϕ_3, and θ_2 are considered. Figure 7 shows conformation energy maps as a function of ϕ_2 and θ_2, when another angle ϕ_3 is fixed at the minimum position, and Table 2 gives the most stable angles, minimum energies and the areas surrounded by the contour of 500 cal/mol higher than the energy of each minimum position. Some important features of these figure and table are noted: (1) Only three conformations are stable in 3-phenylpentane. Other conformations can be ignored because of the high potential energies and small areas on the energy maps around each minimum position. This result reduces the number of conformations to be taken into consideration. (2) The minimum positions of the angle ϕ_2 in those

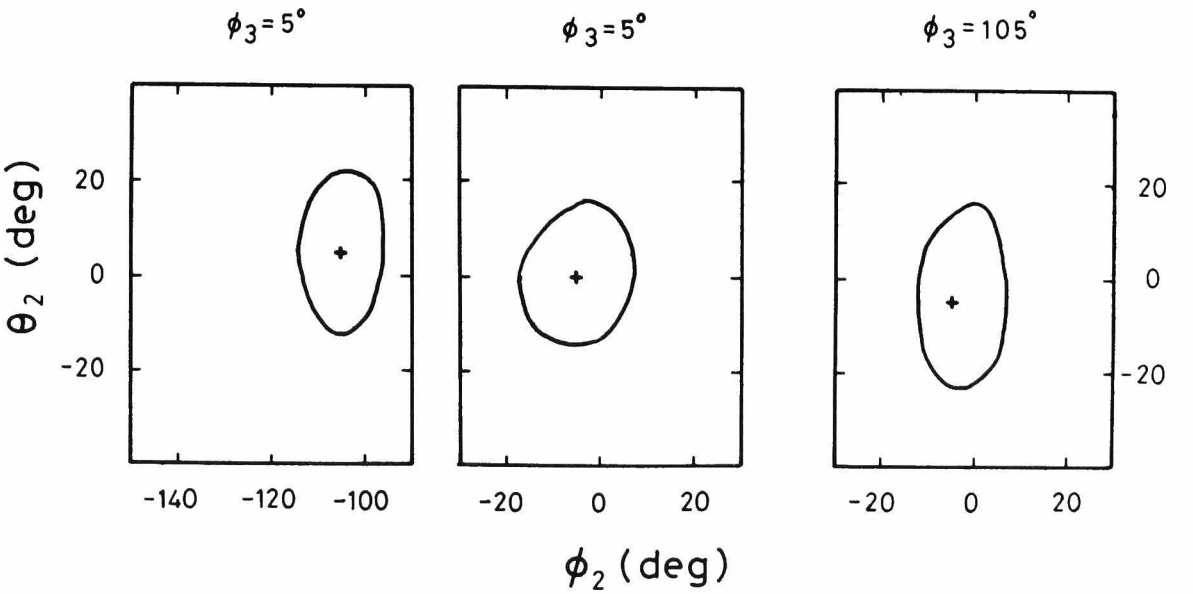

Fig. 7. Conformational energy maps of 3-phenylpentane. The energy minima are marked by the sign, +. The contour lines indicate the 500 cal/mol higher energies than each minimum.

Table 2. Stable conformations and their energies of 3-phenylpentane.

	ϕ_2 (deg)	θ_2 (deg)	ϕ_3 (deg)	W_i	E_i (kcal/mol)
t t	-5	0	5	4.4	0
t g^+	-5	-5	105	5.0	0.4
g^-t	-105	5	5	4.1	0.4

stable conformations are consistent with the results for the monomeric model compounds, 2-naphthylbutane which were described in Chapter 6. This means that the stable conformations of the right hand part of the molecule are little affected by those of the left hand part. So, these trimer model compounds may be treated as two dimer molecules connected at the carbon atom, C_3. (3) In the stable conformations, the angle, θ_2 is found in the range of $\pm 5^o$, and the areas for each minimum are almost the same. Then, the rotational angle, θ_2 and the weighting factor for the middle aromatic group are eliminated from the following consideration.

The minimum position and weighting factor for corresponding dimeric model compounds, 1-(2-naph-

Table 3. Stable conformations and their energies, fractions of trimer model compounds.

1,5-DNPe	n	E_i (kcal/mol)	f_i
tttt	1	0	0.26
tttg	4	0.5	0.19
ttgt	4	0.7	0.33
N S N	**n**	**E_i**	**f_i**
tttt	1	0	0.45
ttgt	2	0.4	0.37
N N N	**n**	**E_i**	**f_i**
tttt	1	0	0.40
ttgt	2	0.4	0.38

n: number of equivalent conformations.

thyl)-3-phenylbutane and 1,3-di(2-naphthyl)butane are calculated. The data for 1,3-DNBu were already shown in Chapter 6. Using the results for the dimer model compounds and Table 2, stable conformations and their energies and fractions for NNS and NNN are obtained, and the results are given

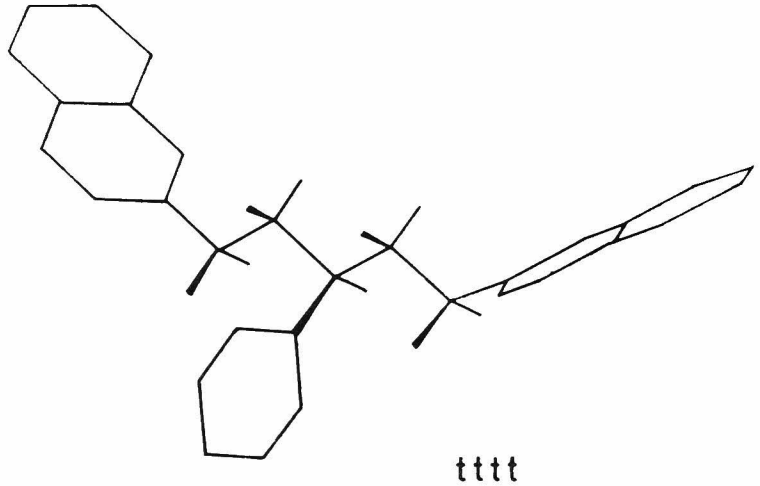

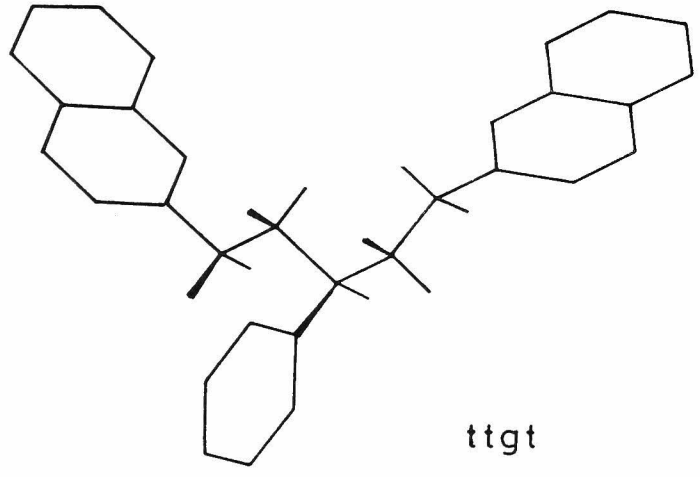

Fig. 8. Stable conformations of the trimer model compound, NSN.

in Table 3 together with 1,5-DNPe. Two conformations of NSN having high probabilities are shown in Fig. 8.

7-4. Discussion

7-4, 1. Decay Process of the Naphthyl Groups in NSN

The emission behavior of 1,3,5-triphenylpentane was reported by Hirayama and the mechanism of the excimer formation was discussed. He also observed the lack of excimer formation in 1,5-diphenylpentane, but he did not deny the possibility of excimer formation between two phenyl groups attached to the terminal carbon atoms of skeletal chain. Owing to the presence of the middle phenyl group, relative positions and motion of chromophores may be sufficiently different from those of 1,5-diphenylpentane to enable the close approach of two terminal phenyl groups. In order to discuss the mechanism of the intramolecular excimer formation in the trimer model compound, NNN, it is necessary to clarify the interaction between each pair of naphthalene chromophores.

As shown in the previous section, the compound, NSN shows no interaction between two naphthalene chromophores as in the case of 1,5-DNPe. The excited naphthyl groups of NSN behave like an isolated chromophore. According to the conformational analysis of NSN and 1,5-DNPe, the fraction of fully extended all-trans conformation, tttt for 1,5-DNPe is smaller than that for NSN. Therefore, it seems that the middle phenyl group of NSN makes several gauche forms of the skeletal chain unstable and tends to decrease the degree of freedom of the con-

formational changes. The terminal naphthyl groups of NSN are, in average, more distantly separated than those of 1,5-DNPe, then, from a view of the conformation in the ground state, the trimer model compound, NSN has less advantage than 1,5-DNPe for the intramolecular excimer formation. In the excited state, if an intramolecular excimer is formaed in this compound, the skeletal chain must take such a conformation as shown in Fig. 9. This is the unstable g^+g^- conformation due to the so-called, four bond interaction between the methylene groups of C_1 and C_5, and the interaction energy is con-

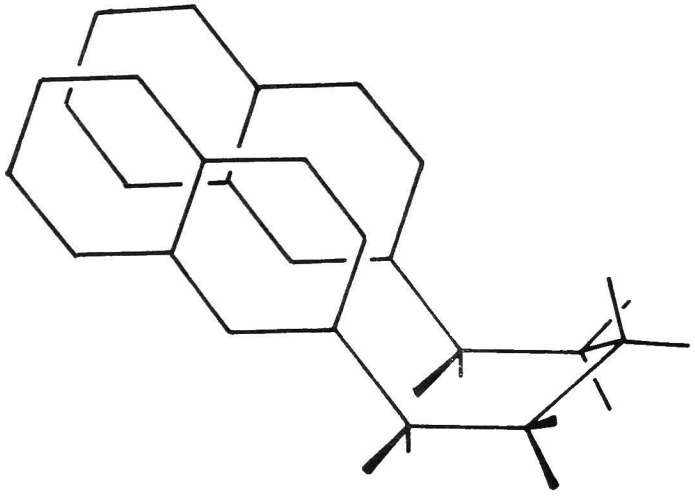

Fig. 9. Excimer conformation of 1,5-DNPe.

sidered to be 3 kcal/mol. The steric hindrance in this conformation mainly prevents the intramolecular excimer formation, and this instability is not mitigated by the presence or absence of the aromatic group at the C_3 position. Then, the compound NSN can not form the intramolecular excimer.

Since the stable positions of the skeletal bonds and the conformation energies are little affected by changing the chromophore from S to N, there are no appreciable differences in the conformation between NSN and NNN. It is concluded from these results that in the trimer model compound, NNN, the intramolecular excimer is formed only between the adjacent chromophores.

7-4, 2. Intramolecular Excimer Formation Process in NNS

The photophysical properties of NNS are identical with those of 1,3-DNBu, which were described in Chapter 5. The quantum yields, Φ_M and Φ_D, the association rate constant, k_{21} and its activation energy for NNS are almost the same as those for 1,3-DNBu. In the calculation of the conformation energies, the tt conformation for trimers corresponds to the tg conformation of 1,3-DNBu denoted in Chapter 6, where the tg conformation was shown to be most stable and adjacent conformation of the excimer state. The results for NNS in Table 3 show the same fraction of the tt form as that for 1,3-DNBu. The population of the conformation adjacent to the excimer conformation is little affected by the additional benzyl group to the end of the dimer. Furthermore, the

conformational relaxation process to the excimer state after excitation of the chromophore is the same internal rotation process from trans to gauche in both compounds. Then, it may safely be said that the exchange of one terminal aromatic group from S to N brings no appreciable change for the conformation of the other terminal naphthyl group and its relaxation processes. Therefore, the kinetic rate constants of NNS show the rates of photophysical processes of each adjacent pair of naphthyl groups in the trimer, NNN. On the basis of these rate constants, the photophysical processes of NNN can be discussed quantitatively.

7-4, 3. Kinetic Treatment for Excimer Formation in NNN

An efficient intramolecular excimer formation was observed in this compound, and it is due to the increase of the association rate constant, k_{21}. The values are 1.4 - 1.6 times larger than those for NNS as shown in Table 1. The results for NSN indicate that the excimer formation between two terminal naphthyl groups is excluded from the photophysical processes of NNN. So, the intramolecular excimer is formed only between the adjacent naphthyl groups along the skeletal chain. Since the equilibrium conformation and the relaxation process of trimers are not seriously affected by changing the kind of the terminal chromophore from S to N, the increase of the association rate constant can be explained by the following reason; the excited naphthalene chromophore at the middle of the trimer

NNN, can form excimers either with the two terminal naphthyl groups, although the excited naphthyl groups at the end of the trimer have the same probability as those of NNS. So, the efficiency of the intramolecular excimer formation in NNN becomes higher than that of NNS. As mentioned in the previous sections, the association rate of one adjacent pair of naphthyl groups is decided by the rotational motion of the skeletal chain from trans to gauche conformation, whose process is independent of the other pair's conformation. Then, it can be assumed that the association rate, k_{21} for the excited middle chromophore is twice as large as that for the excited terminal chromophores. If the excimer formation rate is averaged for one middle chromophore and two terminal chromophores of NNN, it becomes 4/3 times larger than that of NNS.

In detail, these discussions must be followed on the basis of the reaction kinetic equations. As an averaging process of excitation energy among the chromophores, an energy migration process is taken into consideration. For steady excitation with light of intensity I_o, the kinetic equations are given as follows,

$$d[M_e]/dt = 2I_o/3 + k_{12}[D]/2 + 2k_t[M_m] - (k_{01} + k_{21} + k_t)[M_e] , \quad (1)$$

$$d[M_m]/dt = I_o/3 + k_{12}[D]/2 + k_t[M_e] - (k_{01} + 2k_{21} + 2k_t)[M_m] , \quad (2)$$

$$d[D]/dt = k_{21}[M_e] + 2k_{21}[M_m] - (k_{12} + k_{02})[D]. \quad (3)$$

where $[M_m]$ and $[M_e]$ are concentrations of the excited monomer state of middle and terminal naphthyl groups, respectively, and k_t represents the rate constant of the energy migration process between adjacent naphthyl groups. Under photostationary conditions, $d[M_e]/dt = d[M_m]/dt = d[D]/dt = 0$, the ratio of the quantum yield, Φ_D/Φ_M is given as follows,

$$\Phi_D/\Phi_M = 2k_{21}k_{02}^f(2k_{01} + 3k_{21} + 6k_t) / k_{01}^f\{k_2(3k_{01} + 5k_{21} + 9k_t) - k_{21}k_{12}/2\}. \quad (4)$$

On the other hand, the ratio for NNS is given by Eq. 2-9,

$$\Phi_D/\Phi_M = k_{21}\, k_{02}^f / k_{01}^f\, k_2 .$$

Then, in Eq. 4, the ratio, Φ_D/Φ_M for NNN becomes 4/3 =1.33 times larger than that of NNS under the condition, $k_t \gg k_{21}$ or $k_{12} \gg k_{02}$.

Experimentally, the ratio was found to be ca. 1.4 times larger value than NNS in the temperatures below T_c, and also it is somewhat larger than the expected value in Eq. 4. Since the dissociation rate constant, k_{12} of the intramolecular excimers is smaller than the other rate constants, the experimental results show that the excitation energy is diffusing among the chromophores with considerably fast rate as compared with k_{21}. Similar phenomena were observed for αβ-DNPr in Chapter 4.

To analyze the transient behavior of NNN after excitation by a δ function light pulse, we must consider three rate equations similar to Eqs. 1, 2, and 3. Solving the equations with appropriate

initial conditions: $[M_e]_0 = 2/3$, $[M_m]_0 = 1/3$, and $[D]_0 = 0$, the response functions of the monomer and the excimer emission are generally represented as the sums of three exponential functions,

$$I(t) = \alpha \exp(-\lambda_1 t) + \beta \exp(-\lambda_2 t) + \gamma \exp(-\lambda_3 t), \quad (5)$$

where α, β, γ, λ_1, λ_2, and λ_3 are constants which are determined by the rate constants. The transient

Table 4. Decay parameters of the monomer and excimer fluorescence in the absence or presence of energy migration process.

$k_t = 0$	$\lambda_1 = 1.22$ α	$\lambda_2 = 35.7$ β	$\lambda_3 = 18.9$ γ
$I_M(t)$	0.101	1.04	1.86
$I_D(t)$	2.83	-1.02	-1.81
$k_t = 100$	$\lambda_1 = 1.21$ α	$\lambda_2 = 330.$ β	$\lambda_3 = 24.7$ γ
$I_M(t)$	0.102	0.002	2.90
$I_D(t)$	2.84	-0.002	-2.84

units of k_t, λ_1, λ_2, and λ_3: 10^7 s^{-1}

equations were solved numerically under two conditions where the rate constant k_t takes a sufficiently large value as compared with k_{21}, or takes a very small value. The decay parameters calculated with the rate constants of NNS, are shown in Table 4, and the response functions for both typical values of k_t are shown in Fig. 10. When the migration rate is negligibly small, λ_1, λ_2, and λ_3 relate to the

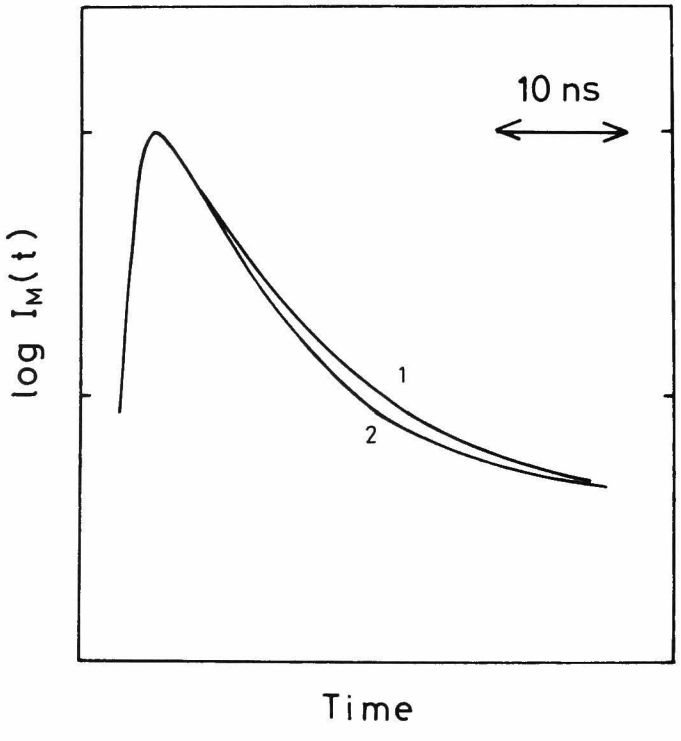

Fig. 10. Decay curves of the monomer fluorescence for NNN simulated by the rate constants of NNS at 0 °C: (1) $k_t = 0$, (2) $k_t = 1.0 \times 10^9$ s^{-1}.

the decay time of the excimer state, of the monomer state for the middle chromophore, and of the monomer state for the terminal chromophore, respectively. As increasing the migration rate, the weight, β for the decay component $\exp(-\lambda_2 t)$ becomes extremely small, and the response functions are represented with the ordinary two component decay functions. They are identical with the function derived for the kinetic scheme assuming that the middle and the terminal naphthyl groups are not distinguished and the association rate constant takes 4/3 times larger than NNS. Experimentally, the decay curves are treated as the sum of two exponential functions, and the averaged association rate constants are determined with the ordinary procedures. Thus obtained values are given in Table 1. The rate constants at various temperatures are found to be 1.4 - 1.6 times larger than those of NNS, and somewhat larger than the values predicted by the above discussion.

The kinetic equations are based on the assumption that the excited monomer states of the middle and the terminal chromophores can be always distinguishable and each excited chromophore forms an excimer with a given rate constant decided by its position on the skeletal chain. But, if the migration rate becomes extremely fast as compared with the conformational relaxation time, the validity of such assumption appears doubtful. When the excitation energy is delocalized among the chromophores, the association rate should be proportional to the probability that the excimer conformation is generated in either of adjacent naphthalene pairs

of the trimer, NNN. Then, the association rate constant of NNN will be doubled by the delocalization of excitation energy, as compared with NNS. The somewhat larger values than those predicted by the kinetic equations seems to be indicative appearance of such delocalization effect.

In this chapter, three trimer model compounds have been examined using the time-resolving technique. By the analysis of these compounds, interactions of each pair of naphthyl groups in the trimer, NNN, can be discussed separately. An enhancement of the excimer formation rate constant was observed for NNN, and the behavior was interpreted with two reasons in addition to those described in the previous chapters. First, the excited middle naphthalene chromophore of the trimer, NNN can chose either of two terminal naphthalene chromophores as the partner of intramolecular excimer. This effect increases the formation rate up to ca. 1.3 times larger than that of NNS. It appears to be an increase of the intramolecular concentration of chromophores. Secondly, the rapid migration of the excitation energy among the chromophores enables to make the excimer conformation more efficiently. Then, it will enhances the association rate still higher in addition to the enhancement due to the first effect. The migration of excitation energy becomes an even more important process in polymer systems, where a lot of aromatic chromophores are linked by a polymer chain.

From the discussion to this point, several factors governing the intramolecular excimer formation processes are clarified:

(1) Configuration of the compound, which decides the stability of the excimer state and the following conformational factors.

(2) Conformational distribution in the ground state, which relates to the intramolecular effective concentration of chromophores and the pathways to the excimer conformation.

(3) The rate of conformational changes from the eqilibrium conformation to the excimer conformation, which are influenced by the environment of the compound, e.g., temperatures and viscosities.

(4) Energy migration between chromophores, which plays an important role in the compound having three of more chromophores on a molecule.

In the following chapters, the photophysical characteristics of polymer systems will be discussed on the basis of the knowledge obtained by various model compounds.

PART III

Excimer Formation Mechanism in Polymer Systems

CHAPTER 8

Polymer Effect on Intramolecular Excimer Formation in Poly(2-vinylnaphthalene)

8-1. Introduction

Inter- and intramolecular excimer formation of various naphthalene derivatives have been investigated in the previous chapters. Particularly, the quantitative study of dinaphthyl and trinaphthylalkanes demonstrated clearly the characteristics of intramolecular excimers. It was shown that a primary condition to form intramolecular excimer is the micro-structure of the compound, in which two aromatic chromophores have to be separated by exactly three carbon atoms along the alkane chain. Vinyl aromatic polymers such as poly(vinylnaphthalene) satisfy this configurational condition, and they appear to show efficient intramolecular excimer formation.

Since the first observation of excimer emission in polystyrene,[1] many spectroscopic investigations of vinyl aromatic polymers have been reported,[2] e.g., poly(vinylnaphthalene),[3] poly(vinylcarbazole),[4] poly(acenaphthylene),[5] poly(vinylpyrene),[6] and poly(arylmethacrylate).[7] In dilute solution, the above mentioned polymers show excimer fluorescence from intramolecularly formed excimers between the pendant chromophores along the polymer chain. The effect of molecular configuration of the polymer

have been examined for various polymers.[8] The excimer formation in polystyrene and poly(vinylnaphthalene) has been considered to be mainly due to interaction between adjacent chromophores on the polymer chain.[9] The photophysical behavior in dilute solutions of these polymers is very similar to their dimeric model compounds, and the excimer formations are thermally activated processes as described in the previous chapter. The phenomena of intramolecular excimer formation seem to be closely connected with micro-structure, conformation of the molecule, and rotational motion of the skeletal chain. Particularly, considering the fact that the relaxation times of polymer molecules obtained by various methods are in the order of magnitude ranging from 10^{-8} s to 10^{-10} s,[10] it can be expected that the phenomena of intramolecular excimers provide some significant information about the micro-Brownian motion of polymer chain segments. On the other hand, it is said that in solid films, energy migration between chromophores plays an important role in the excimer formation, since efficient excimer formation is observed in spite of the restriction of rotational freedom in films.[11] Some workers[12] include the energy migration process in the general kinetic scheme in dilute polymer solutions as well as in films.

The excimer formation mechanism in polymers has not been established yet. It is due to the complexity of polymer systems. In order to clarify the photophysical processes of intramolecular excimer formation in polymers, two approaches are taken in

this chapter. One is to observe the fluorescence behavior of various model compounds designed to clarify interactions of a pair of chromophores. Such studies were first reported by Hirayama[13] and developed by Chandross et al.[14] The other is to determine all rate constants of photophysical process using the time-resolved technique, which has been applied for polymer systems, lately.[15] On the basis of these measurements, the mechanism of the excimer formation in polymers are discussed, and polymer effect on intramoleculae excimer formation are indicated.

8-2. Experimental

Poly(2-vinylnaphthalene) (PVN) was prepared by radical and anionic polymerization of synthesized 2-vinylnaphthalene (VN). The radical polymerization was carried out in benzene solution at 60 °C using α,α'-azobisisobutyronitrile as an initiator. The resulting polymer was reprecipitated several times from benzene solution into methanol and fractionated by the fractional precipitation method. The molecular weight of PVN was determined by vapor pressure osmometry, light scattering measurement, and calibrated GPC measurement. Anionic polymerization was carried out in tetrahydrofuran at 0 °C using sodium-naphthalene as an initiator. In the same way, ABA type block copolymer, poly(VN-block-styrene-block-VN) was prepared from living polystyrene dianion, whose kinetic investigation has been reported by Szwarc et al.[16] The degree of polymerization of middle styrene block was ca. 100. The compositions were

determined by IR spectra, using the bands at 820, 690, and 470 cm^{-1}, and found to be 47, 56, 65 mole% for VN residue. Preparation of model compounds were described in the previous chapters.

Solutions of these samples were prepared in 2-methyltetrahydrofuran (2MTHF) and in tetrahydrofuran (THF) at the concentration of ca. 10^{-4} mol/l for the naphthalene residue. Each solvent was purified by several distillations before use, and its purity was tested by UV absorption spectroscopy. All measurements were carried out in a deaerated condition, and details were described in the previous chapters.

8-3. Results and Discussion

8-3. 1. Emission Properties of PVN in Photostationary Condition

Fluorescence spectra of PVN are shown in Fig. 1, and the temperature dependence of the quantum yields, Φ_M and Φ_D are shown in Fig. 2. The absorption and the monomer fluorescence bands of the polymer are almost idential with those of the dimeric model compounds, except for the shift of both absorption and fluorescence peaks to the longer wavelength of ca. 1 nm. For the excimer band, there is no difference between that of the model compounds and the polymer. Because of the similar molecular structure in the dimeric unit of the polymer, its excimer has the same binding energy and arrangement of the naphthalene chromophores as the dimers. The quantum yield of each emission band shows the same tendency as the dimers with variations in temperature. At

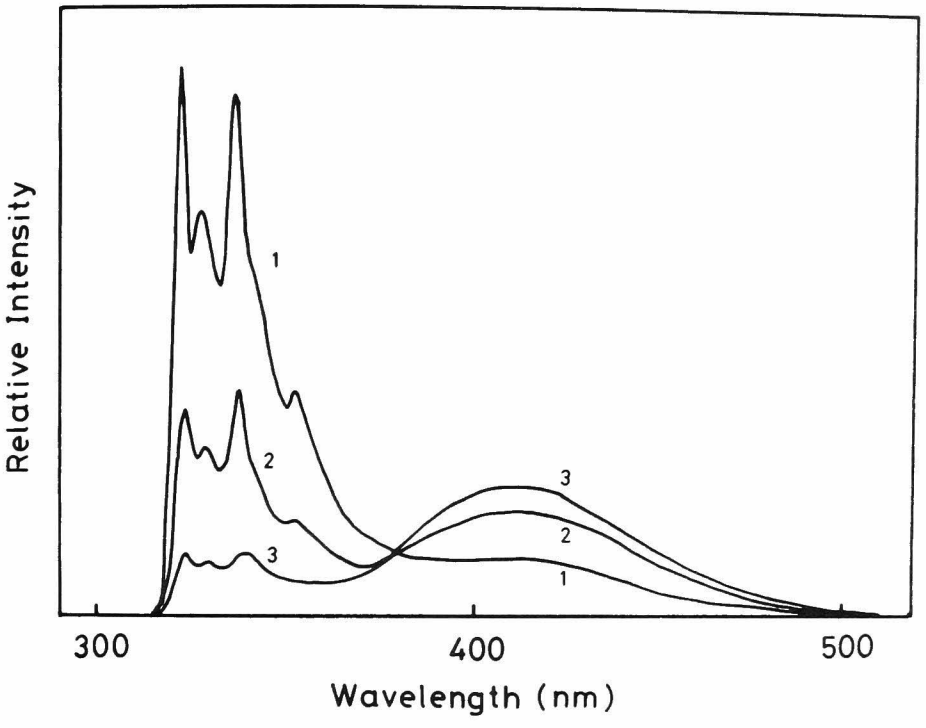

Fig. 1. Fluorescence spectra of PVN in THF: (1) -80 °C, (2) -50 °C, and (3) -20 °C.

77 K, there is no excimer emission on the fluorescence spectra, and at temperatures below -100 °C, the monomer fluorescence quantum yield approaches that of 2-ethylnaphthalene. This indicates that the naphthalene side groups of PVN behave like an isolated naphthalene unit when their molecular motion is suppressed. There are only few suitable conformations to form intramolecular excimers in the polymer chain

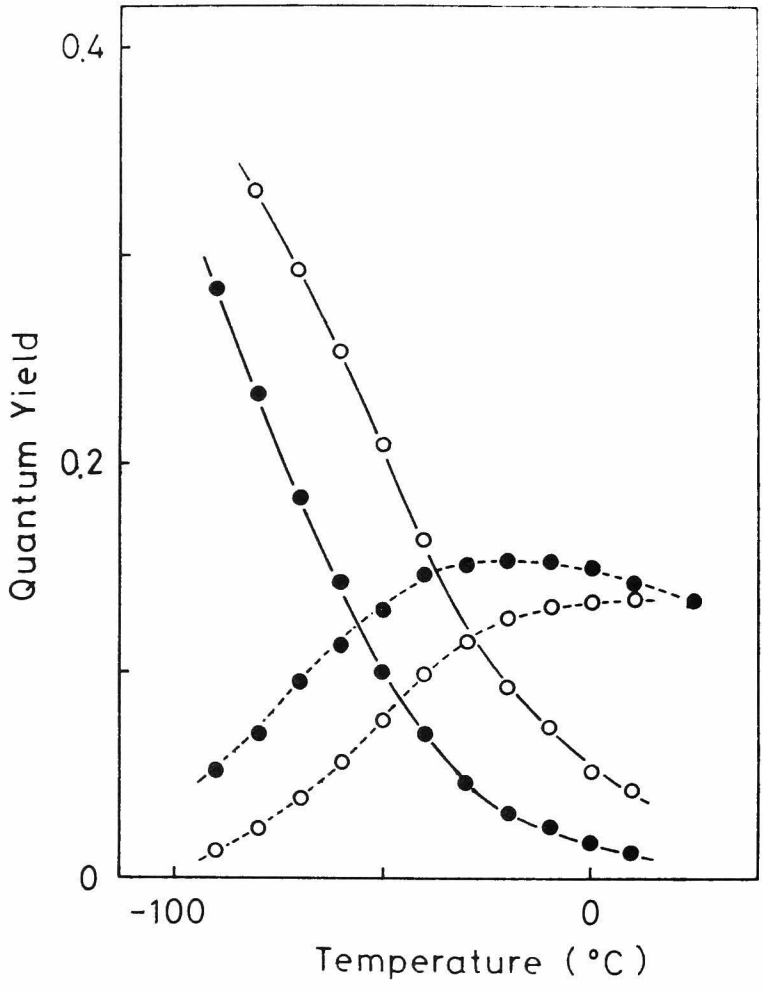

Fig. 2. Temperature dependence of the quantum yields in THF. ○ : 1,3-DNPr and ● : PVN. Full lines are the quantum yields of the monomer fluorescence and broken lines are the quantum yields of the excimer fluorescence.

at such low temperatures, because of the instability of the excimer conformation. With increasing temperature, the excimer formation of PVN becomes more efficient than that of the dimers, and conversely, the monomer fluorescence of PVN is quenched more than that of the dimers. Then, it shows that the intramolecular excimer in polymer systems is formed through dynamical processes due to thermally activated molecular motion of the polymer chain. The activation energy of the association process of PVN is obtained from the slope of the plot, Φ_D/Φ_M against 1/T as shown in Fig. 3, and the energy is found to be 4.8 kcal/mol, which is the same as that of dimers. The excimer formation processes seem to be very much alike with each system, and the polymer excimers are probably formed between adjacent naphthalene chromophores on the polymer chain. These results qualify the application of the scheme of the excimer formation in dimers to the high molecular weight polymers. The excimer conformation is unstable in the ground state, and fairly high conformation energy is assigned to the polymer chain: 2 - 3 kcal/mol.[17] At initial stage of excitation, most of chromophores lie in the monomeric state and then intramolecular excimers are formed with conformational relaxation to the excimer conformation. The pathway of the conformational change is deduced easily from the results in the dimer model compounds. The similar activation energy to the dimers represents that the barrier energy of the excimer formation process is decided by the configuration of the dimeric unit of polymer chain.

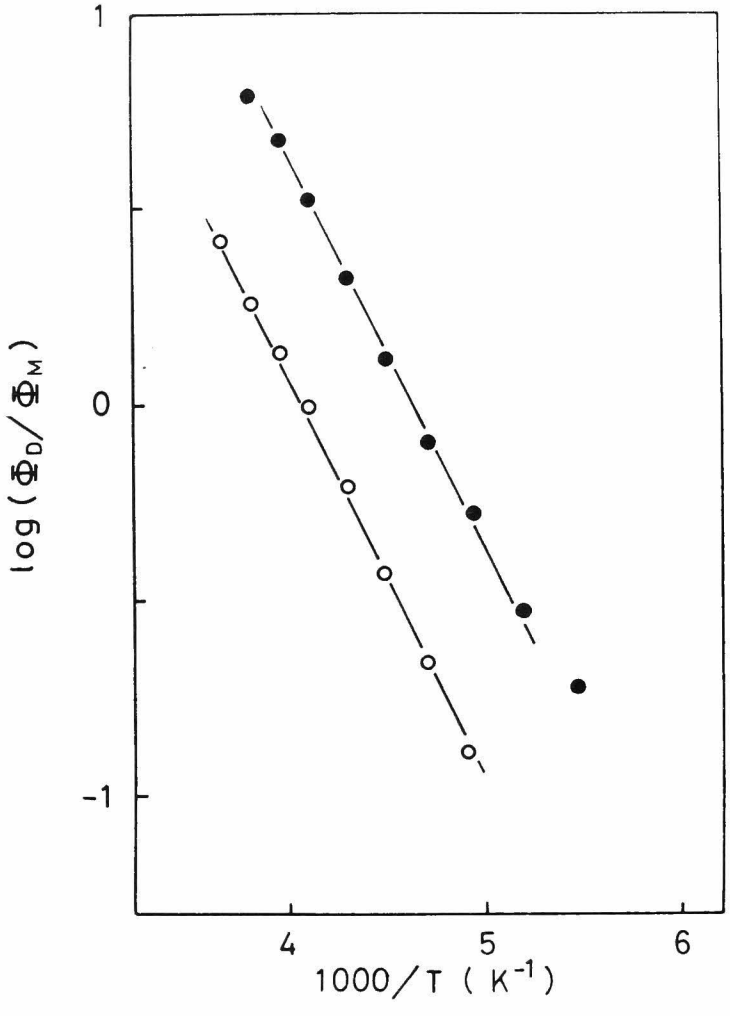

Fig. 3. Arrhenius plots of the quantum yield ratios, Φ_D/Φ_M.
○ : 1,3-DNPr, ● : PVN.

The quantum yield ratio, Φ_D/Φ_M for PVN at a given temperature shows the largest value among the compounds so far observed, and this is probably due to the increase of the association rate constants for PVN. It is exceptional that the emission properties of PVN and 2,4-DNPe(meso) are very much alike. This behavior is again discussed on the basis of the rate constants in the later section.

8-3, 2. Molecular Weight Dependence and Solvent Effect on Emission Properties

Many physical properties of a polymer depend on its molecular weight which is one of the most important characteristics of macromolecules. The photophysical behavior of PVN is measured for the samples having various molecular weight in the range from 4×10^3 to 1×10^6. Figure 4 shows the molecular weight dependence of Φ_M and Φ_D of PVN at several temperatures. In the range of the molecular weight up to ca. 2×10^4 (which corresponds to the degree of polymerization of ca. 100), Φ_D increases as the molecular weight increases, and conversely Φ_M decreases. For the molecular weight higher than that, both quantum yields are invariant with the change of molecular weight. The ratio, Φ_D/Φ_M relates to the association rate constant k_{21}, so the change of k_{21} seems to be the cause of the molecular weight dependence of the intramolecular excimer formation in the polymer.

When considering this effect of molecular weight, the following physical properties affecting the association process must be taken into account:

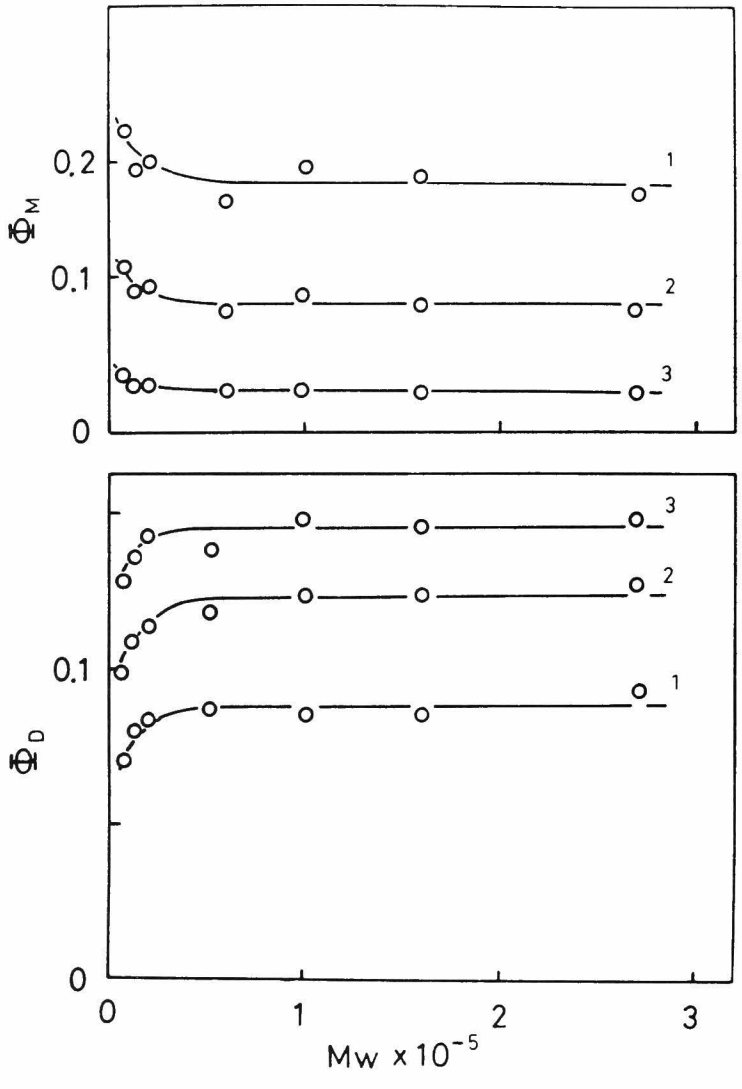

Fig. 4. Molecular weight dependence of the quantum yields, Φ_D and Φ_M in 2MTHF at various temperatures: (1) -70 °C, (2) -50 °C, and (3) -20 °C.

(1) Conformational relaxation time of the segment motion.
(2) Interaction between chromophores situated far apart along the polymer chain, but coming to encounter during their lifetime.
(3) End effect on the configuration and conformation of polymer chain.
(4) Migration of an excitation energy among chromophores on the polymer chain.

The relaxation time of polymer chain has been measured by several methods,[10] i.e., ^{13}C-NMR,[18] ESR,[19] fluorescence depolarization,[20] depolarized Rayleigh scattering,[21] and dielectric dispersion.[22] Their results show that the relaxation time of polymer chain increases with increasing the molecular weight, and indicate that the observed relaxation process consists of two components.[19,20] One is mainly due to the rotatory diffusion of the whole macromolecule which depends on its molecular weight. The other is due to the local segmental motion of the polymer chain which is not so dependent on the variation of the molecular weight. The intramolecular excimer formation is influenced by the micro-motion of the polymer segments, then such a tendency might give an inverse effect of the excimer formation in polymers with increasing the molecular weight. This is in disagreement with the experimental result as shown in Fig. 4.

The interaction between remote parts of the polymer chain has been discussed as as important problem of intramolecular reaction in polymer systems.[23] And if there is such excimer formation

process in the fluid solution of polymers, it might become a cause of the molecular weight dependence. The existence of the intramolecular excimers between remote chromophores along the polymer chain is not completely denied in the present stage. In fact, a very little intramolecular excimer formation has been observed in dilute solution of poly(allylnaphthalene) in which the chromophores are separated from the skeletal chain, and the structure does not satisfy the n=3 rule.[8] But, the following facts indicate that the non-adjacent excimer formation is a negligibly small part of the excimer formation processes in the polymer system.

The fluorescence behavior of polystyrene in various solvents have been reported by Nishihara and Kaneko,[24] and interpreted in terms of the non-adjacent excimer formation. They found a good correlation between the quantum yield ratio, Φ_D/Φ_M and the reciprocal of the intrinsic viscosity $[\eta]$ in various solvents, and the viscosity relates to the mean radius of gyration $\langle S^2 \rangle$ as follows,

$$[\eta] = 6^{3/2} \Phi \langle S^2 \rangle^{3/2} / M$$

where M is the molecular weight of the polymer. Qualitatively, this result indicates that the increase of the segment density of the polymer chain enhances the encounter probability of chromophores attached to the remote part of polymer chain.

Similar tendency is observed for PVN as shown in Fig. 5. THF is a good solvent for PVN and cyclohexane is a poor solvent. The efficiency of intramolecular excimer formation in their mixed

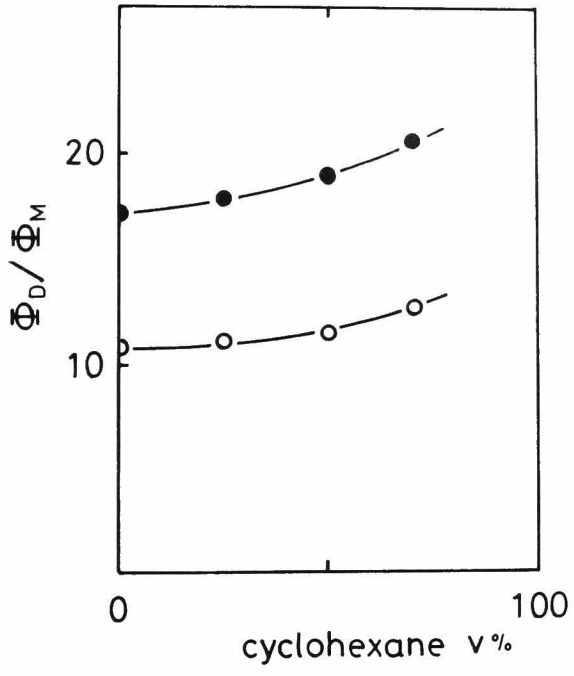

Fig. 5. Quantum yield ratios of PVN in THF-cyclohexane mixed solvents. : 10 °C, : 25 °C.

solvents increases with the component of the poor one. But, it is too hasty to conclude that this indicates the existence of the non-adjacent intramolecular excimers in PVN. Because a difference in the solvent-segment (chromophore) interaction may give a different efficiency of the excimer formation between adjacent chromophores. This possibility is examined in various solvents using 1,3-DNPr, which regarded as a dimeric model compound of the segment

Table 1. Solvent effects on the photophysical porperties and rate constants of 1,3-DNPr at 25 °C

solvent	η (cps)	ε	Φ_D/Φ_M	E_a (kcal/mol)	ν_D^{max} (nm)	k_{01}^f	k_{01}	k_{21} (10^7 s^{-1})	k_{12}	k_{02}^f	k_{02}^n
1 hexane	0.30	1.8	10.9		399	0.44	1.61	60.	1.0	0.15	0.9
2 acetonitrile	0.34	37.	8.9		400	0.48	1.75	60.	0.9	0.16	1.2
3 T H F	0.46	7.6	4.0	4.8	400	0.50	1.85	16.	0.3	0.21	1.2
4 M T H F	0.46		4.8	4.8	400	0.41	1.75	26.	0.9	0.16	1.0
5 methanol	0.54	33.	10.6	4.6	399	0.44	1.82	74.	1.2	0.15	1.1
6 cyclohexane	0.90	2.0	6.7		399	0.49	1.67	25.	0.2	0.18	1.0
7 ethanol	1.08	25.	8.9	4.8	399	0.45	1.75	38.	0.2	0.16	1.1
8 iso-butanol	3.9	18.	6.8	5.8	399	0.48	1.72	25.	0.0	0.18	1.1
9 ethylene gly.	18.	38.	1.3	8.2	401	0.58	1.99	4.9	0.0	0.17	1.0
10 propylene gly.	44.		1.0	11.		0.52	1.89	3.9	0.1	0.19	1.1

of polymer chain. Physical properties of the solvents and photophysical rate constants of 1,3-DNPr at 25 ^{o}C are given in Table 1. The wavelength (ν_D^{max}) showing the maximum intensity of excimer emission and all rate constants except for the association rate constant, k_{21} are almost the same in various solvents. Then, the electronic states of the monomer and excimer are not affected by the physical properties of solvent e.g., polarity of solvent. The direct measurement of rate constant k_{21} enables discussion of the difference of the formation processes without considering the intrusion of the other processes. As shown in Fig. 6, the plot of reciprocal of the association rate constant against the viscosity indicates two dominant factors controlling the association process of the intramolecular excimer: viscosity and solubility. It is natural that the excimer formation process is controlled by the viscosity of the medium, since the process is attended with conformational relaxation in itself. However, the relationship between the association rate and viscosity of the solvent is not clear, except for the series of alcoholic solvents in which the rate constant is fairly correlated to the viscosity.[25] In comparison of the rate constants in several solvents having similar value in viscosity, it can be safely said that the association rate constants are closely correlated with the solubility of the compound rather than the viscosity. In a good solvent, THF, the rate constants are found to be much smaller than those in a poor solvent, methanol. Because of a strong segment-solvent interaction force, the fre-

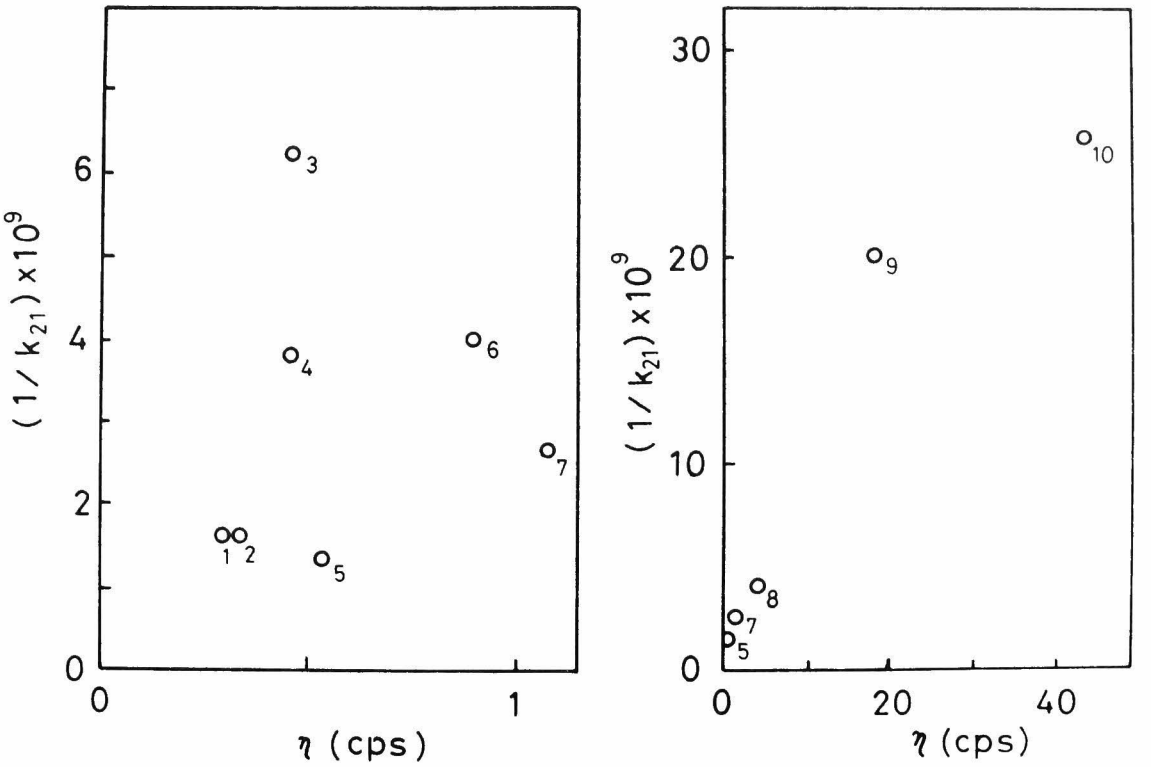

Fig. 6. Viscosity dependence of the association rate constant, k_{21} at 25 °C. Numerals in the figures correspond to the numbers of solvents in Table 1.

quency of the contact between two naphthalene chromophores in the dimeric model compound, becomes smaller in a good solvent than in a poor solvent. Some cases can be considered to give such an effect on the association process. First, the strong interaction of solvent increases the fraction of extended conformation in the ground state and decreases the intramolecular effective concentration of chromophores as described in Chapter 6. Secondly, the efficiency of the excimer formation per an encounter of chromophores becomes small by the solvent-chromophore interaction. In the present stage, further quantitative discussion about the solvent effect on the excimer formation process cannot be given, but this effect must vary the association rate of the adjacent chromophores on the polymer chain, too. Then, it is easily predicted that the excimer formation efficiency of PVN in cyclohexane becomes larger than that in THF in spite of the increase of the viscosity as shown in Fig. 5.

On the other hand, an interesting result was obtained in Chapter 4. It was found that no intramolecular excimer is formed in the compounds, α,ω-dinaphthylalkanes, in the whole range of temperature. This result shows that the naphthalene chromophore cannot interact with another one attached to a remote part along the methylene chain during its lifetime. Although the observation was carried out for the compounds up to n=12, the increase of the methylene chain length seems to be more and more disadvantageous for the intramolecular excimer formation, since the chain instability at the ring closure conforma-

tion is already relaxed in the compound, n=12.[26]

From these results, it can be said that the non-adjacent intramolecular excimer formation is a negligibly small part of the excimer formation processes in the polymer system, supposing that it exists in that system. Then, another mechanism should be considered for the cause of the molecular weight dependence.

8-3, 3. Molecular Weight Dependence of PVN and Block Copolymers Prepared by Anionic Polymerization

The fluorescence spectra of the samples prepared by anionic polymerization are identical with those by radical polymerization. Figure 7 shows the molecular weight dependence of the quantum yield ratio, Φ_D/Φ_M in the low molecular weight region with the plot against reciprocal of the degree of polymerization. The dependence is marked for these samples, too. As compared the ratios with those for samples prepared by radical polymerization, they show somewhat larger values for the anionic polymers than the radical polymers at the same degree of polymerization. This may be attributable to the difference in the tacticity of the polymer chain. As mentioned in Chapter 5, it can be expected that the polymer containing a larger fraction of isotactic sequence shows more efficient intramolecular excimer formation.

The quantum yield ratio for the block copolymers is also given in Fig. 7. As the values on the abscissa, the reciprocal of degree of polymerization

for the VN part in the one end of copolymer chain is chosen. Although the degree for the middle styrene part of these block polymers is about a hundred, the fluorescence behavior is similar to the homo PVN

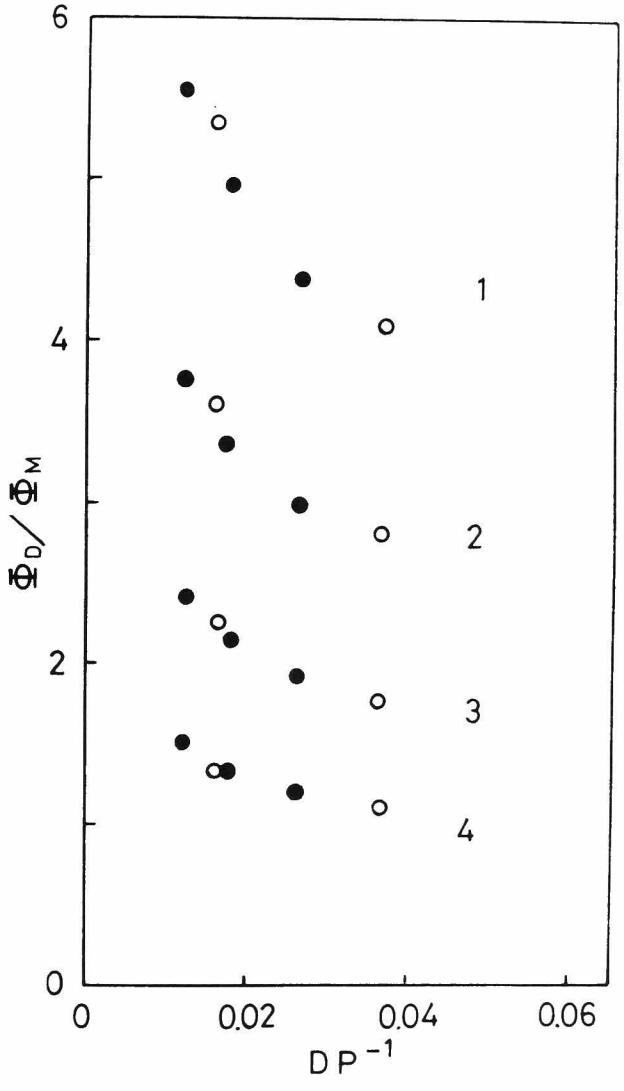

Fig. 7. Quantum yield ratios of PVN homopolymers (O) and block copolymers (●) prepared by the anionic polymerization: (1) -20 °C, (2) -30 °C, (3) -40 °C, (4) -50 °C.

polymers having the degree of polymerization corresponding to the chain length of VN part. This indicates that the molecular weight dependence is not due to the physical properties concerned with the whole molecular weight of polymers, but due to the length of consecutive alignment of chromophores.

8-3, 4. Photophysical Rate Constants and Excimer Formation in PVN

Decay curves for the monomer emission were approximately given by single exponential functions, $\exp(-t/\tau)$, and this shows that the dissociation rate constant of intramolecular excimer is negligibly small, compared with the association process. Figure 8 shows temperature dependence of the rise and decay curves of the excimer emission for dilute THF solution of PVN. All photophysical rate constants can be determined from these decay data using the ordinary methods as described in the previous chapters, and listed in Tables 2 and 3. Compared with the rate constants for the various dimer model compounds, there is a large difference in the association process, k_{21}, although little difference is observed in the other processes. Temperature dependence is mainly due to the change of the association rate constant which reflects the conformational change of the polymer chain. Arrhenius plot of k_{21} for PVN gives the activation energy of the association process and the same values as those for the dimeric model compounds are obtained: 5.3 kcal/mol. Then, the difference between the behavior of the dimeric compounds and that of polymer is due to the difference in the frequency factor of the association process:

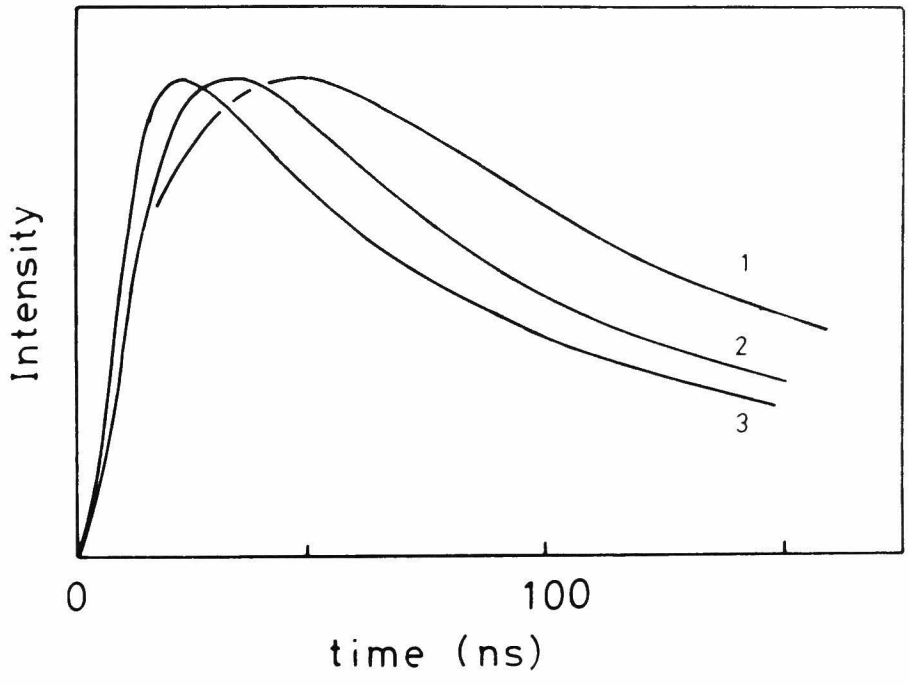

Fig. 8. Rise and decay curves of the excimer emission of PVN at various temperatures: (1) -60 °C, (2) -40 °C, (3) -20 °C.

1.4×10^{12} for 1,3-DNPr, 2.5×10^{12} for 1,3-DNBu, 4.6×10^{12} for 2,4-DNPe(meso), and 6.0×10^{12} for PVN. The frequency factor of the association process in the polymer is much larger than that in the dimers in spite of the same barrier energy of the process.

The photophysical behavior of PVN and 2,4-DNPe (meso) is very similar in the photostationary and the

Table 2. Photophysical rate constants of PVN and its trimer and dimer model compounds at 0 °C.

	PVN	1,3,5-TNPe	1,3-DNPr
k_{21}	41.	26.	12.
k_{12}	0.7	0.9	0.6
k_{02}^{f}	0.23	0.22	0.19
k_{02}^{n}	1.2	1.1	0.99

Table 3. Association rate constants of PVN and its trimer and dimer model compounds at various temperatures.

Temp. (°C)	PVN	1,3,5-TNPe	1,3-DNPr
25	74.	49.	21.
0	41.	26.	12.
-20	18.	10.	4.8
-40	7.3	4.4	1.9
-60	—	1.4	0.7
E_a (kcal/mol)	5.3	5.4	5.1

transient measurements. As shown in Chapter 5, the racemo DNPe which corresponds to the syndiotactic sequence of PVN shows a very small association rate compared with the meso isomer. This indicates that the intramolecular exicmer of PVN is mainly formed at the isotactic sequence of the polymer chain, and the syndiotactic sequence makes few contributions to the excimer formation. In this place, two incomprehensible points are raised. First, the polymer was prepared by radical or anionic polymerization, so it has random distribution of isotactic and syndiotactic sequences on the polymer chain. But, there is no indication of the photophysical behavior concerning the syndiotactic sequence, which will appear in the time-resolved measurements as a longer decay time for the monomer emission and a slower rise component for the excimer emission. Experimentally, the decay profile can be analyzed with the association rate constant much similar to that of 2,4-DNPe(meso). Secondly, the intramolecular excimer formation is controlled by the conformational changes of the polymer chain. Then, some accelerative mechanism for the association process must be taken into consideration in order to interpret the large frequency factor of the polymer, since the segmental motions in the polymer will be slower than those of the dimers.

From this view point, the results in the trimer model compounds in Chapter 7 are very interesting. As an effect of the interaction among successive three or more chromophores along a methylene chain, it was shown that the intramolecular effective con-

centration with respect to the chromophore having its adjacent partners on either side can be evaluated to be twice the concentration of an adjacent pair. Furthermore, the energy migration among chromophores makes the differences in the dissipation processes due to configurational factors unimportant, and also enhances the formation rate of the intramolecular excimer. These phenomena must occur to the polymer systems in the same way.

Here, the mechanism of the intramolecular excimer formation in PVN can be easily estimated from these results. An excitation energy absorbed by a naphthyl group migrates the chromophores on the polymer chain. A part of the excitation energies is released as monomer fluorescence or thermal energy with an intrinsic rate constant for the chromophore. On the other hand, micro-Brownian motions of the polymer chain produce various conformational changes and arrangements of adjacent chromophores, and most probable rotational conversion seems to be tg - gt transition via tt conformation at isotactic sequence where the tt conformation is an excimer conformation. So, the isotactic sequence mainly participates in the intramolecular excimer formation. If the chromophore situated at the isotactic sequence is being excited at just the time that the conformational changes are carried out from tg conformation to tt conformation, the intramolecular excimer can be formed. It is also true that the other formation processes due to different modes of conformational changes exist in the polymer systems, but they can not become main part of the excimers, since the ex-

citation energy will be caught by the fastest mode to make the excimer arrangement of chromophores and scarcely come back to the excited monomer state with the dissociation of the excimer. The effective concentration of the chromophores is taken to be twice that of dimers because two adjacent chromophores are found at the both side of an excited chromophore. Furthermore, the association rates in polymer systems are enhanced by the fast migration of the excitation energy, which averages the heterogeneity of the relaxation processes due to the sequence distribution of the vinyl aromatic polymer. A primary factor in determining the association rate constant is the rate of conformational relaxation as mentioned above, but in addition to this, there are such accelerative factors for the polymer system. The observed rate, 7×10^8 s^{-1} at 25 ^{o}C, is a result of these processes. Although the rate of conformational relaxation process is not exactly estimated form this association rate constant without determining the migration rate at the present stage, but according to the results for the trimer model compounds, the rate seems to be in the same range with the observed rate constant of the excimer formation rate.

In the samples having the degree of polymerization below ca. 100, the accelerative effect due to the energy migration becomes inefficient, since the extent of energy migration on the polymer chain is larger than the chain length of the polymer. It appears to be an evidence of the migration effect that the photophysical behavior of the ABA type block copolymer does not depend on the whole degree

of polymerization of the copolymer, but depends on the chain length of the VN block in the copolymer. Then, they seem to be cause for the molecular weight dependence observed at the oligomer region. Further discussion for the polymer systems will be made on the basis of the photophysical behavior of random copolymers in the next chapter.

References

1) L.J. Basile, J. Chem. Phys., 36, 2204 (1962).
S.S. Yanari, F.A. Bovey, and R. Lumry, Nature, 200, 242 (1963).

2) M.T. Vala, J. Haebig, and S.A. Rice, J. Chem. Phys., 43, 886 (1965).
J.W. Longworth and F.A. Bovey, Biopolymers, 4, 1115 (1966).
J.W. Longworth, Biopolymers, 4, 1131 (1966).
F. Heisel and G. Laustriat, J. Chim. Phys., 66, 1881 (1969).
C. David, M. Lempereur, and G. Geuskens, Eur. polym. J., 9, 1315 (1973).
H. Odani, Bull. Inst. Chem. Res., Kyoto Univ., 51, 351 (1973).
T. Ishii, T. Handa, and S. Matsunaga, Macromolecules, 11, 40 (1978).

3) M.T. Vala, J. Haebig, and S.A. Rice, J. Chem. Phys., 43, 886 (1965).
Y. Nishijima, J. Polym. Sci., C, 31, 353 (1970).
Y. Nishijima, M. Yamamoto, K. Mitani, S. Katayama, and T. Tanibuchi, Repts. Progr. Polym. Phys. Japan, 13, 417 (1970).

C. David, W. Demarteau, and G. Geuskens, Eur. Polym. J., 6, 1397 (1970).
L.A. Harrah, J. Chem. Phys., 56, 385 (1972).
R.B. Fox, T.R. Price, R.F. Cozzens, and J.R. McDonald, J. Chem. Phys., 57, 534 (1972).
C. David, M. Piens, and G. Geuskens, Eur. polym. J., 8, 1019 (1972).
Y. Nishijima, Y. Sasaki, M. Tsujisaki, and M. Yamamoto, Repts. Progr. Polym. Phys. Japan, 15, 453 (1972).

4) W. Klöpffer, J. Chem. Phys., 50, 2337 (1969).
P.C. Johnson and H.W. Offen, J. Chem. Phys., 55, 2945 (1971).
C. David, M. Piens, and G. Geuskens, Eur. Polym. J., 8, 1291 (1972).
Y. Nishijima, Y. Sasaki, K. Hirota, and M. Yamamoto, Repts. Progr. Polym. Phys. Japan, 15, 449 (1972).
M. Yokoyama, T. Tamamura, M. Atsumi, M. Yoshimura, Y. Shirota, and H. Mikawa, Macromolecules, 8, 101 (1975).

5) C. David, M. Lempereur, and G. Geuskens, Eur. Polym. J., 8, 417 (1972).
C. David, M. Piens, and G. Geuskens, Eur. Polym. J., 8, 1019 (1972).
Y. Nishijima, Y. Sasaki, M. Tsujisaki, and M. Yamamoto, Repts. Progr. Polym. Phys. Japan, 15, 453 (1972).

6) J.R. McDonald, W.E. Echols, T.R. Price, and R.B. Fox, J. Chem. Phys., 57, 1746 (1972).
M. Yokoyama, T. Tamamura, T. Nakano, and H. Mikawa, Chem. Lett., 499 (1972).

K. Hirota, M. Yamamoto, and Y. Nishijima, Repts. Progr. Polym. Phys. Japan, 16, 509 (1973).
7) A.C. Somersall and J.E. Guillet, Macromolecules, 6, 218 (1973).
R.B. Fox, T.R. Price, R.F. Cozzens, and W.H. Echols, Macromolecules, 7, 937 (1974).
8) Y. Nishijima, M. Yamamoto, S. Katayama, K. Hirota, Y. Sasaki, and M. Tsujisaki, Repts. Progr. Polym. Phys. Japan, 15, 445 (1972).
9) R.B. Fox, T.R. Price, R.F. Cozzens, and J.R. McDonald, J. Chem. Phys., 57, 534 (1972).
10) A.T. Bullock, J.H. Butterworth, and G.G. Cameron, Eur. Polym. J., 7, 445 (1971).
A.M. North and I. Soutar, J. Chem. Soc. Faraday I, 68, 1101 (1972).
M. Uchida, Doctoral Thesis, Kyoto University, Kyoto, Japan, 1977.
W.H. Stockmayer and K. Matsuo, Macromolecules, 5, 766 (1972).
11) W. Klöpffer, J. Chem. Phys., 50, 2337 (1969).
C.W. Frank and L.A. Harrah, J. Chem. Phys., 61, 1526 (1974).
C. David, M. Piens, and G. Geuskens, Eur. Polym. J., 9, 533 (1973).
12) C. David, M. Piens, and G. Geuskens, Eur. Polym. J., 8, 1019 (1972).
C. David, M. Lempereur, and G. Geuskens, Eur. Polym. J., 9, 1315 (1973).
A.M. North, Br. Polym. J., 7, 119 (1975).
R.F. Reid and I. Soutar, J. Polym. Sci., Polym. Lett. Ed., 15, 153 (1977).
R.F. Reid and I. Soutar, J. Polym. Sci., Polym. Phys. Ed., 16, 231 (1978).

13) F. Hirayama, J. Chem. Phys., 42, 3163 (1965).
14) E.A. Chandross and C.J. Dempster, J. Am. Chem. Soc., 92, 3586 (1970).
15) K. Hirota, M. Yamamoto, and Y. Nishijima, Repts. Progr. Polym. Phys. Japan, 16, 509 (1973).
G.E. Johnson, J. Chem. Phys., 62, 4697 (1975).
C. David, M. Piens, and G. Geuskens, Eur. Polym. J., 12, 621 (1976).
C.E. Hoyle, T.L. Nemzek, A. Mar, and J.E. Guillet, Macromolecules, 11, 429 (1978).
C.E. Hoyle, and J.E. Guillet, J. Polym. Sci., Polym. Lett. Ed., 16, 185 (1978).
K.P. Ghiggino, R.D. Wright, and D. Phillips, J. Polym. Sci., Polym. Phys. Ed., 16, 1499 (1978).
16) M. Szwarc, "Carbanions Living Polymers and Electron Transfer," Interscience, New York, 1968.
17) T. Moritani and Y. Fujiwara, J. Chem. Phys., 59, 1175 (1973).
D.Y. Yoon, P.R. Sundararajan, and P.J. Flory, Macromolecules, 8, 776 (1975).
18) A. Allerhand and R.K. Hailstone, J. Chem. Phys., 56, 3718 (1972).
19) A.T. Bullock, G.G. Cameron, and P.M. Smith, J. Phys. Chem., 77, 1635 (1973).
20) M. Uchida, Doctoral Thesis, Kyoto University, Kyoto, Japan, 1977.
21) D.R. Bauer, J.I. Brauman, and R. Pecora, Macromolecules, 8, 443 (1975).
22) W.H. Stockmayer and K. Matsuo, Macromolecules, 5, 766 (1972).
23) N. Goodman and H. Morawetz, J. Polym. Sci., C, 31, 177 (1970).

N. Goodman and H. Morawetz, J. Polym. Sci., A, 9, 1657 (1971).
M. Sisido, Polym. J., 3, 84 (1972).
M. Sisido, Polym. J., 4, 534 (1973).
C. Cuniberti and A. Perico, Eur. Polym. J., 13, 369 (1977).
G. Wilemski and M. Fixman, J. Chem. Phys., 60, 866 (1974).
S. Sunagawa and M. Doi, Polym. J., 7, 604 (1975).
24) T. Nishihara and M. Kaneko, Makromol. Chem., 124, 84 (1969).
25) P. Avouris, J. Kordas, and M.A. El-Bayoumi, Chem. Phys. Lett., 26, 373 (1974).
M. Goldenberg, J. Emert, and H. Morawetz, J. Am. Chem. Soc., 100, 7171 (1978).
26) K. Zachariasse and W. Kühnle, Z. Phys. Chem. N.F., 101, 267 (1976).

CHAPTER 9

Kinetic Analysis of Excimer Emission of Vinylnaphthalene-Styrene Copolymers in Solution

9-1. Introduction

In the previous chapters, intramolecular excimer formation in polymer solutions were discussed, and various results showed the existence of the energy migration process on the pendant chromophores attached to the polymer chain. This migration process makes an important role in the excimer formation of polymers. In homopolymers, it appears that the migration mainly takes place along the row of cosecutive adjacent aromatic groups and the rapid migration enables to catch the excimer conformation on the polymer chain, efficiently. In random or alternative copolymers, such migration process seems to be interrupted by the insertion of the photophysically inert species on the polymer chain, and even if the migration exists in polymers, it mainly occurs between non-adjacent chromophores within the domain of the polymers.

Luminescence characteristics of various copolymers have been investigated by many workers,[1,2] and their experimental data suggest effective migration of excitation energy in films and in solutions.[2] But, there has been no report still now which deals with the quantitative relationship between the energy migration and the excimer formation phenomena in co-

polymers, i.e., sequence distribution of the chromophores, excimer formation rate of an adjacent pair, and migration rate of the energy among chromophores. These points seem to have fundamental significance in interpreting the photophysical properties of polymer systems.

In this chapter, the photoluminescence characteristics of copolymers of 2-vinylnaphthalene with styrene have been studied under photostationary and transient conditions, in order to investigate the interactions between the adjacent chromophores and also between the non-adjacent chromophores in a polymer chain. The observed luminescence behavior can be explained very well with a kinetic treatment including energy migration process between chromophores.

9-2. Experimental

2-Vinylnaphthalene (VN) - styrene random copolymers were prepared by radical polymerization at 60 ^{o}C using α,α'-azobisisobutyronitrile as an initiator. The polymerization was stopped at the conversion below 5%. The resulting polymer was reprecipitated several times from benzene solution into methanol. The copolymer compositions were determined by IR spectra using the bands at 820, 690, and 470 cm^{-1}, and the calibration curves were shown in Fig. 1. The relationship between the composition of the copolymer and the composition of the starting monomer mixture is given in Fig. 2. From the Fineman-Ross plot as shown in Fig. 3, the monomer reactivity ratios were obtained: r_{VN} = 1.43, $r_{styrene}$ = 0.53.

The ratios were in accordance with the value reported by Price at al.[3] Triad probabilities of the naphthalene units in the copolymer chain, P_{SNS}, P_{SNN}, and P_{NNN}, in which subscripts N and S refer to the vinylnaphthalene and styrene units, respectively, were estimated from the reactivity ratios. Molecular weights of the copolymers were determined by a calibrated GPC. The characteristics of these co-

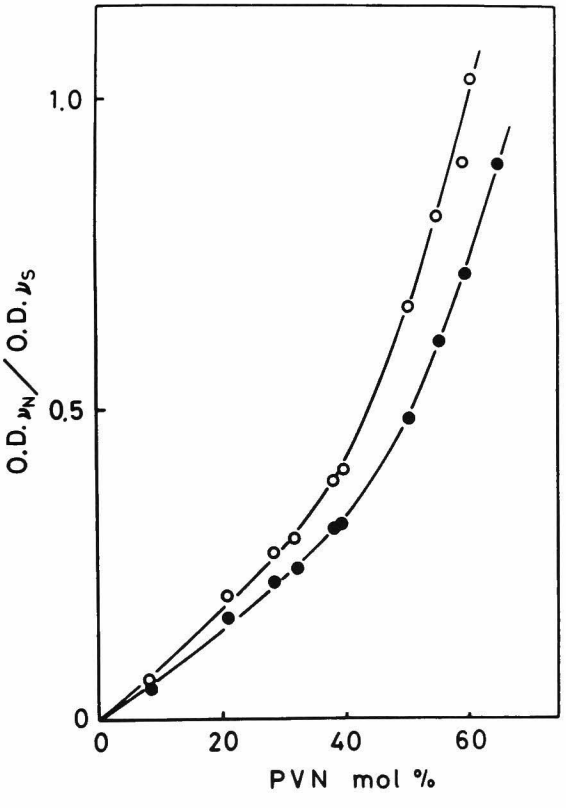

Fig. 1. Calibration curves of IR absorption to determine the compositions of VN-styrene copolymers. ○: ν_N= 820 cm^{-1}, ν_S= 690 cm^{-1}, ●: ν_N= 470 cm^{-1}, ν_S=690 cm^{-1}.

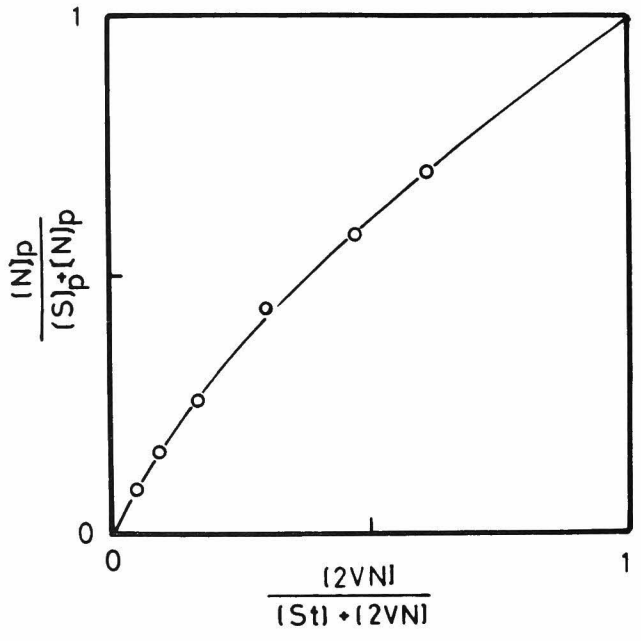

Fig. 2. Relationship between the composition of the copolymer and that of the monomer mixture.

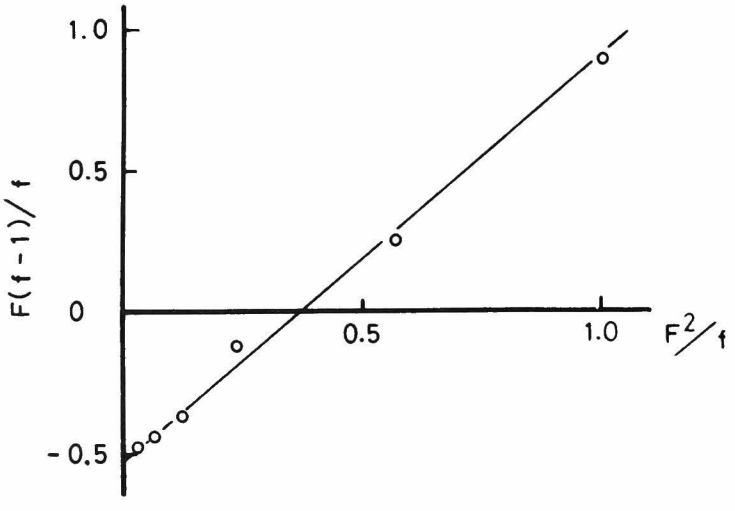

Fig. 3. Fineman-Ross plot, where F = [VN]/[St] and f = $[N]_p/[S]_p$.

Table 1. Characteristics of vinylnaphthalene-styrene copolymers

St-2VN COPOLYMER	$\frac{[2VN]}{[St]+[2VN]}$	$\left(\frac{[N]}{[S]+[N]}\right)_P$	CONV. %	$M \times 10^4$	P_{NNN}	P_{SNN}	P_{SNS}
C 1	0.05	0.09	2.9	18	0.006	0.15	0.85
C 2	0.09	0.16	5.3	18	0.02	0.23	0.75
C 3	0.17	0.26	2.3	21	0.05	0.34	0.62
C 4	0.30	0.44	3.9	27	0.17	0.48	0.35
C 5	0.47	0.58	3.3	34	0.31	0.49	0.20
C 6	0.61	0.70	4.7	25	0.47	0.43	0.10

polymers are summarized in Table 1. In quenching experiments, biacetyl was chosen as a quencher. The concentrations of biacetyl were adjusted to be 5×10^{-4} - 3×10^{-3} mol/l.

All measurements were carried out in deaerated THF solutions, and the concentrations were adjusted to be ca. 10^{-4} mol/l for the naphthalene chromophore, Details of measerements were described in the preous chapters.

9-3. Results and Discussion

9-3, 1. Stationary State Behavior of the Copolymers and Their Triad Probabilities

In stationary state, fluorescence intensities from the dilute solutions of the copolymers in THF were measured at various temperatures. The energy level of the singlet excited state of naphthalene chromophore lies in lower than that of the phenyl group, then we may pay attention only to the dis-

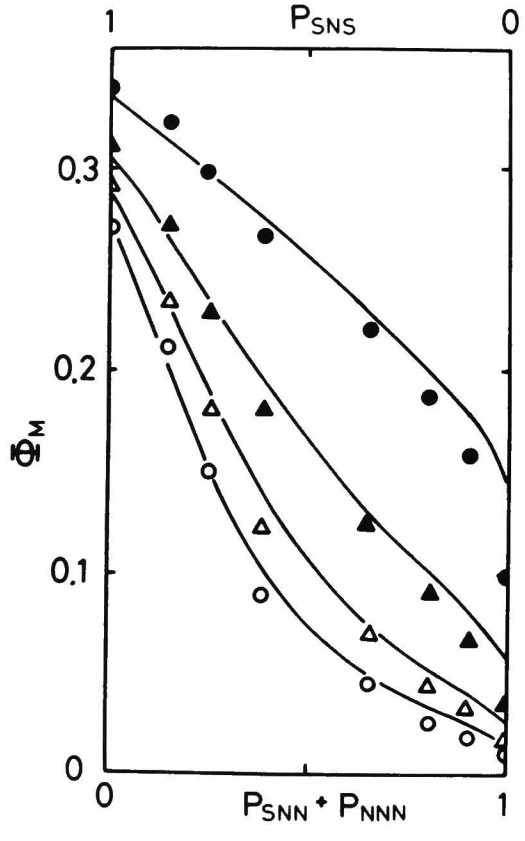

Fig. 4. Quantum yields of the monomer fluorescence at various temperatures. ○: 25°C, △: 5°C, ▲: -20°C, ●: -50°C. Solid lines are calculated values of Φ_M with Eqs. 7 - 11.

sipation processes of the excited naphthalene chromophores. In Figs. 4 and 5, the quantum yields of the monomer fluorescence, Φ_M and the excimer fluorescence, Φ_D are plotted against the probability that an excited naphthalene chromophore has the adjacent naphthalene unit, i.e., $P_{SNN} + P_{NNN} = 1 - P_{SNS}$.

Under the assumption that isolated naphthalene chromophores situated in the local sequence of SNS, do not any contribution to the intramolecular excimer

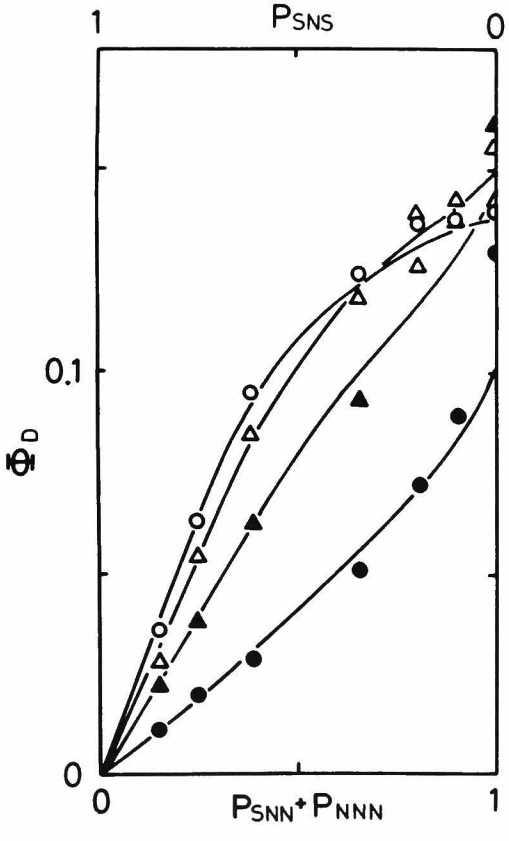

Fig. 5. Quantum yields of the excimer fluorescence at various temperatures. ○: 25°C, △ : 5°C, ▲ : -20°C, ●: -50°C. Solid lines are calculated values of Φ_D with Eqs. 7 - 11.

formation in the copolymers, and that the excimer formation efficiencies in the sequence of SNN and NNN are not distinguished, the quantum yields, Φ_M and Φ_D can be expressed in the following form, respectively,

$$\Phi_M = P_{SNS}\,\phi_M + (1 - P_{SNS})\,\phi_M' \qquad (1)$$

$$\Phi_D = (1 - P_{SNS})\,\phi_D' , \qquad (2)$$

where ϕ_M is the fluorescence quantum yield of the isolated naphthalene groups, and ϕ_M', ϕ_D' refer to the quantum yields of the monomer fluorescence and the excimer fluorescence, respectively, for the non-isolated naphthalene chromophores. The quantum yields, ϕ_M, ϕ_M', and ϕ_D' are written by the kinetic rate constants as follows,

$$\phi_M = k_{01}^f / k_{01} \qquad (3)$$

$$\phi_M' = k_{01}^f\, k_2 / (k_1\, k_2 - k_{21}\, k_{12}) \qquad (4)$$

$$\phi_D' = k_{02}^f\, k_{21} / (k_1\, k_2 - k_{21}\, k_{12}). \qquad (5)$$

These equations imply that Φ_M and Φ_D should both have linear relationship with the probability $P_{SNN} + P_{NNN}$. However, neither of the obtained results are in accordance with these simple linear relationships as shown in Figs. 4 and 5. At low temperatures, as the contents of naphthalene chromophores in polymers increase, Φ_M decreases particularly in the high content region, and intramolecular excimers are formed more efficiently than expected by the above relationship. At high temperatures,

the monomer fluorescence is quenched notably even in the relatively low contents of naphthalene chromophores. These observed facts indicate that the isolated naphthalene units also contribute to the intramolecular excimer formation of polymer molecules in solution. This conclusion is confirmed by the measurements of emission decays using a single photon counting technique.

9-3, 2. Time-Resolved Measurements of Monomer and Excimer Emission

Decay curves of the monomer and the excimer fluorescence at 25 °C in THF were measured. Figure 6 shows the decay curves $I_M(t)$ of the monomer fluorescence for various copolymers. For the copolymers of the low content of naphthalene, the obtained $I_M(t)$ shows simple exponential decay, but its lifetime are 48, 38, and 28 ns for C1, C2, and C3, respectively. Those are shorter than the lifetime of the monomeric model compound, MNEt in the same condition: 54 ns. If the isolated excited naphthalene chromophores situated in the sequence of SNS, do not play any role in the excimer formation and dissipate to the ground state with the intrinsic rate constant of the chromophore, the component of this corresponding lifetime, 54 ns ($= k_{01}^{-1}$), should be contained within the decay curves of those copolymers as follows,

$$I_M(t) \propto P_{SNS} \exp(-k_{01}t) + C\,(1 - P_{SNS})\{\exp(-\lambda_1 t) + A \exp(-\lambda_2 t)\} \quad (6)$$

where C is a constant. Then, the results as shown

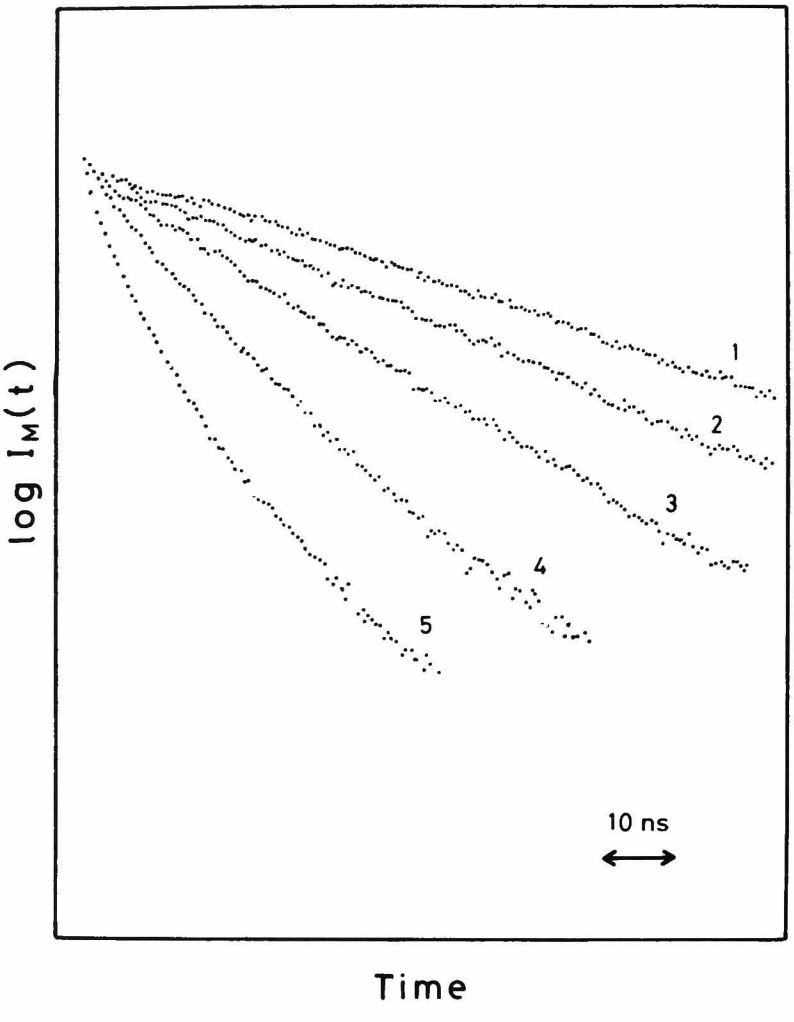

Fig. 6. Decay curves of the monomer fluorescence for various copolymers: (1) C1, (2), C2, (3) C3, (4) C4, and (5) C5.

in Fig. 6 show that the isolated excited naphthalene units are intramolecularly quenched in solution. These phenomena suggest the effective diffusion of naphthalene units or the excitation energy in the polymer molecules. For the copolymers of high naphthalene contents, the observed decays of $I_M(t)$ consist of two of more components indicating the contribution of the excimer dissociation process.

The decay curves of the excimer fluorescence $I_D(t)$ for PVN and various copolymers are shown in Fig. 7. It can be noted that the rise of excimer emission for the copolymers of low naphthalene contents is much slower than that PVN. For example, the rise time of C1's excimer emission are estimated to be apparently ca. 11 ns, although some faster rise components than that are observed in the decay curve. The composition of naphthalene units in C1 is only about 9%, but the evaluated value for the probability of P_{SNN} is about 15%. The predominant portion of the excimer fluorescence of C1 can reasonably be assumed to be emitted from the excimer formed between such adjacent naphthalene chromophores. Then, the relatively slow rise time for the copolymers suggests that the segment motion controlling the excimer formation in polymer chain is considerably slower than the expected value from the k_{21} observed for homopolymer, PVN. To be exact, the excimer formation processes in the copolymers are complex, and more detailed and quatitative discussion must be made on the basis of kinetic rate equations followed by experimental data.

On the other hand, the rise time of PVN is ca.

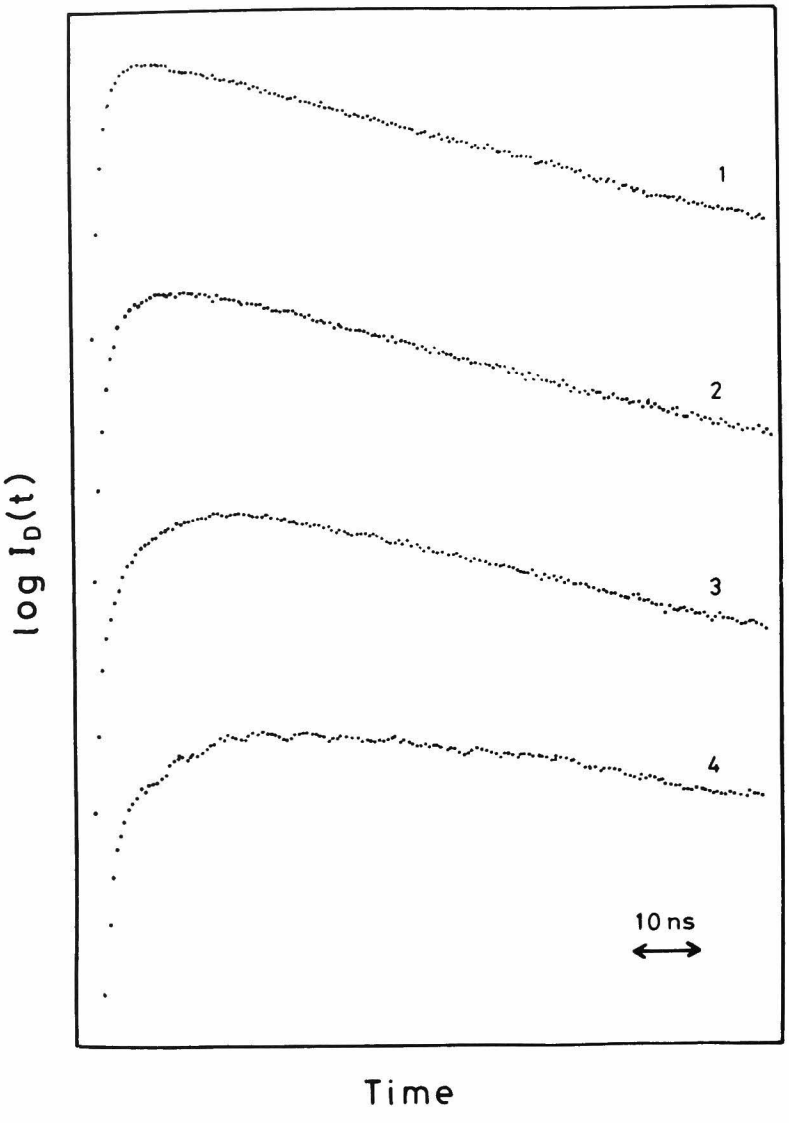

Fig. 7. Rise and decay curves of the excimer fluorescence for various copolymers: (1) PVN, (2) C6, (3) C4, and (4) C2.

1.4 ns at 25 °C in THF, and the obtained association rate constant is ca. 7×10^8 s^{-1}, as described in the previous chapter. The markedly large value of k_{21} for homopolymer, PVN, implies the important role of the row of the consecutive adjacent aromatic groups for the formation of the intramolecular excimer in the polymer chain.

9-3, 3. Energy Migration in Copolymers and Kinetic Treatments of the Emission Behavior

When considering the observed quantum yields and decay profile, we must take into account the following two facts; First, the excimer formation efficiency of the excited naphthalene chromophores having different sequence were examined with trimer model compounds NNS and NNN in Chapter 7, and it was indicated that the excimer formation rate constant of the excited naphthalene units situated in the sequence of NNN should be at least twice as large as that in the sequence of SNN. Secondly, as shown in Chapter 7 and Chapter 8, energy migration among naphthalene chromophores can make averaged the dissipation processes of the excitation energy, which is originally decided by the local sequence of the pendant naphthalene chromophores in the absence of the migration process.

Here, taking into account these two facts, the following steady state kinetic equations are written,

$$d[M^*_{SNS}]/dt = P_{SNS} I_o + k_t P_N P_{SNS}([M^*_{SNN}] + [M^*_{NNN}]) - \{k_{01} + k_t P_N (P_{SNN} + P_{NNN})\} [M^*_{SNS}] \quad (7)$$

$$d[M^*_{SNN}]/dt = P_{SNN}I_o + k_t P_N P_{SNN}([M^*_{SNS}] + [M^*_{NNN}]) + k_{12}[D^*_{SNN}] - \{k_{01} + k_{21} + k_t P_N (P_{SNS} + P_{NNN})\}[M^*_{SNN}] \quad (8)$$

$$d[M^*_{NNN}]/dt = P_{NNN}I_o + k_t P_N P_{NNN}([M^*_{SNS}] + [M^*_{SNN}]) + k_{12}[D^*_{NNN}] - \{(k_{01} + 2k_{21} + k_t P_N (P_{SNS} + P_{SNN})\}[M^*_{NNN}] \quad (9)$$

$$d[D^*_{SNN}]/dt = k_{21}[M^*_{SNN}] - (k_{12} + k_{02})[D^*_{SNN}] \quad (10)$$

$$d[D^*_{NNN}]/dt = 2k_{21}[M^*_{NNN}] - (k_{12} + k_{02})[D^*_{NNN}] , \quad (11)$$

where M^*_{SNS}, M^*_{SNN}, and M^*_{NNN}, represent the singlet excited naphthalene groups situated in the sequences of SNS, SNN, and NNN, respectively, k_t is the intramolecular migration rate constant of the excitation energy from an excited naphthalene monomer to another naphthalene chromophore on the polymer chain, P_N is the composition of VN unit in the copolymer, and $P_N P_{SNS}$, $P_N P_{SNN}$, and $P_N P_{NNN}$ represent the intramolecular concentration of the local sequences, SNS, SNN, and NNN, respectively. The other rate constants are the same notation as mentioned on the previous chapter, but particularly, the association rate constant, k_{21} means the excimer formation rate constant of the isolated dimer sequence NN on the polymer chain. Then, this rate is closely concerned with the conformational changes of the polymer segments. Using the solutions of Eqs. 7 - 11, the quantum yields Φ_M and Φ_D are given by,

$$\Phi_M = k_{01}^f([M_{SNS}^*] + [M_{SNN}^*] + [M_{NNN}^*]) / I_o \qquad (12)$$

$$\Phi_D = k_{02}^f([D_{SNN}^*] + [D_{NNN}^*]) / I_o \ . \qquad (13)$$

The decay curves of the monomer and the excimer emission, $I_M(t)$ and $I_D(t)$ can be given by solving the differential equations similar to the Eqs. 7 - 11. under appropriate initial conditions,

$$[M_{SNS}^*]_o = P_{SNS} \ , \quad [M_{SNN}^*]_o = P_{SNN} \ ,$$

$$[M_{NNN}^*]_o = P_{NNN} \ , \quad [D_{SNN}^*]_o = [D_{NNN}^*]_o = 0 \ . \qquad (14)$$

In these kinetic equations, several rate constants for the naphthalene chromophore have been already decided from the measurements of various dimer model compounds and polymers. Then, unknown rate parameters are only two: k_t and k_{21}. In Fig. 8, the association rate constant dependence of Φ_M and Φ_D calculated for various k_t's at $P_{SNS} = 0.7$, is shown, and the same way, the dependence of lifetime of the monomer emission decay, τ_M is shown in Fig. 9, where the decay curve, $I_M(t)$ can be approximated to be single exponential function in the low naphthalene content samples. It is obvious in Figs. 8 and 9 that the quantum yields and decay times are mainly dominated by the association rate constants k_{21} in the region of small k_{21} value, and by the migration rate constants k_t in the region of large k_{21} value, in which the migration process of excitation energy from an isolated SNS chromophore to an adjacent naphthalene pair, SNN or NNN, means substantially quenching process of the excited monomer

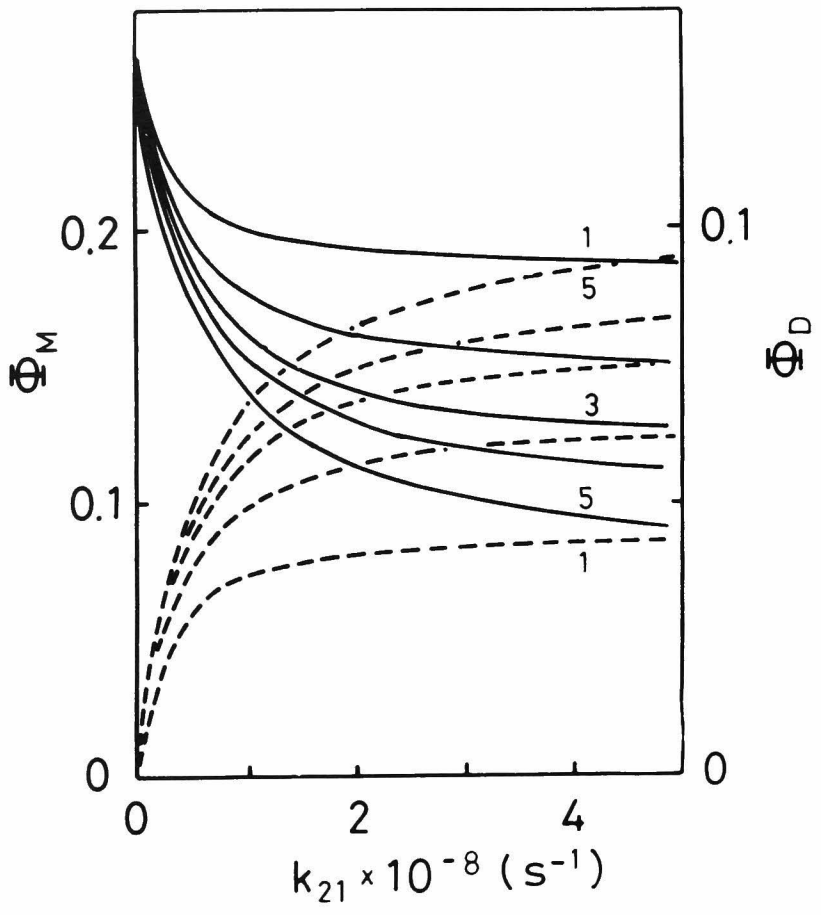

Fig. 8. Association rate constant dependence of Φ_M and Φ_D at P_{SNS}= 0.7 for various k_t values. Full lines are the quantum yields Φ_M, and broken lines are the quantum yields Φ_D. (1) k_t= 1 x 10^7 s^{-1}, (2) k_t= 1 x 10^8 s^{-1}, (3) k_t= 2 x 10^8 s^{-1}, (4) k_t= 3 x 10^8 s^{-1}, (5) k_t= 5 x 10^8 s^{-1}. Numerals are put in order from the top for full lines and from the bottom for the broken lines.

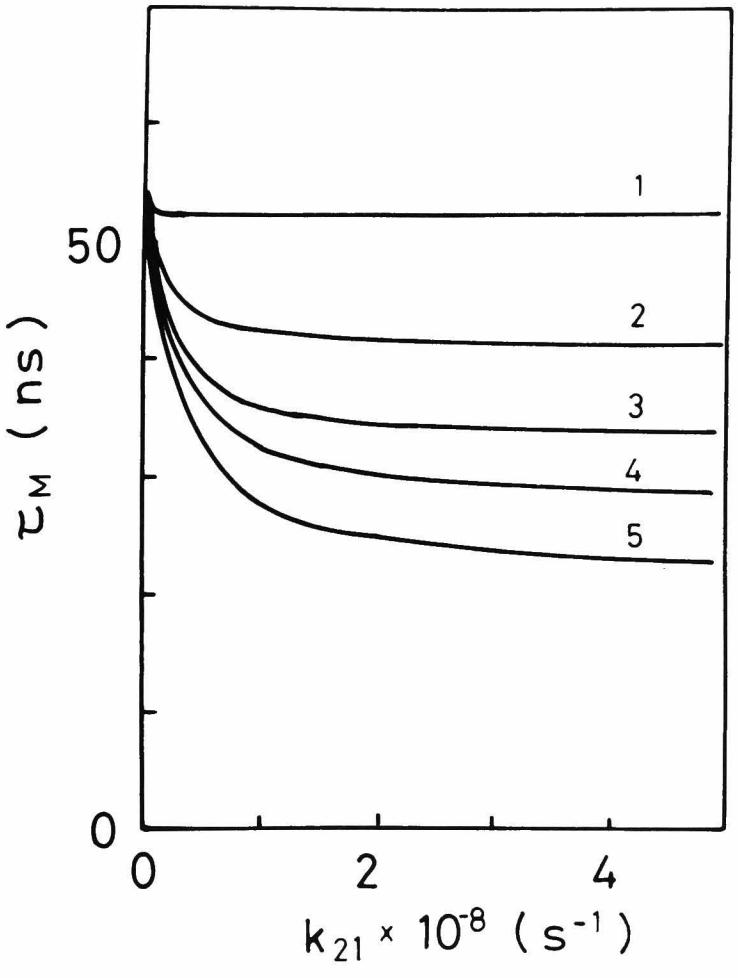

Fig. 9. Association rate constant dependence of the lifetime, τ_M, at P_{SNS}= 0.7 for various k_t values. Numerals represent the same k_t values as those in Fig. 8.

state M^*, because almost all of the excitation energy in M^*_{SNN} and M^*_{NNN} are to go to the corresponding excimer states, and scarcely go back to the isolated naphthalene units, SNS. Appropriate values of k_{21} and k_t ($k_{21} = 2 \times 10^8\ s^{-1}$, $k_t = 3 \times 10^8\ s^{-1}$) are chosen in Figs. 8 and 9, and the agreement between calculated and found values is examined for samples having various naphthalene contents.

Figures 10 and 11 show the observed decay curves of $I_M(t)$ and $I_D(t)$ and calculated decay curves, $I(t)$ given by the following equation,

$$I(t) = \int_o^t p(t')\ F(t - t')\ dt' \qquad (15)$$

where $F(t)$ is calculated response function from the differential equations, and $p(t)$ is the exciting pulse shape. These curves agree very well those experimental curves in wide range of naphthalene contents. As mentioned above, the decay curve, $I_M(t)$ for the low content region of naphthalene chromophore can be approximated by a single exponential function. Actually, the decay functions given by the equations consist of five exponential functions.

When the dissociation rate constant, k_{12} is neglected in order to make clear the decay profile, the decay curves of $F_M(t)$ and $F_D(t)$ can be expressed by sums of three or four exponential functions, respectively, as follows,

$$F_M(t) = \Sigma_{i=1}^{3}\ A_{M,i}\ \exp(-t/\tau_i) \qquad (16)$$

$$F_D(t) = \Sigma_{i=1}^{3}\ A_{D',i}\ \exp(-t/\tau_i). \qquad (17)$$

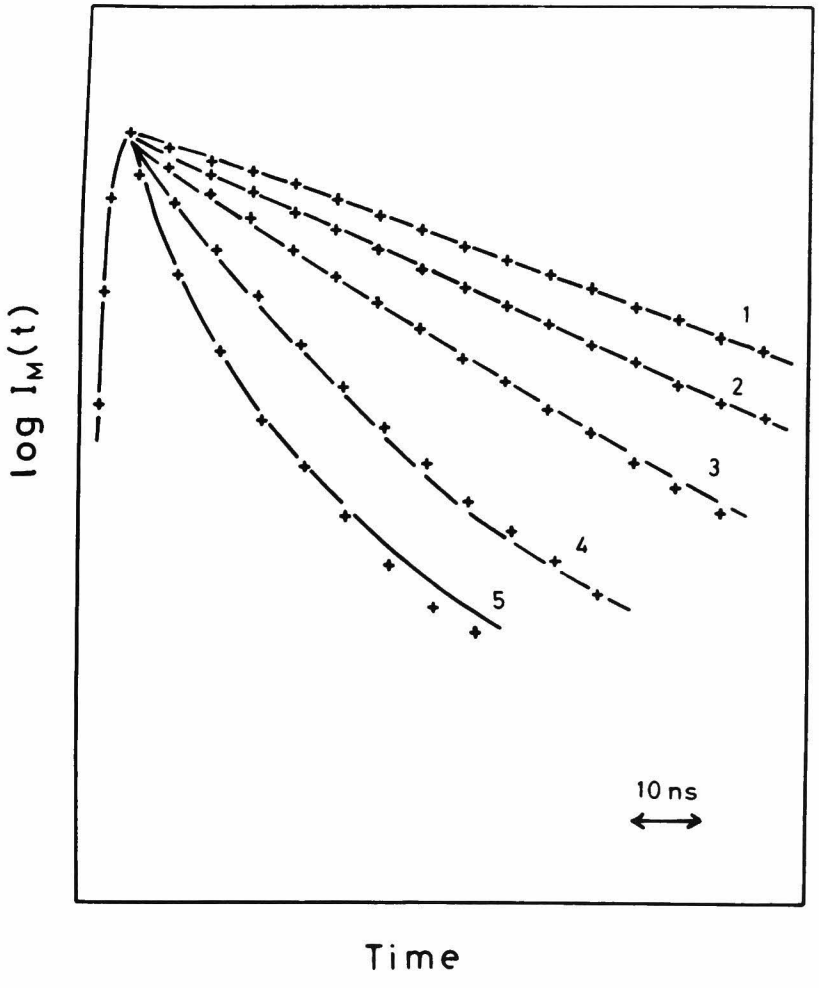

Fig. 10. Calculated decay curves for the monomer fluorescence. The sign, + represents the experimental value in Fig. 6. (1) C1, (2) C2, (3) C3, (4) C4, and (5) C5.

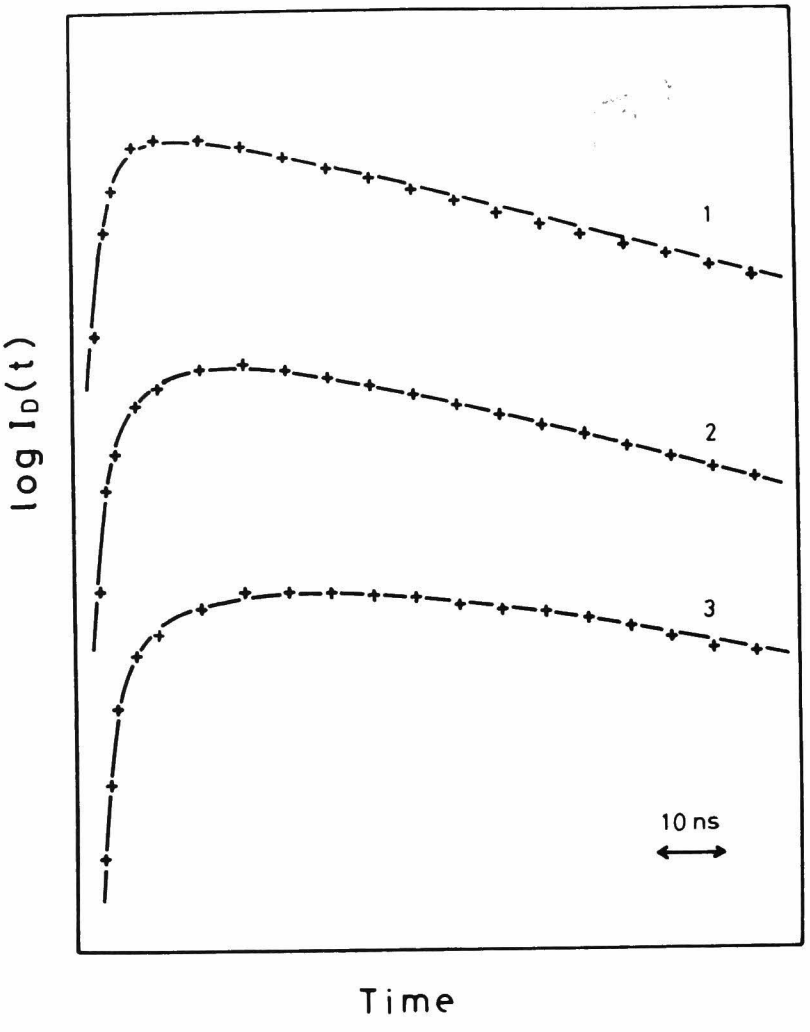

Fig. 11. Calculated rise and decay curves for the excimer fluorescence. The sign, + represents the experimental value in Fig. 7. (1) C6, (2) C4, and (3) C2.

These parameters in Eqs. 16 and 17 are listed in Table 2 for the samples, C1, C2, and C3. The decay times, τ_1, τ_2, and τ_3 are originally the decay times of the naphthalene chromophores at the sequences of

Table 2. Decay parameters of the monomer and excimer fluorescence for the low naphthalene content samples.

C1 (P_{SNS}= 0.85)

	i = 1	i = 2	i = 3	i = 4
τ_i (ns)	46.	4.1	2.2	65.
$A_{M,i}$	0.88	0.11	0.01	—
$A_{D,i}$	-0.82	-0.17	-0.01	1.0

C2 (P_{SNS}= 0.75)

	i = 1	i = 2	i = 3	i = 4
τ_i (ns)	35.	3.9	2.1	65.
$A_{M,i}$	0.82	0.16	0.01	—
$A_{D,i}$	-0.79	-0.19	-0.02	1.0

C3 (P_{SNS}= 0.62)

	i = 1	i = 2	i = 3	i = 4
τ_i (ns)	25.	3.7	2.0	65.
$A_{M,i}$	0.76	0.21	0.03	—
$A_{D,i}$	-0.74	-0.23	-0.03	1.0

SNS, SNN, and NNN respectively, but calculated decay times deviate from those values owing to the mixing of the location of excitation energy. For the decay curve, $F_M(t)$, the pre-exponential factor, A_1 is dominant in Eq. 16, then the monomer emission shows a single exponential decay with the longest lifetime τ_1, except the time immediately after the exciting pulse. For the decay curve, $F_D(t)$, the τ_1, τ_2, and τ_3 become the rise time of the excimers, and the decay profiles of $F_D(t)$'s are considerably affected by the rise components, τ_2 and τ_3 not only for the samples of high naphthalene contents but for those of low contents. The observed decay curves, $I_D(t)$'s can be simulated by using such two or three rise components for the rise time of excimers.

The stationary state behavior is also examined using the Eqs. 7 - 11, under the conditions, $d[M^*]/dt = d[D^*]/dt = 0$ for the naphthalene chromophore of each sequence. Figures 4 and 5 show the quantum yields, Φ_M and Φ_D calculated for various naphthalene contents of copolymers. In low temperatures, the association rate constants k_{21}'s are evaluated from the value at 25 °C, 2×10^8 s^{-1}, using the activation energy, 5.3 kcal/mol, which is obtained for various model compounds and PVN, and k_t is chosen to fit in with the measurements. The other rate constants are given by the results for PVN described in Chapter 8. These rate constants are summarized in Table 3. As shown in Figs. 4 and 5, these calculation can reproduce both the found quantum yields, Φ_M and Φ_D for wide region of naphthalene contents at various temperatures.

Table 3. Photophysical rate constants obtained for the copolymers at various temperatures.

T (°C)	25	5	-20	-50
k_{01}^f	0.49	0.49	0.49	0.50
k_{01}	1.80	1.70	1.60	1.48
k_{12}	0.60	0.50	0.35	0.20
k_{02}^f	0.23	0.22	0.22	0.21
k_{02}	1.55	1.35	1.25	1.20
k_{21}	20.0	12.0	4.5	1.2
k_t	30.0	16.0	8.0	2.5

Unit: $10^7 \cdot s^{-1}$

The kinetic equations indicate important characteristics of the polymer systems. The large value for the migration rate constant (k_t = 3 x 10^8 s^{-1}) shows considerably fast migration of excitation energy among the pendant chromophores on the polymer chain. It has been said that there are mainly two mechanisms in these singlet-singlet migration systems, Coulombic interaction between electronic excited states of chromophores and exchange interaction between the overlapping electron clouds of the chromophores.[4] The former Coulombic interaction

usually operates in the longer distance of chromophores than the latter mechanism, but the spectroscopic data for MNEt in THF gives ca. 12 Å as the critical distance, R_o, with the next equation for the dipole-dipole interaction of Coulombic interactions, at which energy migration and internal deactivation processes have equal probability,

$$R_o = \frac{(9000 \ln 10)\, K^2}{128\, \pi^5\, n^4\, N_o} \int_0^\infty f(\nu)\, \varepsilon(\nu)\, \frac{d\nu}{\nu^4} \quad . \qquad (18)$$

where n is the solvent refractive index, K^2 is an orientation factor, $\varepsilon(\nu)$ is the molar extinction coefficient at wavenumber ν, and $f(\nu)$ is the relative donor fluorescence quantum intensity at ν.

In a low viscosity medium satisfying the condition, $R_o \ll \sqrt{2D\tau_M}$, the migration obeys Stern-Volmer kinetics.[5] Then, the rate equation can be written by the time-independent migration rate constant, k_t and the concentration of energy acceptor, [A] as follows,

$$d[M^*]/dt = -\,(\, k_{01} + k_t\, [A]\,)\, [M^*] \quad . \qquad (19)$$

In the Eqs. 7 - 9, [A] is replaced by the intramolecular concentrations, $P_N P_{SNS}$, $P_N P_{SNN}$, and $P_N P_{NNN}$ for the corresponding naphthalene sequence in the polymer molecules. Here, the rate constant, k_t is closely concerned with the Brownian motion of the polymer segments. Supposing that the migration is a diffusion controlled process and has the conditions that probability of reaction p, is equal to 0.5 for $r < R_o$, and $p = 0$ for $r > R_o$,[5] the experimental data mean that the polymer segments collide with

the other part of the polymer chain with the rate of $6 \times 10^8\ s^{-1}$.

In high content region of naphthalene chromophores or in homopolymer PVN, a different migration process will be taken place in the polymers. In such high content samples, most of the naphthyl groups situate in the row of consecutive chromophores on the polymer chain, so the excitation energy can migrate along the chromophores row with a faster rate than that described above. In the next section, a quenching experiment for the monomer and excimer fluorescence is shown and the result is discussed in comparison with the migration rate obtained by the kinetic analysis of decay curves.

9-3, 4. Quenching Rate for the Monomer and Excimer Fluorescence

The quenching of naphthalene fluorescence by biacetyl has been found to be diffusion controlled process with a quenching radius: R = 11 Å.[6] This interaction distance is the same as the transfer distance between naphthalene chromophores estimated from spectroscopic data. First, the results for MNEt and extremely low naphthalene content copolymer (ca. 1%) are described briefly.

The naphthalene chromophore in this copolymer shows only monomer fluorescence, and is considered as a fluorescent probe singly introduced on the polymer chain. The quenching rate by biacetyl is expected to reflect the encounter frequency between a polymer chain and a biacetyl molecule. The quenching process in fluid solutions has been treated by Stern-

Volmer kinetics,

$$\Phi_o / \Phi = \tau_o / \tau = 1 + k^q \tau_o [Q] , \qquad (20)$$

where Φ_o, τ_o are the quantum yield of fluorescence, its lifetime in the absence of quencher, respectively, and k^q is the quenching rate constant. This

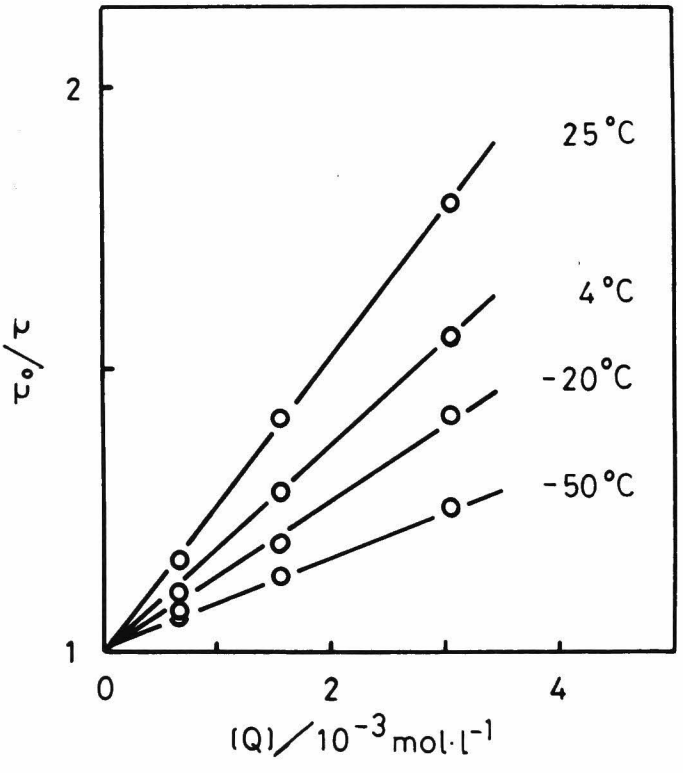

Fig. 12. Stern-Volmer plots for the lifetime of monomer fluorescence τ of 1% copolymer at various temperatures.

Table 4. Quenching rate constants and activation energies

T / °C	MNEt	1% Copolymer
25	8.7×10^9	4.6×10^9
4	6.5×10^9	3.0×10^9
-20	5.0×10^9	2.1×10^9
-50	3.0×10^9	1.3×10^9
$\frac{E(k_{01}^q)}{\text{kcal mol}^{-1}}$	1.8	2.0

relation is plotted in Fig. 12. From the slope of a line and lifetime τ_o, the quenching rate constant, k^q is obtained. The rate constant and its activation energy, $E(k_{01}^q)$, for MNEt and the 1% copolymer are listed in Table 4. Here, two important points in Table 4 are noted: (1) the activation energies, $E(k_{01}^q)$'s are found to be 1.8 - 2.0 kcal/mol, and these values are very close to the activation energy of solvent viscosity, (2) the quenching rates of MNEt are 2.0 to 2.5 times larger than those of the 1% copolymer. These facts indicate that the quenching

reaction is a diffusion controlled process. In the Smoluchowski expression for the rate parameter of a diffusion controlled process,

$$k^q = 4 \pi N' D R \{1 + R(\pi D t)^{-1/2}\} , \qquad (21)$$

the mutual diffusion coefficient, D is given as the sum of the diffusion coefficients of the two species: naphthalene moiety and quencher ($D = D_N + D_Q$). The diffusion coefficient of naphthalene moiety attached to the polymer chain is negligibly small as compared with low molecular weight molecules. Then, the quenching rate between polymers and small molecules are expected to reduce half the rates between two small molecules.

On the basis of these characteristics, the results for various naphthalene content copolymers are discussed, hereinafter. The copolymers having naphthalene contents of more than 10% show excimer emission besides the monomer fluorescence. In order to obtain both the quenching rate constants, k_{01}^q for the excited monomer state, and k_{02}^q for the excimer state, two different methods were used. First, the results obtained by the photostationary method is described.

Under the steady state condition, the next equation must be held for both kinds of dissipation processes,

$$(k_{01}^f + k_{01}^n + k_{01}^q [Q]) [M^*] + (k_{02}^f + k_{02}^n + k_{02}^q [Q]) [D^*] = I_o , \qquad (22)$$

where I_o is the intensity of incident light. Equa-

tion 22 can be rewritten as follows,

$$\{(k_{01}^{f} + k_{01}^{n} + k_{01}^{q}[Q])/\ k_{01}^{f}\}\ \Phi_M + \{(k_{02}^{f} + k_{02}^{n} + k_{02}^{q}[Q])/\ k_{02}^{f}\}\ \Phi_D = 1\ . \qquad (23)$$

In Eq. 23, unknown parameters are two quenching rates, k_{01}^{q} and k_{02}^{q}, and the other have already been obtained. It was confirmed in this system that reciprocal of the excimer's lifetime ($1/\tau_D$) is almost equal to the sum of rate constants for the excimer state,

$$\tau_D^{-1} = k_{02}^{f} + k_{02}^{n} + k_{02}^{q}[Q]\ , \qquad (24)$$

because the equilibrium at the excited state lies so heavily to the excimer state. The quenching rate constant, k_{02}^{q} is obtained by the simple Stern-Volmer plot for the lifetime of excimer emission. Therefore, k_{01}^{q} is given by the measurements of quantum yields, Φ_M and Φ_D.

In the second method, the analysis of transient decay curves are carried out using the kinetic equations already mentioned. The rate constants, k_{01}^{q} and k_{02}^{q} are chosen in such a way that the calculated decay curves for both the monomer and excimer emission fit with the observed transient curves. This method can be applicable for the low naphthalene content samples and the quenching rate thus obtained agreed with those from photostationary method.

The rate constants, k_{01}^{q} and k_{02}^{q} at 25 °C are plotted against the content of naphthalene unit in Fig. 13. The observed k_{02}^{q}'s show no change in the whole range of naphthalene content. The value is

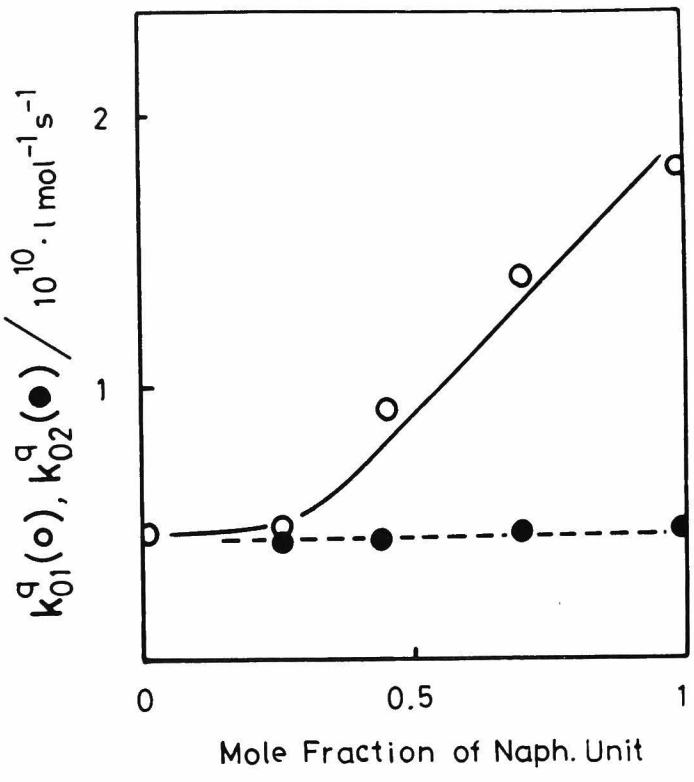

Fig. 13. Quenching rate constants, k_{01}^q and k_{02}^q against the contents of naphthalene units of copolymers.

almost the same as that of monomer fluorescence for the low naphthalene content copolymers, in which the quenching process is known to be diffusion controlled: 4.6×10^9 l $mol^{-1}s^{-1}$. It is clear that biacetyl molecules quench the naphthalene excimers with diffusion controlled reaction rate, and excimers are localized on the polymer chain since the quenching rates show no variation with increase of naphthalene

content in the copolymers.

On the other hand, the rate constant, k_{01}^{q} shows remarkable increase in the region above 40% of naphthalene content. As mentioned above, the diffusion coefficient of polymer chain is negligibly small. So, the mutual diffusion coefficient is written by the sum of D_Q and migration coefficient of excitation energy Λ. Hence, it seems that the large k_{01}^{q}'s for high naphthalene content polymers are due to the increase of Λ. If D_Q is taken as 2×10^{-5} $cm^2 s^{-1}$,[7] then Λ is estimated to be 6×10^{-5} $cm^2 s^{-1}$ for homopolymer, PVN. These polymer systems are too complex for a make quantitative discussion using the simple diffusion model, but the results suggest that the excitation energy can migrate among chromophores of PVN about three times faster than the diffusion of biacetyl molecule, and the migration effect becomes marked in the copolymers whose naphthalene contents are larger than 40%. In the present stage, there is no appropriate model to quantify the migration rate in polymers, but the migration will be carried out in the time range of picosecond.[8]

It is interesting to compare this fast migration process with the migration rate obtained by the kinetic analysis of monomer and excimer fluorescence decay curves: $k_t = 3 \times 10^8$ s^{-1}. The latter type of energy migration takes place even in the naphthalene content below 40%, since the excitation energy can migrate from an excited chromophore to another one with the intramolecular collision of the polymer segments. This type of energy migration is assisted by the micro-Brownian motion of polymer chain, and

hence, does not enhance the quenching rate constant by biacetyl. With increasing naphthalene contents, another type of energy migration takes place. In the high naphthalene content samples, most of the naphthalene units situated in a row of consecutive chromophores on the polymer chain, so the excitation energy can migrate along the chromophore's row at a faster rate than the segment motion of polymer chain. This type of energy migration should increase the quenching rate of monomer fluorescence.

Table 5. Photophysical processes in the copolymer system

1	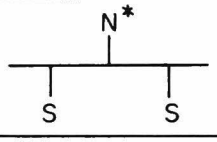	isolated N excited $\longrightarrow i_M$
2	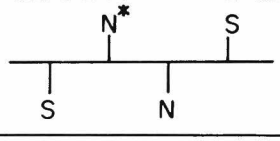	non-isolated N excited but no excimer formed $\longrightarrow i_M$
3	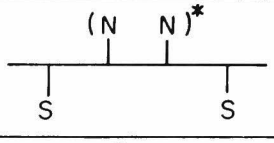	non-isolated N excited and excimer formed $\longrightarrow i_D$
4	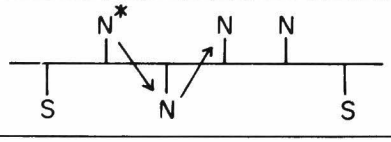	non-isolated N excited energy transfer to adjacent N
5	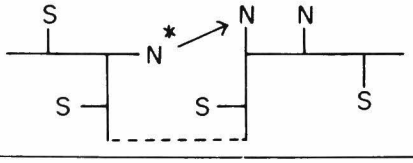	isolated and non-isolated N excited, energy transfer to non-adjacent N

The marked increase of k_{01}^{q} is attributable to this type of energy migration.

It has been already shown in Chapter 7 and 8 that fast migration of excitation energy enables to enhance the excimer formation efficiencies. As shown in Figs. 4 and 5 in high content region, the more efficient quenching of the monomer fluorescence and formation of the excimer than the prediction of the calculation are probably due to this

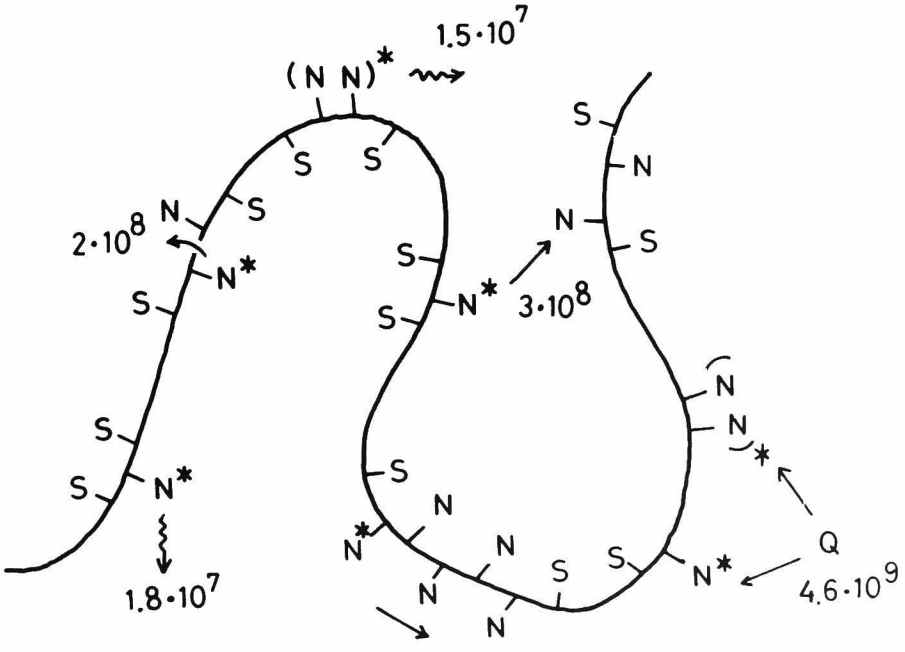

Fig. 14. Dissipation processes of the excitation energy and their rate constants in the copolymer system. The rate constants are in unit of s^{-1}.

fast migration along chromophores, which seems to be also the cause of molecular weight effect observed for PVN in Chapter 8. This migration effect will be easy to appear under the condition that the molecular motion is suppressed in low temperatures or rigid matrix. This is discussed again in the next chapter using polystyrene films containing trace amounts of PVN.

Lastly, the photophysical processes in the copolymer system are summarized in Table 5, and the rate constants are shown in Fig. 14.

References

1) S.S. Yanari and F.A. Bovey, Nature, 200, 242 (1963).
Y. Nishijima, J. Polym. Sci., C, 31, 353 (1970).
Y. Nishijima, K. Mitani, S. Katayama, and M. Yamamoto, Repts. Progr. Polym. Phys. Japan, 13, 425 (1970).
F. Schneider and J. Springer, Makromol. Chem., 146, 181 (1971).
R.B. Fox, T.R. Price, R.F. Cozzens, and J.R. McDonald, J. Chem. Phys., 57, 534 (1972).
C. David, M. Lempereur, and G. Geuskens, Eur. Polym. J., 9, 1315 (1973).
C. David, M. Piens, and G. Geuskens, Eur. Polym. J., 12, 621 (1976)
2) A.C. Somersall and J.E. Guillet, Macromolecules, 6, 218 (1973).
C. David, M. Piens, and G. Geuskens, Eur. Polym.

J., 9, 533 (1973).
R.B. Fox, T.R. Price, R.F. Cozzens, and W.H. Echols, Macromolecules, 7, 937 (1974).
C. David, V. Naegelen, W. Piret, and G. Geuskens, Eur. Polym. J., 11, 569 (1975).
M. Yokoyama, T. Tamamura, T. Nakano, and H. Mikawa, J. Chem. Phys., 65, 272 (1976).
A. Ueno, T. Osa, and F. Toda, J. Polym. Sci., Polym. Lett. Ed., 14, 521 (1976).
C. David, N.P. Lavareille, and G. Geuskens, Eur. Polym. J., 13, 15 (1977).
R.F. Reid and I. Soutar, J. Polym. Sci., Polym. Lett. Ed., 15, 153 (1977).
R.F. Reid and I. Soutar, J. Polym. Sci., Polym. Phys. Ed., 16, 231 (1978).

3) C.C. Price, B.D. Halpern, and S.T. Voong, J. Polym. Sci., 11, 575 (1953).

4) D.L. Dexter, J. Chem. Phys., 21, 836 (1953).
Th. Förster, Discuss. Faraday Soc., 27, 7 (1959).
J.B. Birks, "Photophysics of Aromatic Molecules," Wiley-Interscience, London 1970.

5) O. Stern and M. Volmer, Physik. Z., 20, 183 (1919).
R. Voltz, G. Laustriat, and A. Coche, J. Chim. Phys., 63, 1253 (1966).
M. Yokota and O. Tanimoto, J. Phys. Soc. Japan, 22, 779 (1967).
I.Z. Steinberg and E. Katchalski, J. Chem. Phys., 48, 2404 (1968).

6) J.B. Birks, M. Salete, and S.C.P. leite, J. Phys. B., 3, 417 (1970).

7) This is a normal value as the coefficient of organic molecules in low viscosity solvents.

Leroy et al. (Biopolymers, 13, 507 (1974)) have reported the diffusion coefficient of biacetyl in dichloroethane to be 1.9×10^{-5} $cm^2 s^{-1}$.

8) The decay time of the monomer fluorescence of PVN has been found to be ca. 1.4 ns.

CHAPTER 10

Excimer Emission of Poly(2-vinylnaphthalene) Dispersed in Polystyrene Matrix

10-1. Introduction

In the studies on the intramolecular excimer formation of high polymers in solution, it has been clarified that the energy migration along the polymer chain besides the micro-Brownian motion of the polymer chain, plays an important role in the formation of excimer. The manifestation of the energy migration seems to become more pronounced when the micro-Brownian motion is inhibited, e.g., when a polymer having aromatic side groups is imbedded in solid matrix. In such a situation, the excimer formation is mostly through the migration of excitation energy to the excimer site. In solid systems, it is expected that the phenomena of energy migration along a polymer chain are observed explicitly. Several interesting studies on the emission properties of high polymers in solids have been reported by David,[1] Fox,[2] and Frank.[3] They pointed out the important role of energy migration in photophysical properties of polymer systems.

In the present chapter, the photoluminescence characteristics of poly(2-vinylnaphthalene) (PVN) and vinylnaphthalene-styrene copolymers in polystyrene (PSt) film have been studied. A marked molecular weight dependence of excimer formation

efficiency was observed for various PVN samples, and it will be tried to interpret the result as an effect of energy migration on the polymer chain.

10-2. Experimental

The characteristics of PVN homopolymers used in this chapter are summarized in Table 1. The PVN-A polymers were prepared by anionic polymerization in THF using sodium naphthalene as an initiator. The PVN-R polymers were prepared by radical

Table 1. Characteristics of PVN homopolymers and observed quantum yield ratio, Φ_D/Φ_M and the lifetime of the excimer emission.

	$M \times 10^{-4}$	D.P.	Φ_D/Φ_M	τ_D (ns)
PVN-A1	0.55	36	0.46	67
PVN-A2	0.97	63	0.76	66
PVN-A3	1.3	88	0.90	62
PVN-R1	0.75	49	0.61	67
PVN-R2	1.3	86	1.0	67
PVN-R3	2.0	130	1.3	67
PVN-R4	5.0	330	1.9	69
PVN-R5	8.1	520	2.1	69
PVN-R6	14.	920	2.4	
PVN-R7	26.	1700	3.6	68
PVN-R8	47.	3100	11.	65
T N Pe	0.045	3	0.05	

polymerization in bezene solution at 60 °C. The polymer samples were fractionated by the fractional precipitation method. The molecular weight were determined by GPC, some points of which were calibrated by light scattering measurements, vapor pressure osmometry and viscosity. The trimer model compound, 1,3,5-tri(2-naphthyl)pentane (TNPe) was synthesized by the method described in Chapter 7.
The characteristics of the copolymers are summarized in Table 2, whose samples are the same used in Chapter 9. P_N is the mole fraction of VN unit in the copolymer, and P_{NN} is the fraction of the adjacent pair of naphthalene on the polymer chain which are

Table 2. Characteristics of vinylnaphthalene-styrene copolymers and observed quantum yield ratio, Φ_D/Φ_M and the lifetime of the excimer emission, τ_M in polystyrene films.

	$M_w \times 10^{-4}$	P_N	P_{NN}	Φ_D/Φ_M	τ_D(ns)
C4	27	0.44	0.16	0.19	67
C5	34	0.58	0.33	0.88	66
C6	25	0.70	0.49	1.36	61

estimated from the copolymerization reactivity ratios. Polystyrene was obtained from Nakarai Chemicals Ltd., and purified by repeated precipitation from benzene solution with methanol. The molecular weight was determined to be 2×10^5 by GPC measurements. Sample film was casted on a wall in quartz cell by slow vacuum distillation from spectrograde benzene solution. The PVN concentration in PSt matrix was 0.2 - 0.3 wt%, and the thickness of the film was about 100 μm. The casting temperature was fixed at 25 °C. Fluorescence spectra were observed by front surface excitation (excitation wavelength: 300 nm); the spectra were unchanged with the exciting wavelength between 290 nm and 320 nm.

10-3. Results

The fluorescence spectra of the copolymers, C4, C5, and C6 dissolved in PSt matrix are shown in Fig. 1. As the content of naphthalene chromophores in the polymer increases, the quantum yield ratio Φ_D/Φ_M increases markedly. In Fig. 2, the ratios are plotted against the probability, P_{NN} which seems to be proportional to the intramolecular concentration of the excimer forming sites between adjacent chromophores on the polymer chain. The result obviously deviates from the linear relationship. This indicates that besides the number of adjacent pairs of chromophores, an additional mechanism to enhance the excimer formation plays more and more important role as increasing the naphthalene content of the copolymers. Such a process can be easily presumed to be migration of excitation energy along the polymer

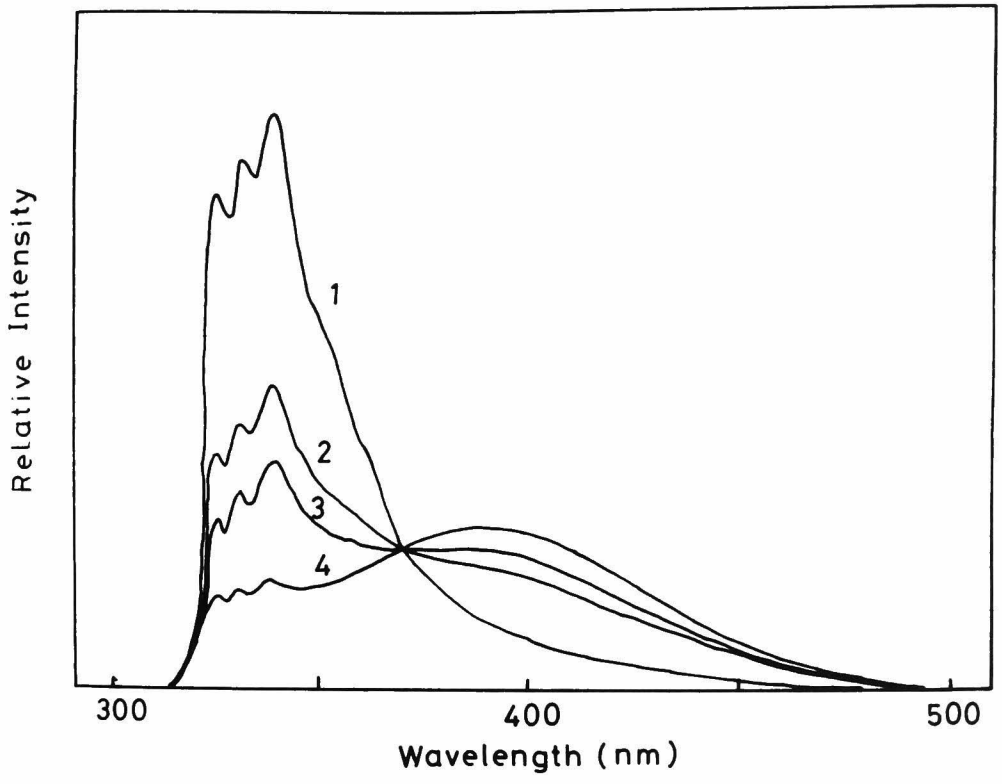

Fig. 1. Fluorescence spectra of vinylnaphthalene-styrene copolymers in PSt matrix: (1) C4, (2) C5, (3) C6, and (4) PVN-R7. There is no appreciable excimer emission for C1, C2, and C3.

chain. The copolymers containing the naphthalene units less than the fraction of C4 (P_N= 0.44) show no appreciable excimer emission in films, although in solutions, even the copolymers C1 and C2

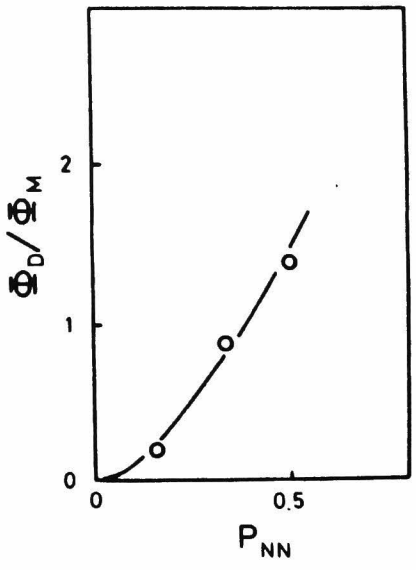

Fig. 2. Quantum yield ratios, Φ_D/Φ_M as a function of the probability P_{NN}.

show efficient excimer formation as described in the previous chapter.

The fluorescence spectra of PVN homopoymers with various molecular weights were measured in PSt matrix and they are shown in Fig. 3. The trimeric model compound, TNPe dose not show excimer emission, and its fluorescence characteristics are similar to those of 2-ethylnaphthalene (MNEt). But, as the molecular weight increases, the quantum yield ratio, Φ_D/Φ_M increases markedly. The value of Φ_D/Φ_M and the decay time of the excimer emission, τ_D are given in Table 1. The decay times are approximately constant for all samples: 65 - 69 ns, these values are almost identical with the decay time of excimer emission of PVN in solutions. The ratio, Φ_D/Φ_M, is

plotted as a function of the molecular weight M, up to 8×10^4 in Fig. 4, and up to 5×10^5 in Fig.5.

10-4. Discussion

10-4, 1. Copolymers

A photophysical kinetic scheme for excimer formation in films is given as follows,

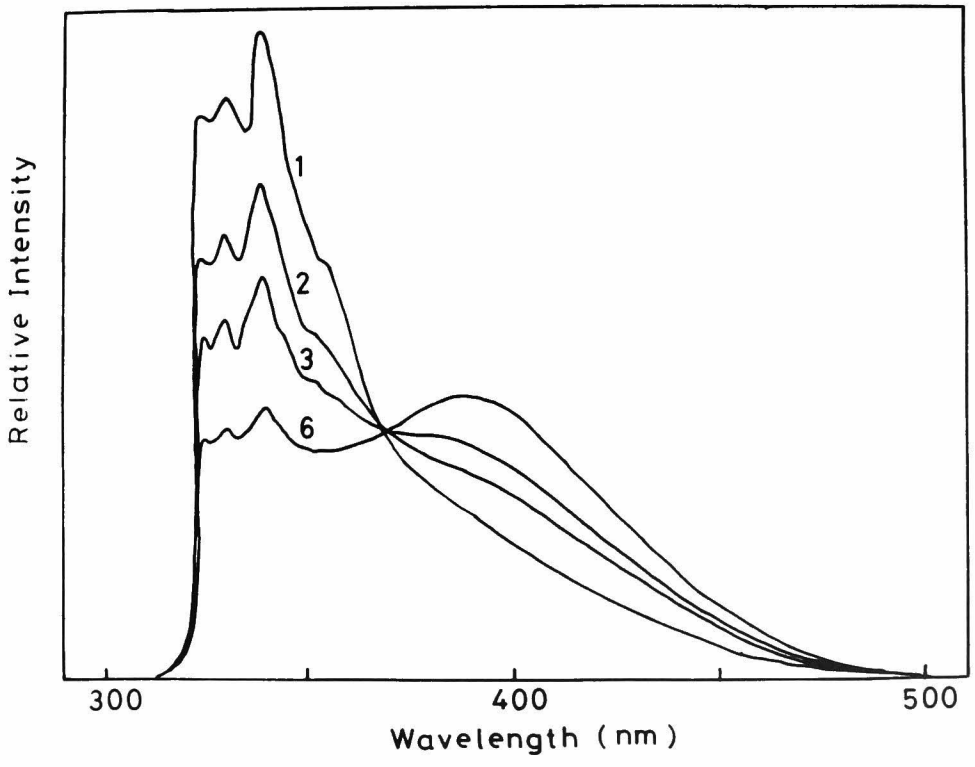

Fig. 3. Fluorescence spectra of various PVN homopolymers in PSt matrix: (1) PVN-R1, (2) PVN-R2, (3) PVN-R3, and (6) PVN-R6.

$$
\begin{aligned}
&{}^1M^* && \rightarrow && {}^1M && + && h\nu && k_{01}^f \\
&{}^1M^* && \rightarrow && {}^1M && && && k_{01}^n \\
&{}^1M^* && + (M\text{-}M) && \rightarrow && {}^1M && + && {}^1D^* && k_{21} \\
&{}^1M^* && + {}^1M && \rightarrow && {}^1M && + && {}^1M^* && k_t \\
&{}^1D^* && && \rightarrow && (M\text{-}M) && + && h\nu' && k_{02}^f \\
&{}^1D^* && && \rightarrow && (M\text{-}M) && && && k_{02}^n \\
&{}^1D^* && + {}^1M && \rightarrow && (M\text{-}M) && + && {}^1M^* && k_{12}
\end{aligned}
$$

where (M-M) is the excimer site on the guest polymer chain. Under photostationary condition: $d[{}^1M^*]/dt = d[{}^1D^*]/dt = 0$, the ratio of the quantum yields of excimer emission to monomer fluorescence, Φ_D/Φ_M can be expressed in the following form,

$$\Phi_D/\Phi_M = k_{02}^f\, k_{21}[(M\text{-}M)]/k_{01}^f(k_{02} + k_{12}) \qquad (1)$$

where $k_{02} = k_{02}^f + k_{02}^n$. This equation implies that the quantum yield ratio reflects directly the rate of excimer formation process and the concentration of the excimer forming sites. Since the micro-Brownian motion of polymer chain is suppressed in films, it is impossible to form excimers between adjacent chromophores by conformational changes of polymer chain during the lifetime. Furthermore, energy migration between non-adjacent chromophores assisted by micro-Brownian motion seems to be inefficient under such solid condition; in solution, this type of energy migration causes efficient excimer formation in the low naphthalene content samples. This is the reason

that the copolymers C1, C2, and C3 show no appreciable excimer emission in films. As increasing the naphthalene content of copolymers, another type of energy migration will become efficient; energy migration along the row of chromophores on the polymer chain. As shown in Eq. 1, the excimer formation efficiency is not only affected by the concentration of excimer forming sites but also affected by the migration rate of excitation energy in the domain of guest polymer. Energy migration rates vary with the naphthalene contents of the samples, and the changes have to taken into account in addition to the concentration of excimer site. As shown in Fig. 2, this migration process enhances the ratio, Φ_D/Φ_M for C4, C5, and C6, well ahead of the expected values from the probability of adjacent pair, P_{NN}.

One of the major problems is how to determine the migration rate of excitation energy in the copolymer systems. Soutar et al. reported a good proportionality between the ratio, Φ_D/Φ_M and the mean square length of naphthalene unit on the polymer chain in the solid system: PVN in PMMA matrix.[4] In the present system, however, such a relationship was not obtained for PSt films. Accurate evaluation of the migration rate in the copolymers has not been clarified yet. But, with regard to this migration process, the observation for the homopolymer samples having various molecular weights seems to provide rather significant information, since the diffusion length of excitation energy is restricted within the chain length of the guest polymer, PVN.

10-4, 2. Excimer Formation Mechanism in Homopolymers

Marked molecular weight dependence of the quantum yield ratio Φ_D/Φ_M are observed. The decay times for the excimer emission are approximately constant for all samples, therefore, the observed molecular weight dependence is caused by the excimer formation

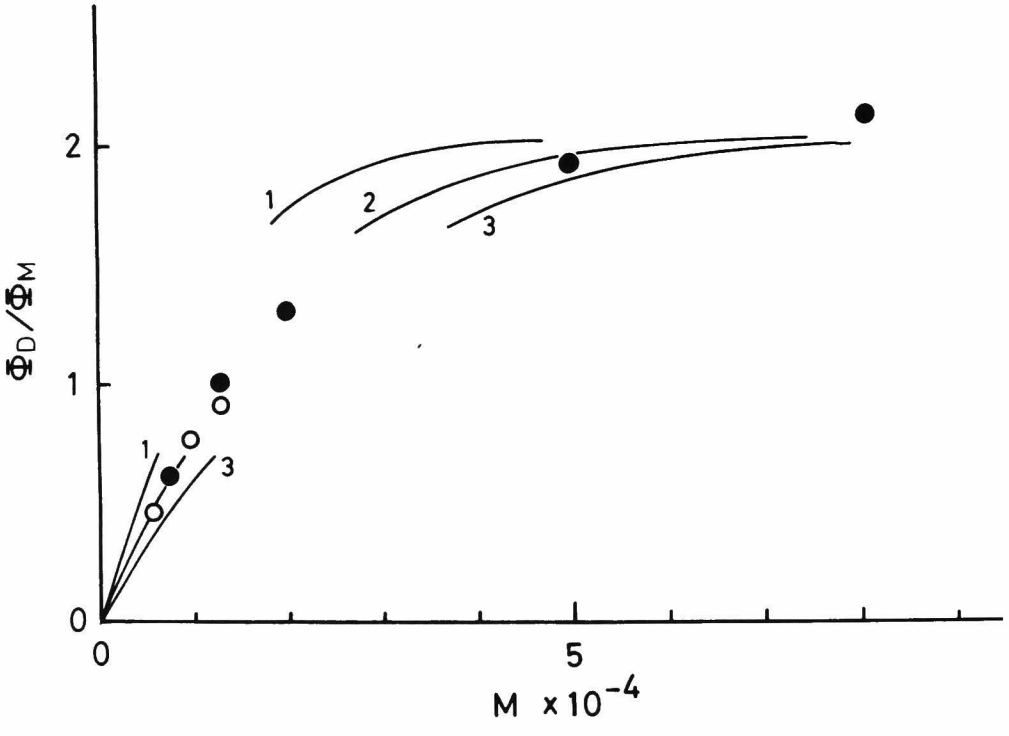

Fig. 4. Molecular weight dependence of Φ_D/Φ_M up to 8 x 10^4. ○: PVN-A and ●: PVN-R. Solid lines show calculated values from the probability, (1) p= 1/40, (2) p= 1/60, and (3) p= 1/80.

processes. In the first place, let us consider the dependence of the quantum yield ratio on M up to 8 x 10^4, the results of which is shown in Fig. 4.

If W(k,n) is the probability that k excimer sites are formed in a guest polymer whose degree of polymerization is n, the observed ratio Φ_D/Φ_M is given by,

$$\Phi_D/\Phi_M = \sum_{k=1} q_D(k,n)\ W(k,n)/\{q_M(0,n) + \sum_{k=1} q_M(k,n)\ W(k,n)\} \qquad (2)$$

where $q_M(k,n)$ and $q_D(k,n)$ are the quantum yields of monomer fluorescence and excimer emission, respectively, for the polymer molecule whose degree of polymerization is n and whose excimer site is k. Now, the probability that an adjacent naphthalene pair becomes an excimer site is denoted by p. If the probability is not affected by neighbors, W(k,n) is given by a Bernoulian distribution, and for large values of n, it can be approximated by a Poisson distribution as follows,

$$W(k,n) = \lambda^k\ e^{-\lambda}\ /\ k! \qquad (3)$$

where λ is the average number of excimer sites in a single guest polymer molecule, and is given by $\lambda = np$. For large values of n, the ratio Φ_D/Φ_M should reach a limiting value, since the encounter probability of diffusing excitation energy to an excimer site becomes independent of n, in the case that the polymer chain length is sufficiently longer than the diffusion length of excitation energy during chromophore's lifetime. This appears to be in the region

of M above 5×10^4 as seen in Fig. 4. For small values of n, the ratio Φ_D/Φ_M will be small, since the probability p is fairly low; almost all guest molecules have no excimer site on the polymer chain. The excitation energy of such a guest molecule cannot contribute to excimer formation, regardless of its migration efficiency.

On the assumption that in films the dissociation rate k_{12} is negligibly small compared with k_{02}, the quantum yields, Φ_M and Φ_D are given by,

$$\Phi_M = k_{01}^f / (k_{01} + k_{21})$$
$$\Phi_D = \tau_D k_{02}^f k_{21} / (k_{01} + k_{21}) \qquad (4)$$

where $k_{01} = 1/\tau_M = k_{01}^f + k_{01}^n$. By use of the limiting value $(\Phi_D/\Phi_M)'$ of high molecular weights in Fig. 4, the rate of excimer formation $k_{21}(p)$ for a site con-

Table 3. Rate constants obtained for PVN in polystyrene matrix

k_{01}^f	0.49×10^7
k_{01}	1.85×10^7
k_{02}^f	0.23×10^7
k_{02}	1.55×10^7
$k_{21}(p)$	7.0×10^7

unit: s^{-1}

centration of p, is given by

$$k_{21}(p) = (\Phi_D/\Phi_M)' \; k_{01}^f \; / \; \tau_D \; k_{02}^f \quad . \qquad (5)$$

Here, let k_{21} be proportional to the concentration of excimer site as follows,

$$k_{21}(k,n) = k_{21}(p) \; (k/\lambda) \quad . \qquad (6)$$

From Eqs. 2, 3, 4, 5, and 6, we can evaluate the quantum yield ratio Φ_D/Φ_M with those rate parameters and λ (= np). The rate parameters were obtained experimentally as listed in Table 3. The calculated values of Φ_D/Φ_M are shown by curves in Fig. 4 for various p values. All experimental data gave excellent agreement with the curve for p = 1/60. From this value, the energy of excimer conformation based on the energy of stable chain conformation, ΔE is estimated to be 2400 cal/mol, from the relation, $\Delta E = -RT \ln p$.

The problem of random walks with spontaneous emission has been treated by Rosenstock,[5] Levinson,[6] and Rudemo.[7] They assumed that there exist two kinds of sites in one or three dimensional lattice, e.g., "ordinary site" and "absorbing site" whose fraction is p. In their treatment, the excitation energy at an ordinary site may be emitted at the site, and leaves the lattice with probability, α. In one dimensional lattice, the emission probability, $Q(\alpha, p)$ is given as follows,

$$Q(\alpha,p) = 2/\pi^{3/2} - (2/\pi) \; t \; \exp(t^2)\{1 - \mathrm{Erf}(t)\} + (2/\pi^2) \; G(t) \qquad (7)$$

where $t = \pi p/(2\alpha)^{\frac{1}{2}}$, Erf(t) is the usual error function and G(t) is given explicitly in ref. 5. In three dimensional lattice, the $Q(\alpha,p)$ is given as follows,

$$Q(\alpha,p) = (1 + 0.66\ p\ /\ \alpha)^{-1} \qquad (8)$$

In their discussion, if the ordinary site and the absorbing site are regarded as monomer excited state of naphthalene chromophore on the polymer chain and as excimer state, respectively, the equation derived by them can be applied to the present work.

Using the value of $(\Phi_D/\Phi_M)'$ and rate parameters, we can estimate the probability, $Q(\alpha,p)$

$$\Phi_M = (k_{01}^f\ /\ k_{01})\ Q(\alpha,p)$$
$$\Phi_D = (k_{02}^f\ /\ k_{02})\ \{1 - Q(\alpha,p)\}$$

then,

$$(\Phi_D/\Phi_M)' = (k_{02}^f\ k_{01}/\ k_{01}^f\ k_{02})\ \{Q(\alpha,p)^{-1} - 1\} \qquad (9)$$

From the observed value: $(\Phi_D/\Phi_M)' = 2.0$, $Q(\alpha,p)$ is found to be 0.21. In one dimensional random walk model, this value gives $\alpha = 1.3 \times 10^{-4}$ and by use of the dissipation rate of excited monomer, $k_{01} = 1.8 \times 10^7\ s^{-1}$, energy migration rate constant k_t is obtained to be $1.5 \times 10^{11}\ s^{-1}$. On the other hand, the three dimensional model gives $\alpha = 2.9 \times 10^{-3}$ and the migration rate constant k_t is obtained to be $6 \times 10^9\ s^{-1}$. These values indicate that the number of jumps of excitation energy during the lifetime is ca. 300. Although the adequacy of the models is not clear, both of the results led from the one and three dimensional models indicate very fast

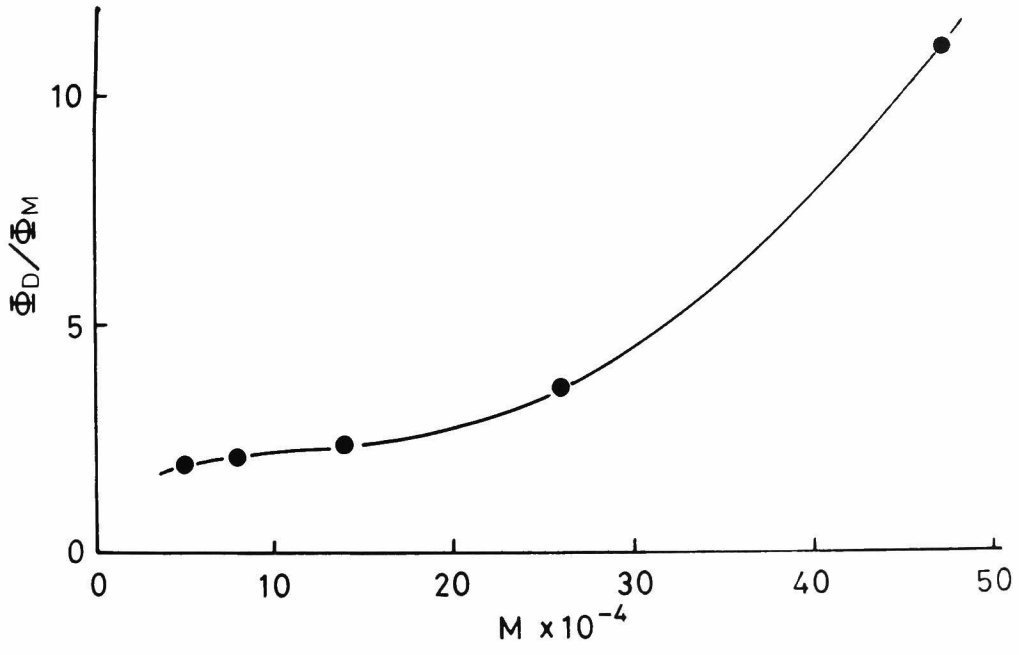

Fig. 5 Molecular weight dependence of Φ_D/Φ_M up to 5 x 10^5.

energy migration on the polymer chain in the range of 10^{10} - 10^{11} s^{-1}.

The behavior of Φ_D/Φ_M in the range of higher molecular weights above M = 2 x 10^5 cannot be explained by this energy migration scheme. If the polymer molecules in PSt matrix are dispersed monomolecularly, the ratio must be independent of M for very high molecular weight region, or decrease in such a region. The further increase of Φ_D/Φ_M with M as shown in Fig.

5, may be due to the intermolecular aggregation of PVN in PSt matrix, since the emission properties become similar to those of PVN neat film.[8] The phenomena are interesting in connection with compatibility of polymer solids.

References

1) C. David, M. Lempereur, and G. Geuskens, Eur. Polym. J., 9, 1315 (1973).
2) R.B. Fox, T.R. Price, R.F. Cozzens, and J.R. McDonald, J. Chem. Phys., 57, 534 (1972).
3) C.W. Frank and L.A. Harrah, J. Chem. Phys., 61, 1526 (1974).
4) R.F. Reid and I. Soutar, J. Polym. Sci., Polym. Lett. Ed., 15, 153 (1977).
R.F. Reid and I. Soutar, J. Polym. Sci., Polym. Phys. Ed., 16, 231 (1978).
5) H.B. Rosenstock, J. Soc. Indust. Appl. Math., 9, 169 (1961).
6) N. Levinson, J. Soc. Indust. Appl. Math., 10, 442 (1962).
7) M. Rudemo, SIAM J. Appl. Math., 14, 1293 (1966).
8) C.W. Frank and M.A. Gashgari, Macromolecules, 12, 163 (1979).

SUMMARY

In Chapter 1, some fundamental characteristics of excimers were described, and two important points were noted: (a) excimer formation is a dynamic process due to a diffusion controlled collision between two chromophores during the excited lifetime, (b) excimers are formed by short range attractive interactions, and the geometry of two aromatic molecules in the excimer state is the sandwich parallel arrangement at the distance of 3 - 4 Å. On the basis of these characteristics, two purposes for the study of intramolecular excimers in polymer systems were described. The first is fundamental interest for the relaxation processes of excitation energy in polymer systems. It has been known that the excitation of pendant chromophores of vinyl aromatic polymers brings about predominant excimer formation. It was pointed out that the detailed knowledge of the intramolecular excimers is essential for understanding of the photophysical and photochemical phenomena in polymer systems. The second is application of the excimers for the study of physical properties of polymers. The formation of intramolecular excimers was considered to be closely related to the molecular motion of polymer segments and their micro-structures.

In Chapter 2, detailed experimental methods for studying the excimer formation processes of naphthalene chromophores, were mentioned. In order to

obtain all rate constants in the kinetic scheme, it was necessary to make quantitative measurements under photostationary and transient conditions. In the photostationary measurements, quantum yields of the monomer and excimer fluorescence were determined relative to the fluorescence of quinine sulfate. These measurements were meticulously carried out at various temperatures. In the time-resolved mesurements, rise and decay curves of the monomer and excimer fluorescence were directly observed by a pulsed nanosecond fluorometer, and two decay parameters, λ_1 and λ_2 were determined. The kinetic treatments for the excimer formation processes were described, where all rate constants could be obtained by thus observed values of quantum yields and decay parameters. The procedures mentioned in this chapter were used in the following works of this thesis.

In Chapter 3, the inter- and intramolecular excimer formation processes were analyzed in practice with the photophysical reaction kinetics. The rate constants were determined, and the characteristics of inter- and intramolecular excimers of 2-ethylnaphthalene and 1,3-di(2-naphthyl)propane, respectively, were discussed. For the intermolecular excimers, a little slower association rate constant and somewhat larger activation energy compared with pyrene chromophore, were observed. This results indicated that the steric condition necessary for the formation of excimers is strict in the case of naphthalene chromophore. For the intramolecular excimers, it was demonstrated that both the association and dissociation processes are depressed by the methylene chain

restriction. Efficient intramolecular excimer formation was observed even at room temperature; the intermolecular excimers could not be found at room temperature, because of the predominant dissociation process. The association rate constant was also smaller than the value evaluated from the apparent concentration of naphthalene units. From these facts, it was concluded that the characteristics of intramolecular excimers exist in the association and dissociation processes, which reflect the binding effect of methylene chain and its rotational relaxation processes.

In Chapter 4, the geometrical requirements for intramolecular excimer formation were investigated. The n=3 rule was examined for α,ω-dinaphthylalkanes up to n=12. Although corresponding dipyrenylalkanes having the same number of carbon atoms showed the excimer emission, no appreciable excimer emission could not be observed in the case of naphthalene chromophores. Hence, it was concluded that there are some strict geometrical conditions for the intramolecular excimers of naphthalene chromophores, and it is due to the small binding energy of the excimers and the short lifetime of the excited state. Next, the emission behavior of unstable excimers were observed. The molecular axes of naphthalene units were not parallel, although the structures were close to the sandwich arrangements. In αβ-DNPr, the axes of naphthalene chromophore were rotated by an angle of ca. 40° from the parallel conformation, and in cis-DNCb, the long in-plane axis was tilted by an angle of ca. 50° from the parallel arrangement. These compounds

formed unstable excimers in the excited states, which showed some extraordinary behavior: small enthalpy gain for the association process, large dissociation rate of the excimer, and increase of non-radiative dissipation process. These results indicated that the aromatic rings must take the parallel sandwich arrangement at the stable excimer state. The strict configurational requirements of naphthalene excimers were expected to provide useful information for the conformation of molecules and their rotational motions.

In Chapter 5, various dinaphthylalkanes in which two naphthalene units are separated by three carbon atoms were prepared, and intramolecular excimer formation was investigated. All rate constants were determined by the steady state and time-resolved measurements. A large difference in the association rate constant was observed with variation of molecular structure. The results indicated that intramolecular excimer formation is directly controlled by the rotational relaxation processes of the molecules from their neighboring conformations to the excimer conformation. A large formation rate (7.9 x 10^8 s^{-1} at 25 ^{o}C) was observed for meso-2,4-dinaphthylpentane, the rate for the racemo isomer being found to be one tenth of that for the meso isomer. This indicated that the isotactic sequence in vinyl aromatic polymers plays an important role in the intramolecular excimer formation.

In Chapter 6, the pathway of internal rotation from the most stable conformation to the excimer conformation was clarified. By the use of this re-

sult, the rate constants of intramolecular excimer formation were interpreted excellently. The rate constants k_{21}'s obtained in Chapter 5, were 2.1 x $10^8 s^{-1}$ for 1,3-DNPr, 2.8 x $10^8 s^{-1}$ for 1,3-DNBu, and 8.7 x $10^8 s^{-1}$ for 2,4-DNPe(meso). These values were consistent with the results of calculation; the fractions of the conformation neighboring to the excimer state were estimated to be 0.4 for 1,3-DNPr, 0.6 for 1,3-DNBu, and 0.98 for 2,4-DNPe(meso). From these facts, it was concluded that intramolecular excimers are mainly formed by the internal rotation, trans → gauche, of the naphthalene unit and the fraction of the tg state which is the adjacent conformation to the excimer one, serves as an effective concentration of the intramolecular reaction. It was also demonstrated that the small formation rate for 2,4-DNPe (rac) is due to the unfavorable rotational mode ($g^+ \rightleftarrows g^-$) necessary to achieve the excimer conformation.

In Chapter 7, three trimer model compounds were investigated using the time-resolved technique. By the analysis of these compounds, interactions of each pair of naphthyl groups in the trimer, NNN, could be discussed separately. An enhancement of the excimer formation rate constant was observed, and the behavior was interpreted with two factors in addition to those described in the previous chapters. First, the excited middle naphthyl group of NNN can chose either of two terminal naphthyl groups as the partner of intramolecular excimer. This effect increased the formation rate up to ca. 1.3 times larger than that of NNS. It can be regarded as

an increase of the intramolecular concentration of chromophores. Secondly, the rapid migration of the excitation energy among chromophores enhances the association rate still higher in addition to the enhancement due to the first effect. The trimer, NNN, can be cinsidered as a smallest model compound having polymer effects on the relaxation processes. Hence, these results provided many useful information about the photophysical behavior of excitation energy in polymer systems.

In Chapter 8, the mechanism of intramolecular excimer formation in poly(2-vinylnapthalene) (PVN) were discussed on the basis of the photostationary and transient emission behavior. It was found that the intramolecular excimers are formed efficiently in PVN (k_{21}= 7 x 10^8 s^{-1}), and the efficiency increases with the increase of the molecular weight up to 2 x 10^4. In order to explain these phenomena some physical properties concerning with polymer molecules were considered: interaction between non-adjacent segments, variation of rotational relaxation times, end effect of polymer chain, and effect of energy migration. The measurements for α,ω-dinaphthylalkanes and for PVN in various solvents made the existence of non-adjacent excimers improbable. Furthermore, end effect of polymer chain became also unlikely as a cause of the molecular weight dependence, because the emission behavior of ABA type block copolymers did not depend on the whole degree of polymerization but on the chain length of the vinylnaphthalene block in the copolymer. From these results, it was suggested strongly that the energy migration takes place

with fairly fast rate, and it accelerates the intramolecular excimer formation.

In Chapter 9, kinetic analyses of vinylnaphthalene-styrene copolymer systems were carried out. The migration rate of excitation energy and association rate of an adjacent naphthalene pair were taken into the treatment, and their rates were obtained: $k_t = 3 \times 10^8\ s^{-1}$, $k_{21} = 2 \times 10^8\ s^{-1}$. The results indicated that the considerably fast migration of excitation energy brings about the quenching of the excited monomer state, and causes the efficient excimer formation. Next, it was shown from the quenching experiment that two types of energy migration should be considered in the copolymers; the first is the migration above mentioned, which mainly appears in low naphthalene content samples, and is assisted by the intramolecular collision of the polymer segments. The second type of migration takes place in the samples of the naphthalene content above 40%, where most of the naphthalene units situate in a row of chromophores, and the excitation energy can migrate along the chromophore's row with a fast rate than the segment motion. This rate was estimated to be in the time range of picosecond.

In Chapter 10, intramolecular excimer formation of PVN in polystyrene rigid matrix was investigated. A marked molecular weight dependence in the range below 10^4 was observed, and well interpreted by the energy migration model among chromophores. For the samples of the molecular weight above 4×10^4, the quantum yield ratio, Φ_D/Φ_M reached a limiting value, because the chain length was sufficiently

longer than the diffusion length of excitation energy during the chromophore's lifetime. From the results, the probability of the formation of excimer sites, p, and the migration rate of excitation energy, k_t were estimated to be p = 1/60, $k_t = 10^{10} - 10^{11} s^{-1}$. These results indicated the existence of very fast migration of excitation energy and showed clearly the role of energy migration on the intramolecular excimer formation.

LIST OF PAPERS

Excimer Emission of High Polymers in Solution (V) Intramolecular Excimer Formation of Poly(2-vinylnaphthalene) and its Dimeric Model Compound.

Shinzaburo Ito, Masahide Yamamoto, and Yasunori Nishijima

Repts. Progr. Polym. Phys. Japan, 19, 421 (1976).

Excimer Emission of High Polymers in Solution (VI) Excimer Emission of Vinylnaphthalene-Styrene Copolymers in Solution.

Shinzaburo Ito, Masahide Yamamoto, and Yasunori Nishijima

Repts. Progr. Polym. Phys. Japan, 20, 481 (1977).

Excimer Emission of High Polymers - Effects of Molecular Structure and Molecular Motion on Intramolecular Interaction of Electronically Excited States.

Yasunori Nishijima, Masahide Yamamoto, and Shinzaburo Ito

Ann. Rept. Res. Inst. Chem. Fibers, 34, 55 (1977).

Excimer Emission of Poly(2-vinylnaphthalene) Dispersed in Polystyrene Matrix.

Shinzaburo Ito, Masahide Yamamoto, and Yasunori Nishijima

Repts. Progr. Polym. Phys. Japan, 21, 393 (1978).

Configurational Requirements of Intramolecular Excimer Formation in α,ω-Dinaphthylalkanes.

Shinzaburo Ito, Masahide Yamamoto, and Yasunori Nishijima

Repts. Progr. Polym. Phys. Japan, 22, 453 (1979).

A Kinetic Study of Excimer Formation in Poly(2-vinylnaphthalene-co-Styrene) and its Trimer Model Compounds.

Shinzaburo Ito, Masahide Yamamoto, and Yasunori Nishijima

Repts. Progr. Polym. Phys. Japan, 22, 457 (1979).

Kinetic Studies of Fluorescence Quenching and Energy Migration in Vinylnaphthalene-Styrene Copolymers.

Shinzaburo Ito, Tohru Shiga, Masahide Yamamoto, and Yasunori Nishijima

Repts. Progr. Polym. Phys. Japan, 23, 543 (1980).

Kinetic Studies on Intramolecular Excimer Formation in Dinaphthylalkanes.

Shinzaburo Ito, Masahide Yamamoto, and Yasunori Nishijima

Bull. Chem. Soc. Jpn., in press.

Unstable Excimer Formation in Dinaphthylcyclobutanes.

Shinzaburo Ito, Masahide Yamamoto, and Yasunori Nishijima

Chem. Phys. Lett., submitted.

Conformational Analysis for Intramolecular Excimer Formation in Dinaphthylalkanes.

Shinzaburo Ito, Masahide Yamamoto, and Yasunori Nishijima

Bull. Chem. Soc. Jpn., submitted.

Kinetic Analysis of Excimer Emission of Vinylnaphthalene-Styrene Copolymers.

Shinzaburo Ito, Masahide Yamamoto, and Yasunori Nishijima

Polym. J., submitted.

ACKNOWLEDGMENTS

The present thesis is based on the studies which the author has carried out at the Department of Polymer Chemistry, Kyoto University, Kyoto, from 1973 to 1980, under the guidance of Professor Yasunori Nishijima. The author wishes to express his sincere gratitude to Professor Nishijima for his constant guidance and encouragement throughout the course of this work.

The author is sincerely grateful to Assistant Professor Masahide Yamamoto, Department of Polymer Chemistry, Kyoto University, for his invaluable guidance and discussions throughout this work.

The author wants to express his sincere appreciation to Drs. Tokuji Fujimoto and Yoshihiko Onogi for their insightful comments and suggestions. He wishes to express his thanks to Mr. Masataka Ohoka for his many valuable discussions and comments.

Thanks are also expressed to Messrs. Toshiji Kanaya and Tohru Shiga for their kind collaboration during this work.

The author wishes to thank Dr. Yoshiteru Sakata, Osaka University, for the separation of the isomers of 2,4-DNPe by a recycle gel permeation chromatography.

Finally, the author wishes to express his thanks to his colleagues in the Nishijima Laboratory for their kind help in many ways.